Experimental Study on the Engineering Properties of Gelfill

By

Najlaa Abdul-Hussain

A thesis submitted
under the supervision of Dr. Mamadou Fall

in partial fulfilment of the
requirements for the degree of
Master of Applied Science
in Civil Engineering

Department of Civil Engineering
University of Ottawa
Ottawa, Canada
March, 2011

The M.A.Sc. in Civil Engineering is a joint program
with Carleton University administrated by
Ottawa-Carleton Institute for Civil Engineering

To my Parents

ABSTRACT

Gelfill (GF) is made of tailings, water, binder and chemical additives (Fillset, sodium silicate gel). The components of GF are combined and mixed on the surface and transported (by gravity and/or pumping) to the underground mine workings, where the GF can be used for both underground mine support and tailings storage.

Thermal (T), hydraulic (H), and mechanical (M) properties are important performance criteria of GF. The understanding of these engineering properties and their evolution with time are still limited due to the fact that GF is a new cemented backfill material.

In this thesis, the evolution of the thermal, hydraulic, mechanical, and microstructural properties of small GF samples are determined. Various binder contents of Portland cement type I (PCI) are used. The GF is cured for 3, 7, 28, 90, and 120 days. It is found that the thermal, hydraulic and mechanical properties are time-dependent or affected by the degree of binder hydration index. Furthermore, a relationship is found between the compressive strength and the saturated hydraulic conductivity of the GF samples.

The unsaturated hydraulic properties of GF samples have also been investigated. The outcomes show that unsaturated hydraulic conductivity is influenced by the degree of binder hydration index and binder content, especially at low suction ranges. Simple functions are proposed to predict the evolution of air-entry values (AEVs), residual water content, and fitting parameters from the van Genuchten model with the degree of hydration index (α). Furthermore, two columns are built to simulate the coupled thermo-hydro-mechanical (THM) behaviour of GF under drained and undrained conditions. The obtained results from the GF columns are compared with the small samples. It is observed that the

mechanical properties, hydraulic properties (suction and water content), and temperature development are strongly coupled. The magnitude of these THM coupling factors is affected by the size of the GF. The findings also show that the mechanical, hydraulic and thermal properties of the GF columns are different from samples cured in plastic moulds.

Acknowledgements

I would like to express my sincere gratitude to my supervisor, Dr. Mamadou Fall, for his guidance and support throughout all the stages of this investigation.

I would like to thank Dr. J. J. Beaudoin for his help and interest in this research. I would also like to acknowledge Mr. G. Chan from the NRC.

Special thanks to Dr. Muslim Majeed and Mr. Jean Claude Celestin for their continual help and useful information.

Finally, I would like to thank my husband, Bessam, for his help and support, and my children, Reeham and Haider, for their understanding and patience.

Table of Contents

List of Figures

List of Tables

Chapter 1

Introduction

1.1 General Statement

Tailings are waste products that remain when valuable metals are extracted from mineral rocks. Huge voids, which are called stopes, are created by the ore extraction process; these voids are generally filled by using waste products (tailings). This process is called mine backfilling.

Backfilling has become the standard practice in mining operations. One of the main reasons behind the extensive use of backfill in mines is that it can lead to a significant reduction of the amount of waste disposed on the surface (Li and Aubertin, 2007). Furthermore, backfilling allows an increased amount of ore that can be safely extracted, and increases mine productivity and work safety. There are several types of mine fills; however, the most recent, cost-effective and popular type is cemented paste backfill (CPB), a mix of tailings, water, and binder.

However, the cost of CPB is still high. Typically, the costs of CPBs range between 10% to 20% of mine operations. Binder cost represents a significant fraction of operation costs in underground mining operations (Hassani et al., 2007). The binder can represent up to 75% of the cost of the cemented backfill (Fall et al., 2008). The most common binder used in the preparation of CPBs is Portland cement (PC). PC is not only a costly binder, but its production is highly energy-intensive and thus generates a large amount of carbon dioxide (CO_2). Cement production is making up approximately 5 to 7 percent of global anthropogenic CO2 emissions (CEMBUREAU, 1999), and the mining industry is the second

largest cement consumer in Ontario (Environment Canada, 2006). These factors mentioned above have compelled mining companies to seek for alternatives to cement that increase the strength of the fill and reduce the cement content. Sodium silicate is the most recent chemical additive that is used to reduce the binder content in CPB. This new product is named gelfill (GF), a mix of tailings, water, cement and sodium silicate (sodium silicate has many applications in different industries, see Section 2.6). The aim is to add small amounts of sodium silicate (0.3-0.4% by weight of solids) to the mix of backfill with a solid concentration of 73%. The addition of sodium silicate results in an increase of the compressive strength of GF structures (Hassani et al., 2007).

Mechanical stability and environmental performance are important engineering design criteria of GF structures. They are functions of the mechanical (M), hydraulic (H), thermal (T) and chemical (C) properties of the GF material as discussed below.

- Mechanical properties

GF can be considered as a safe underground working material when certain mechanical stability requirements are accomplished. Uniaxial compressive strength (UCS) is frequently used to judge the mechanical stability of GF (see Section 2.3).

- Hydraulic properties

The mechanical properties are influenced by the hydraulic properties or behaviour of GF structures. Indeed, movement of water through GF structures at early ages and development of pore water pressure (positive and negative) can contribute to decreases or increases in the strength of GF.

Furthermore, it is noted that hydraulic properties are the main factors that influence environmental performance and durability of cemented backfill structures (Fall et al., 2009). The main problem that is often associated with the mining process is the formation of acid mine drainage (AMD). The tailings used in CPBs and GF often contain ferrous sulphide minerals in form of pyrite and pyrrhotite (Elberling et al., 1994). The percentage of sulphide in the tailings can vary from 2% to 60% (Fall and Benzaazoua, 2005), depending on the composition of the ores. The accessibility of oxygen and water inside the GF structures leads to an increase of the sulphate concentration by the oxidation of sulphide tailings. This process causes degradation in GF strength through sulphate attacks and helps the generation of AMD. The hydraulic properties of GF are responsible for controlling the flow of hostile elements (water and oxygen). Furthermore, earlier, there was the assumption that in situ cemented backfill was saturated; however, recent studies show that in situ cemented material are unsaturated (e.g., Le Roux et al., 2005). This means that there is the opportunity for oxygen to diffuse through unsaturated GF structures (oxygen has low solubility in water). This unsaturated condition will also affect the UCS; decreasing the moisture content due to higher suction leads to increases in the compression strength of GF structures.

- Thermal properties

This binder hydration process leads to the development of the microstructure of GF, which in turn, decreases the permeability of the structure and increases strength. Since the hydration of binder compounds is exothermic, the heat evolution in hydrated binder indicates the rate of hydration (Neville, 1995; Simon, 2005). Due to the relatively low thermal conductivity (K) of cementitious materials and large mass of GF structures, steep

temperature gradients could occur between the interior and the exterior of the GF (the exterior loses some of the heat to the surrounding). This behavior can cause serious cracking in GF structures. On the other hand, the heat of hydration affects the mechanical behavior of GF at early ages (higher temperature results in higher early strength in cementitious material).

- Chemical properties and factors

The chemical properties or factors include several parameters such as the type of binder, degree of binder hydration and sulphate content. The binder proportions and type as well as the degree of binder hydration influence the mechanical, hydraulic, and thermal properties of cementitious materials. For example, the amount of heat developed and the variation in the temperature of the filling mass is strongly influenced by the binder concentration and type (chemistry of the binder). Furthermore, studies show that the strength of cementitious material is considerably affected by the binder contents and type, and α (e.g. Celestin, 2009). Moreover, sulphate can contribute to the increase of the early age strength of cemented backfill or the decrease of its long-term strength (i.e mechanical stability) through sulphate attack (e.g., Fall and Benzaazoua, 2005). Sulphate attack not only decreases mechanical stability, but also contributes to the development of cracks in cemented backfill. This may result in the generation of AMD and a potentially environment-hostile leachate.

Further details on GF properties are discussed in Technical Paper I (Chapter 3).

Therefore, mechanical, hydraulic, thermal, and chemical properties are essential performance criteria for GF structures. Since GF is new cemented backfill material, only a

few studies (e.g. Doucet et al., 2007, and Hassani et al., 2007) have been conducted to investigate the mechanical properties of GF. However, the understanding of these properties and their evolution with time is still limited. No studies have been conducted to study the hydraulic (unsaturated) and thermal properties of GF. There is the need to increase our knowledge about the thermal, hydraulic and mechanical properties of GF because the understanding of these properties is essential for a reliable assessment and prediction of mechanical stability, durability and environmental performance of GF. In addition, most of the previous studies did not take into consideration the coupled effects of these thermal (heat produced by binder hydration or from external sources, such as rock or air), chemical (α, sulphate content), hydraulic (fluid flow, positive and negative pore water pressure), and mechanical (external and internal mechanical loads) factors (Figure 1-1). The understanding of these coupled factors and their evolution is important for engineers to design safe and economical GF structures. For example, recent studies (Le Roux et al., 2005; Grabinsky et al., 2008) that focused on the relationship between the actual in situ properties of cemented backfill and laboratory properties showed that the in situ properties are different from laboratory properties. This is because the GF structure is subjected in the field to strong coupled thermal, hydraulic, mechanical (THM) loadings conditions. No studies have been performed on the coupled THM behaviour of GF. Thus, there is the need to address these issues. Indeed, in reality (i.e. the field), the GF is simultaneously subjected to various THM loadings conditions.

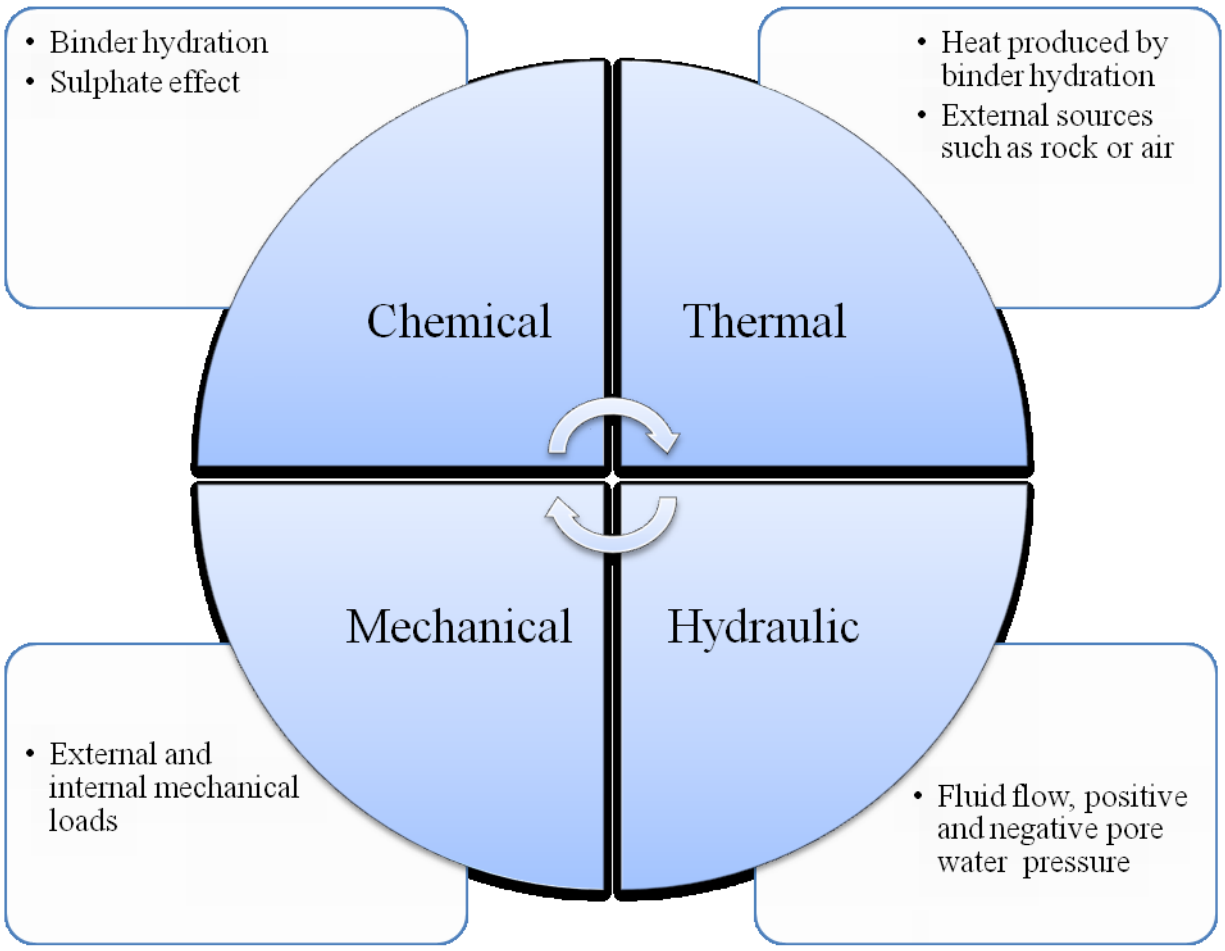

Figure 1-1 Main coupled factors in GF structures

1.2 Objectives and scope

The main objectives of this investigation are:

- to study the evolution of the thermal, hydraulic and mechanical properties of GF by conducting experimental studies on small samples;
- to study the time-dependent evolution of the unsaturated hydraulic properties of GF;
- to investigate the coupled thermal, hydraulic and mechanical behavior of cemented GF columns; and
- to gain a good understanding of coupled THM behavior of GF.

In order to achieve the objectives of this thesis, experimental studies on mould (small) samples and GF columns have been conducted. Tests are carried out in the geotechnical laboratory at the University of Ottawa following prescribed standard recommendations (Revision 2004 of the ASTM).

1.3 Organization of manuscript

The thesis is organized in the form of technical papers, and divided into six chapters.

Chapter One contains the introduction, while Chapter Two provides the literature review. Five sections are included in Chapter Two; Section One discusses the technology of mine cemented backfill; Section Two provides background information on binder hydration and cement paste characteristics; Section Three presents the unsaturated hydraulic properties of porous media and the methods used to determine them; Section Four discusses the K of porous media and their determination by using KD2; and finally, Section Five gives

background information on sodium silicate and its effect on binder hydration and performance of cementitious materials.

Chapter Three provides the first technical paper. In this paper, the evolution of the thermal, hydraulic, mechanical, and microstructural properties of GF is studied.

Chapter Four presents the second technical paper, which deals with the unsaturated hydraulic properties of GF.

Chapter Five provides the third technical paper. This chapter studies the coupled THM behaviour of GF in column experiments.

Finally, Chapter Six includes the conclusion and final recommendations for future studies.

It should be mentioned that because the main results of the thesis are presented as technical papers, some information is repeated in the papers. This is because each paper is independently written (i.e. without taking into account the content of the other papers or the rest of the document) and in accordance to the manuscript preparation instruction of the corresponding publication medium.

Below is a flow chart that shows the experimental study on GF material.

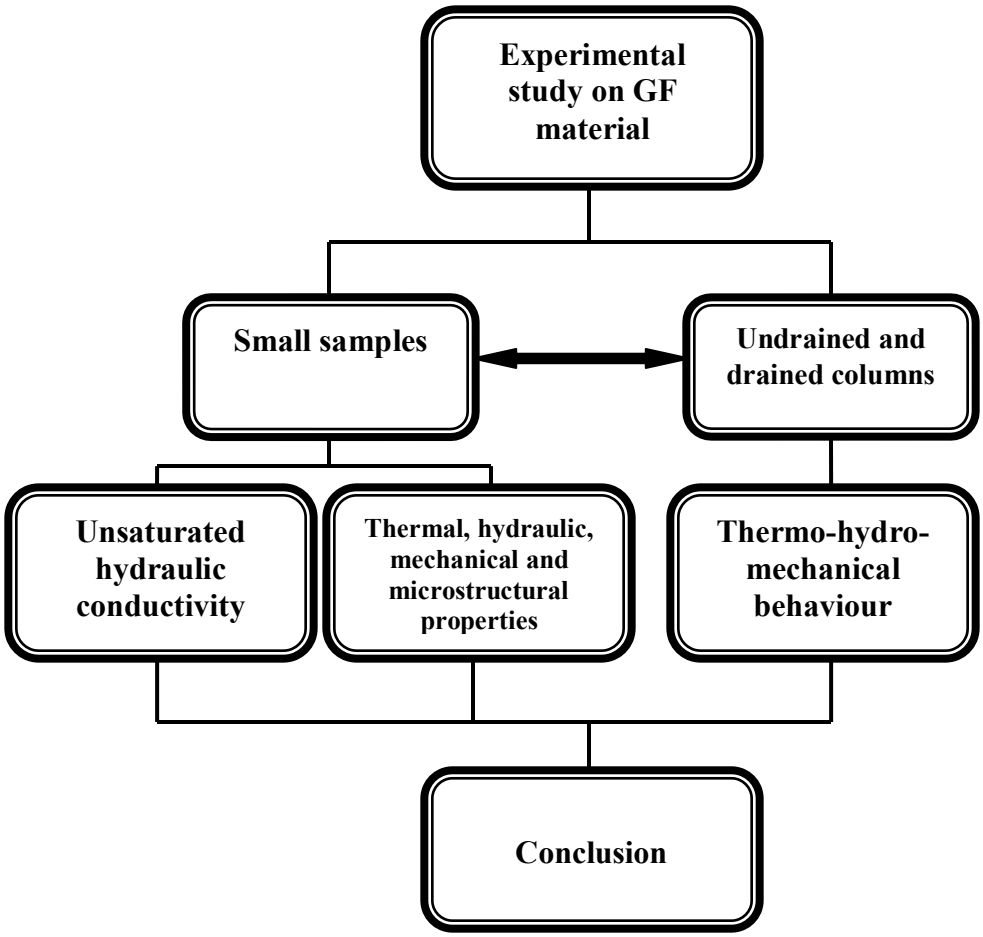

Figure 1-2 Schematic diagram that illustrates the experimental study on GF material.

1.4 References

American Society for Testing and Materials, Test method for compression strength of cylindrical concrete specimens: C39/C39M-03 Annual book of ASTM, Pennsylvania, 2004.

American Society for Testing and Materials, Test method for measurement of hydraulic conductivity of saturated porous materials using a flexible wall permeameter: D5084-00, Annual book of ASTM, Pennsylvania, 2004.

CEMBUREAU, Environmental Benefits of Using Alternative Fuels in Cement Production, CEMBUREAU, 1999.

Doucet, C., Tarr, K., Swan, G. Evaluation of the Effect of Mixing Method, Sequence and time on the properties of gelfill. Minefill 2007, 2488.

Elberling, B., Nicholson, R.V., Scharer J. M. A combined kinetic and diffusion model for pyrite oxidation in tailings: a change in controls with time. Journal of Hydrology 157 (1994) 47-60.

Environment Canada (2006). National Inventory Report: Greenhouse Gas Sources and Sinks in Canada, 1990–2004. Greenhouse Gas Division, Ottawa, Library Archives Canada, 482 p.

Fall, M., Adrien, D., Celestin, J.C., Pokharel, M., Toure, M. Saturated hydraulic conductivity of cemented paste backfill. Minerals Engineering 22 (2009) 1307-1317

Fall, M. and Benzaazoua, M.. Modeling the effect of sulphate on strength development of paste backfill and binder mixture optimization. Cement and Concrete Research 35 (2005) 301–314.

Fall, M., Benzaazoua, M. and Saa, E.G. Mix proportioning of underground cemented tailings backfill. Tunnelling and Underground Space Technology 23 (2008) 80–90.

Fall, M., Nasir, O., and Celestin, J. Paste backfill responses in deep mine temperature conditions. In: 9th International Symposium of mining with backfill. Montreal, Canada: CD-Rom; 2007 paper 2522.

Grabinsky, M., Bawden, W., Simon, D., Thompson, B. In situ properties of cemented paste backfill in an Alimak Stope. Canadian Geotechnical Conference Edmonton(2008): 790-796.

Hassani, F, Razavi, S.M., and Isagon, I. A study of physical and mechanical behaviour of gelfill. Minefill, 2007 Paper 28.

Le Roux, K., Bawden, William F. and Grabinsky, Murray F. Field properties of cemented paste backfill at the Golden Giant mine, Mining Technology (Trans. Inst. Min. Metall. A). (2005) 1-16.

Li, L., Aubertin, M. An improved solution to estimate the stress state in sub-vertical backfilled stopes. Canadian Geotechnical Conference Ottawa 2007; 1-8.

Marland, G., T.A. Boden, R.C. Griffin, S.F. Huang, P. Kanciruk and T.R. Nelson. Estimates of CO2 Emissions from Fossil Fuel Burning and Cement Manufacturing, Based on the United Nationals Energy Statistics and the U.S. Bureau of Mines Cement Manufacturing Data. Report No. #ORNL/CDIAC-25, 1989.

Carbon Dioxide Information Analysis Centre, Oak Ridge National Laboratory, Oak Ridge, Tennessee, USA.

Nasir, O. Modeling of Coupled Processes in Hydrating Cemented Paste Backfill Structures and Application to the Analysis of their Performance. University of Ottawa. (2008) 1-144.

Neville, A. M. Properties of Concrete. Forth Edition, 1995.

Pokharel, M. Geotechnical and Environmental Responses of Paste Tailings Systems to Coupled Thermo-Chemical Loadings. University of Ottawa. (2008) 1-248.

Rankine, K. J. and Sivakugan, N. R. Cowling. Emplaced geotechnical characteristic of hydraulic fills in a number of Astralian mines. Geotechnical and Geological Engineering (2006) 24: 1-14.

Simon, D. Microscale Analysis of Cemented Paste Backfill. University of Toronto, (2005) 1-282.

Chapter 2

Theoretical and Technical Background

2.1 Introduction

In order to better understand the results presented in the technical papers of this thesis, background information on some of the relevant fundamental mechanisms and techniques are given in this chapter.

First, the technology of mine cemented backfill is highlighted. Several types of mine fills are discussed. The focus is on CPB and GF because they are the most recent and popular techniques of mine backfills. CPB technology is considered superior to conventional slurry backfill methods in terms of both economic and environmental benefits (Fall et al., 2007).

Furthermore, the purpose of filling the stopes is to provide support to the adjacent wall as mining progresses. The fills should also withstand static and dynamic loads applied during their service life in underground mining. Therefore, the design criteria of cemented backfill are discussed.

Moreover, due to the presence of binder in the cemented backfill, the materials undergo a hydration process and self-desiccation, while it is hydrating. Depending on the relative humidity (RH) of the mine atmosphere, the cement backfill can undergo some desiccation too. For that, it is of importance to go through the mechanisms of binder hydration, the main products of the hydration process (e.g., calcium silicate hydrates, C-S-H), pore structure of the hardened cement paste (hcp), and the state of water and diffusion

mechanisms in the hcp. The latter is helpful to understanding the drying and wetting phenomena in hcps.

In addition, cemented backfill materials change from a saturated to unsaturated state during their service life. These changes have an impact on their hydraulic properties. For this reason, technical background on unsaturated hydraulic conductivity of porous media is provided.

This is followed by a discussion about the thermal properties of porous material, which can provide information on the heat exchange of the material with its surrounding. This is important for the understanding of heat development and dissipation within cemented backfill structures and their thermal interactions with the surrounding rock mass.

Finally, as sodium silicate is the chemical additive used in the preparation of GF, technical information on sodium silicate and their interactions with the binder is given. This will help to better understand the different types of sodium silicate and their applications, and the impact of sodium silicate on the performance of cementitious materials.

2.2 The technology of mine cemented backfill

2.2.1 Introduction

Tens to hundreds of meters in one dimension as a minimum are the excavations that may result from underground mining operations. These excavations are made by a carefully controlled series of blasts. After the blasted ore is extracted, voids are filled using products of ore extraction and mineral processing by a process called mine backfilling. Before the fill can be delivered to the stope through pipelines and boreholes, the construction of barricades is required. Barricades are like conventional retaining walls made of bricks,

rocks, masonry, shotcrete, and even concrete (Figure 2-1). The purpose of constructing a barricade is to provide a barrier between the fill and active mine workings. The structures of barricades should be designed to withstand the expected maximum head pressure with an appropriate level of safety. It is important to point out that barricade failure can lead to significant consequences, including endangering the safety of personnel, property damage, and production losses and delays. Filling may take from several days to several months, depending on the size and geometry of the stopes. Water is used as the transport medium to place several types of backfill. Following settlement and consolidation of fill under its own weight soon after placement, excess water drains from the stope through two mechanisms; it can drain through the fill and barricades or by decanting through upper barricades (Rankine, 2006).

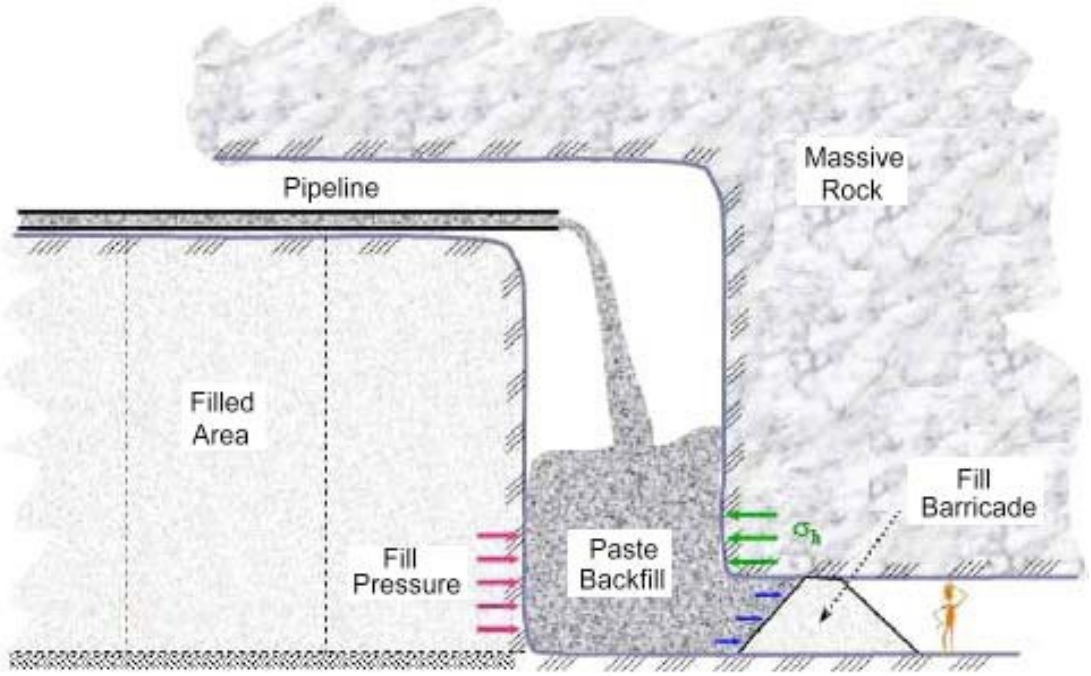

Figure 2-1 Cemented paste backfill placements to underground mines (Yilmaz, 2004)

2.2.2 Main types of cemented backfill

Several types of mine backfills are used to fill stopes, such as sand fill (hydraulic fill), cemented sand fill (cemented hydraulic fill), rock fill, paste backfill and GF. Below is a brief explanation on the main types of mine backfill.

- **(Cemented) Hydraulic fill**

Sandfill, which is also called hydraulic fill, is prepared from concentrator tailings by hydrocyclone treatments to remove the slimes or clay size fraction. Typical hydraulic fill density is around 70% solids by weight and no more than 10% by weight of size fractions less than 10 μm to ensure acceptable permeability of the placed fill (Grice, 1998). Ideally, the hydraulic fill should be free draining to allow removal of water from the stope as soon as possible, and avoid any build up of excess pore water pressure. The advantage of using this method is the simplicity and low cost while the disadvantages are that first, permeable barricades should be designed and constructed to retain backfill and allow free drainage of excess water. These barricades are built with porous concrete and bricks, and take a two man crew between 2-3 shifts to complete (Grice, 1998). Secondly, excess water in the fill should be pumped out of the mine or else it can result in the ponding of water in the stopes which can cause barricade failure.

To overcome the lack of true cohesion of sandfill, various cementing agents are added to the sand mass and the new product is called cemented sandfill (or cemented hydraulic backfill). Cemented sandfill is transported underground as a suspension at about 70% solids by weight. Flow velocities required to maintain homogeneous dispersion of the fill components in the slurry that exceed about 2 m/s (Brady and Brown, 1993). However,

segregation may occur after discharge, with the coarser particles settling close to the discharge point. This leads to a degree of heterogeneity in the fill mass as the result of different local settling rates of coarse and fine particles.

- **Rockfill**

To improve the performance of cemented sandfill or in large stopes when the demand for fill material can exceed the available supply, rockfill or cemented rockfill is used. Rockfill is the waste rock from the surface or underground, typically crushed into a size around 40 mm which can be placed as is or with cemented sandfill. The procedure is done by simultaneously discharging cemented sandfill slurry and rockfill into the stope. The advantage of adding rock to the fill is to treble the tonnage of filling and doubling the volumetric rate, increase the strength performance, and reduce cement consumption to below 2% (Grice, 1998).

- **Cemented Paste Backfill**

To lower the water content of the backfill and improve its strength, CPB is introduced. It is a relatively recent development that has high fines content around 15% by weight passing through a 20 μm sieve. CPB is prepared by mixing tailings with a solid percentage between 70% and 85%, water which can be fresh or mine processed, and a hydraulic binder which is between 3% and 7% by weight. CPB is mixed in a plant located on the surface and then transported by gravity and/or pumping to the underground mine (Figure 2-2). To transport fill material from the surface to the underground stopes, three possible configurations can be used; the gravity/pump system, the gravity system, and the

pump/gravity system (Figure 2-3). It should be noted that each method of transportation has its own advantages. As discussed by Thomas (1979), the gravity/pump system is entirely operated underground, which causes no disruption to surface activities. In addition, the ratio of the vertical to horizontal distance is so favourable that little or no pumping energy is required. The gravity system is another way of transportation that can be used to progressively convert vertical head to horizontal pressure which allows shorter and lighter pipes to be used. Finally, the advantage of using the pump/gravity system is easy installation, inspection and maintenance, with no special underground level requirements and no disruption of the main shaft. As recommended by Paynter and Dodd (1997), prior to pumping, all pipelines and borehole are wetted to prevent moisture from being absorbed by the dry network that would result in the formation of plugs in the circuit.

In order for the CPB to smoothly flow through the pipelines, rheological properties should be obtained. The standard slump test can be used to determine the consistency of the CPB which is widely used due to its simplicity. Slump can be defined as a measure of the drop in height of a material when it is released from a truncated metal cone. As mentioned by Clark (1995), determination of the slump provides a way to characterize a material's consistency that can be related to its transportability. According to Landriault et al. (1997), the ideal slump of the paste must be in a range between 150 mm (6") and 250 mm (10").

For economic reasons as discussed by Paynter and Dodd (1997), a CPB with two different strengths is poured into the stope depending on the position. The first mix at the bottom of the stope generally consists of adding a relatively high binder content to reach a rapid

setting which minimizes horizontal stress over the barricade. The second part occupies most of the stope volume and only needs to carry the necessary strength for final application of the stope. Thus, less binder content is used for this layer. The last layer, which is at the top, has the same binder content as the bottom layer to form the mucking floor and provide strength capable of supporting working equipment.

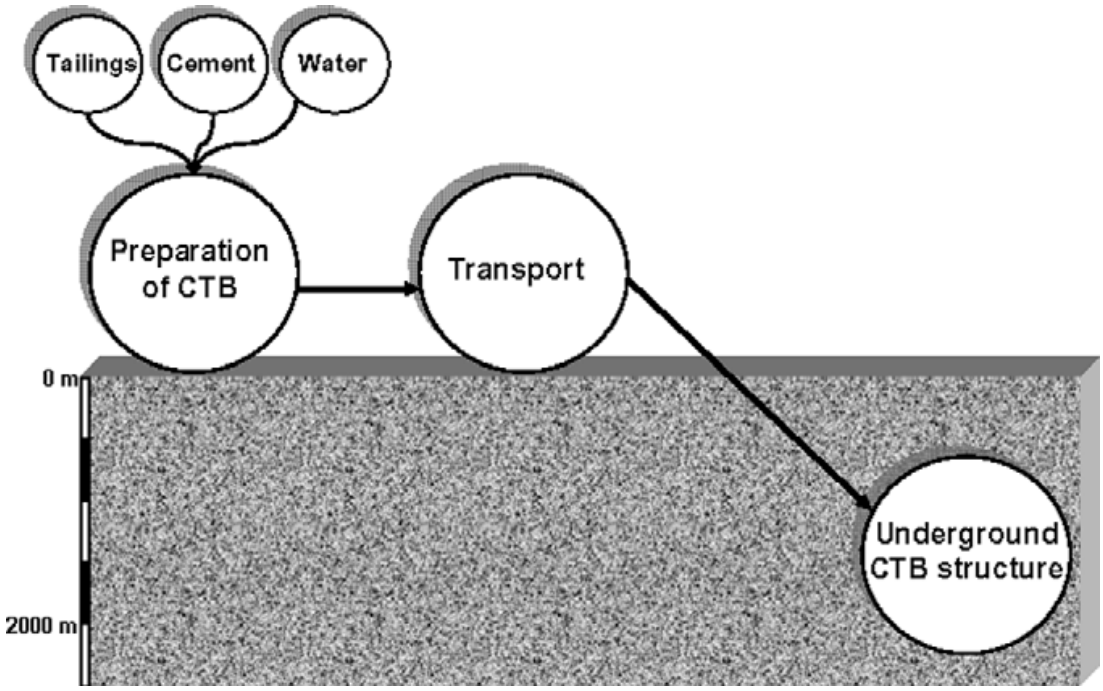

Figure 2-2 Schematic presentation of the different phases of the technology of cemented paste backfill (CPB): preparation, transport and underground placing of the CPB, where it builds CPB structure (Fall et al., 2008)

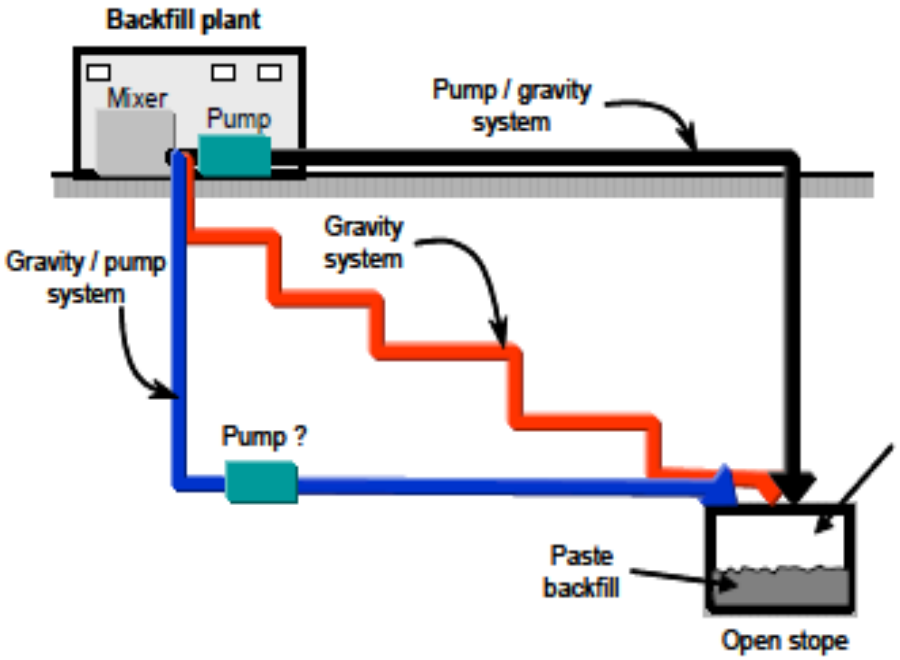

Figure 2-3 Basic configurations for cemented paste backfill distribution systems (Thomas et al., 1979)

The mechanical stability of hardened CPB is considered to be the most important quality factor. The mechanical stability is usually evaluated by using the UCS of the CPB. Nevertheless, the UCS value required for each underground mining operation varies, depending on the application or function of the CPB (Fall and Benzazoua, 2005). When CPB is used to fill voids, underground disposal, or to eliminate the risk of liquefaction, UCS values of 150-300 kPa are used (Bloss, 2002) while the values of the UCS can reach up to 1 MPa when CPB is used in open stoping operations, to maintain stability (free-standing wall faces are exposed during pillar recovery). However, strength values higher than 4 MPa are required when the CPB is used to support a roof (Belem, 2003). In general, the range of the UCS values is between 0.7 and 2 MPa (Celestin, 2008). The permeability

plays an important role in the durability and environmental performance of CPBs (Fall et al., 2009).

Several factors can affect the UCS and permeability values of CPB. The main factors are: binder content, binder type, water/cement ratio, sulphate content and external parameters, such as temperature and curing time, as discussed below.

- **Effect of binder content**

Different types of binding agent are used to prepare the CPB mix; however, the most common one is Portland cement type I (PCI). Admixtures with pozzolanic materials such as fly ash (FA) and ground blast furnace slags (BFS) are also used to reduce the amount of cement in the CPB and then the cost. Hardening of the CPB occurs due to the use of binder. Binder is defined as a reactive material that has the ability to transform into hardened material. This process happens under a chemical reaction which is called hydration, and occurs between cement components (e.g., tricalcium silicate (C_3S), dicalcium silicate (C_2S), and tricalcium aluminate (C_3A)) in the presence of water to form hydration products. Hydration also gives the binder its bonding property (more details are given in Section 2.3). For that, increasing the amount of cement or binder leads to an increase in the CPB compressive strength (Figure 2-4) as well as a decrease in the permeability of the CPB (Figure 2-5). Higher cement content leads to the formation of more cement hydration products, which in turn, leads to refinement of the pore structure and reduction in the porosity (*n)*. As a result, the strength of the cement matrix increases and the permeability decreases. However, even a slight reduction in the cement content leads to considerable

cost savings. Therefore, many studies have been carried out to determine the right amount of cement that is needed to give the required strength.

- **Effect of water-cement ratio (w/c)**

The water-cement (w/c) ratio is known as one of the most valuable factors in controlling paste quality. Water is essential for proper hydration and workability of the mix. A small amount of water is used for hydration; the rest is usually required to pump the CPB to the underground. However, excess water in the CPB affects the porosity of the mix due to an increase in the amount of voids in the hardened matrix. These voids might be filled or partially filled with water or air which reduces the compressive strength and increases the hydraulic conductivity of the CPB. It can be concluded that the relationship between the UCS and w/c ratio is inversely proportioned (Figure 2-4). This relationship is clearly shown in Fall et al. (2008), in which a lower w/c ratio for any given binder proportion or tailing grain size means a higher CPB compressive strength (Figures 2-4 and 2-6) and lower hydraulic conductivity (Figure 2-7) (Fall et al., 2009).

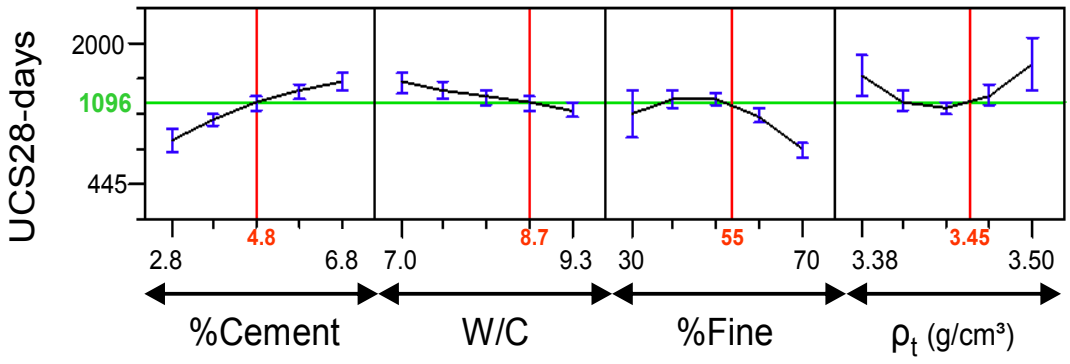

Figure 2-4 Effect of binder content, water-cement ratio, tailings fineness and tailings density on the UCS (kPa) of CPB (Fall et al., 2008).

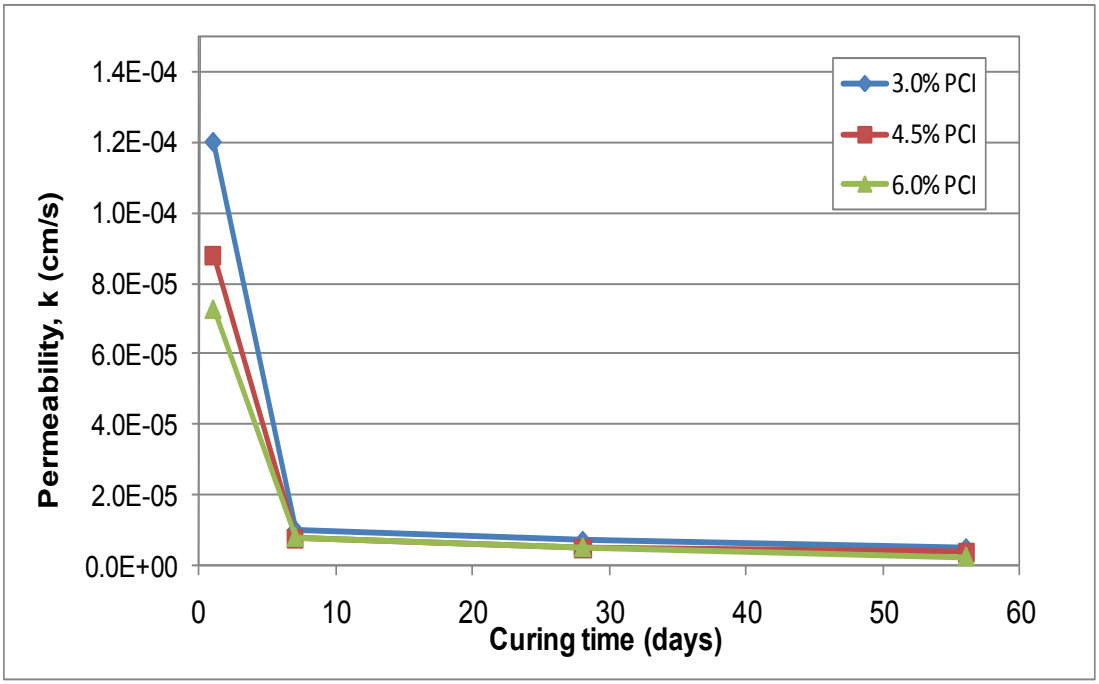

Figure 2-5 Effect of binder content on the permeability of CPB (PCI; slump = 18 cm; SI used) (Fall et al., 2009)

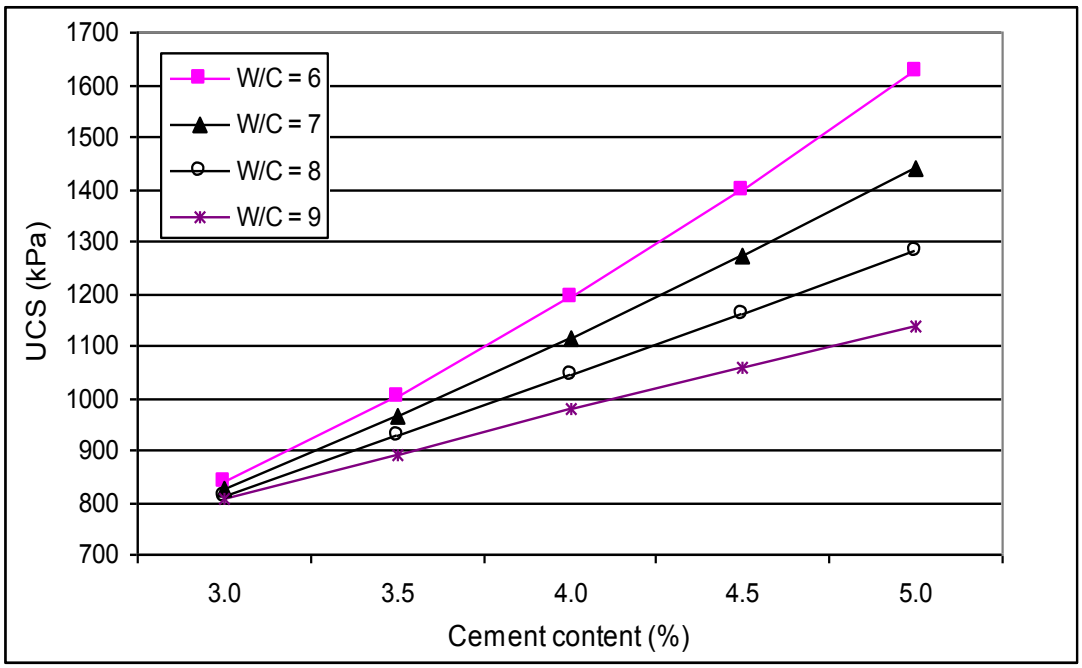

Figure 2-6 Effect of water-cement ratio on UCS 28 days of the CPB for different binder contents (%Fine = 40%; tailings density, ρ_t = 3.459 g/cm3) (Fall et al., 2008).

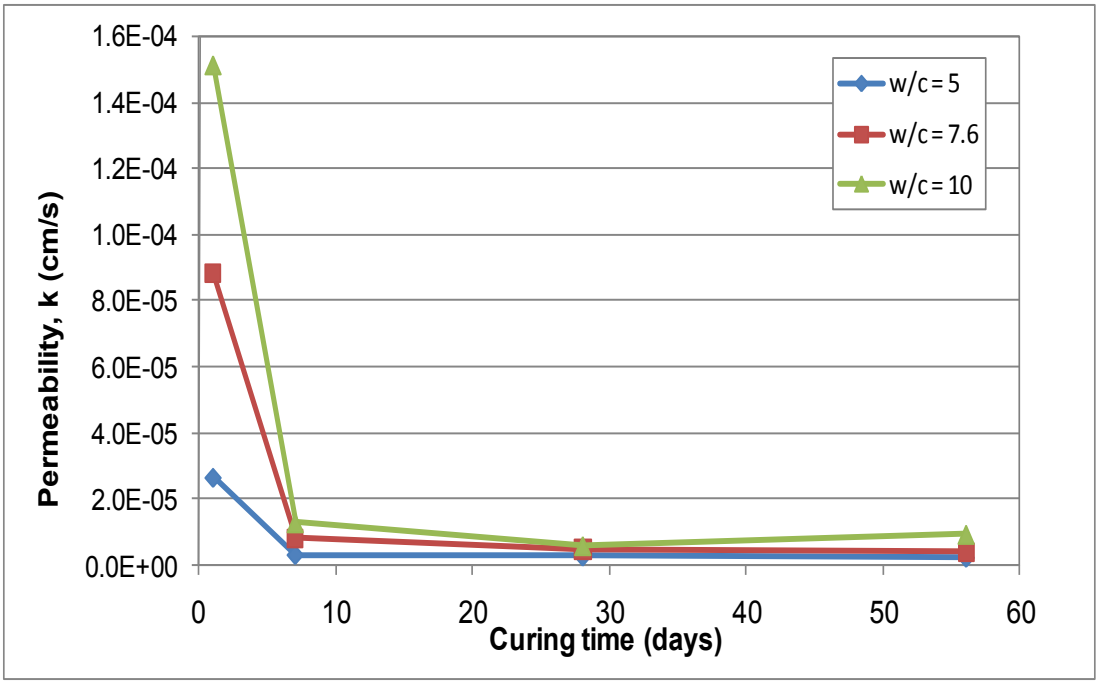

Figure 2-7 Effect of w/c ratio on the permeability of CPB (4.5% PCI; SI used) (Fall et al., 2009)

- **Effect of tailings fineness**

The strength and hydraulic conductivity of CPBs are influenced by the particle size distribution of the tailings. According to Fall et al. (2008), the highest compressive strength is reached when the tailings contain 40-45% fine particles (20 µm) (Figure 2-4). The increase of CPB compressive strength with tailings coarseness is due to the fact that increases in tailings coarseness reduce CPB porosity and the w/c ratio which lead to compressive strength gain. However, the strength of CPBs slightly decreases when tailings coarseness reaches 25-35% fineness (Figure 2-4). On the other hand, a lower hydraulic conductivity is reached when the tailings with a 45% fineness is used (Figure 2-8). Using coarse tailings (20% and 32% fineness) leads to higher hydraulic conductivity. The increase in hydraulic conductivity is attributed to the reduction of the packing density of

the tailings materials and coarsening of the pore structure as the fineness content decreases from 45% to 20% (Fall et al., 2009).

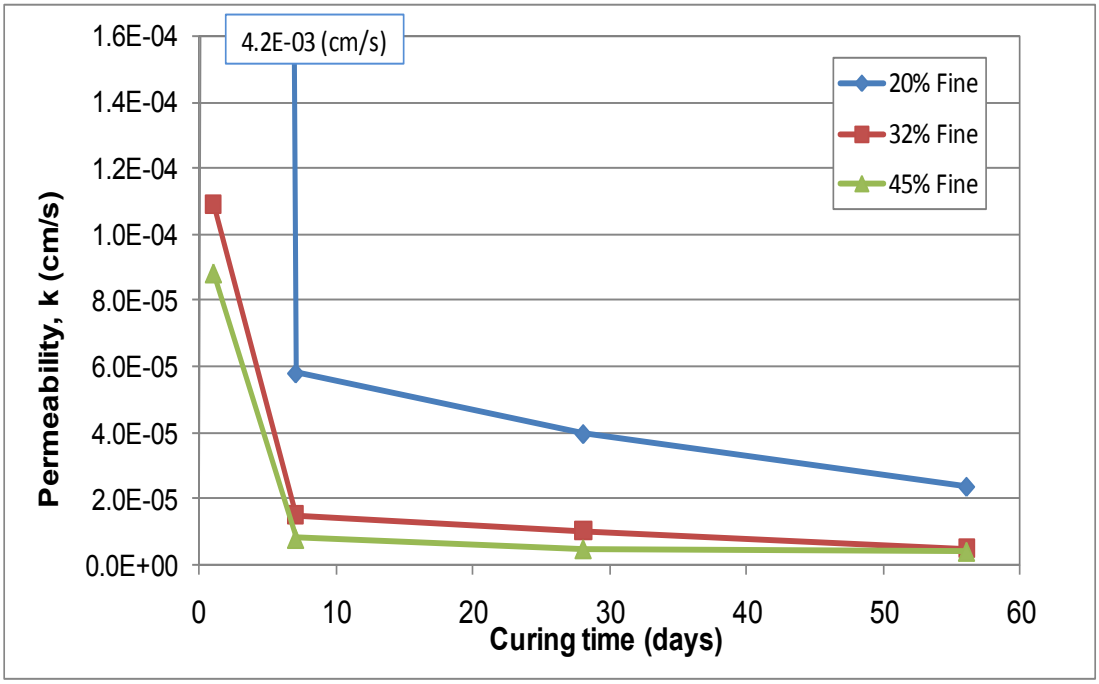

Figure 2-8 Effect of tailings fineness on the permeability of CPB (4.5% PCI; slump = 18 cm; SI used) (Fall et al., 2009)

- **Effect of sulphate content**

The strength and hydraulic conductivity of CPBs are significantly influenced by sulphate. This influence is based on several factors, such as sulphate concentration, curing time, and the amount and chemical composition of the cement (Pokharel, 2008). When the concentrations are relatively low, sulphate contributes to early strength gain and reduces the hydraulic conductivity of the CPB through a decrease of the internal porosity (Figures 2- 9 and 2-10). This is due to the filling of the CPB pores with hydrated cement products and the precipitation of hydrated sulphate as gypsum and/or ettringite which modify the

microstructure of the CPB. Nonetheless, for advanced curing times, the strength of the CPB can be deteriorated, independent of the sulphate concentration and cement proportion (Figure 2-11). The hardened CPB becomes progressively weaker mainly due to the destructive action of expansive minerals that form in the CPB pores (Fall and Benzazzoua, 2005). It is also noticed that for advanced curing times, the hydraulic conductivity of CPB specimens with high initial sulphate concentrations is slightly higher than those with low initial sulphate content or without sulphate (Figure 2-10).

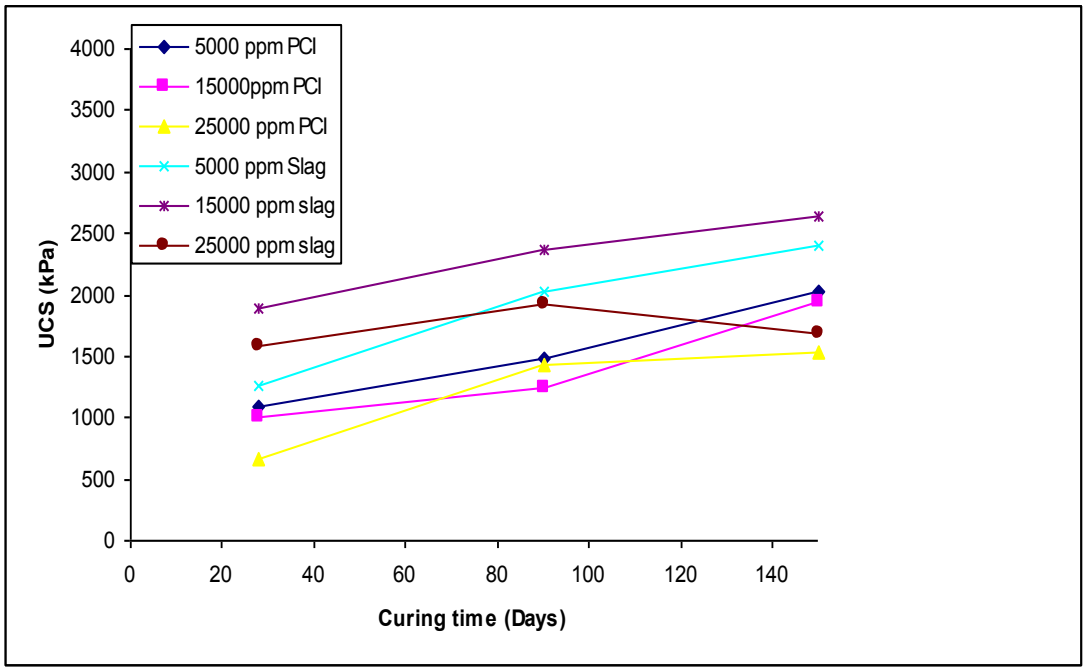

Figure 2-9 Evolution of UCS of CPB with different sulphate concentrations at 20°C at different curing times (Pokharel, 2008)

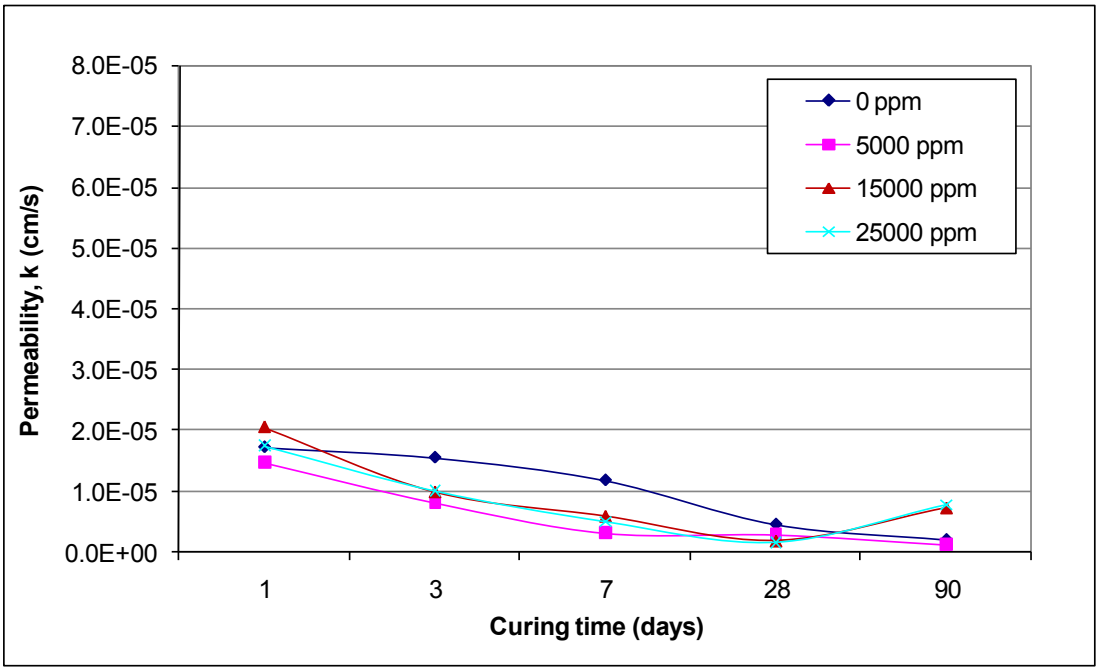

Figure 2-10 Effect of sulphate content on the permeability of CPB (4.5% PCI; slump = 18 cm; SI used) (Fall et al., 2009)

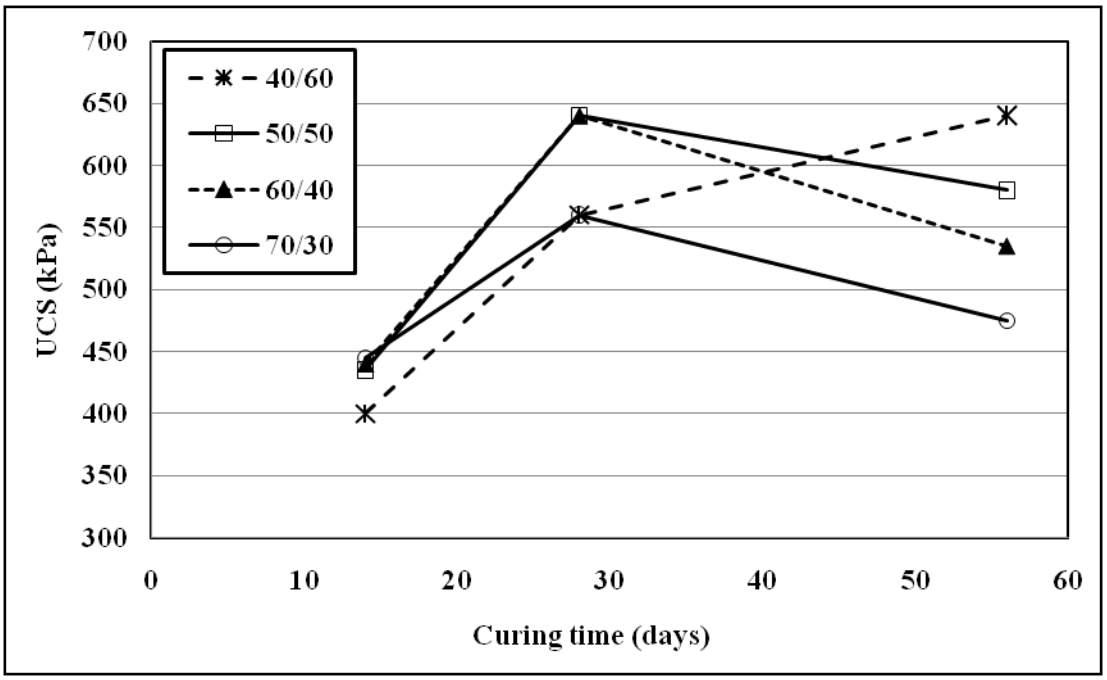

Figure 2-11 Strength development of the paste backfill in relation to the binder ratio for mixing water that contains 2000 ppm sulphate (binder content = 4.5%) (Fall and Benzazzoua, 2005)

- **Effect of temperature and curing time**

Curing temperature has a significant impact on the mechanical properties and saturated hydraulic conductivity of CPBs. It is observed that curing temperature increases the compressive strength of CPBs (Figure 2-12) and decreases hydraulic conductivity (Figure 2-13). A study conducted by Celestin (2008) showed that changes in hydraulic conductivity with curing time are more significant in early age samples, up to 7 days, and changes are more significant at low curing temperatures than at higher curing temperatures. In addition, samples cured at low curing temperatures bear higher hydraulic conductivity despite curing time (Figure 2-13). Higher curing temperatures accelerate the cement hydration process which lead to the formation of more cement hydration products and thus to a reduction in the total porosity, while lower curing temperatures tend to slow down or inhibit the hydration process which lead to coarse pore size distribution. In other words, CPBs cured at high temperatures (up to 35ºC) have lower hydraulic conductivity and therefore higher durability than CPBs cured at lower temperatures. However, it should be emphasized that overly high curing temperatures can lead to a decrease of the strength and coarsening of the pore structure of CPBs in the long term (Fall et al., 2010). This phenomenon of temperature inversion in the compressive strength of cementitious materials is commonly called the "crossover effect" (Alexander and Taplin, 1962). However, studies (e.g., Fall et al., 2010) have shown that that the effect of a high initial curing temperature on the strength development of CPBs is not entirely similar to that on conventional PC concrete and mortar materials.

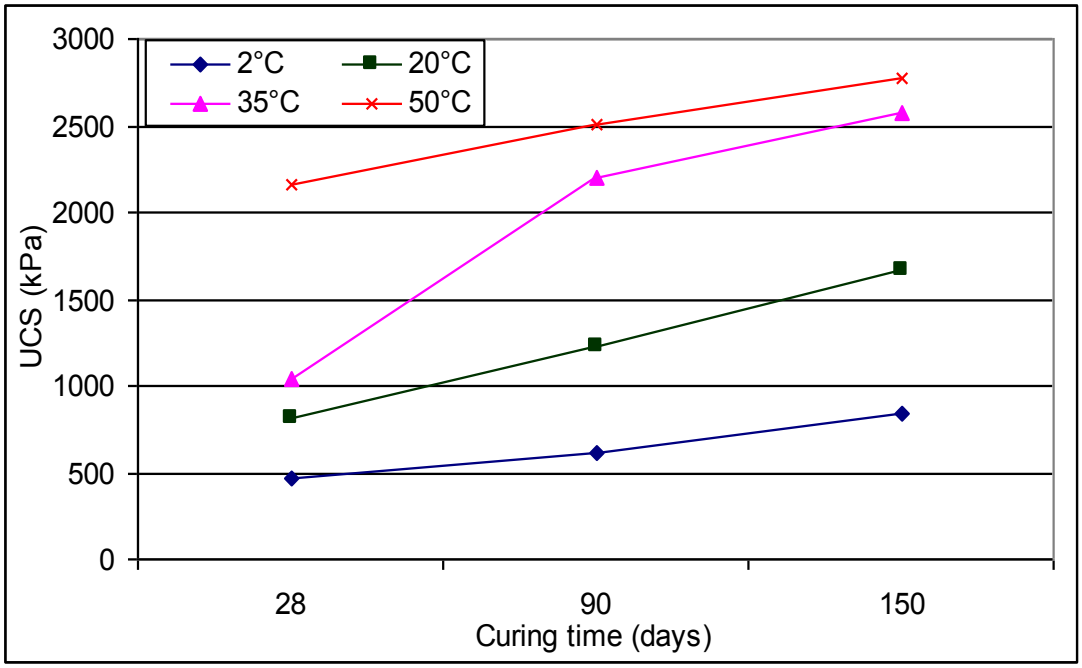

Figure 2-12 Effect of curing temperature on UCS development of CPB with ordinary Portland cement (4.5% cement, slump~ 17 cm) (Fall et al., 2010)

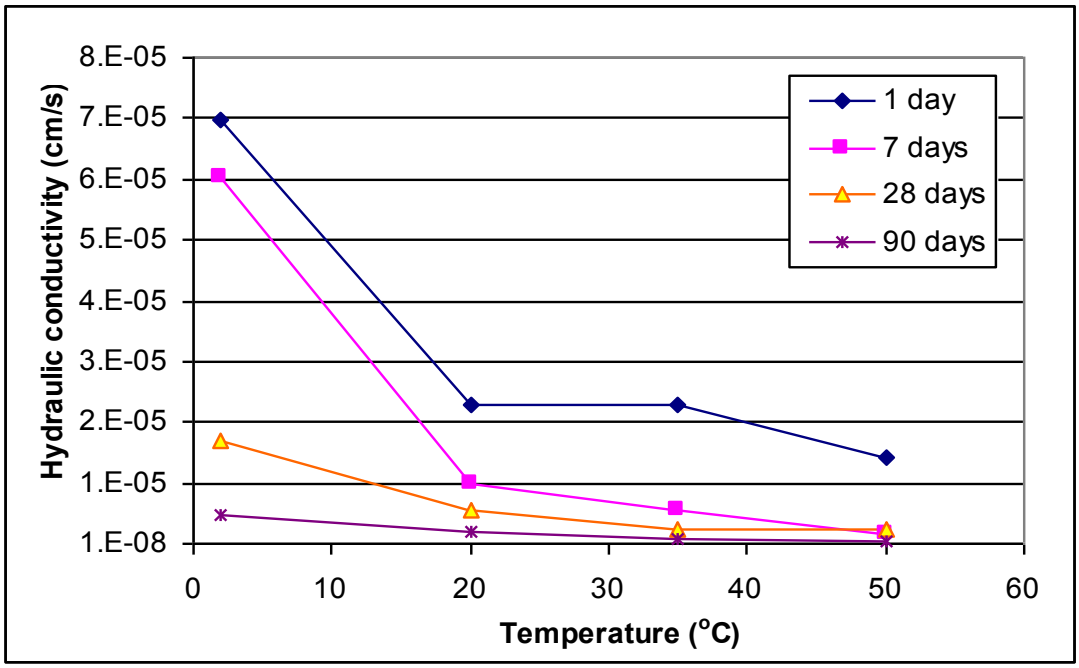

Figure 2-13 Effect of curing temperature and curing time on hydraulic conductivity of CPB (Celestin, 2008)

- **Gelfill**

GF is produced by adding a small amount of sodium silicate, about 0.3-0.4% by weight of solids, to the binder, water and tailings with a solid percentage of 73%. One of the purposes of adding a small quantity of sodium silicate is to reduce the w/c ratio of GF, thereby reducing the quantity of free water in stopes which results in GF strength improvement. It is stated that the (silica sodium) gel has the ability to capture water which results in decreasing the drained water (Hassani et al., 2007). In addition, sodium silicate produces lower hydration heat compared to cement which can lower the threat of thermal cracking in the backfill mass (Hassani et al., 2007). Nevertheless, the GF technique is still new and only a few studies are available to explain the effects of adding sodium silicate on the mechanical and saturated hydraulic properties of GF. It is assumed that the mechanical and hydraulic properties of GF follow the same trend as CPBs (see previous section); however, studies need to be conducted to prove this hypothesis. This will be addressed in this thesis. Furthermore, no information about the impact of silicate sodium on the hydration of GF and its consequence on the performance (mechanical, hydraulic, thermal properties) of GF is available. This issue will also be discussed in this thesis.

As in the case of CPBs, the GF is usually prepared in a plant often located on the mine surface and then transported to the underground stopes (Figure 2). Originally, sodium silicate is added to the GF at the point of stope discharge underground; however, a demonstration made by the Onaping Depth Project showed that sodium silicate could be added to the GF at the backfill plant (Doucet et al., 2007). It is necessary to have a good mixing after the addition of sodium silicate to obtain consistent results and it is expected to be achieved in practice by the turbulent action of transporting the mix through fill lines to

the stope (Doucet et al., 2007). Transport systems and mechanisms similar to those used in CPBs are also used for the transport of GF (Figure 2.3).

Mechanical stability and durability are also considered as the most important quality factors of GF. While mechanical stability is commonly assessed by using the UCS of the GF, permeability is a good indicator of the durability and environmental properties of GF. The UCS values required are similar to those described in the previous section for CPBs. It is important to mention that there are many factors that affect the UCS and permeability of GF, such as variability of tailings chemistry and particle size distribution, variability in chemical components of binder used (Figure 2.14), mixing method, mixing time, and curing conditions (Doucet et al., 2007). According to Doucet et al. (2007), the curing time, tailings particle size distribution, sulphur content, sodium silicate content (Figure 2.14), drain conditions, curing temperature, mixing method, mixing time, binder content, and binder type influence the strength of GF. Some of these factors are discussed below. However, it should be emphasized that there is a paucity of studies on the impact of these factors on GF performance properties. As such, more studies are needed to be done in this field.

- **Effect of curing environment and conditions**

Curing environment is an essential factor that should be considered when evaluating the performance of GF from laboratory results. It is a well known fact that comparisons should only occur between samples that have the same curing conditions when determining the effect of other variables. Results show that samples cured at high temperatures yield higher strength at a given curing time. The results obtained from Doucet et al. (2007) showed an

increase in strength for samples cured at 45ºC compared to those cured at ambient conditions after 28 days. Furthermore, higher strength is observed when samples are allowed to drain during curing time (Doucet et al., 2007). In addition, the difference in strength between drained and undrained samples is dependent on the moisture content of the samples; higher moisture content means larger differences in strength between drained and undrained samples. This is due to the fact that a high percentage of water is trapped in the undrained samples while the extra amount of water can be drained out in the drained samples (Doucet et al., 2007).

- **Effect of sodium silicate content**

The strength of cemented backfill is influenced by the addition of sodium silicate. Furthermore, the gel has the ability to capture water which results in decreasing the drain water (Doucet et al., 2007). A study carried out by Doucet et al. (2007) indicated the capacity of sodium silicate to remove up to 60% of the hydraulic fill drain water which reduces the drain water from 15 m^3/h to 6 m^3/h. This means that the drain water decreases as the sodium silicate content increases. However, increasing the sodium silicate content beyond a certain threshold leads to a reduction in the strength of the GF because the binder becomes starved of water for complete hydration during the curing process (Doucet et al., 2007). Studies (e.g. Doucet et al., 2007) show increasing the dosage of sodium silicate beyond 0.4% by weight of solids reduces the strength of the mix due to an increase in its porosity (*n)*.

Furthermore, when the sodium silicate increases beyond 0.3-0.4%, the benefits of reduced drain water begin to decrease (Doucet et al., 2007). The optimum sodium silicate dosage is

influenced by the binder content and proportions. According to Doucet et al., (2007), the percentage of sodium silicate in GF should be lower than 0.5% by weight of solids (0.3-0.4%). However, experimental works conducted by Hassani et al. (2007) showed that the UCS values for samples with 2% (total binder weight) sodium silicate are greater than the corresponding values for samples prepared with 4% (total binder weight) sodium silicate (Figure 2-14). Furthermore, Hassani et al. (2007) carried out mercury intrusion porosimetery (MIP) analyses and the results showed that samples with 4% sodium silicate have higher porosities and larger pore diameters than similar samples with 2% sodium silicate.

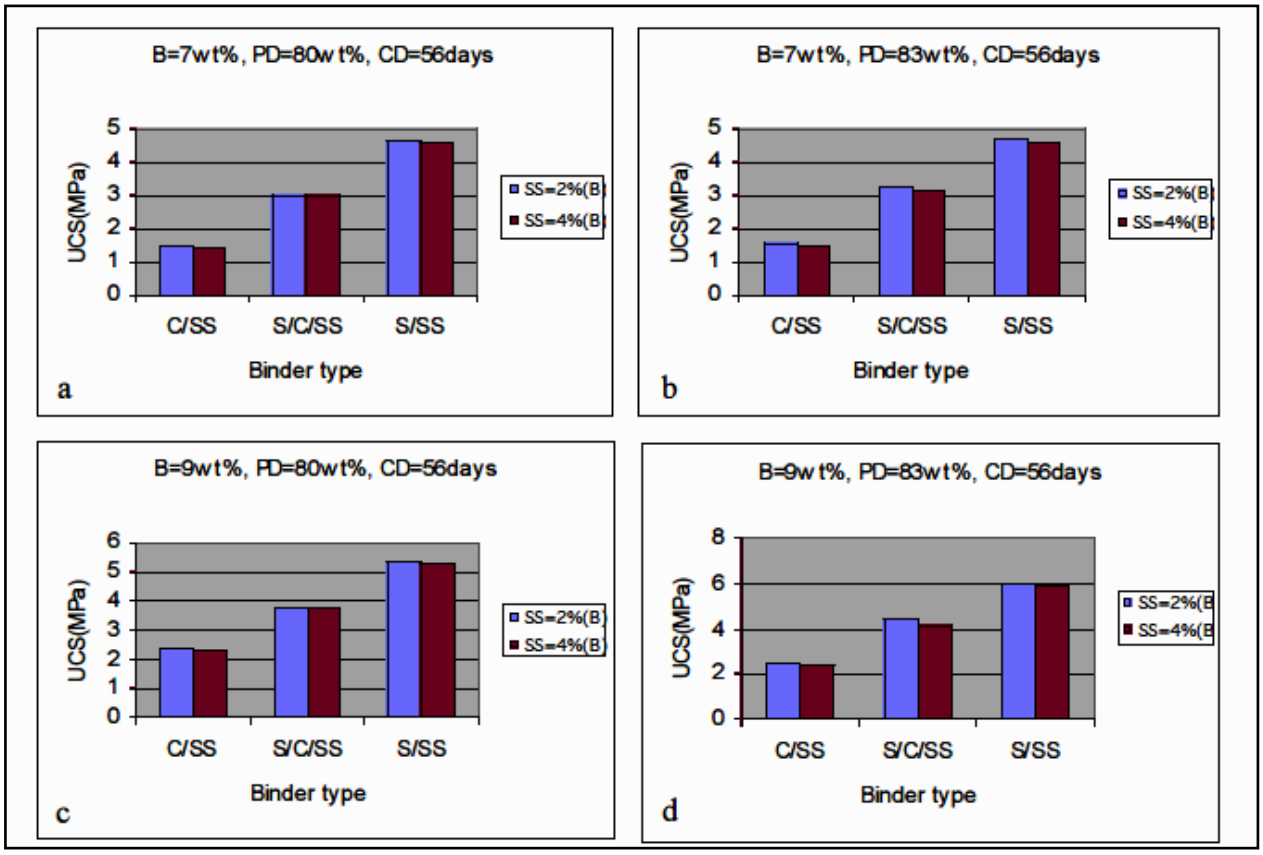

Figure 2-14 Effect of sodium silicate concentration on the mechanical strength (UCS) of sand paste backfill mixtures made with 7 wt% (a, b) and 9 wt% (c, d) binder at 80% and 83 wt% pulp density (Hassani et al., 2007)

- **Mixing effects**

The strength and water retention of GF are affected by the sequence of ingredients added into the mix, mixing method, and mixing time. The best result is achieved by using a typical sequence; tailings, binder and water are mixed first and then followed by addition of the gel, which is also recommended by the supplier of the sodium silicate gel (Doucet et al., 2007). It is also recommended to mix the gel with water before adding it to the mix. On the other hand, different mixing methods result in strength differences. According to Doucet et al. (2007), samples prepared using a mini-loop apparatus yields higher strengths than those prepared using a stand-up propeller mixer. It was observed that samples prepared with a mini-loop apparatus retain more water. Furthermore, a noticeable amount of segregation was observed in the samples prepared with the mixer (Doucet et al., 2007). Finally, the experimental work shows that the first 20 minutes is the optimum mixing time to reach the required strength. Longer mixing times have less effect on GF strength.

2.2.3 Design criteria of cemented backfill

In order for the cemented backfill to be a suitable backfill material, specific static and dynamic requirements should be achieved. The static design requirements are reached when cemented backfill is able to remain stable after vertical faces are exposed, to support the weight of loading equipment and roof, confine the rock mass around the stope, and allow mining underneath the fill. The dynamic requirements are attained when the cemented backfill withstands the effects of close blasting and earthquakes, as summarized by Grice and Bloss (2001). In addition, the geometric boundaries of the fill, such as high and narrow or low and wide, should be taken into account when cemented backfill is

designed. A UCS test is adopted to examine the strength of backfill structures. It is important to mention that the cost of cemented backfill should be considered during the designing. The target is to design an optimal mix in which the cost is minimal, but does not affect the strength of the structures.

In general, the conventional design of backfill is based on standing walls that require a UCS equal to the overburden stress at the bottom of the filled stope. Nevertheless, in many cases, the adjacent rock walls can help support the fill through boundary shear and the arching effect.

The fill rigidity can range between 0.1 and 1.2 GPa, while the rigidity of the ore pillars varies between 20 and 100 GPa. For that, it is assumed that vertical loading will be the result of roof deformation (Figure 2-15) and the design UCS is estimated according to Donavan (1999) by the following relationship:

$$UCS = \left(E_p \frac{\Delta H_p}{H_p} \right) FS \qquad \text{Equation 2-1}$$

where

E_p = pillar modulus of elasticity,

ΔH_p = strata deformation,

H_p = strata initial height, and

FS = factor of safety.

However, when the stope walls deform before backfilling, the maximum load will never approach the total weight of the deformed overlying strata and the design of the UCS can be estimated by the following relationship (Donavan, 1999):

$$UCS_{design} = k(\gamma_p \times H_p)FS \qquad \text{Equation 2-2}$$

where

k = scaling factor (vary from 0.25 to 0.5), and

γ_p = strata unit weight

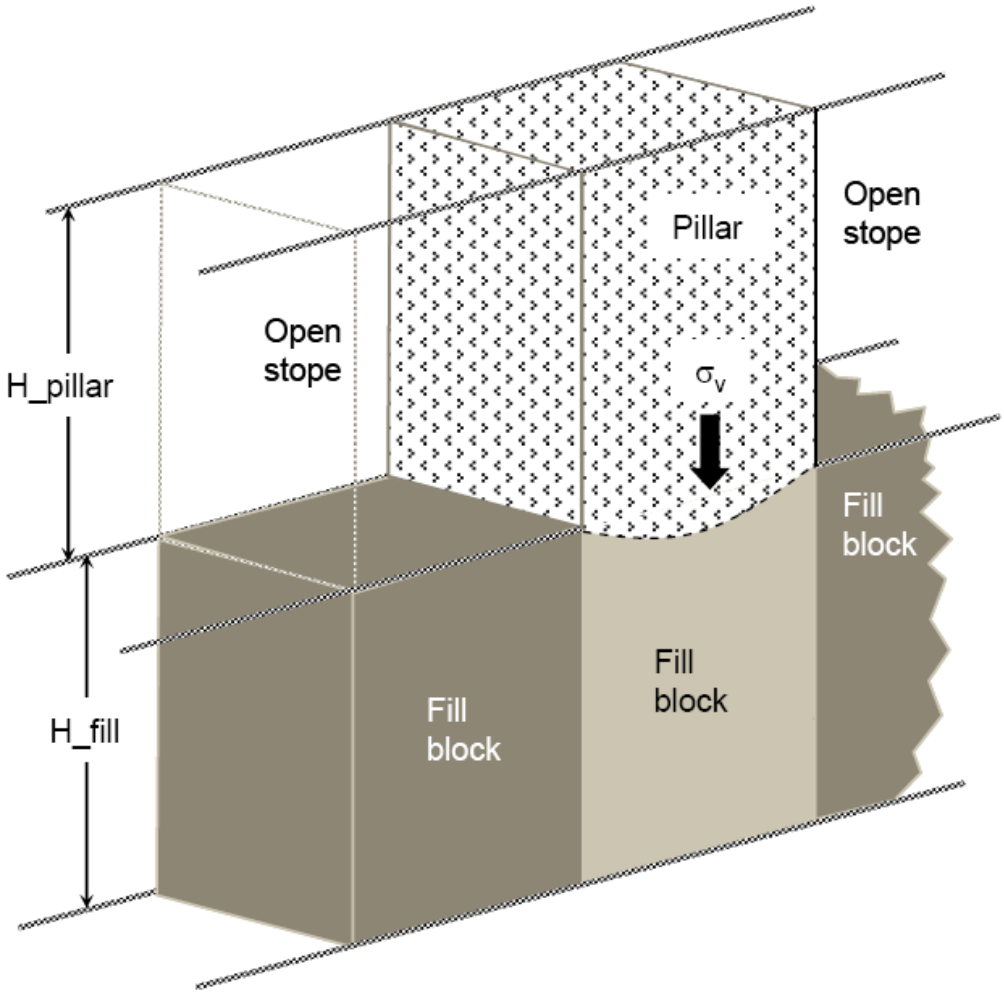

Figure 2-15 Deformation of the backfill block under vertical loading (Belem, 2004)

During pillar recovery, the fill can be exposed to more than two faces. This means that the walls that confine the fill are removed and the fill block is subjected to gravity loading (Belem and Benzaazoua, 2004). The design UCS can be estimated by this relationship:

$$UCS_{design} = (\gamma_f H_f) FS \qquad \text{Equation 2-3}$$

where

γ_f = fill bulk weight,

H_f = fill height, and

FS = factor of safety.

In the case of a narrowly exposed fill face, the arching is taken into account when the UCS is designed:

$$USC_{design} = \frac{1.25B}{2K \times \tan\phi}\left(\gamma - \frac{2C}{B}\right) \times \left[1 - \exp\left(-\frac{2H \times K \times \tan\phi}{B}\right)\right] FS \qquad \text{Equation 2-4}$$

where

B = width of the stope,

C = fill cohesion strength,

ϕ = fill internal friction angle, and

K = fill pressure coefficient and can be determined using Terzaghi's earth pressure coefficient.

$$K = \frac{1 + \sin^2\phi}{\cos^2\phi + 4\tan^2\phi} = \frac{1}{1 + 2\tan^2\phi} \qquad \text{Equation 2-5}$$

By assuming there is a friction between the fill and two stope walls, the design UCS proposed by Mitchell (1993) is given by:

$$UCS_{design} = \left(\frac{\gamma \times L - 2C}{L}\right) \times \left[1 - \frac{B}{2}\tan\left(45 + \frac{\phi}{2}\right)\right] \times \sin\left(45 + \frac{\phi}{2}\right) FS \qquad \text{Equation 2-6}$$

When no friction develops between the stopes and the fill, the design UCS is given by:

$$UCS_{design} = \left(\frac{\gamma \times L \times H}{L + H}\right) FS \qquad \text{Equation 2-7}$$

where

L = strike length of stope, and

H = total height of fill.

When the fill is used for ground support or working platform, the strength is determined by using calculations similar to the bearing capacity method for shallow foundations. Craig (1995) proposed the following equation which corresponds to the modification of the Terzaghi bearing capacity.

$$Q_f = 0.4\gamma B N_\gamma + 1.2 C N_c \qquad \text{Equation 2-8}$$

where

N_γ and N_c = bearing capacity factors,

B = width of square foot in at surface contact, and

C = fill cohesive strength.

2.3 Background on binder hydration and some characteristics of the binder

2.3.1 Binder hydration

Since two types of binder (Portland cement and slag) are used in this study, background information on the hydration of these two binders is provided in the next section. This will help provide a better understanding of the results presented in this thesis.

- Portland cement hydration mechanism

The raw materials used to manufacture PC are lime, silica, alumina, and iron oxide. These compounds interact with each other in the kiln to form a series of more complex products which shape into balls called clinker.

The major constituents of cement are C_3S, C_2S, C_3A, and tetracalcium aluminoferrite (C_4AF). According to Neville (1995), C_3S occupies more than 50% of the total PC and forms as small, equidimensional colourless grains. On the other hand, C_2S has rounded shape grains and occupies almost 20% of the total mass of the PC. C_3A forms rectangular crystals and comprises about 3-8% of the total PC while C_4AF is a solid solution that ranges from C_2F to C_6A_2F. Minor components of the clinker are magnesium oxide (MgO), titanium dioxide (TiO_2), manganese oxide (Mn_2O_3), potassium oxide (K_2O), and sodium oxide (Na_2O). Gypsum is also added to clinker before grinding to control the rate of hydration of aluminates which helps to avoid flash set.

In the presence of water, these components react to form hydration products (e.g. calcium silicate hydrates, C-S-H; calcium hydroxide, CH; tricalcium aluminate hydrate, C_3AH_6), and calcium sulphoaluminate (ettringite) which produce a firm and hard mass with time. Table 2-1 shows a summary of the hydration of cement compounds.

C-S-H is an amorphous, poorly crystalline gel which is the final product of the hydration of both C_3S and C_2S. The reaction of hydration can be written as shown below (Skalny et al., 2002):

$$2C_3S + 11H \rightarrow C_3S_2H_8(CSH) + 3CH + Heat$$

$$2C_2S + 9H \rightarrow C_3S_2H_8(CSH) + CH + Heat$$

On the other hand, the C_3AH_6 forms a prismatic dark interstitial material. The reaction of pure C_3A with water is very violent and leads to immediate stiffening of the paste, known as flash set. Gypsum ($CaSO_4$) is added to slow down the reaction. The outcomes of the reaction are ettringite and monosulfoaluminate, and the reaction can be written as follows (Skalny et al., 2002):

$$C_3A + 3C\bar{S}H_2 + 26H \rightarrow C_6A\bar{S}_3H_{32} + Heat$$

$$2C_3A + C_6A\bar{S}_3H_{32} + 4H \rightarrow 3C_4A\bar{S}H_{12} + Heat$$

where

$3C\bar{S}H_2$ gypsum,

$C_6A\bar{S}_3H_{32}$ ettringite, and

$3C_4A\bar{S}H_{12}$ monosulfoaluminate.

The amount of gypsum added to the cement should be monitored because an excess of gypsum can lead to expansion and disruption of the set cement paste (sulphate attack) (Skalny et al., 2002).

$$C_4A\bar{S}H_{12} + 2C\bar{S}H_2 + 16H \rightarrow C_6A\bar{S}_3H_{32} + Heat$$

Table 2-1 Summary of hydration of cement compounds (CVG 6303)

Compound	Reaction rate	Strength	Setting	Heat liberated
C_3S	Moderate	High	Low	High
C_2S	Slow	Low initially, high later	Low	Low
C_3A	Fast	Low	High	Very high
C_4AF	Moderate	Low	Moderate	Moderate

- Hydration mechanism of slag

The hydration mechanism of slag is not similar to that of PC. When slag comes into contact with water, initial hydration is much slower than PC mixed with water. The latent hydraulicity of slag needs to be activated by activators, such as the solutions of alkalis or sulphates (Regourd, 1998). The hydration of PC produces calcium lime (liberated by the hydration of the clinker silicates) and sulphate (from the gypsum). Thus, a mixture of slag and PC is a group of binders with good reactivity and performance. The hydration of slag in the presence of PC depends upon the breakdown and dissolution of the glassy slag structure by hydroxyl ions released during the hydration of PC and also the alkali content in cement. CH is consumed during the hydration of slag which results in the formation of additional C-S-H. Several authors (e.g. Regourd, 1980; Vanden Boschm, 1980; and Roy and Idorn, 1982**)** have indicated that in general, the hydration of slag blended with PC, in normal stages, is a two-stage reaction. Initially and during early hydration, the predominant reaction is with alkali hydroxide, but subsequent reactions are mainly with CH (Mantel 1994). The hydration and hardening step of slag cement can be explained as follows: first, C–S–H gel and ettringite form from the hydration of the clinker minerals and liberate CH.

This ensures that the CH not only maintains a certain pH value in the solution to activate the hydration of slag, but also reacts with all ions of slag separation to form new hydration products (Vanden Bosc, 1980).

2.3.2 Calcium silicate hydrate (C-S-H)

C-S-H is not a well-crystallized material (amorphous) with extremely small particles and high surface area (400 m^2/g). It has a layer structure similar to some clay minerals, such as montmorillonite and halloysite. C-S-H is largely responsible for the strength of the hcp and occupies around 50-60% of the volume of the completely hydrated products. The chemical composition of C-S-H is not well defined because the ratio of the oxides changes due to several factors, such as the change in α, w/c ratio, and temperature. The C/S ratio varies from 1.5-2; different test methods to measure this ratio yield different results. However, at the end of hydration, it corresponds to the formula $C_3S_2H_3$ (Neville, 1995).

2.3.3 Pore structure of the hardened cement paste

The mechanical properties of hcp depend on the physical structure of the hydration products more than on the chemical composition of the hydrated cement (Neville, 1995). For that, familiarity with the physical properties of the cement gel is indispensable.

The hardened paste consists of very poorly crystallized hydrates of different compounds of C-S-H, crystals of CH, some minor components, unhydrated cement, and the voids filled with water in fresh paste. All the aforesaid components are referred to as a gel. The voids are divided into capillary pores and gel pores (within the gel itself). The diameter of gel pores is about 3 nm while the capillary pores are larger by one or two orders of magnitude (Neville, 1995).

Since hydration products are colloidal (the ratio of C-S-H to $Ca(OH)_2$ being 7:2 by mass), during hydration, the surface area of the solid phase enormously increases and large amounts of free water become adsorbed in the surface (Neville, 1995).

2.3.4 State of water in hardened Portland cement pastes

There are three states of water in the hcp (Figure 2-16);

- capillary water which contains free water when the capillary pores are greater than 50 nm and water held by capillary tension with capillary pores between 5-50 nm. The capillary pores are emptied when the ambient RH falls below about 45% (Neville, 1995);
- gel water that is divided into adsorbed water when it is held by the surface force of the gel particles (removal of this water causes shrinkage when RH is less than 30%) and interlayer water when it is held between the surfaces of the C-S-H planes which can be lost only upon strong drying (RH < 11%) and leads to considerable shrinkage of the C-S-H structure (CVG 6303); and
- chemically combined water. This is non-evaporable water, which can be lost only when the hydration products decompose.

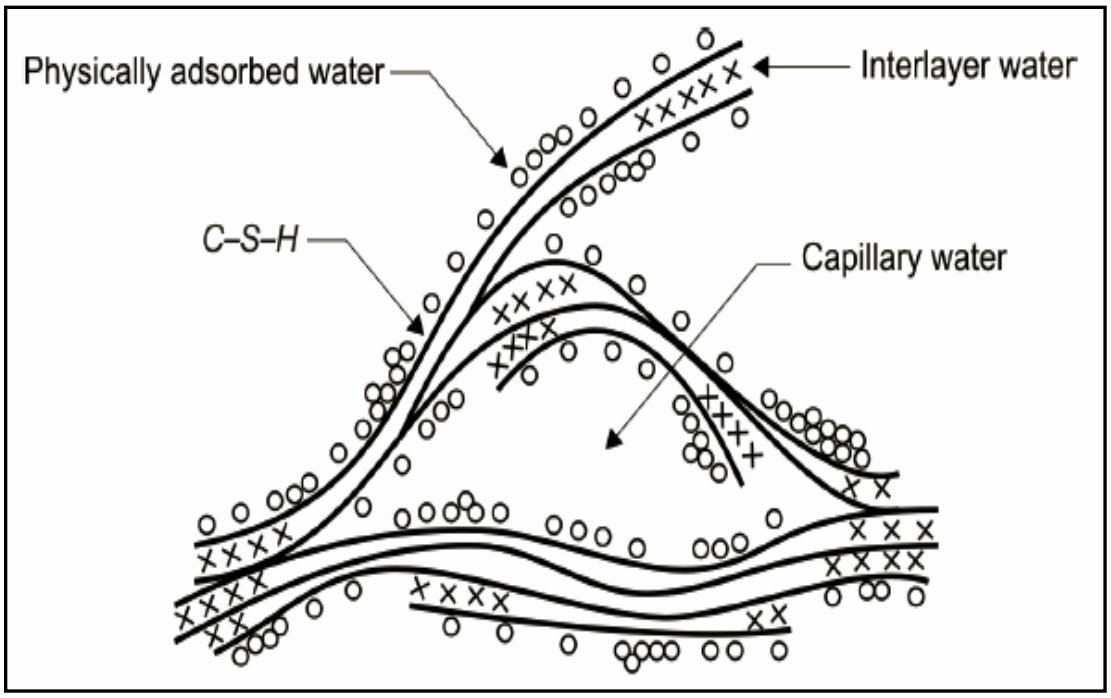

Figure 2-16 Feldman-Sereda model of C-S-H structure (Feldman and Sereda, 1968)

2.3.5 Diffusion mechanisms of water in hardened cement paste

Diffusion mechanisms are influenced by the pore structure of the hcp. Three main diffusion mechanisms can occur in cemented-based material.

- **Molecular diffusion (in pores 50 nm-10 µm = capillary pores)**

When the RH level is low in the pores, the adsorptive force of the pore wall captures only one layer of water molecules. As the humidity increases, the number of layers adsorbed by the pore wall is increased. As a result, the space available to vapor in the macropore decreases, also the force that acts on the water molecules decreases i.e. decrease of diffusion resistance. When RH reaches a certain threshold, the adsorbed water will form a meniscus. Then processes of condensation and evaporation which occur at the neck will accelerate the diffusion (Figure 2-17).

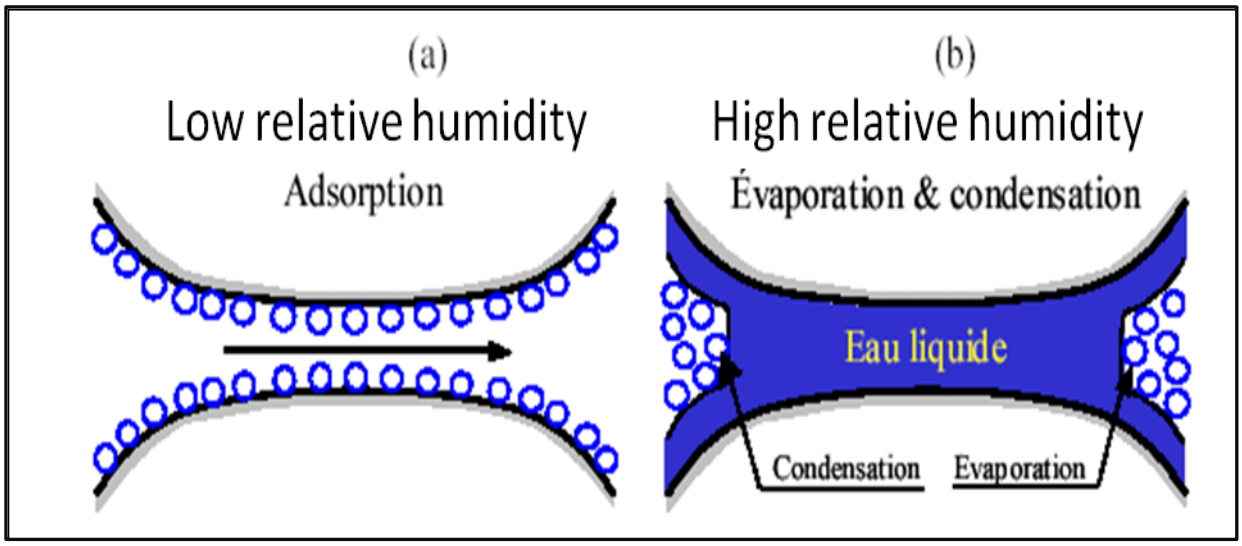

Figure 2-17 Molecular diffusion mechanisms at different humidity levels (Xi et al. 1994)

- **Knudsen diffusion (in nanopores < 50 nm)**

The nanopores represent a large portion of pores in the hcp. In these small pores, the collisions between the water molecules and against pore walls are the main source of diffusion resistance (Figure 2-18). When the pores are small, resistance is higher and thereby, there is less diffusivity.

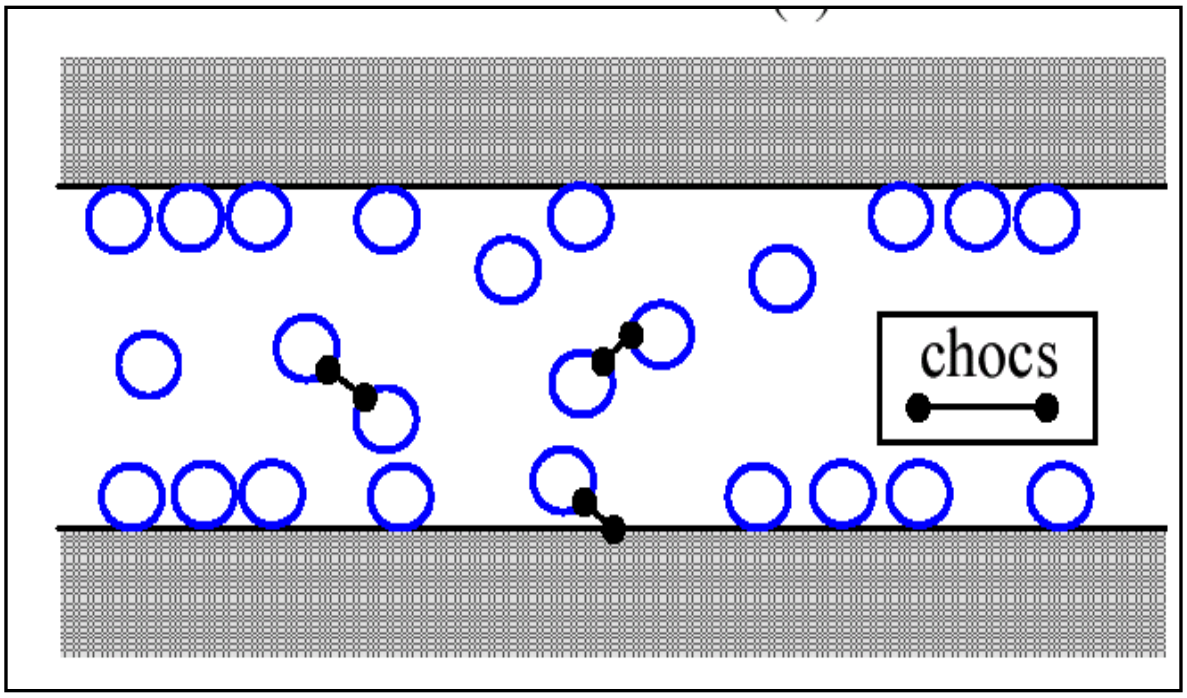

Figure 2-18 Knudsen diffusion mechanisms (Xi et al., 1994)

- **Surface diffusion (in nanopores < 50 nm)**

This mechanism occurs in low RH when water molecules are totally adsorbed by the pore surface. The water molecules are unable to escape the adsorptive force of the pore surface. This diffusion process is characterized by the jump of the molecules between adsorption sites (Figure 2-19). Therefore, surface diffusion has greater resistance to transport than Knudsen diffusion.

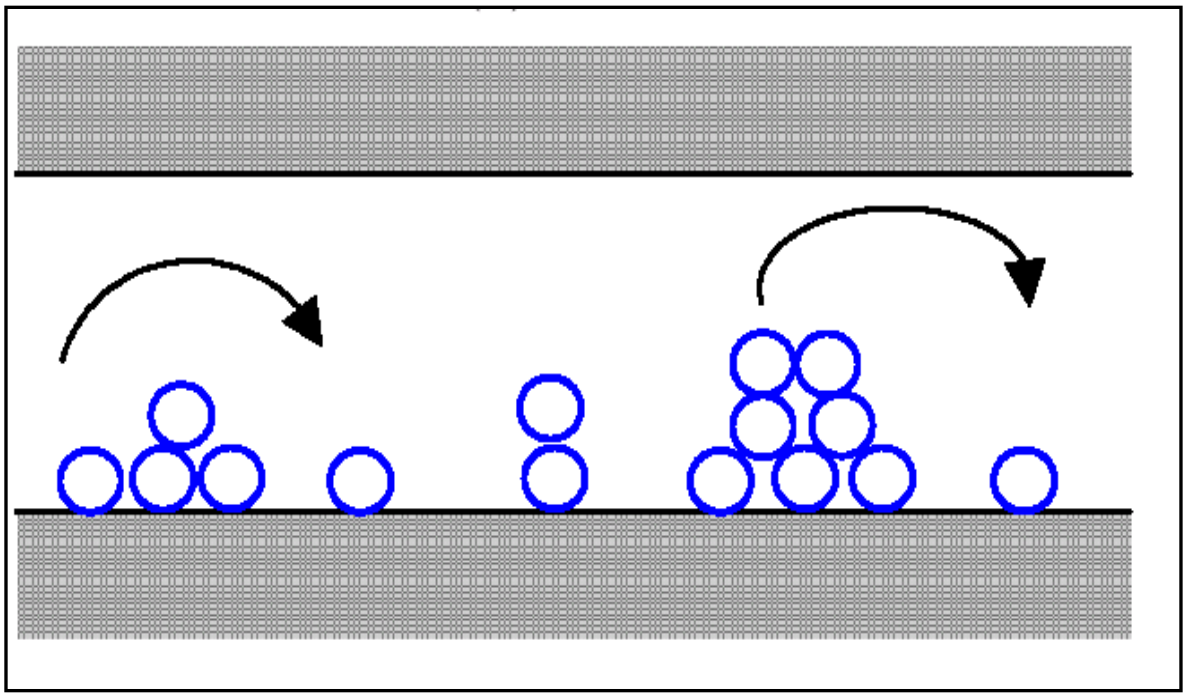

Figure 2-19 Surface diffusion mechanisms (Xi et al. 1994)

2.4 Unsaturated hydraulic properties of porous media and methods to determine them

The two fluid phases of unsaturated porous media can be commonly classified into water and air. The flow of water through an unsaturated porous media has been explained using several concepts. For instance, water content, matrix suction, and hydraulic head gradients have all been considered as driving potentials. However, the most appropriate concept to define flow as a fundamental driving potential is the hydraulic head gradient, which is a combination of the pressure and elevation gradients (Fredlund and Rahardjo, 1993).

Darcy's law is commonly used to describe the flow of water in a saturated porous media. It is also applied to the flow of water in unsaturated porous media (Fredlund and Rahardjo, 1993). The coefficient of permeability is relatively constant for a specific saturated porous

media. Nonetheless, the coefficient of permeability of unsaturated porous media cannot be assumed to be constant. It is a function of the water content or matrix suction gradient.

The second phase of fluid that can flow through an unsaturated porous media is air. This phase can be found in two forms, continuous air phase and occluded air bubble. The flow of air in the continuous phase form is governed by concentration or pressure gradient. The latter is considered to be the only driving potential for the air phase (Fredlund and Rahardjo, 1993). Fick's and Darcy's laws have been used to describe the flow of air through a porous media.

Saturated and unsaturated hydraulic conductivities are used to determine the transportation of fluids through porous media. The unsaturated hydraulic conductivity of porous media is determined using the water retention curve (WRC) and the saturated hydraulic conductivity. WRC is the most widely used method for characterizing hydraulic properties of unsaturated porous media.

2.4.1 Water retention curve (WRC)

The WRC, which is also called the soil-water characteristic curve (SWCC) if the porous medium is soil, is defined as the relationship between water content and suction for soil (Fredlund and Xing, 1994). Water content is the ratio of the weight of water to the weight of solids (Budhu, 2000). In soil science, volumetric water content, θ, is most commonly used. In geotechnical engineering practices, gravimetric water content, w, which is the ratio of the mass of water to the mass of solids, is most commonly used. The degree of saturation, S, is another term commonly used to indicate the percentage of the voids that are filled with water (Fredlund and Xing, 1994). However, it is suggested that the term

WRC is used to represent the relationship between the volumetric water content and matrix suction. The suction may be matrix suction ($u_a - u_w$ where u_a is the pore air pressure and u_w is the pore water pressure) or total suction (matrix plus osmotic suction). Figure 2-20 shows the general features of the desorption (drying) and adsorption (wetting) branches of a WRC. The most critical point on the curve is the air entry value (AEV) (bubbling pressure), which is the matrix suction where air starts to enter the largest pores in the porous media. Another key characteristic of the curve is the residual water content which is the water content where a large suction change is required to remove additional water from the porous media.

The WRC can be used as a tool to predict the unsaturated hydraulic conductivity of porous media. Figure 2-21 illustrates the relationship between the WRC and the coefficient of permeability function for the unsaturated portion of a porous media profile.

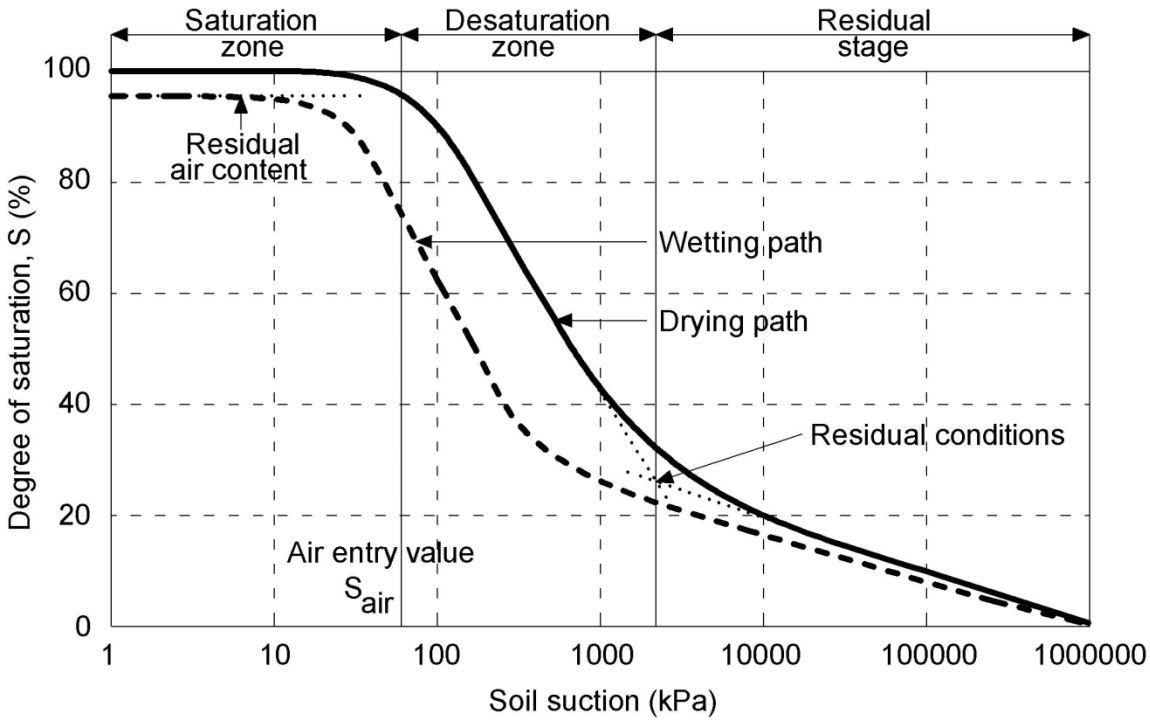

Figure 2-20 General feature of a water retention curve (Tsiampousi et al., 2010)

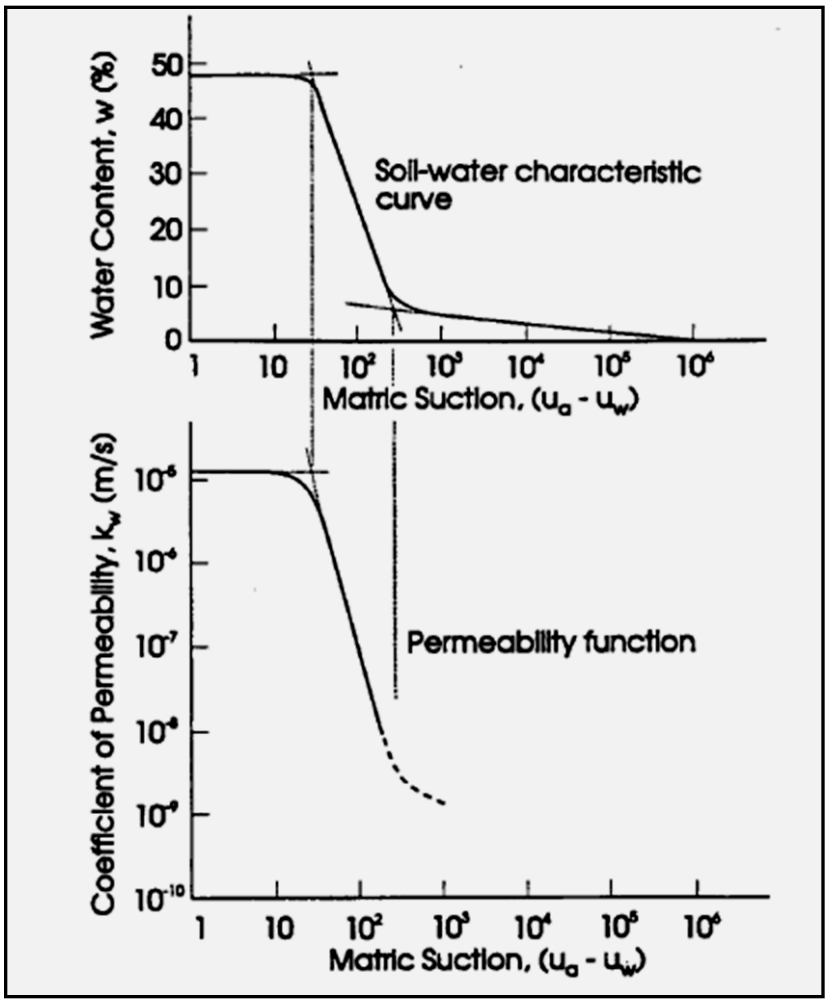

Figure 2-21 Visualization of the relationship between the coefficient of permeability function and the water retention curve (Murray, 1997)

Numerous empirical equations have been proposed to simulate the WRC. Among all of them, the one proposed by Fredlund and Xing (1994) (Equation 5-5) best fits the WRC (Murray, 1997).

Furthermore, the WRC can be measured in the laboratory. The measurement of suction is becoming increasingly a routine for engineering work that deals with unsaturated porous media. Various devices have been developed to measure the matrix or total suction in the laboratory and field. The most commonly used methods available for measurement of porous media suction and their suitability or unsuitability for the determination of the WRC of GF will be discussed below.

- **Psychrometers**

Psychrometers can be used to measure the total suction of a porous media by measuring the RH in the air phase of soil pores or the region near the soil. Psychrometers are useful for measuring high suctions in soils within a range between 400-8000 kPa in the field. However, psychrometers show low sensitivity in low suction ranges and their sensitivities deteriorate with time, and the results are insignificant when there are even small fluctuations in temperature. This could affect the reliability of the results from the tests on GF.

- **Filter paper**

The filter paper method can be used to measure either the total or matrix suction of a porous media. The method is based on the assumption that filter paper can come to equilibrium with unsaturated porous media specimens that have a specific value of suction through water exchange between the soil and the filter paper in a liquid or vapour form. The filter paper technique is a convenient and economical method to measure the total suction both in the laboratory and the field with a reasonable degree of accuracy. However,

the measurements must be performed with extreme care. The results can be significantly affected by small delays. For example, a delay of 1 min results in an increase in the measured suction of about 10% (Navaneethan et al., 2004). Furthermore, due to the cemented nature (hard material) of GF, filter paper will be not appropriate for the determination of the WRC of GF.

- **Tensiometers**

A tensiometer measures negative pore-water pressure in a porous media in a range of 0 to 90 kPa. It consists of a high air entry porous ceramic cup connected to a pressure measuring device through a small bore tube. The tube is made of plastic material to avoid heat loss and corrosion. The tensiometer can be used to measure the matrix suction of unsaturated soil in the laboratory and the field. There is a difficulty associated with using a tensiometer as it is not accurate after 70 kPa because of cavitations and air diffusion through the ceramic cup. The tensiometer is therefore appropriate for the monitoring and measurement of the matrix suction within the GF for a low suction range.

- **Null type plate pressure (axis translation)**

A null pressure plate apparatus can be used to measure the matrix suction of an unsaturated porous media specimen directly in a laboratory using the axis translation technique with reasonable success and accuracy. It can be used to measure matrix suction up to 1500 kPa. The technique has a few limitations; air diffusion through the disk, water loss from the specimen, and secondary consolidation. Due to the relatively lengthy time needed to measure the suction, this technique will not be appropriate to determine the WRC of the

hydrating GF. The same argument applies for the apparatuses described below, i.e. the tempe pressure cell apparatus and volumetric pressure plate extractor.

- **Tempe pressure cell apparatus**

The tempe pressure cell is commonly used for matrix suction up to 100 kPa. It operates on the same principle as the pressure plate apparatus.

- **Volumetric pressure plate extractor**

The maximum amount of matrix suction that can be attained with the volumetric pressure plate extractor is 200 kPa. This apparatus can be used to study the hysteresis of the WRCs associated with the drying and wetting of porous media. The drying and wetting processes are performed on the same soil specimen. The volumetric pressure plate extractor has been used to measure the coefficient of permeability in unsaturated porous media.

- **Thermal conductivity sensor**

The K sensor is a promising device for laboratory measurements and long-term in situ monitoring of porous media suction (Fredlund and Rahardjo, 1993). The K of soil increases with an increasing water content. However, different porous media require different calibrations in order to relate the K measurements to the water content. This makes the K sensor inappropriate for the determination of the WRC of hydrating GF.

- **Saline solution method**

The range of the suction that is measured using this method is between 3 MPa and 1000 MPa. In other words, the saline solution method is used to measure high suction ranges. It is an indirect method to measure the suction from the RH by using the Kelvin equation (2-9). The procedure is done by placing samples in desiccators that contain a salt solution with a known RH, and the samples are supported by a rigid grid above the salt solution. Saturated salt solutions are generally used in the saline solution method (Tang and Cui, 2005). The advantage of using a saturated solution is that the molar fraction of water in a solution does not change with humidity exchanges between the liquid and gaseous phases. The imposed suction which is related to the molar fraction of water is therefore maintained constant (Tang and Cui, 2005). However, the time that is taken by samples to reach equilibrium is about one to two months. From the information presented above, it can be concluded that the saline solution is a suitable method to determine the WRC of hardened GF, since it is known that hardened cemented backfill can show high suction values.

$$\psi = -\frac{RT}{v_{wo} w_v} \ln(RH) \qquad \text{Equation 2-9}$$

where

ψ = total suction (kPa)

R = universal (molar) gas constant [8.31432 J/mol K]

T = absolute temperature [273.16 + t˚ (K)]

t˚ = temperature (˚C)

v_{wo} = specific volume of water [$(1/\rho_w)$ (m³/kg)]

w_v = molecular mass of water vapour (18.016 kg/ml)

RH = relative humidity

- **WP4 Dewpoint Potentiameter**

The WP4 dewpoint potentiameter is the fastest instrument for measuring water potential. It measures water potential from 0 to 60 MPa with an accuracy of ±0.1 MPa from 0 to 10 MPa and ±1% from 10 to 60 MPa (WP4 and WP4-T manual, 2003). The method is used to only measure the total suction. Samples should be kept for at least 16 hours for equilibration time before reading the suction. This procedure is done by placing the sample in a WP4 cup and immediately placing a lid on the cup, then sealing the edges with tape and placing the cup into a container. After the equilibration time is reached, each WP4 cup is unsealed and placed into a calibrated device for reading. After each suction measurement, the specimen is taken out of the WP4 chamber, weighed and then left to air dry for about 10–15 min before the next suction measurement. This process is repeated several times to obtain the WRC. At the end of the testing, the specimen is placed into an oven to determine the dry weight. Its ability to quickly measure the water potential makes the WP4 dewpoint potentiameter suitable to determine the WRC of the hydrating GF, i.e. when the pore structure of GF is still changing due to binder hydration.

2.4.2 Unsaturated hydraulic conductivity (k_{unsat})

Several experimental methods are available to determine the flow behaviour in unsaturated porous media. However, unsaturated flow behaviour is commonly predicted and not measured. This has become a conventional engineering practice since the direct measurements of unsaturated flow properties require complicated equipment and qualified personnel, which prove to be time consuming and expensive (Fredlund and Rahardjo, 1993). Due to these reasons, several investigators have focused their research on developing procedures to predict unsaturated hydraulic conductivity by using saturated hydraulic conductivity and the WRC.

The coefficient of permeability for a porous media can be determined using either direct or indirect techniques. Direct measurements of permeability can be performed in the laboratory and field. Indirect methods can also be used to compute the coefficient of permeability.

- **Direct methods to measure coefficient of permeability**

When using direct methods to measure permeability, the hydraulic head gradient and the flow rate are determined from pore-water pressure and water content measurements. Laboratory tests are most economical, but in situ tests may better represent actual conditions. However, the in situ field methods are not as advanced and standardized as the laboratory methods. All methods assume the validity of Darcy's law. Direct methods can be categorized into two groups, namely, steady-state and unsteady-state methods.

- **Steady-state method**

The steady-state method to measure the coefficient of permeability is performed by maintaining a constant hydraulic head gradient across an unsaturated porous media specimen. The matrix suction and water content of the porous media are also maintained as constant. The constant hydraulic head gradient produces a steady-state water flow across the specimen. Steady-state conditions are achieved when the flow rate entering the soil is equal to the flow rate leaving the soil. The coefficient of permeability which corresponds to the applied matrix suction or water content is computed. The experiment can be repeated for different magnitudes of matrix suction or water content. The steady-state method can be used for both compacted and undisturbed specimens. The coefficient of permeability is computed as follows:

$$k_w = (\frac{Q}{At})(\frac{d_t}{h_{w3} - h_{w4}}) \qquad \text{Equation 2-10}$$

where

k_w = coefficient of permeability

Q = volume of water flowing

A = cross-sectional area of the soil

t = time

d_t = distance between tensiometers

h_{w3}, h_{w4} = hydraulic heads

There are several difficulties associated with the steady-state method (Fredlund and Rahardjo, 1993):

- the main difficulty arises from the low permeability of unsaturated soils or porous media. As a result, the water flow rates during the testing are extremely low and a lengthy amount of time is required to complete a series of permeability measurements,
- air diffusion through the water and water loss from the apparatus can cause errors in the volume of water measurements, and
- water is commonly used as a permeating fluid in the permeability test. However, in some cases, an osmotic suction gradient may develop between the pore-water within the soil and pure water.

Another testing difficulty is related to the contact between the soil specimen and the permeameter. As matrix suction increases, the soil specimen may shrink and separate from the permeameter wall and the high air entry ceramic plates.

- **Instantaneous profile method/unsteady-state method**

This method can be used either in the laboratory or in situ. The method uses a cylindrical specimen of porous media that is subjected to a continuous water flow from one end of the specimen. The test method has several variations. These differ mainly in the flow process used and the measurement of the hydraulic head gradient and the flow rate. The flow process can be a wetting process where water flows into the specimen or a drying process where water flows out of the specimen.

The hydraulic head gradient and flow rate at various points along the specimen can be obtained using one of several procedures. For the first procedure, the water content and

pore-water pressure head distributions can be independently measured. The water content distribution can be used to compute the flow rate. The pore-water pressure gradient can be calculated from the measured pore-water pressure head distribution. The gravitational head gradient is obtained from the elevation difference. For the second procedure, the water content distribution is measured while the pore-water pressure head is inferred from the WRC. A third procedure entails the measurement of the pore-water pressure head distribution and the inference of water content from the WRC (Fredlund and Rahardjo, 1993).

The coefficient of permeability is computed by dividing the flow rate by the average hydraulic head gradient.

$$k_w = \frac{v_w}{i_{ave}} \qquad \text{Equation 2-11}$$

where

i_{ave} = average hydraulic gradient

v_w = flow rate

Computations for the coefficient of permeability can be repeated for different points and different times. As a result, many coefficients of permeability can be computed corresponding to various water contents or suction values obtained from one test.

The difficulties that may be met using the unsteady-state method are similar to those described at steady-state method.

- **Indirect methods to measure coefficient of permeability**

Many studies have tried to predict the coefficient of permeability theoretically based on the soil pore size distribution. These predictions are referred to as an indirect method to determine permeability. The indirect method can be performed using the WRC and the saturated coefficient of permeability.

There are three types of permeability functions that can be identified: empirical equations, macroscopic models, and statistical models. These categories of functions were suggested by Mualem (1986) as an indication of the degree of theoretical sophistication, with the statistical models being the most rigorous (Leong and Rahardjo, 1997).

In the statistical models, the coefficient of permeability is derived from the WRC. There are many statistical equations to predict the coefficient of permeability, but the most popular models are the van Genuchten equation (1980) (Equation 2-12), and Fredlund and Xing equation (1994) (Equation 2-13).

$$k_r = \frac{\left\{1-(\alpha\psi)^{n-1}\left[1+(\alpha\psi)^n\right]^{-m}\right\}^2}{\left[1+(\alpha\psi)^n\right]^{m/3}} \qquad \text{Equation 2-12}$$

$$k_r = \frac{\int_{\ln\Psi}^{\ln 10^6} \frac{\theta(e^y)-\theta(\psi)}{e^y}\theta'(e^y)dy}{\int_{\ln\Psi_b}^{\ln 10^6} \frac{\theta(e^y)-\theta_s}{e^y}\theta'(e^y)dy} \qquad \text{Equation 2-13}$$

$$m = 3.67\ln\left[\frac{\theta_s C(\psi_i)}{\theta_i}\right]$$

$$n = \frac{1.31^{m+1}}{mC(\psi_i)} 3.72 s'$$

$$s' = \frac{s}{\theta_s} - \frac{\psi_i}{1.31^m (\psi_i + C_r) \ln[1 + (1000000 / C_r)]}$$

$$s = \frac{\theta_i}{\ln(\psi_p / \psi_i)}$$

where:

$k_r =$ relative coefficient of permeability

$\psi =$ matric suction (kPa)

$\psi_i =$ air entry value (kPa)

a, α , n, m = fitting parameters

$\theta =$ volumetric water content

$\theta_s =$ saturated water content

$\theta' =$ derivative of volumetric water content

$C_r =$ constant related to the matrix suction corresponding to the residual water content

y = dummy variable of integration representing the logarithm of suction

e = natural number, 2.71828

$C(\psi_i) =$ correction function

$s =$ the slope of the tangent line at inflection point.

$s' =$ correction factor

$\psi_p =$ intercept of the tangent line and the matrix suction axis.

2.5 Thermal conductivity of porous media and their determination by using KD2

It is very important to study the thermal properties of a material. The K, thermal diffusivity, and specific amount of heat can provide information about the heat exchange of a material with its surrounding. For example, the K gives information about how fast heat is travelling in a mass, thermal diffusivity shows the rate of heat that can be transferred by absorption or removal, and specific amount of heat provides an indication about the amount of heat stored in the material.

According to Fourier (1768-1830), the rate of heat transfer is proportional to the temperature gradient (Tae, 2005). The ratio of heat flux density to temperature gradient in a material is given by the following equation. Steady state and transient state methods can be used to determine the K of materials.

$$\lambda = dQ / dT \qquad \text{Equation 2-14}$$

where:

Q is the heat in joules

T is the temperature in ˚C

A KD2 thermal properties analyzer is used to measure the thermal properties of GF in this study. It is a compact, portable meter that consists of a hand- held readout and a single-needle sensor that can be inserted into the medium in order to conduct measurements. KD2 is used to measure K and resistivity (R) by monitoring the dissipation of heat from a line heat source. The method used is generally called the transient line heat source or transient

heated needle method. Figure 2-22 shows a KD2 thermal properties analyzer from Decagon Devices Inc.

Figure 2-22- KD2 thermal properties analyzer (Decagon Devices Inc.)

2.6 Sodium silicate and its effect on cementitious materials

2.6.1 Introduction

Soluble silicates are water soluble glasses generally manufactured from varied proportions of an alkali metal and SiO_2. It is manufactured by smelting sand with sodium carbonate at 1100ºC to 1200ºC. Aside from being used as an admixture for cement, soluble sodium

silicate is also used for a number of applications in various industries or fields, such as the paper industry (e.g., for binding packaging), geotechnical engineering (e.g., soil grouting, mine backfill), soap and detergent manufacturing, waterproofing, textile processing, and foundries. Soluble sodium silicates are silicate polymers. A higher degree of polymerization means a greater proportion of oxygen shared between $SiO4^{2-}$ tetrahedra and hence a smaller Na_2O:SiO_2 ratio (Turner, 2004). A range of different SiO_2 and Na_2O polymers can exist. Hence, one of the key determinants of the properties and functional activities of a particular type of sodium silicate is its "SiO_2/Na_2O" ratio usually expressed as a ratio by weight. This ratio determines the physical properties of the product as well as its chemistry (Turner, 2004). Varying this ratio enables various uses for sodium silicate.

In the present thesis, soluble sodium silicate is used as an admixture for the cement or binder for the preparation of cemented backfill. Two types of binder, PC and slag, are used. Thus, it is necessary to provide some background information about the effect of sodium silicate on the hydration and performance of these two binders and cemented materials that contain them. This is the objective of the next two sections.

2.6.2 Sodium silicate-activated slag binder

Ground granulated blast furnace slag (slag) has latent hydraulic properties that result in its extensive use as a partial replacement for PC, where it is activated by alkali and lime generated by the cement hydration. It can also be directly activated with alkali salts to provide a clinker-free binder. The production of alkali-activated slag (AAS) needs less energy than ordinary PC and is associated with low greenhouse gas emissions (CO_2). Such AAS materials have been used in many countries, such as China, Eastern Europe, Scandinavia, and the former USSR (Chang, 2003). Several studies have been conducted on

AAS and concretes (e.g., Glukhoskij et al., 1983; Wang et al., 1995; Shi, 1996; and Brough and Atkinson, 2001). It is generally agreed that AAS based materials show lower porosity, higher early strength and higher durability than PC based materials. Moreover, it is commonly accepted that the main reaction product of the alkali-activation of slag is a poorly crystalline C-S-H, broadly similar to that formed from ordinary Portland cements (OPC), but with a lower calcium silicate Ca/Si ratio (Wang et al., 1994). The alkali hydration of slag corresponds to a complex process that is composed of several steps. The exact reaction mechanism, which explains the setting and hardening of alkali-activated binders, is not yet perfectly understood. However, many authors agree that the reaction mechanism of alkali-activated binders exists in a three step model of dissolution, orientation and hardening. The reaction products also depend on the activator, prime materials, and systems (Si + Ca), which have a C–S–H gel as the main reaction product (e.g.,Wang et al., 1994; Fernández-Jiménez et al., 1999; Chao et al., 2010). Fernández-Jiménez and Puertas (2001) showed that the nature of the anion in the solution also plays a significant role in activation, particularly in early ages and especially with regard to paste setting (Fernández-Jiménez and Puertas 2003). These authors proposed a descriptive model based on the model proposed by Glasser (1990) in 1990 (Figure 2-23).

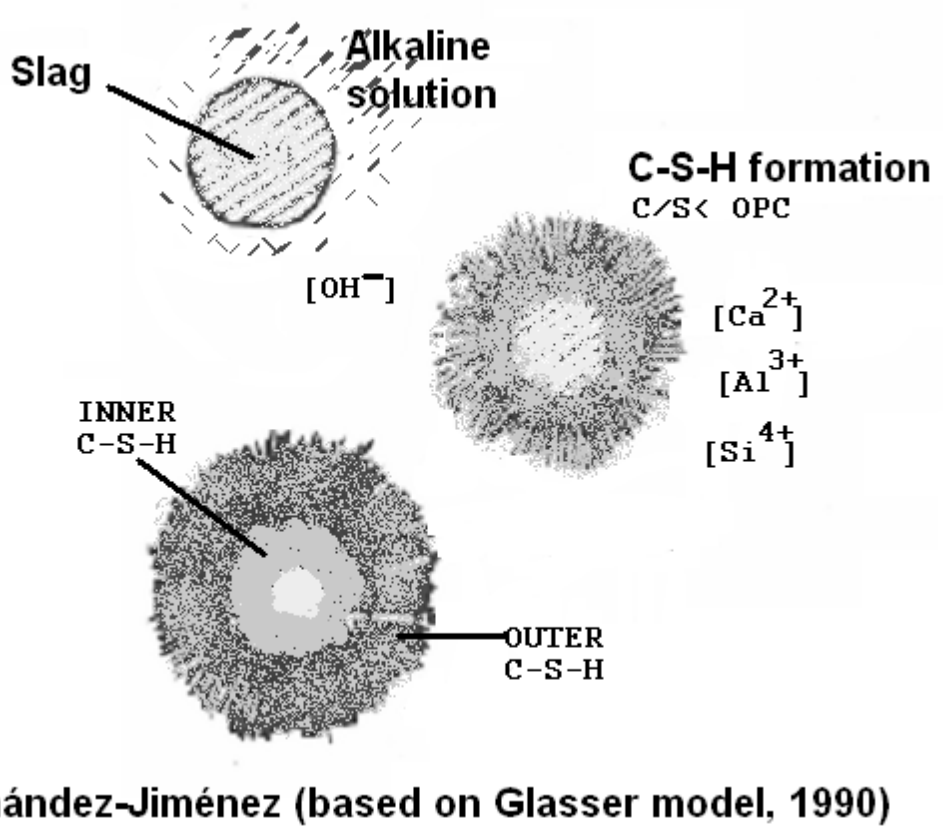

Figure 2-23- Theoretical model for the reaction mechanism in alkali-activated slag (Fernández-Jiménez and Puertas 2003)

The most commonly used alkaline activators are a mixture of sodium or potassium hydroxide (NaOH or KOH), with sodium silicate or water glass ($n SiO_2$. Na_2O) or potassium water glass ($n SiO_2$. K_2O). It has been reported that the strength development of AAS depends on the activator type and concentration (Shi, 1996; Fernández-Jiménez et al., 1999). The activator based on sodium silicate (water glass) is commonly found to have the best performance on strength development because it contributes a silica-gel that helps to form a compact matrix of hydration products (Escalante-Garcia et al., 2003). It is generally accepted that water glass doubly contributes to strength development, both by acting as an

alkaline activator and giving rise to the formation of a silica gel (Fernandes- Jiménez et al., 2009). Variations in the SiO_2/Na_2O ratio are known to significantly modify the degree of polymerization of the dissolved species.

2.6.3 Effect of sodium silicate on Portland cement system

Compared to the number of studies conducted on the sodium silicate-activation of binders such as slag and fly ash, there is a paucity of studies on the effect of sodium silicate on the hydration and performance of Portland cement system. The view that compounds of alkali metals (sodium and potassium) stimulate the hydration of the main phases of PC, at least in the early stages of the hydration mechanism, and accelerate the setting of cement paste has long been recognized in cement research (e.g., Jawed and Skalny, 1978; Taylor, 1990). However, there is no common view on how their presence affects the later stages of hydration, although most researchers have a tendency to believe that alkalis negatively influence the final strength and durability of the PC material. Brykoz et al. (2002) showed that the hydration of cement clinker minerals occurs at a high rate in the presence of sodium silicates due to a decrease in the initial pH of the pore solutions of cement pastes and intensive formation of calcium hydrosilicates. Previous studies have reported that depending on the molar ratio SiO_2/Na_2O, soluble sodium silicates affect the pH value of the liquid phase, hydration rate of clinker minerals, and morphology of the C-S-H gel formed differently as a result of hydration (Aborin et al., 2001; Brykov et al., 2002). Studies conducted by Skripkiunas and Janavicius (2010) confirmed that due to its high chemical activity, SiO_2 can bind free portlandite ($Ca(OH)_2$) in hcp. They showed that the reaction of SiO_2, formed in the hydrolysis of a sodium silicate solution (Equation 2-15), and $Ca(OH)_2$

from the cement hydration results in the formation of C-S-H, which later causes more intensive binding under natural conditions (Equation 2-16).

$$Na_2O.SiO_2 + H_2O = 2Na^+ + 2OH^- + SiO_2 \quad \text{Equation 2-15}$$

$$SiO_2 + mCa(OH)_2 + (n-1)H_2O = mCaO\text{-}SiO_2.H_2O \quad \text{Equation 2-16}$$

Skripkiunas and Janavicius (2010) also indicated that sodium hydroxide arouse in a sodium silicate hydrolysis reaction (Equation 2-15) forms an amorphous phase, which covers the surfaces of cement hydration products. Sodium hydroxide has an accelerating effect on the mechanisms of PC hydration. This formation of the amorphous phase was also graphically demonstrated by a comparison of SEM images on hcp without soluble sodium silicate with that of hcp with 0.5% soluble sodium silicate (Skripkiunas and Janavicius, 2010). From Figure 2.24a, which represents the microstructure of the hcp without sodium silicate, high amounts of ettringite (needle shaped long crystals) and amalgamated to coarse agglomerates crystals of splinting form C-S-H crystals and large forms of CH crystals were observed (Skripkiunas and Janavicius, 2010). On the contrary, the SEM micrographs of hcp with soluble sodium silicate clearly show high amounts of amorphous (irregular shape) phases, which coat the C-S-H and CH crystals.

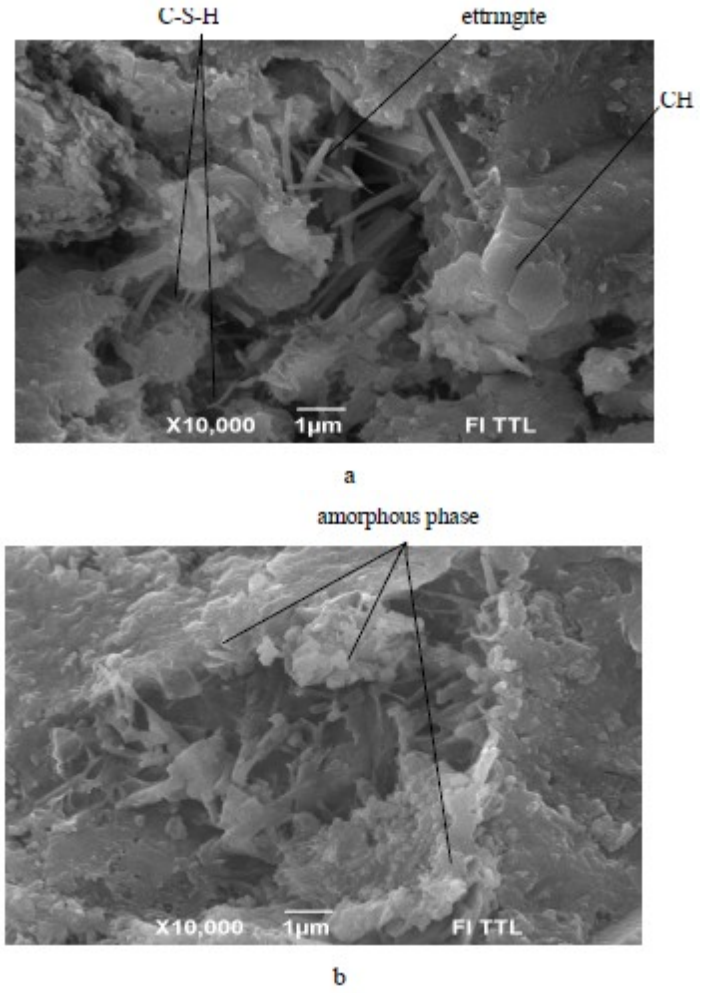

Figure 2-24- SEM micrographs of hcp with 0% (a) and 0.5% (b) of sodium silicate solution after 180 days curing (Skripkiūnas and Janavičius, 2010)

2.7 Summary and conclusions

In this chapter, theoretical and technical background information relevant to a better understanding of the main issues addressed in the present thesis is provided.

Background information on cemented backfill has been provided. The technology for mine cemented backfill is highlighted. Several types of mine fills are discussed. The focus is on CPBs and GF due to their popularity as well as because some behaviours of CPBs will be compared to those of GF in this thesis.

Different design procedures have been discussed in the section on the design criteria of cemented backfill. The target is to design an optimal mix that reduces the cost without affecting the strength of the structures.

Brief explanations of the mechanisms of binder hydration, the main products of the hydration process (e.g. C-S-H), pore structure of the hcp, and the state of water and diffusion mechanism in the hcp have been presented. The discussions help to create an understanding of the characteristics of hcp.

Technical background details on the unsaturated hydraulic conductivity of porous media are given since cemented backfill, an evolutive porous media, can be in unsaturated state. Direct and indirect techniques to measure the coefficient of permeability are addressed. In addition, WRC is defined. The most commonly used methods available for the measurement of porous media suction will be discussed shortly. This allows us to determine the methods suitable for the determination of the WRC of the hardening of the GF as well as hardened GF.

A short review on sodium silicate and its effect on the hydration of binder and performance of cementitious material that contains sodium silicate are provided. From this review, it can be noticed that the effect of sodium silicate on the performance cementitious materials, especially PC material, is not perfectly understood.

In addition, information on the thermal properties of porous material is discussed as well as the technique adopted in this thesis to measure the K of the GF.

In conclusion, the purpose of providing a technical background in this thesis is to draw attention to the achievements of previous research and focus on unaddressed issues. From

the information given in this chapter, it is noted that only a few studies (e.g. Doucet et al., 2007, and Hassani et al., 2007) have been carried out to examine the mechanical properties of GF. However, the understanding of the mechanical properties and their evolution with time is incomplete. No studies have addressed the thermal and hydraulic (unsaturated) properties of GF. Furthermore, none of the previous studies have considered the coupled THM behaviour of GF.

Consequently, this has inspired the author to perform a laboratory investigation to address these issues.

2.8 References

Aborin, A.V., Brykov, A.S., Danilov, V.V., and Korneev, V.I., Tsement Ego Primen., 2001, no. 3, pp. 40 - 42

ACI, Guide to Durable Concrete, ACI 201.2R-92 (1992)

Alexander K.M., Taplin J.H., Concrete strength, cement hydration and the maturity rule, Aust. J. Applied Sciences 13 (1962), pp. 277–284.

Belem, T. and Benzaazoua, M. An overview on the use of paste backfill technology as a ground support method in cut-and-fill mines. Proceedings of the 5th Int. Symp. On Ground support in Mining and Underground Construction, (2004) 637-650.

Brady, B.H.G. and Brown, E.T. Rock Mechanics for underground mining, (1993) 408-429.

Brakebusch, F.W. Basics of paste backfill systems. Mining Engineering. 46, (1994) 1175–1178.

Brisson, P. Unsaturated Flow in Tailings. University of Ottawa. (2006) 1-205.

Brough A.R., Atkinson A. (2001). Sodium silicate-based, alkali-activated slag mortars. Part I. Strength, hydration and microstructure. Cement and Concrete Research 32, 2002: 865-879.

A. S. Brykov, V. V. Danilov, V. I. Korneev, and A. V. Larichkov**.** Effect of Hydrated Sodium Silicates on Cement Paste Hardening. Russian Journal of Applied Chemistry, Vol. 75, No. 10, 2002, pp. 157731579

Budhu, Muni. Soil Mechanics and Foundation, 2000, 586 pp.

Celestin, J.C. Geotechnical Properties of Cemented Paste Backfill and Tailings Liners: Effect of Mix Components and Temperature. University of Ottawa, (2008) 1-221.

CEMBUREAU, Environmental Benefits of Using Alternative Fuels in Cement Production, CEMBUREAU, 1999.

Chang, J.J. A study on the setting characteristics of sodium silicate-activated slag pastes. Cement and Concrete Research 33 (7), 2003, 1005-1011.

Craig, R.F. Soil mechanics. Fifth Edition, Chapman and Hill Publishing, London, 1995. 427 p.

Doucet, C., Tarr, K., and Swan, G. Evaluation of the Effect of Mixing Method, Sequence and time on the properties of gelfill. Minefill 2007, 2488.

Escalante-Garcia J.I., Fuentes A.F., Gorokhovsky A., Fraire-Luna P.E. Mendoza-Suarez G. (2003). Hydration products and reactivity of blast-furnace slag activated by various alkalis. Journal of American ceramic Society 86 (12), 2003: 2148-2153.

Fall, M. and Benzaazoua, M. Modeling the effect of sulphate on strength development of paste backfill and binder mixture optimization. Cement and Concrete Research 35 (2005) 301–314.

Fall, M., Benzaazoua, M. and Ouellet S. Experimental characterization of the influence of tailings fineness and density on the quality of cemented paste backfill. Minerals Engineering 18 (2005) 41–44.

Fall, M., Belem, T., Samb, S. and Benzaazoua, M. Experimental characterization of the stress–strain behaviour of cemented paste backfill in compression. Springer Science Business Media. (2007) 1-9.

Fall, M., Nasir, O., and Celestin, J. Paste backfill responses in deep mine temperature conditions. In: 9th International Symposium of mining with backfill. Montreal, Canada: CD-Rom; 2007 paper 2522.

Fall, M. and Samb S.S. Pore structure of cemented tailings materials under natural or accidental thermal loads. Materials Characterization. 5 9 (2008) 5 9 8 – 6 0 5.

Fall, M., Benzaazoua, M. and Saa, E.G. Mix proportioning of underground cemented tailings backfill. Tunnelling and Underground Space Technology 23 (2008) 80–90.

Fall, M., Adrien, D., Celestin, J.C., Pokharel, M., Touré, M.. Saturated hydraulic conductivity of cemented paste backfill. Journal of Mineral Engineering (2009) 22(15):1307-1317.

Fall, M., Célestin, J.C., Pokharel, M., Touré, M.. A contribution to understanding the effects of temperature on the mechanical properties of cemented mine backfill. Engineering Geology (2010) 14 (3-4), 397-413.

Feldman R. F., Sereda P. J. A model for hydrated Portland cement paste as deduced from sorption –length change and mechanical properties. Material and structures, (1968) No. 6, pp. 509-19 Paris.

Fenga, X., Garboczia, E.J., Bentza, D.P., Stutzmana, P.E., and Masonb, T.O. Estimation of the degree of hydration of blended cement pastes by a scanning electron microscope point-counting procedure. Cement and Concrete Research 34 (2004) 1787-1793.

Fernández-Jiménez, A., Palomo J.G., Puertas, F. Alkali-activated slag mortars mechanical strength behaviour. *Cem. Concr. Res.* 29 8 (1999) 1313–1321.

Fernández-Jiménez A. and Puertas F.“Setting of alkali-activated slag cement. Influence of activator nature” Adv. Cem. Res. 13 (3), (2001)115-121.

Fernández-Jiménez A., Puertas F., Sobrados I., Sanz J., aStructure of calcium silicate hydrate formed in alkaline activated slag. Influence of the type of alkaline activator .J. Am. Ceramic Soc. 86(8), (2003a) 1389-1394.

Fernández-Jiménez, A. Palomo, A. Revuelta, D. Alkali activation of industrial by-products to develop new earth-friendly cements. Proceeding of the 11th International Conference on Non-Conventional Materials And Technologies (NOMAT 2009) 6-9 September 2009, Bath, UK

Fredlund, D. G. and Rahardjo, H. Soil Mechanics for Unsaturated Soils, (1993) 510 p.

Fredlund, D. G., Xing, A., Huang, S. Predicting the permeability function for unsaturated soils using the soil-water characteristic curve. Canadian Geotechnical Journal, 31(3): (1994) 521-532.

Fredlund, D.G. and Xing, A. Equations for the soil-water characteristic curve. Canadian Geotechnical Journal, 31(3): (1994) 521-532.

Fredlund, Murray D., Wilson, G.Ward and Fredlund, Delwyn G. Estimation of Hydraulic Properties of an Unsaturated Soil Using a Knowledge-Based System. Department of Civil Engineering University of Saskatchewan, Saskatoon, Sask., Canada. (1997) 1-7.

Glasser F.P., “cements from micro to macrostructure” Br. Ceram. Trans. J. Vol. 89, nº 6, (1990) 192-202.

Glukhoskij V., Zaitsev Y., V. Pakhomow, Slag-alkaline cements and concretes-structures, properties, technologies and economical aspects of the use. Silic. Ind. 10 (1983) 197–200.

Grice, T. Underground mining with backfill. The 2nd Annual Summit- Mine Tailings Disposal Systems (1998) 1-14.

Hassani, F, Razavi, S.M., Isagon, I. A study of physical and mechanical behaviour of gelfill. Minefill, 2007 Paper 28.

Jawed, I. Skalny, J. Alkalies in cement: A review: II. Effects of alkalies on hydration and performance of Portland cement. Cement and Concrete Research, 1978, 8(1), 1978, Pages 37-51.

KD2 Operator's Manual. 1-24.

Lam, L., Wong Y.L., Poon C.S. Degree of hydration and gel/space ratio of high-volume fly ash/cement systems. Cement and Concrete Research, vol. 30, no5, (2000) 747-756.

Leong, E.C. and Rahardjo, H. Permeability functions for unsaturated soils. Journal of Geotechnical and Geo-environmental Engineering (1997) 1118-1126.

D.G. Mantel, Investigation into the hydraulic activity of five granulated blast furnace slags with eight different portland cements. ACI Mater. J. 91 5 (1994) 471–477.

Mehta P. K. Concrete: structure, properties, and materials, (1986) 1-450.

M. Regourd, 'Cements made from blastfurnace slag', in 'Lea's chemistry of cement and concrete', 4th Edn, edited by P. C. Hewlett, (Arnold, London, 1998).

Mitchell, R.J. Earth Structures Engineering. (1983) 1-265.

Mitchell, R.J. Stability of cemented tailings mine backfills. Computer and physical modelling in geotechnical engineering. (1989) 501-508.

Monteiro, P. J. M., Maso, J. C. and Ollivier, J. P. The aggregate-mortar interface. Cement Concrete Research 15 (1985) 953-958.

Mouret, M., Bascoul, A. and Escadeillas, G. Study of the degree of hydration of concrete by mean of image analysis and chemically bound water. Elsevier Science Ltd, 1997.

Murray D. Fredlund, G.W. W., Fredlund, D. G. Estimation of hydraulic properties of an unsaturated soil using a knowledge-based system. Proceedings of Characterization and Measurement of the Hydraulic Properties of Unsaturated Porous Media,California, October 22-24, 1997; 1-13.

Nasir, O. Modeling of Coupled Processes in Hydrating Cemented Paste Backfill Structures and Application to the Analysis of their Performance. University of Ottawa. (2008) 1-144.

Navaneethan, T., Sivakumar, V., Wheeler, S.J., Doran, I.G. Assessment of suction measurements in saturated clays. Geotechnical Engineering 158 Issue GEI (2004) 15-24.

Neville, A. M. Properties of Concrete. Forth Edition, (1995): 1-844.

Orejarena, L. and Fall, M. Mechanical response of a mine composite material to extreme heat. Springer-Verlag. (2008) 67:387–396.

Pakalnis, R., Caceres, C., Clapp, K., Morin, M., Brady, T., Williams, T., Blake, W., MacLaughlin, M. Design Spans – Underhand Cut and Fill Mining Presented at 107th CIM-AGM Toronto. (2005) 1-9.

Paynter, J.T. and Dodd, J.C. The Design, Commissioning and Operation of the Golden Giant Paste Backfill Plant. 29th annual meeting of Canadian mineral processors (division of the CIM). (1997) 382-403.

Pokharel, M. Geotechnical and Environmental Responses of Paste Tailings Systems to Coupled Thermo-Chemical Loadings. University of Ottawa. (2008) 1-248.

Rankine, K. J., Sivakugan, N. R. Cowling. Emplaced geotechnical characteristic of hydraulic fills in a number of Astralian mines. Geotechnical and Geological Engineering (2006) 24: 1-14.

Rankine, Rudd M., and Sivakugan, N. Geotechnical properties of cemented paste backfill from Cannington Mine, Australia. Geotech Geol Eng (2007) 25:383–393.

M. Regourd, Characterization of thermal activation of slag cements. Proceedings of the 7th International Congress on the Chemistry of Cements (Paris) 2 III-3 (1980) 105–111.

D.M. Roy and G.M. Idorn, Hydration, structure and properties of blast furnace slag cements, mortars and concrete. Proc.-Am. Concr. Inst. 79 6 (1982) 445–457.

Shi C., Strength, pore structure and permeability of alkali-activated slag mortars. Cem. Concr. Res. 26 12 (1996) 1789–1799.

Sideris K. K, Konsta-Gdoutos M..Influence of the Water to Cement Ratio W/C on the Compressive Strength of Concrete- An Application of the Cement Hydration Equation to Concrete. Applied Composite Materials 3(1996) 335-343.

G. SkripkiūnAS, E. Janavičius. Effect of Na2O·nSiO2 Nanodispersion on the Strength and Durability of Portland Cement Matrix. Materials Science, 2010(16, No. 1. 2010)

Simon, D. Microscale Analysis of Cemented Paste Backfill. University of Toronto, (2005) 1-282.

Skalny, J., Marchand, J. Odler, I. Sulphate Attack on Concrete. (2002) 1-215.

Tang, A., Cui, Y. Controlling suction by the vapour equilibrium technique at different temperatures and its application in determining the water retention properties of MX80 clay, CERMES-ENPC, Institute Navier, France (2005) 1-32.

Taylor, H.F.W., Cement Chemistry, London: Academic,1990.

Tsiampousi, A., Zdravkovic, L., Potts, D.M. Numerical analysis of excavations in unsaturated soils. Research: Geotechnics, Imperial College London (2007-2010).

Turner C. Chemicals-G-Sodium Silicate-4. Soluble sodium silicate manufacture, IChem Ltd, Morrinsville is ISO9002, 2002, 4p.

V.D. Vanden Bosch, Performance of mortar specimens in chemical and accelerated marine exposure. In: Performance of Concrete in Marine Environment, ACI SP-65, American Concrete Institute, Detroit (1980), pp. 487–507.

Wang, S.D. Pu X.C., Scrivener K.L., Pratt P.L., Alkali-activated slag cement and concrete: a review of properties and problems. Adv. Cem. Res **7** 27 (1995), pp. 93–102.

Wang S. D., Scrivener K. L., P. L. Pratt, "Factors Affecting the Strength of Alkali-Activated Slag, Cement and Concrete Research. 24, 1033–43 (1994).

WP4 and WP4-T Operator's Manual. Version 2.2, (2003) 1-83.

Xi, Y., Bazant, Zdenek P., Molina, L., Jennings, Hamlin M. Moisture diffusion in cementitious materials moisture capacity and diffusivity. Advanced Cement Based Materials. (1994) 1: 258-266.

Yun, T. Mechanical and thermal study of hydrate bearing sediments. Georgia Institute of Technology. (2005) 1-194.

Chapter 3

Technical Paper I

Evolution of the Thermal, Hydraulic, Mechanical, and Microstructural Properties of Gelfill

Abstract

GF is produced by adding small amounts of sodium silicate, about 0.3-0.4% by weight of solids, to binders and tailings with a solid percentage of 73%. It is a new cemented backfill material. Its main roles are underground mine support and tailings disposal. The main performance properties of GF include: thermal, hydraulic, mechanical and microstructural properties. However, the understanding of these engineering properties and their evolution with the degree of binder hydration or time is limited. Therefore, laboratory investigations are conducted to study these engineering properties of GF. Over 200 GF samples have been prepared with various binder proportions, w/c ratios, and 0.4% (by weight of solids) sodium silicate type N. Samples are cured in room temperature for various number of days to study the evolution of the thermal (thermal conductivity), chemical (degree of binder hydration index), hydraulic (saturated hydraulic conductivity), mechanical (strength) and microstructural (cement hydration products, porosity) properties of GF. Valuable results are gained with regards to the evolution of the engineering properties of GF. The study shows that the thermal, microstructural, hydraulic and mechanical properties are time-dependent or affected by the degree of binder hydration index. The mechanical properties

are affected by binder content, binder type, degree of hydration index and curing time while the hydraulic conductivity of GF decreases as the binder content increases and the degree of binder hydration index increases. A relationship between the UCS and saturated hydraulic conductivity is found. It is also noted that the binder content and degree of binder hydration influence the thermal conducity (conductivity) at early ages only. The outcomes obtained from this study will be useful for cost-effective and environmentally friendly design of GF structures.

Keywords: gelfill, cemented paste backfill, thermal properties, binder hydration, hydraulic conductivity, strength

3.1 Introduction

GF is a new cemented tailings backfill material, and a promising backfill technology. GF is typically made of tailings, water, binder and chemical additives (Fillset, sodium silicate gel). The chemical additives (are like a gel, therefore the name, GF) have the ability to absorb (Hassani et al., 2007; Doucet et al., 2007) a high amount of the water (cemented tailings are always prepared with excessive water to allow easy transport to underground voids). This water absorption results in a substantial increase of GF strength (Hassani et al., 2007; Doucet et al., 2007). Recycling the waste (tailings) into GF has economical and environmental advantages for the mining industry. Filling the stopes with GF results in higher ore extraction, while ensuring a safe workplace for the mine worker. Furthermore, this technology reduces the quantity of mine waste on the earth surface.

Mechanical, hydraulic, and thermal properties are key design parameters for GF structures. In order to safely play its role in underground mine support, GF should have adequate mechanical properties. These properties must allow the GF to withstand certain static and dynamic loads; they also have to prevent GF structures from collapsing during adjacent mining operations. Failures of mine backfills can cause injuries, and human and financial lost. UCS is often used to evaluate the mechanical stability of GF. This is because the UCS test is relatively quick and inexpensive. In addition to the use of GF as underground mining support, they are used as tailings storage. In terms of waste disposal, the mechanical properties of GF should prevent it from deterioration, such as cracking (Yilmaz et al., 2003). Mechanical damage (cracking) can significantly increase hydraulic conductivity (Fall et al., 2009). Cracks can create paths for the infiltration of fluids, such as water and oxygen, which weaken the environmental performance and durability of GF structures. The

availability of oxygen and its rate of diffusion through the pore spaces of GF are critical factors that control the rate of acid generation (Nicholson et al., 1989).

Other important parameters that affect the environmental performance and durability of GF are transportability of fluid (e.g. permeability) and its microstructure (e.g. void ratio (e), porosity, and tortuosity). The vulnerability of GF to acid mine drainage (AMD) and capability of transport toxic elements to the mine areas and ground water (when the mine is flooded after closure) are pertinent environmental design criteria of GF structures. Exposure of GF to AMD is dependent on the reactivity of tailings contained in the GF. The reactivity in turn is reliant on the types and quantity of sulphide minerals present in the GF as well as hydraulic properties of the GF (seepage of water and diffusion of oxygen through the GF matrix). These properties can be evaluated by investigating the hydraulic conductivity of the GF. In addition, in order to keep the fresh GF materials from flowing into the mine working areas during stope filling, barricades (retaining wall structures) are constructed in each access to the stope prior to filling. The development of pore water pressure behind the barricades and the permeability of the barricades drastically affect the stability of these retaining walls. The aforementioned factors are influenced by the saturated hydraulic conductivity of GF materials.

Thermal properties are other parameters that affect mechanical and hydraulic properties. One of the main sources of temperature in GF is the heat of binder hydration. When a GF mass is placed in the stope, heat will be generated during the hydration process. Then, heat will be transferred from the GF to the surrounding area. This operation influences both the temperature of the working environment (disturbing the natural temperature of adjacent

rocks especially at permafrost zones where thawing of rocks can create stability problems) and the mechanical behavior of the GF at early ages (higher temperature results in higher early strength in cementitious material). Another source of temperature change comes from the rock or air that surrounds the GF structures (hot rock temperatures in deep mines and cold rock temperatures in permafrost mines). Temperature exchange between the surrounding environment and GF structures has a significant impact on the mechanical stability and durability of GF. Thereby, thermal conductivity knowledge is vital for engineers to design economical and durable GF structures.

In addition, knowing the thermal properties of GF is essential in order to reduce the consumption of energy in deep mining (mining is an energy intensive industry with energy use that accounts for 15-30% of production costs, with the majority of greenhouse gas emission directly related to energy consumption (Celestin and Fall, 2009)) as well as economical reasons. Aside from the advantages of using GF structures to support and stabilize ore, they help to improve ventilation in the mining areas. Backfill also results in reduction of heat induction (up to 53%) through exposed rock into the stoping areas of deep mining (Celestin and Fall, 2009). The continuation of deep mines could be determined by the choice of environmental control systems and the cost of their operation. The contribution of a mine environmental control system is currently 10-15% of the cost of mining (Celestin and Fall, 2009). For that, the role of cemented backfill in improving the environment of deep underground mining should be emphasized. In order to evaluate the performance of GF in terms of ventilation control, understanding of thermal conductivity and heat transfer in GF is required. However, the understanding of the thermal properties of GF is still limited.

Since GF is a new type of cemented backfill material, only a few studies have discussed its mechanical properties (Doucet et al., 2007; Hassani et al., 2007). However, no studies have been conducted on the thermal conductivity of GF or investigated the evolution of the thermal, hydraulic, and mechanical properties of GF with degree of binder hydration.

The objective of this paper is to investigate the evolution of the thermal, hydraulic, mechanical and microstructural properties of GF by conducting experimental tests.

3.2 Experimental programs

3.2.1 Materials

The materials used to prepare GF include binder, tailings, sodium silicate, and water.

3.2.1.1 Binder and mixing water

Portland cement type I (PCI) was used as the binder. It is the most common material used by the mining industry to produce cemented backfill. Blast furnace slag (slag) is also used in this study. The blending ratio of PCI and slag was 50/50 in weight proportion. Table 3-1 shows the physical and chemical properties of the binders. Tap water was used to mix the binders and tailings.

Table 3-1 Characteristics of the different types of binders used

Types of Binder	MgO	CaO	SiO_2	Al_2O_3	Fe_2O_3	SO_3	Relative Density	Specific Surface (m^2/g)
PCI	2.65	62.82	18.03	4.53	2.70	3.82	3.10	1.30
Slag	10.98	41.14	34.23	9.54	-	3.87	3.84	2.20

3.2.1.2 Tailings

Silica tailings (ground silica, TS) are used in this study. The advantage of selecting TS as the tailings material is to accurately control to the mineralogical and chemical compositions of tailings. Furthermore, natural tailings contain various amounts of sulphate and other undesirable minerals which can bring high levels of uncertainty to the obtained results and thus significantly affect the outcomes of the study. For example, the oxidation of the sulphides present in the tailings during the preparation of the GF can produce sulphate. This sulphate can interact with the sodium silicate gel, which can result in significant uncertainty in the analysis and interpretation of the results obtained. TS is made of quartz (an example of a dominant mineral in Canadian hard rock mines) and shows a grain size distribution close to the average of nine Canadian mine tailings (Figure 3-1). It can be observed that TS has about 45 wt.% fine particles (< 20 μm) and can be classified as medium tailings. Tables 3-2 and 3-3 show the physical and chemical properties of TS. From the experimental work performed by Celestin (2008), the used tailings can be classified as sandy silts of low plasticity or the ML group in the Unified Soil Classification System (UCCS). The ML group is characteristic for tailings from hard rock mines as also measured by Vick (1990).

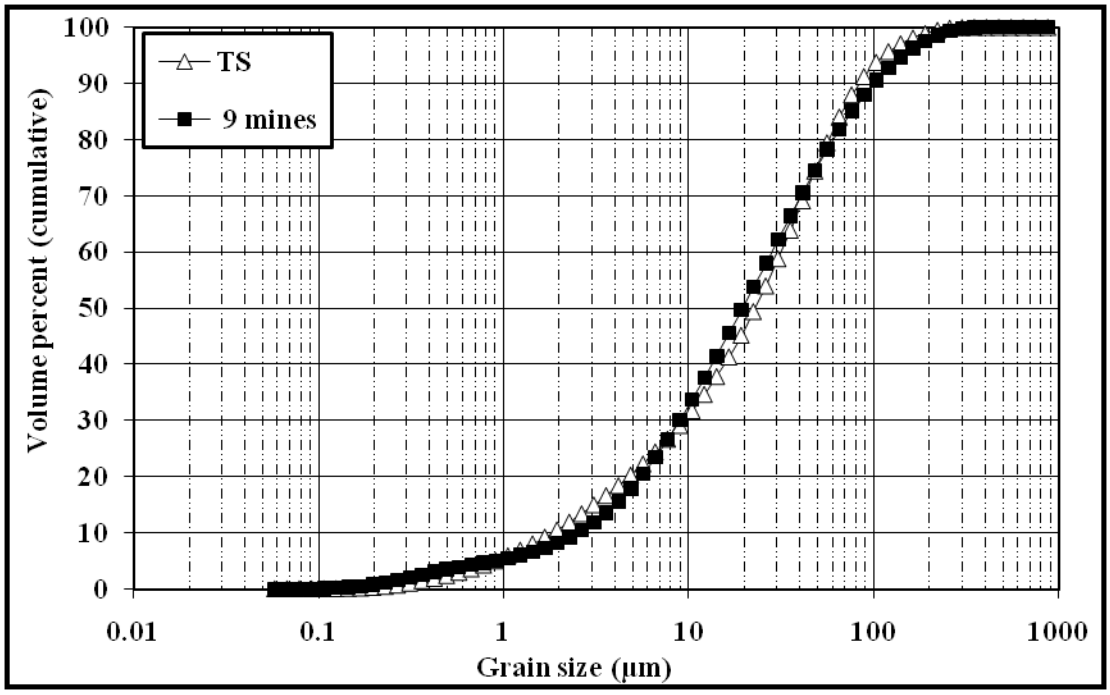

Figure 3-1 Grain size distribution of the tailings used and the average grain size distribution of tailings from nine Canadian mines

Table 3-2 Physical properties of silica tailings (TS)

Element	G_s	D_{10} (µm)	D_{30} (µm)	D_{50} (µm)	D_{60} (µm)	D_{90} (µm)	C_u	C_c
TS	2.7	1.9	9.0	22.5	31.5	88.9	16.2	1.3

Table 3-3 Main chemical elements of TS

Element	Al wt%	Ca wt%	Si wt%	Fe wt%	Na wt%	Pb wt%	S wt%	K wt%
TS	0.1	<0.01	99.8	<0.01	<0.01	0.0	0.0	0.0

3.2.1.3 Sodium silicate

Sodium silicate type N was added to the mix in the liquid form. It is inorganic chemical made by mixing various ratios of sand and soda ash (sodium carbonate) at high temperatures. It is described as clear, colourless, and viscous liquid. Table 3-4 shows sodium silicate properties. The hydrolysis reaction in sodium silicate solution is characterized by the following equation:

$$Na_2O.SiO_2 + H_2O = 2Na^+ + 2OH^- + SiO_2 \quad \text{(Equation 3-1)}$$

Table 5-4 Sodium silicate properties (National Silicates Ltd)

Properties	Values
Na_2O% by weight	8.90
$SiO_{2\%}$ by weight	28.66
Weight Ratio,%SiO_2 /%Na_2O	3.22
Specific Gravity @ 20°C	1.394
Solids%	37.56

3.2.2 Preparation of materials and mix proportions

Over 200 GF samples were prepared to test the thermal, hydraulic, and mechanical properties. The degree of binder hydration index was also determined. The tailings, binder, water, and gel were mixed using a B20F food mixer. The mixing time was 10 minutes for all mixes. The tailings, binder, and water were mixed first, followed by the addition of sodium silicate gel. Preliminary UCS tests were conducted to choose the right dose of gel. Mixes with 0.1, 0.2, 0.3, and 0.4% wt sodium silicate were prepared. The best results were obtained when the sodium silicate is 0.4% wt (Figure 3-2). Hence, this percentage is

selected for this investigation. Various binder proportions were used to prepare the mixes, including 2%, 4.5%, and 6% PCI with a solid mass concentration of 73% which correspond to w/c ratios of 18.5, 8.2, and 6.2, respectively. Furthermore, GF samples made of 4.5% binder of PCI/slag (50/50) were prepared. The slump of the prepared GF was 25 cm. The produced GF were poured into cylindrical plastic moulds that were 5 cm in diameter and 10 cm in height. The prepared samples were then sealed and cured in a laboratory environment at 20 °C ± 2 °C for periods of 3, 7, 28, 90, and 120 days. Furthermore, the mix of GF (i.e. those that contain sodium silicate) with w/c = 2 (to simulate the high w/c ratio of GF) and those without sodium silicate were prepared to investigate the binder hydration products formed and the impact of sodium silicate gel on the hydration of GF.

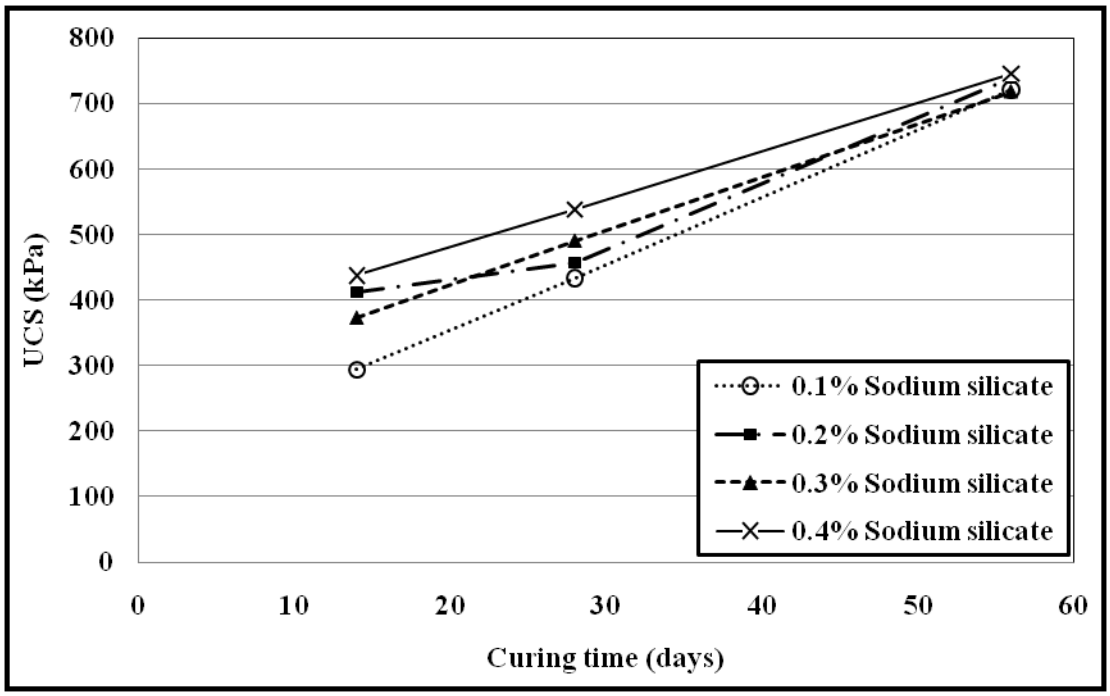

Figure 3-2 Various sodium silicate proportions (0.1%, 0.2%, 0.3%, and 0.4%), 4.5% PCI, and 73% solids mass concentration

3.2.3 Testing and analysis methods

3.2.3.1 Mechanical tests

Uniaxial compression tests (UCS) were performed on GF specimens cured at 3, 7, 28, 90, and 120 days. The specimens were tested according to the ASTM C 39 using a computer-controlled mechanical press. The press has a normal loading capacity of 50 kN. All samples were tested at a constant deformation rate of 1 mm/min. All test data were collected using a computerized data logging system. The results were saved using the computer software LabView. For each age, at least two cylinders were tested to ensure the repeatability of the results obtained.

3.2.3.2 Hydraulic conductivity tests

Saturated hydraulic conductivity tests were conducted on the GF samples. The specimens were tested according to ASTM D5084-00 using a TRI-FLEX II system. A flexible wall technique in constant head mode was employed. The samples were saturated in water for 24 hours prior to the testing. Each hydraulic conductivity test was repeated at least twice to ensure that the results always fall within an accurate limit.

3.2.3.3 Determination of the thermal properties (K)

A KD2 thermal properties analyzer manufactured by Decagon Devices was used to measure the thermal conductivity of GF specimens. The sensor needle of the KD2 contains both a heating element and a thermistor; care should be taken to prevent the bending of the probe. The device computes the values of thermal conductivity and resistivity by monitoring the dissipation of heat from a line source given a known voltage (KD2, 2006).

The thermal conductivity is measured with an accuracy of 5%. The measurement speed is 1.5 minutes, and for this reason, this test is considered as a quick test. The tests were conducted according the guidelines provided by the manufacturer (KD2, 2006).

3.2.3.4 Estimation of binder hydration degree index

The engineering properties of cemented materials, such as strength and durability, are influenced by the microstructure of the hardened paste. The hardening of cementitious material is gradually gained through hydration of the binder, thus, the degree of binder hydration index should be determined. The degree of hydration (α) is defined as the ratio between the quantity of hydrated cementitious material and the original quantity of cementitious material (Schindler and Folliard, 2005). The degree of hydration is a function of time, which ranges between 0% (or 0) at the beginning of hydration, and 100% (or 1) as the hydration is entirely accomplished. Many experimental techniques are used to measure the degree of hydration of PC. For example, measuring the heat of hydration, the non-evaporable water content, and the amount of calcium hydroxide produced in the hydration reactions. All the aforementioned methods are based on comparisons of the measured parameters with the predicted or measured parameters for a fully hydrated paste. In recent years, SEM quantitative techniques are used to estimate the degree of hydration in plain Portland cement paste. In this study, Equation (3-2) is used to estimate α. However, this method is affected by the curing temperature, i.e. the relationship between the compressive strength and α is influenced by curing temperatures. Nonetheless, this limitation is not applicable here because same curing temperatures are used for all mixes.

$$\alpha_n = \frac{UCS_n}{UCS_{final}} \qquad Equation\ (3-2)$$

UCS_n : uniaxial compression strength at n curing time

UCS_{final} : uniaxial compression strength of mature GF (in this study, it is considered that the strength of GF does not increase after 120 days)

α_n: α at n curing time

3.2.3.5 Microstructural analysis

Thermal analyses (thermal gravimetric analysis (TGA)), derivative thermogravimetric analysis (DTA), and differential scanning calorimetry (DSC)) were conducted on hcp that contains sodium silicate (gel) with a high w/c ratio. TGA-DTA/DSC was conducted on hcp of GF for 7 and 28 days curing time. Thermal analyses were carried out using the SDT apparatus from TA Instruments which allows simultaneous registration of weight loss and heat flow along the thermal treatment of the sample. An x-ray diffraction analysis (XRD) was conducted on hcp with and without gel for 28 days of curing time, in order to assess the effect of sodium silicate on the mineralogical composition of the cemented matrix of cemented backfill and degree of cement hydration. X-ray tests were conducted using a Scintag XDS 2000 XRD. The thermal analyses and the x-ray tests permitted the studying of binder hydration products in the GF matrix. The porosity (n) and void ratio (*e)* of the GF samples were evaluated using the following formula:

$$n = \frac{e}{1+e}$$

$$e = \frac{G_s \rho_w (1+w)}{\rho_m} - 1$$

where, w is the water content (%), G_s is the specific gravity, ρ_w is the density of water (1.00 g/cm^3) and ρ_w is the bulk density (g/cm^3).

3.3 Results and discussion

3.3.1 Evolution of the degree of binder hydration index

The degree of hydration index is calculated from the results of UCS tests on GF samples with different binder contents and curing times up to 120 days. Table 3-5 presents the results of the calculations. The table shows that the rate of hydration is almost the same for 6% and 4.5% PCI (rate for 6% is slightly higher), while slower for 2% PCI, especially at early ages up to 7 days (Figure 3-3). Increasing the cement content in GF mixes speeds up the hydration reaction. More cement available in the mix means that more of the surface area is exposed to react with water. Furthermore, the hydration rate is a function of the composition of cementitious materials, the amount of cementitious materials, and water cementitious materials ratio (Schindler and Folliard, 2005). In general, higher cement content implies a higher hydration rate (e.g. Kalinski and Hippley, 2005).

Table 3-5 Degree of hydration index of various binder proportions

Curing time (days)	Degree of hydration (α%)	6% PCI	4.5% PCI	2% PCI
3	α_3	31	37	16
7	α_7	45	44	27
28	α_{28}	69	67	58
90	α_{90}	91	88	86
120	α_{120}	100	100	100

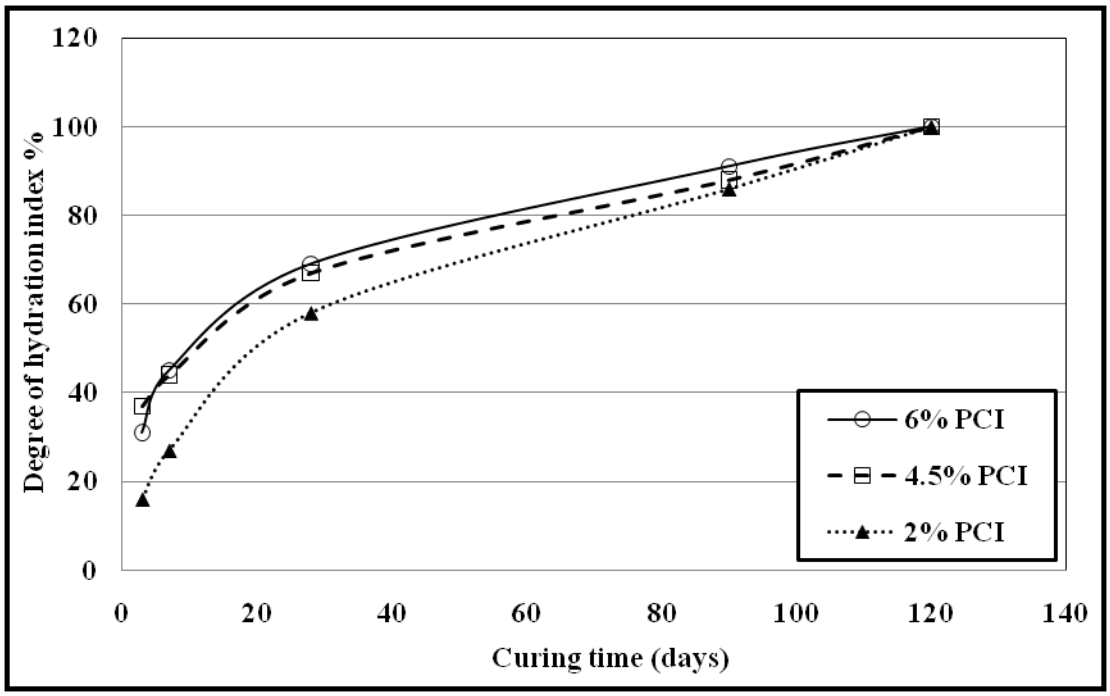

Figure 3-3 Degree of hydration index of various binder proportions

3.3.2 Evolution of the mechanical properties

Figure 3-4 shows the UCS evolution with curing time (Figure 3-4 a) and degree of hydration index (α) (Figure 3-4 b) of GF for different binder contents (6%, 4.5%, and 2%). It can be seen that the development of UCS values is related to the curing time, α, and binder content. A relationship between the UCS values and curing time or α is observed. When the hydration reaction advanced, more hydration products formed to fill the pores of the GF matrix (which enhance the UCS of GF). This is supported by the results of a thermal analysis on the cement paste of GF presented in Section 3.3.5 (will be discussed later). This filling of the pores results in decreasing the overall porosity (Figure 3-5) of the hardening cement matrix and thereby, increasing the strength. Furthermore, it is noticed that increasing the binder content will increase the UCS values of the GF. Increasing the binder content leads to increases in the rate of hydration (Figure 3-3). A higher cement hydration rate means higher UCS values. Indeed, faster cement hydration results in precipitation of larger amounts of cement hydration products, such as C-S-H and CH. C-S-H is the major contributor to strength of cementitious material (e.g., Taylor, 1990). In addition, an increase in binder content results in the precipitation of a larger amount of binder hydration products.

The evolution of porosity with curing time for various binder contents confirms the aforementioned arguments (Figure 3-5). For different binder contents, the differences in the porosity are noticeable at early ages. It can be seen that as the binder content increases, the porosity decreases. Furthermore, as the hydration process proceeds, the porosity of GF samples decreases (more hydration products lead to refining of the pore structures of cementitious materials). This is also in agreement with the results of the effect of binder

contents (7% and 9% wt) on the pore size distribution of GF presented in Figure 3.14 (will be discussed later).

Figure 3-6 shows a comparison between two mixes of different binders. The first mix contains only PCI while the other mix contains PCI and slag, 50:50. Both mixes have the same solids concentrations (73%) and same percentage of sodium silicate (0.4%). It can be observed that the mix with slag gives significantly higher UCS results. It is shown that the UCS value for the PCI-slag (slag-GF) mix at the ages of 28 and 56 days is more than two times the UCS value for the PCI mix. This can be explained as the result of the combined effects of the following mechanisms: (i) the filler effect of the slag grains (a behaviour that PCI grains are not able to achieve), which in addition to the binder hydration products, contribute to filling the pores of the slag-GF matrix, thereby refining its pore structure (Manmohan and Mehta, 1981; Fall and Samb, 2008); (ii) besides the C-S-H from the hydration of PCI, the CH produced by the hydration of PC activates the slag reactions, and thus produces additional C-S-H, which in turn, enhances the strength of the slag-GFs; (iii) the sodium silicate acts as an alkaline activator of the slag, which in turn, results in the stimulation of the hydration of slag and thus contributes to the strength development of slag-GFs. The PCI-slag mix results obtained in this study are in good agreement with the results obtained by Doucet et al. (2007). In summary, the results presented above suggest that the partial replacement of PCI by slag can significantly increase the UCS of GF. This could result in significant saving of binder consumption, i.e. reduction of the production costs of GF.

Furthermore, GF with PCI-slag (w/c = 8.2) has the same UCS values as the cemented paste backfill (slag-CPB) that was prepared by Celestin (2009) with a w/c ratio = 7.6 and the

same tailings and binder proportion (4.5%) and type (PCI/slag in a ratio of 50/50). These observed similar UCS values between the GF and CPB, despite the much higher w/c ratio of the GF, is attributed to the influence of the additive used in the GF (sodium silicate on the binder hydration) the strength development of GF and the evolution of the w/c within the GF. Indeed, it is generally agreed that soluble sodium silicate doubly contributes to strength development, both by acting as an alkaline activator and giving rise to the formation of a C-S-H of low C/S ratio (Fernandes- Jiménez et al., 2009). This activation results in an acceleration of the binder hydration. Combined with the formation of additional C-S-H gel due to the reaction of SiO_2 (formed in the hydrolysis of sodium silicate solution) with CH (generated by the hydration of the PC), this activitation contributes to the increase of GF strength. This scenario is not possible with CPB due to the absence of sodium silicate within this material. Furthermore, Doucet et al. (2007) and Hassani et al. (2007) reported that sodium silicate has the ability to absorb a significant quantity of water, thereby resulting in a decrease of the w/c ratio of the GF. It is well known that a lower w/c ratio is associated with higher strength for a given cementitious material cured in the same conditions (e.g., Sideris and Konsta-Gdoutos, 1996).

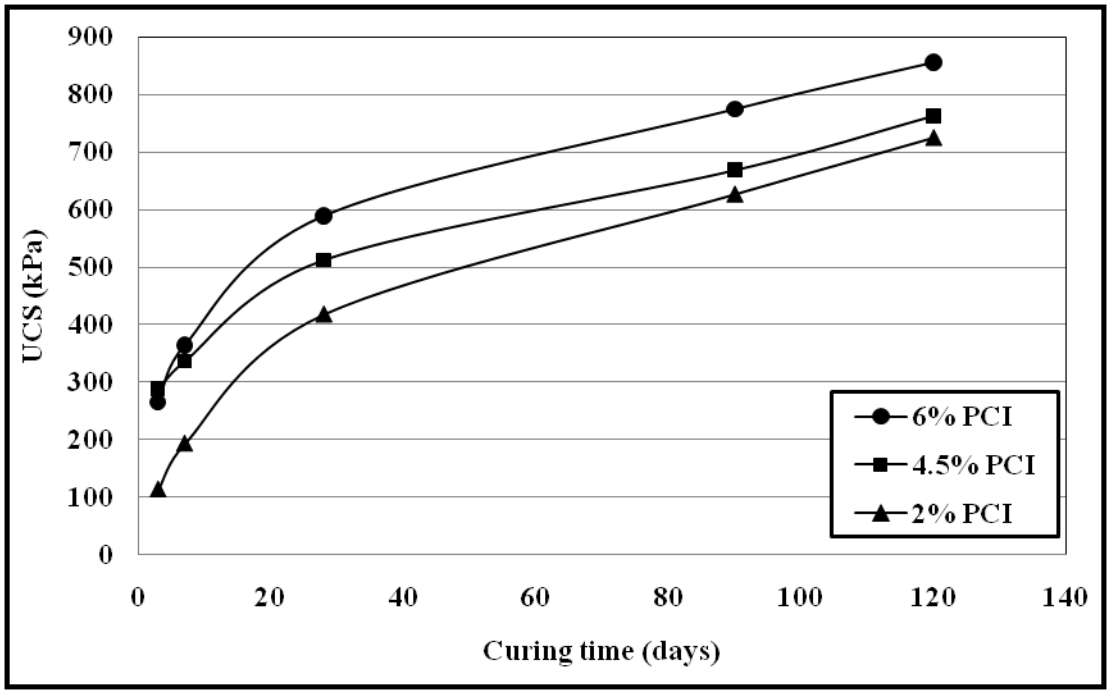

a)

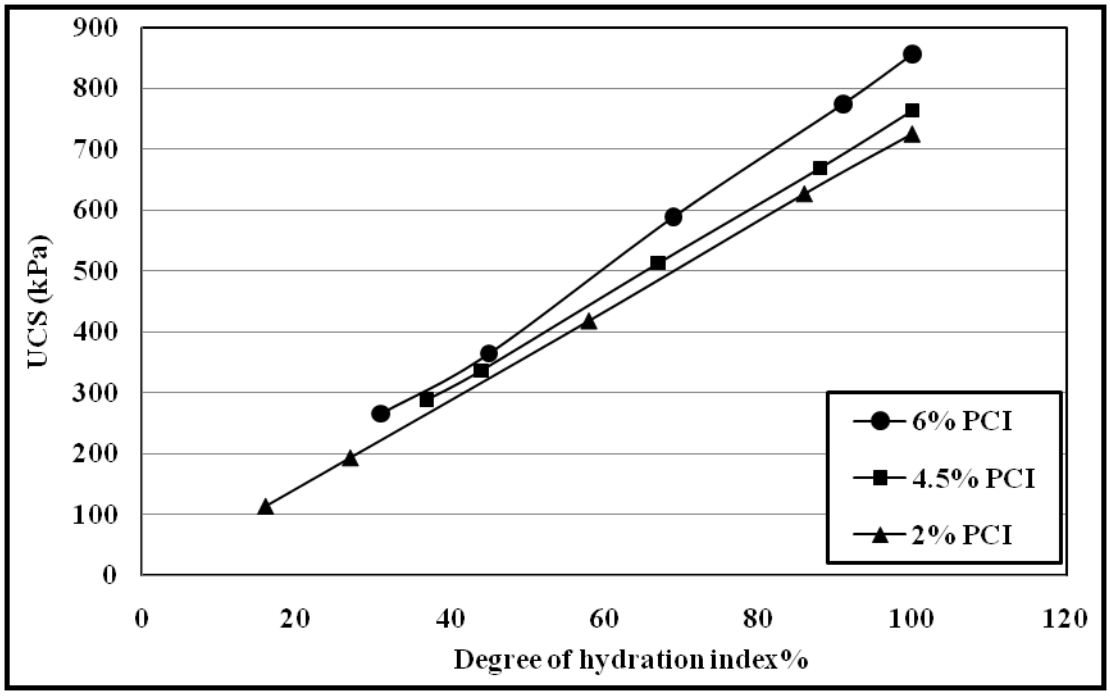

b)

Figure 3-4 UCS evolution of GF for various binder contents with (a) curing time, (b) binder hydration degree index (α)

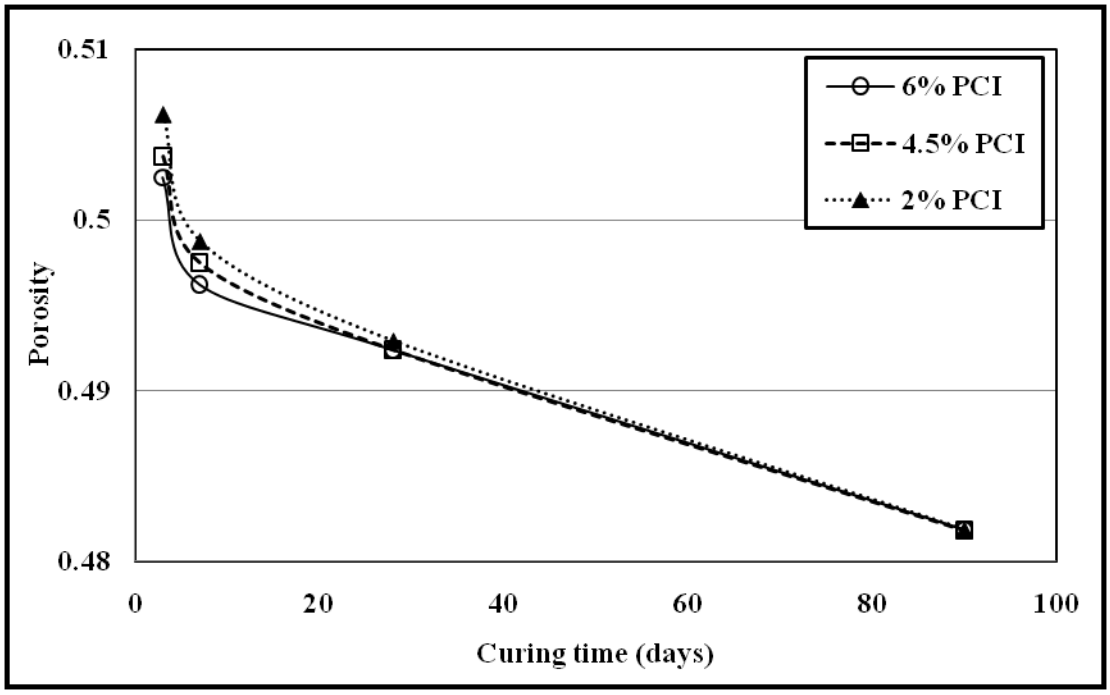

Figure 3-5 Evolution of porosity with curing time for various binder contents

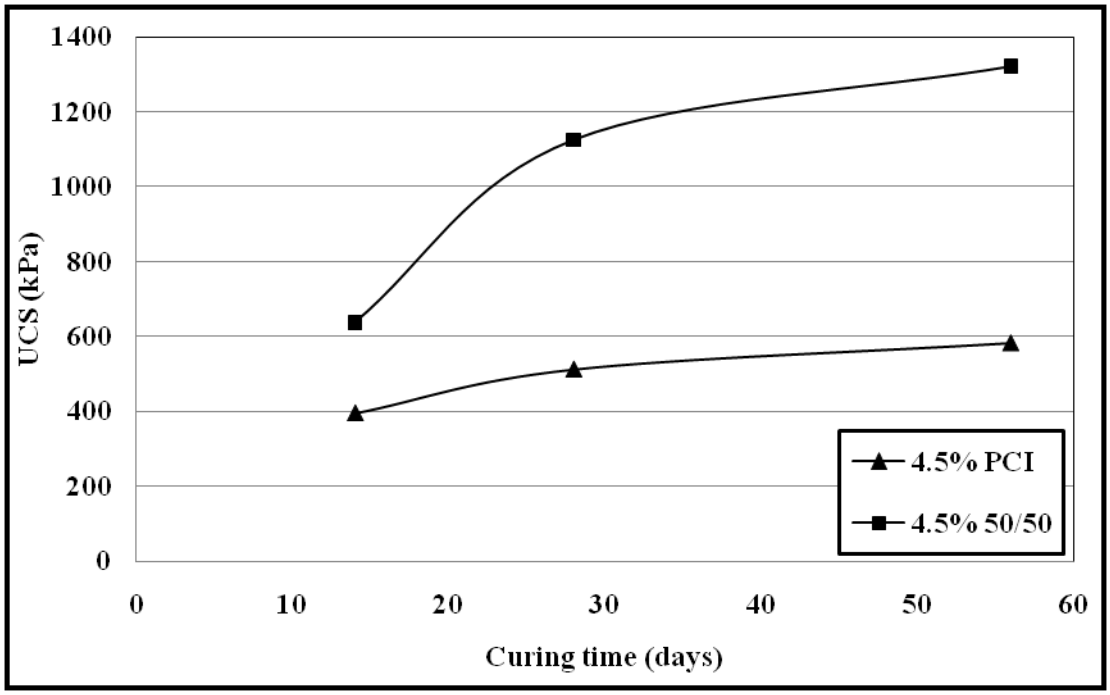

Figure 3-6 UCS evolution of GF for various mixes (PCI, PCI/Slag) with 4.5% binder content

3.3.3 Evolution of the hydraulic properties

The effects of the binder proportion (% PCI), curing time, and degree of binder hydration index on the saturated hydraulic conductivity (k_{sat}) of GF were examined. The results of the saturated hydraulic conductivity tests are illustrated in Figure 3-7. It can be seen that k_{sat} decreases when curing time (Figure 3-7a) and degree of binder hydration index (Figure 3-7b) increases for the three mixes. It is obvious that the effect of curing time or degree of hydration index on saturated hydraulic conductivity is significant. This behaviour is due to the increase in the degree of cement hydration with time (Figure 3-3). As a result, the formation of hydration products (e.g. C-S-H, CH) increases (see Section 3.3.5) which in turn, leads to refinement of the pore structure and reduction in the porosity of the GF materials (Figure 3-5). This reduction occurs by filling the pores of the GF matrix and blocking the interconnected pores with hydration products. This increase of hydration products formed as the curing time increases is graphically demonstrated by the results of a thermal analysis presented in Section 3.3.5 (to be discussed in Section 3.3.5).

On the other hand, it can be observed that the binder content significantly influences the saturated hydraulic conductivity of GF materials especially at early ages. As the binder content increases, the saturated hydraulic conductivity decreases. The reason is that an increase in binder content leads to more precipitation of the hydration products (e.g. C-S-H, CH) in the GF matrix, thus causing a refinement in the pore structure and reduction in the porosity of the GF as shown in Figure 3-14.

The UCS is often used in practice to evaluate the geotechnical properties of cemented backfill structures. In addition, it is assumed that the progress of the UCS of GF gives a good indication of the degree of binder hydration and the microstructure development of

GF. It is known that the GF microstructure (pore size distribution and porosity) influences its hydraulic conductivity. Furthermore, a relationship is found between UCS and hydraulic conductivity of CPB materials (Fall et al., 2009). This formula (Equation 3-3) is used in this paper to predict the k_{sat} of GF materials (Figure 3-8). It can be seen that there is a good agreement between the predicted and experimental values. This means that the model used to predict the k_{sat} for CPB in Fall et al. (2009) is also applicable to predict the k_{sat} for GF.

$$K = k_T A(UCS_t/UCS_{max})^B \qquad \text{Equation (3-3)}$$

where k_T is the saturated hydraulic conductivity of the tailings used, UCS_t (kPa) is the uniaxial compressive strength of the cemented backfill for a given time, UCS_{max} (kPa) is the maximal UCS of the cemented backfill; and A and B are the adimensional fitting parameters to be determined for each cemented backfill mix. In this study; A= 23.8 for 6% PCI, 29.4 for 4.5% PCI, and 18.9 for 2% PCI while B = -1.05 for all mixes.

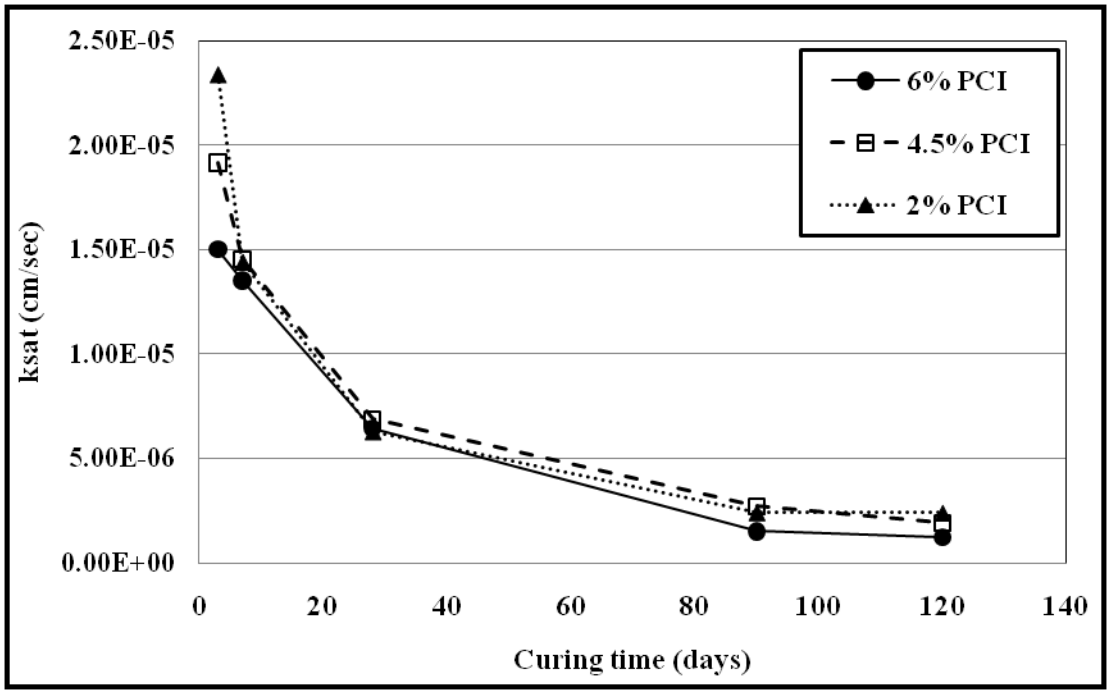

a)

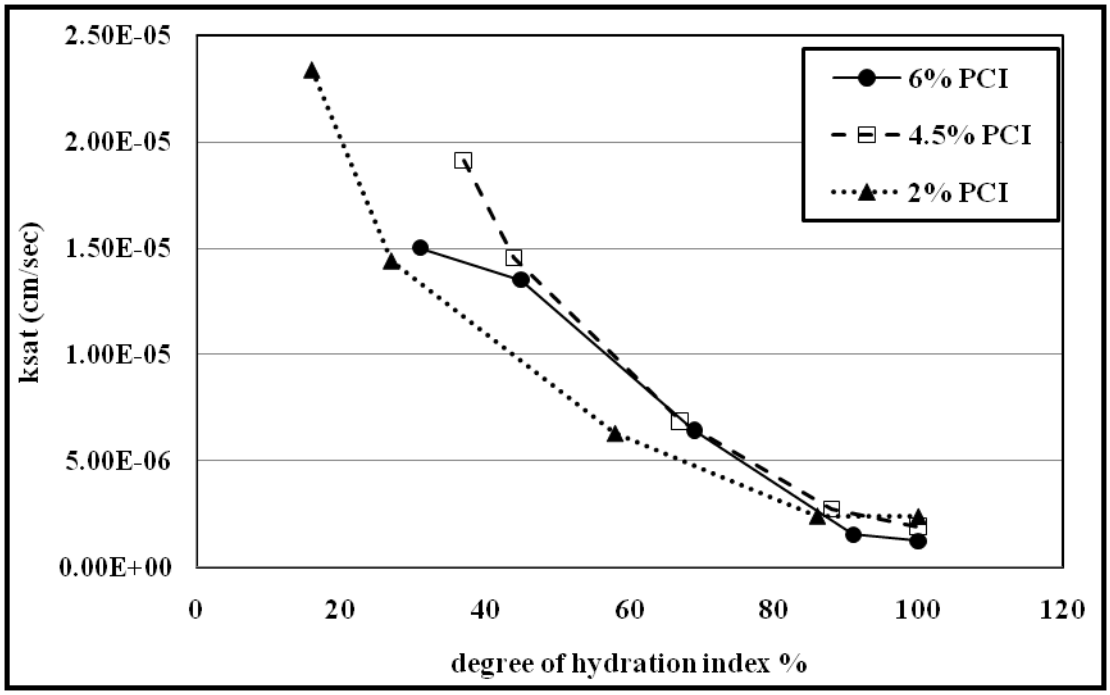

b)

Figure 3-7 The saturated hydraulic conductivity evolution of GF for various binder contents with (a) curing time, (b) degree of binder hydration index (α)

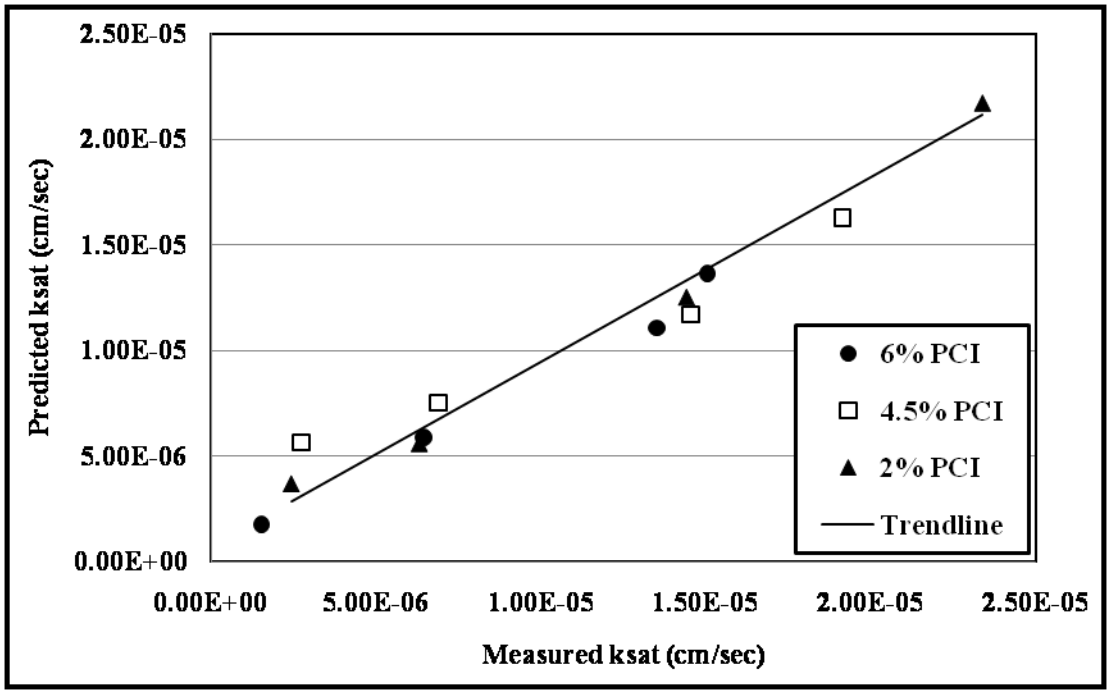

Figure 3-8 Predicted vs. measured saturated hydraulic conductivity of GF

3.3.4 Evolution of the thermal properties

Figure 3-9 shows the variation of the thermal conductivity (K) of GF in relationship to the curing time (Figure 3-9a) and degree of binder hydration index (Figure 3-9b). Samples that contain 2%, 4.5%, and 6% PCI and cured at room temperature were tested to measure their thermal conductivity. The outcomes of this test show that the binder content slightly affects the thermal conductivity of GF. The range of the measured K was 1.0 to 1.75 W/m°C. The differences in the K values are more obvious at early ages. Higher binder proportion in GF causes formation of more hydration products and reduction in w/c ratio. The increase in the hydration products induced porosity reduction in GF (Figure 3-5) and pore size refinement (Figure 3-14). Reducing the porosity and refinement of the pore size of the GF matrix lead to an increase in the density of cemented materials and thus to an increased thermal

conductivity as experimentally observed by Demirboga (2007). From Figure 3-9, it can be seen that the thermal conductivity of GF is dependent on curing age for a given cement content. It can be noticed that there is a drop in the K values of GF between 3 and 7 days curing. In order to understand this drop in K, microstructural analyses are required to perform on gelfill samples cured at 3 and 7 days. However, after 7 days, the K tends to increase with curing time. This increase can be attributed to the reduction of the porosity of the GF with the advancement of the curing time as shown in Figure 3.5. This lower porosity results in more compact or denser GF material, thereby leading to higher thermal conductivity. It is well known that higher density is associated with a higher thermal conductivity (Dmirboga, 2007). Similar observations were made by Celestin and Fall (2008) who studied the thermal conductivity of CPB materials. However, the thermal conductivity of CPB (with the same mix components) found by Celestin (2009) is around 2 W/m°C, which is higher than the K measured in this study. This reduction in the thermal conductivity of GF is due to addition of sodium silicate which has a low thermal conductivity (0.65 W/m°C).

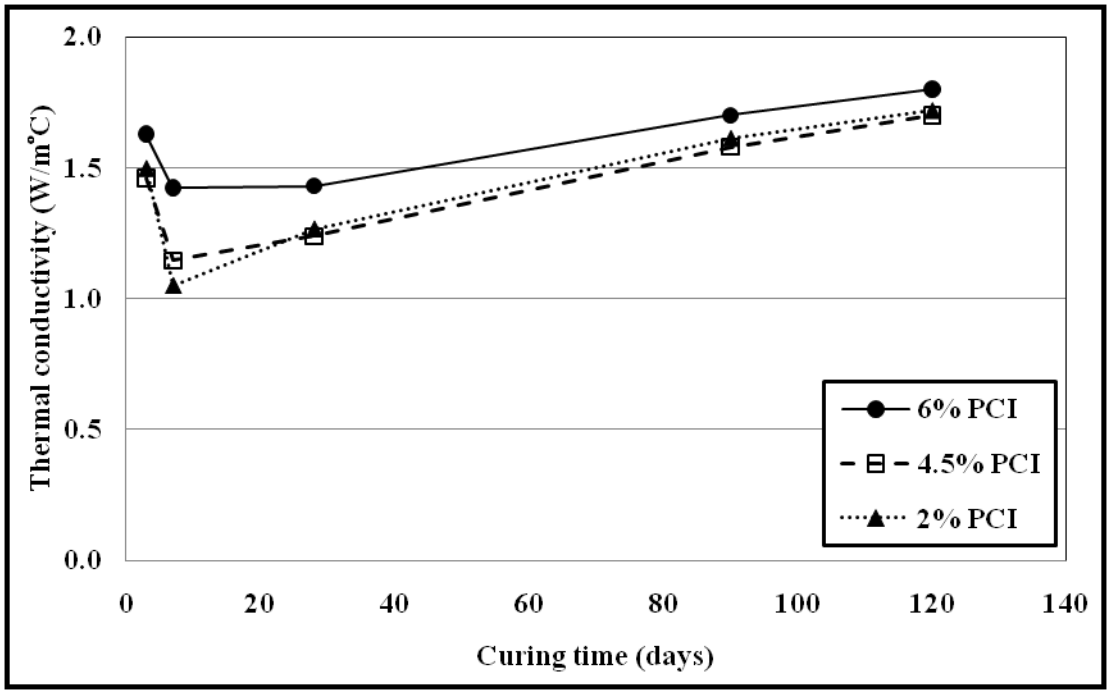

a)

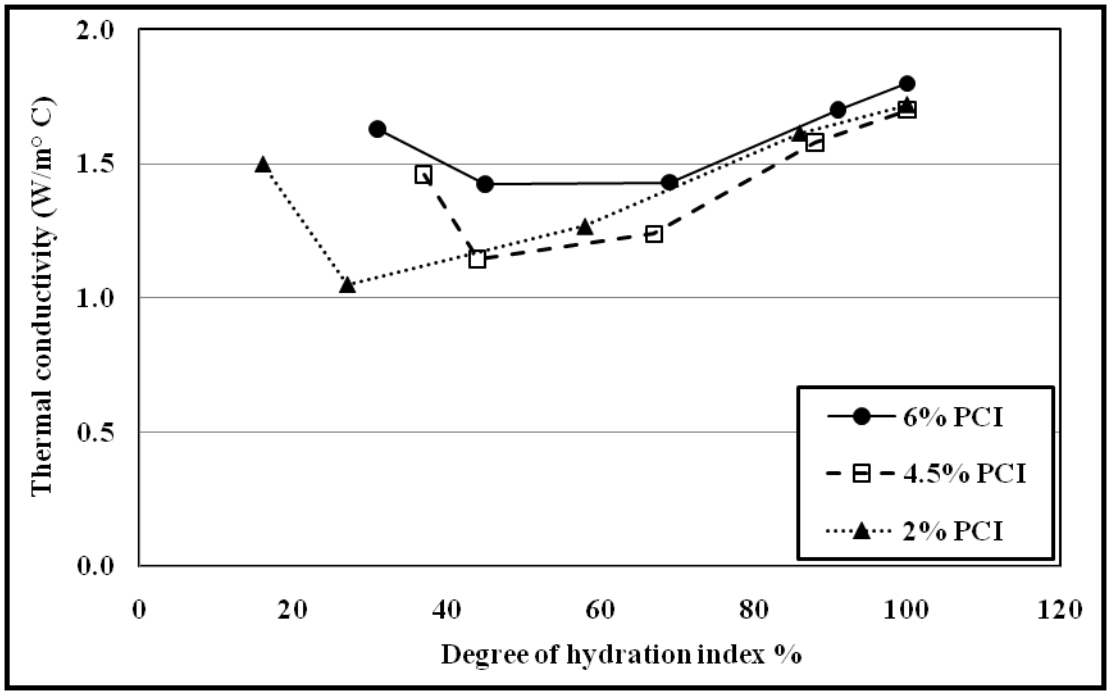

b)

Figure 3-9 Effect of binder proportion on thermal conductivity of GF with (a) curing time, (b) binder hydration degree index (α)

3.3.5 Evolution of the microstructural properties

Figures 3-10, 3-11, 3-12, and 3-13 present a TGA-DTA/DSC diagram of the cement paste of GF made of PCI (i.e. PCI cement paste with sodium silicate) and cured for 7 and 28 days. Figures 3-11 and 3-13 show the heat flow in a relationship with temperature for GF samples cured for 7 and 28 days, while Figures 3-10 and 3-12 show weight loss and derivative weight loss versus temperature. Three endothermic peaks can be seen due to the weight loss and transformations of hydration products (Figures 3-10 and 3-12). The main peak occurs at 400-500ºC, resulting from the decomposition of CH. The first peak or weight loss is located between 80ºC and 200ºC. This peak results from the dehydration reactions of ettringite, gypsum, C-S-H and calcium aluminate (Anderberg, 1997; Zhou and Glasser, 2001). The third peak appears at temperature ranges between 650-750ºC. This loss is attributed to the decomposition of amorphous carbonated phases and well crystallized calcite ($CaCO_3$). When the DTG/DTA diagrams of cement pastes of GF cured at 7 and 28 days were compared, the outcomes showed that the weight losses are higher for cement paste cured at 28 days. This is explained by the increase in the amounts of C-S-H, ettringite, CH and $CaCO_3$ formed with the curing time, which in turn, results in the refinement of the porosity of the GF as shown in Figure 3.5. Furthermore, a refinement of the pore structure of GF, due to the formation of higher amounts of binder hydration products, should also be expected when the binder content of the GF increases. This is confirmed by the results of mercury intrusion porosity (MIP) tests performed on two GF samples with 7 wt% and 9 wt% binder contents, respectively, and presented in Figure 3-14. This figure shows that increasing binder content is associated with increasing proportions of macroporosity (>1 μm). It can be seen that the GF with higher binder content (9 wt %)

has lower proportions of macroporosity (1-10 μm, >10 μm) and higher proportions of fine pores (<1 μm) than GF with lower binder content (7 wt %).

Fall and Samb (2008) conducted a TGA/DSC analysis on cement paste of CPB samples (cement paste with w/c = 2 and without sodium silicate) cured at 20ºC for 28 days (Figure 3-15). It can be noticed that the weight losses from the GF samples at the second and third peaks are higher than the weight losses from the CPB samples. In the first peak, we have an overlap of the signatures of C-S-H, ettringite, gypsum; therefore, the amount of C-S-H gel formed in the cement paste with and without sodium silicate cannot be compared. Thus, it appears that GF samples produce more hydration products than CPB samples due to the influence of sodium silicate on binder hydration, strength development and water absorption as previously explained.

This contribution of sodium silicate to the formation of more hydration products is also confirmed by the results of XRD tests. Examples of XRD patterns of the hardened paste of CPB and GF for 28 days curing times are shown in Figures 3-16 and 3-17. It can be seen that XRD patterns are the same for both mixes. However, the results show that the peak of CH at 18, 47, 51 degree 2-theta for GF samples is higher in intensity than CPB samples, except for the intensity of CH at 34 degree 2-theta for the GF sample, which is lower than the CPB sample. Furthermore, the intensity of C-S-H at 32 degree 2-theta for GF is slightly higher than CPB.

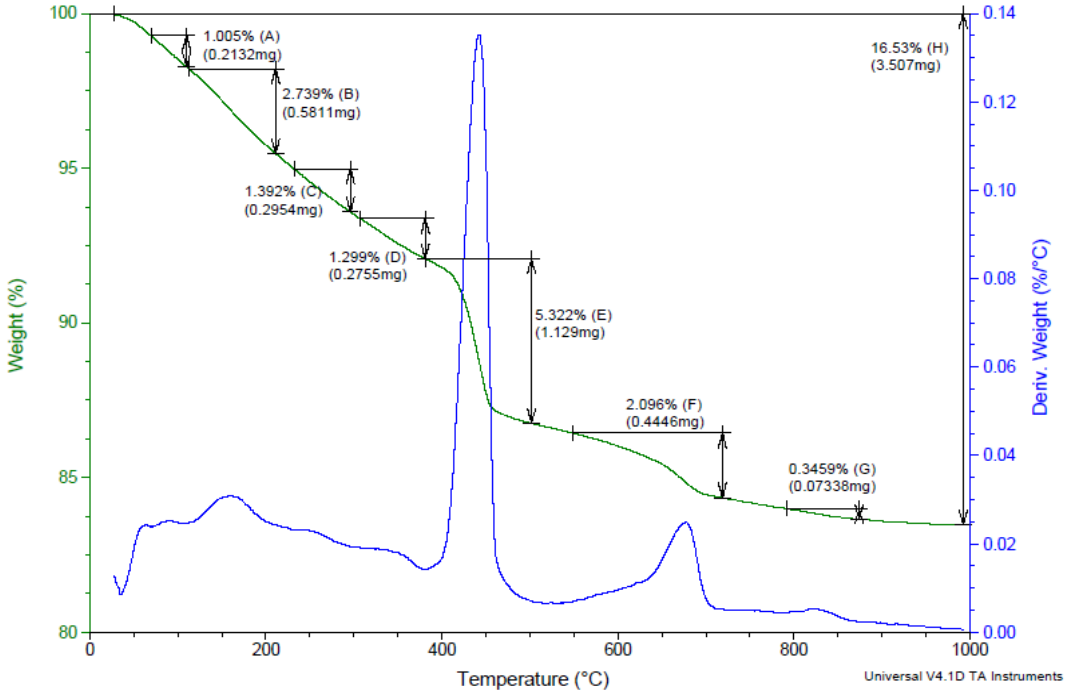

Figure 3-10 Thermal behaviour (TGA/DTA) of the hardened Portland cement pastes of GF with w/c ratio=2 cured at 7 days

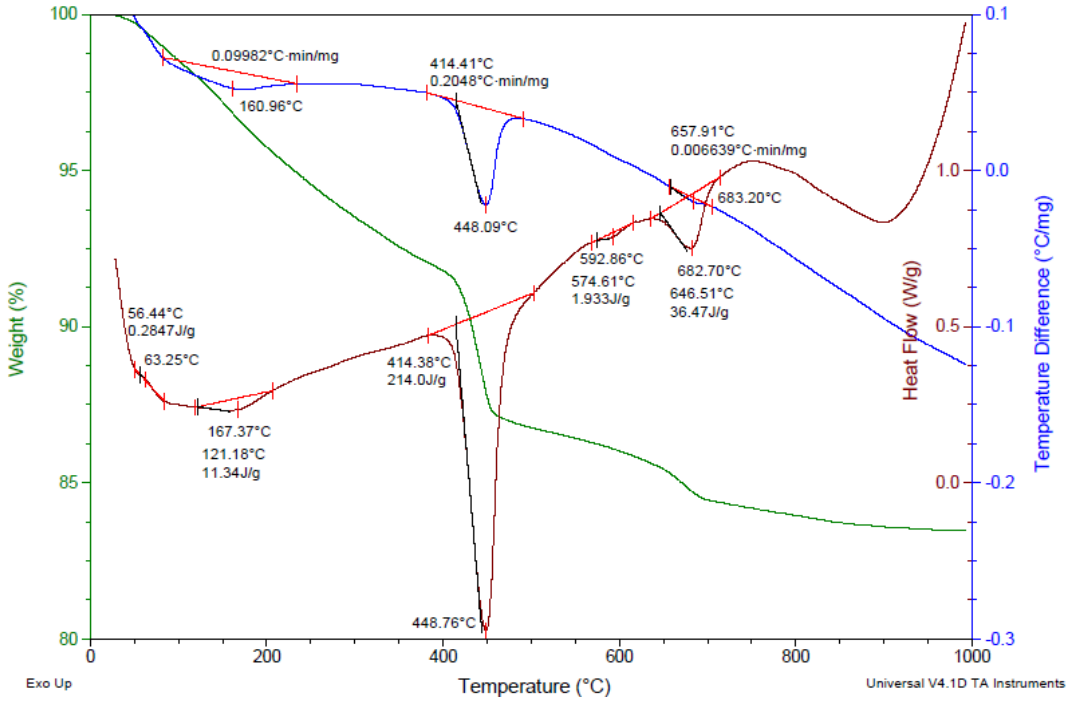

Figure 3-11 Thermal behaviour (DTA/DSC) of the hardened Portland cement pastes of GF with w/c ratio=2 cured at 7 days

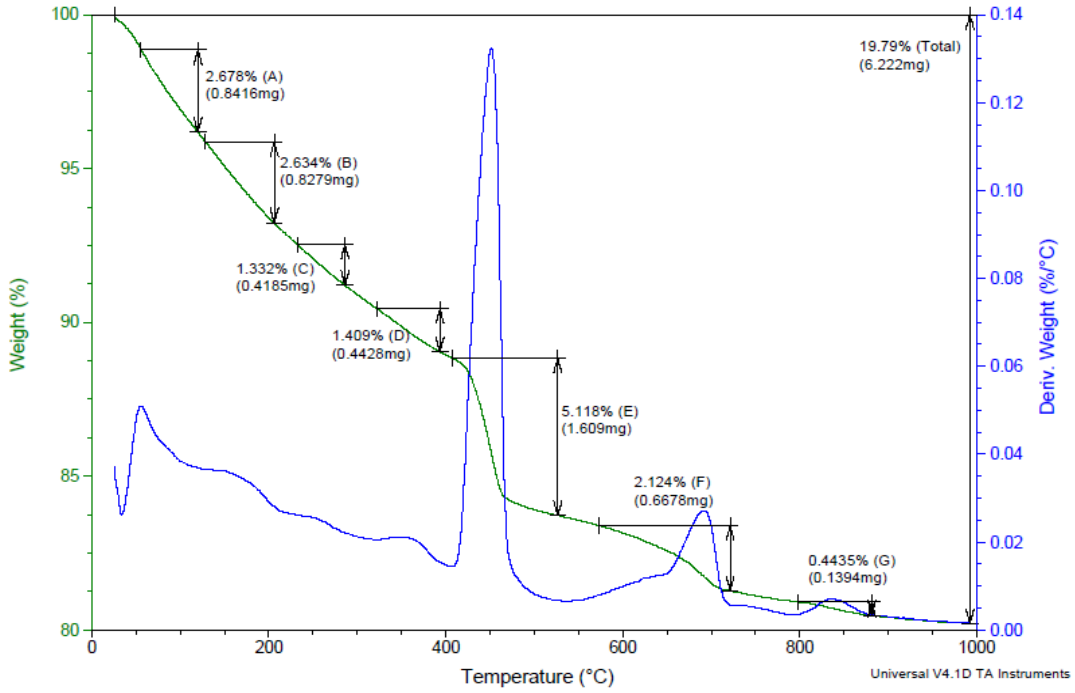

Figure 3-12 Thermal behaviour (TGA/DTA) of the hardened Portland cement pastes of GF with w/c ratio=2 and 28 days curing time

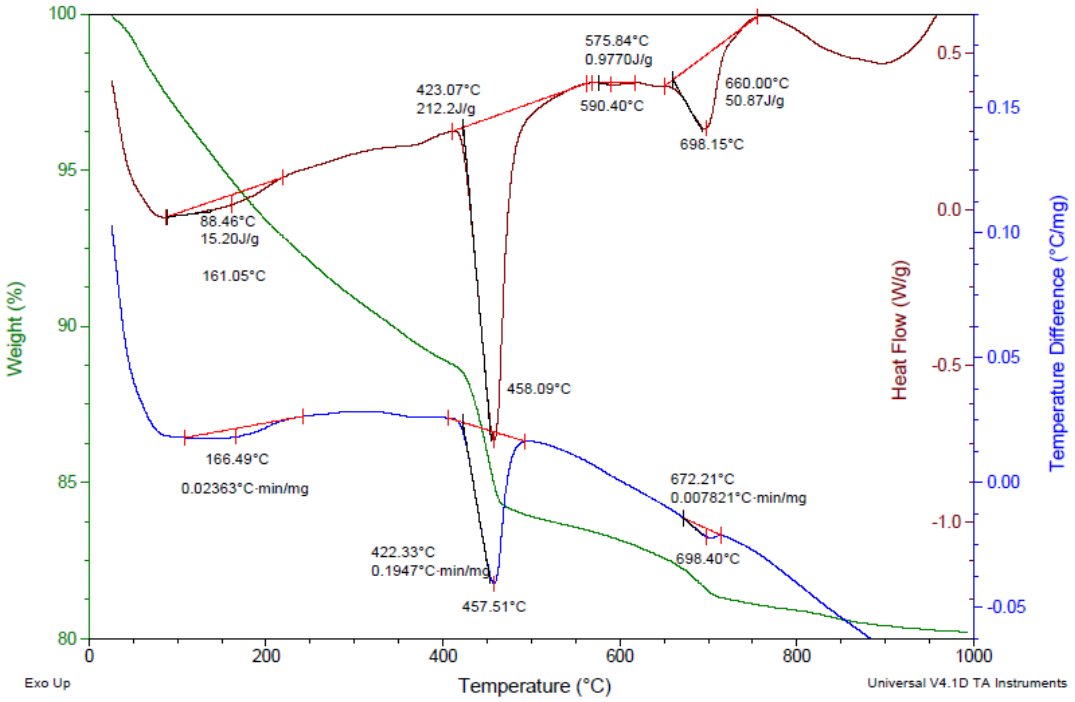

Figure 3-13 Thermal behaviour (DTA/DSC) of the hardened Portland cement pastes of GF with w/c ratio=2 and 28 days curing time

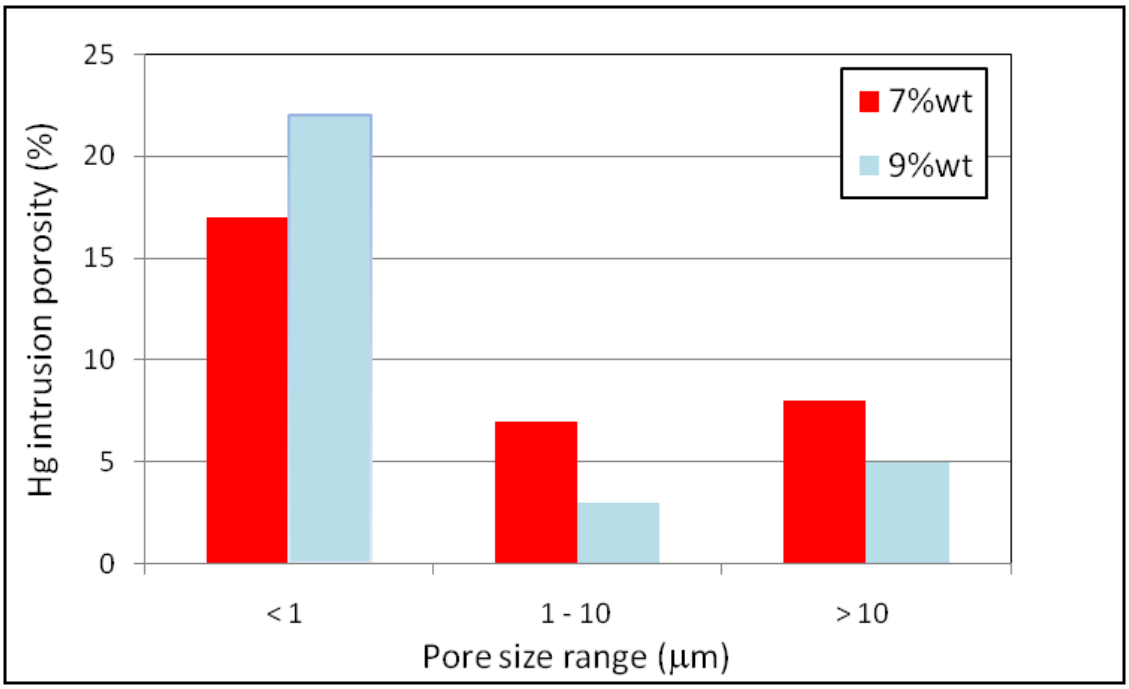

Figure 3-14 Effect of binder content on the pore size distribution of GF paste backfill cemented with PCI/slag vs. content of fines and pore size range (data from Hassani et al., 2007)

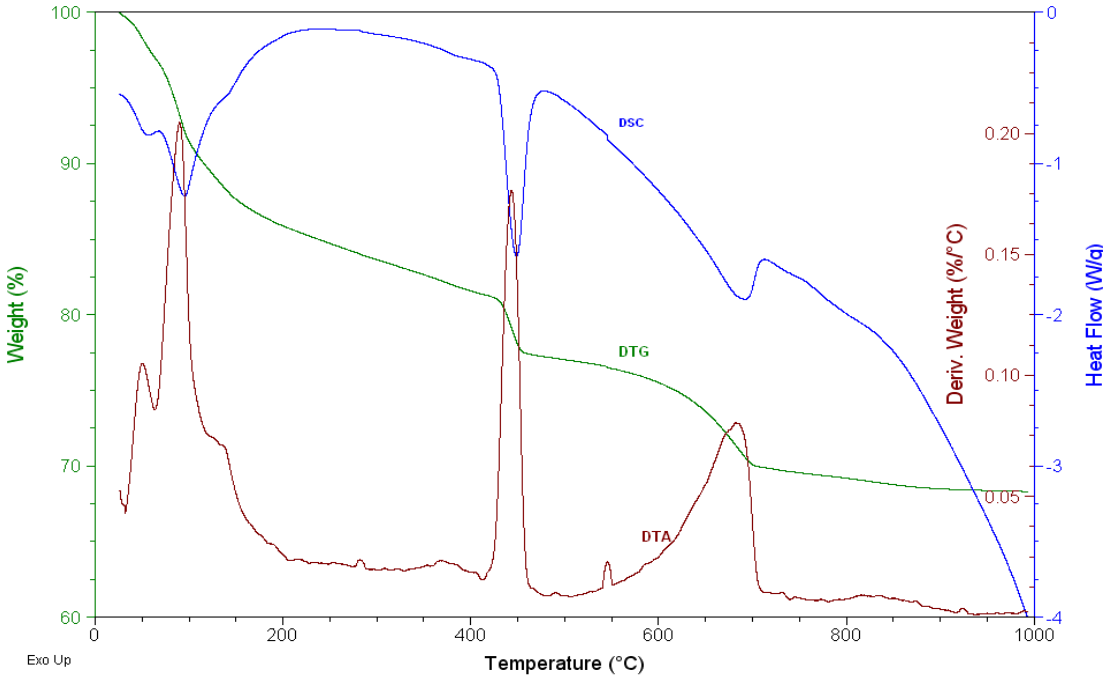

Figure 3-15 Thermal behaviour (DTA/DSC) of hardened Portland cement pastes of CPB with w/c ratio=2 and 28 days curing time (Fall and Samb, 2008)

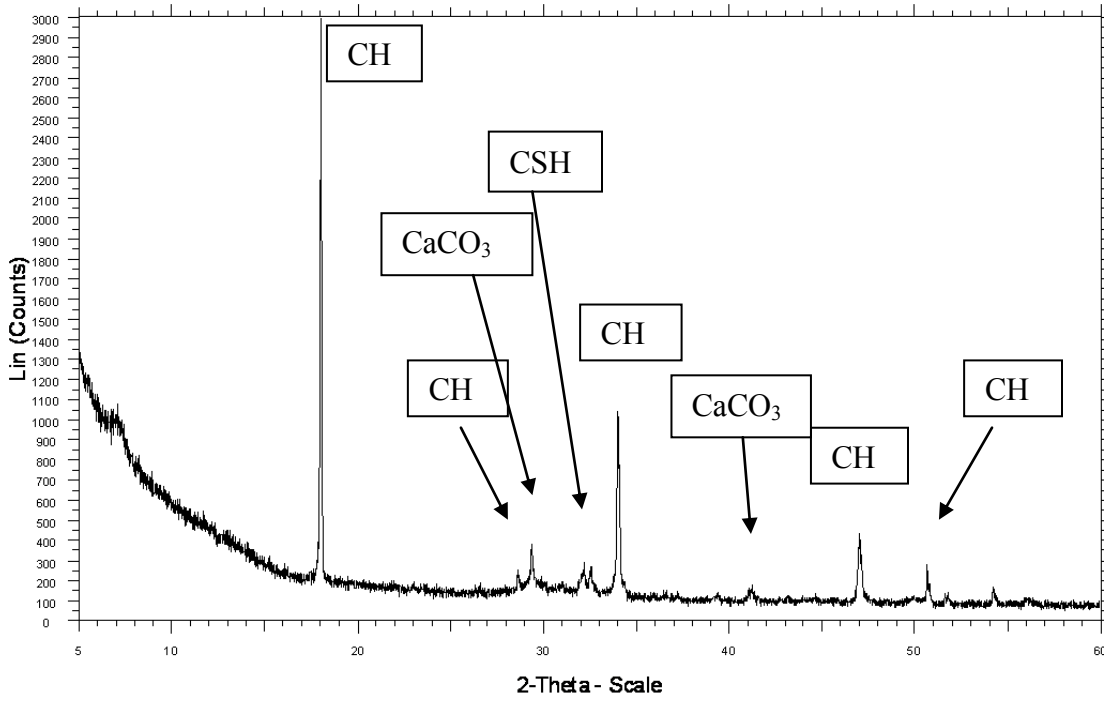

Figure 3-16 XRD patterns of hardened cement without sodium silicate (i.e. hardened cement of CPB) cured at 20ºC for 28 days

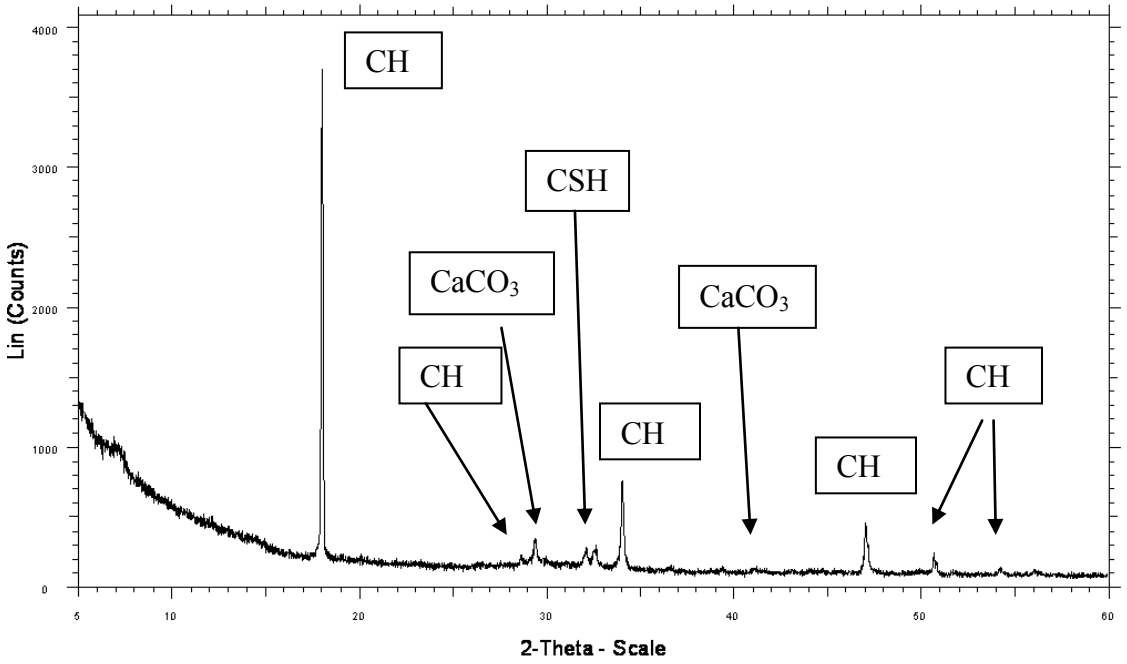

Figure 3-17 XRD patterns of GF cured at 20ºC for 28 days

3.4 Summary and conclusions

In this paper, experimental studies have been conducted on GF samples to investigate the evolution of their thermal, hydraulic, mechanical, and microstructural properties. Samples are tested to obtain their thermal conductivity, saturated hydraulic conductivity, UCS and microstructure. The degree of binder hydration index has been estimated. Different binder contents are adopted (2%, 4.5%, and 6%) which correspond to w/c ratios of 18.5, 8.2, and 6.2, respectively. The used amount of sodium silicate is 0.4 wt %, and the samples were cured in room temperature for 3, 7, 28, 90, and 120 days.

Based on the results, it can be concluded that thermal, hydraulic, mechanical and microstructural properties are strongly time-dependent or affected by the degree of binder hydration index. Mechanical properties are affected by binder content, binder types, degree of hydration index and curing time. The evolution of UCS values is a function of curing time, degree of hydration index and binder content. As the binder contents increase, the UCS values of GF samples increase with curing time or with increases in the degree of binder hydration index. Increasing the cement content in GF mixes speeds up the hydration reaction. More available cement in the mix means more exposed surface area to react with water. In general, higher cement content means higher rate of hydration, and thus higher UCS.

Also, using PCI-slag as a binder in GF mix gives higher strength than a mix that contains only PCI. This is due to the fact that aside from the filler effect of slag, sodium silicate contributes to the activation of the slag and formation of additional C-S-H gel. On the other hand, the UCS values of slag-GF with w/c ratio = 8.2 are the same as slag-CPB with w/c

ratio = 7.6. This is due to the ability of sodium silicate to form gel, quicken the binder hydration and reduce the w/c ratio by absorbing part of the excess water.

The saturated hydraulic conductivity of GF is influenced by binder contents especially at early ages. The hydraulic conductivity of GF decreases as the binder content increases and the degree of binder hydration index increases. In addition, a relationship is found between the UCS and saturated hydraulic conductivity. As the UCS increases, the saturated hydraulic conductivity decreases. In addition, the model used to predict the k_{sat} for CPB in Fall et al. (2009) is also applicable to predict the k_{sat} for GF. This model can be useful for estimating the saturated hydraulic conductivity of GF.

The binder content and curing time significantly influence the thermal conductivity. The thermal conductivity drops between 3 and 7 days and then after 7 days, it tends to increase with curing time. However, the thermal conductivity of GF samples is lower than the thermal conductivity of CPB samples. This reduction in the thermal conductivity of GF is due to the addition of sodium silicate which has a low thermal conductivity (0.65 W/m°C).

When the DTG/DTA diagrams of cement pastes of GF cured at 7 and 28 days were compared, the outcomes showed that the weight losses are higher for cement paste of GF cured at 28 days. This is explained by the increase in the amounts of C-S-H, ettringite, CH and calcite formed with the increase in degree of hydration. Furthermore, TGA/DSC and XRD analyses show that loss of weight and intensity of CH are higher in GF than CPB. This means that sodium silicate enhance the binder hydration process in addition to its ability in capturing the excess water.

This study provides essential information for understanding the evolution of the thermal, hydraulic, mechanical, and microstructural properties of GF. The findings of this paper will help mining operators and engineers who work with GF materials to take into consideration, the design, environmental aspects, and durability assessment of GF structures. It is also useful to predict the potential formation of AMD in GF structures.

3.5 References

American Society for Testing and Materials, Test method for compression strength of cylindrical concrete specimens: C39/C39M-03 Annual book of ASTM, Pennsylvania, 2004.

American Society for Testing and Materials, Test method for measurement of hydraulic conductivity of saturated porous materials using a flexible wall permeameter: D5084-00, Annual book of ASTM, Pennsylvania, 2004.

Anderberg Y. Spalling phenomena of HPC and OC. In Proceeding of the International Workshop on Fire Performance of High-Strength Concrete, NIST (1997).

Celestin, J.C. Geotechnical properties of cemented paste backfill and tailings liners: effect of mix components and temperature. University of Ottawa (2008) 1-221.

Celestin, J. C. H., Fall, M. Thermal conductivity of cemented paste backfill material and factors affecting it. International Journal of Mining, Reclamation and Environment (2009) 1-17.

Demirboga, R. Thermal conductivity and compressive strength of concrete incorporation with mineral admixtures. Building and Environment 42 (2007) 2467−2471.

Doucet, C., Tarr, K., and Swan, G. Evaluation of the effect of mixing method, sequence and time on the properties of gelfill. Mine fill 2007, 2488.

Fall, M., Adrien, D., Celestin, J.C., Pokharel, M., Toure, M. Saturated hydraulic conductivity of cemented paste backfill. Minerals Engineering 22 (2009) 1307-1317.

Fall, M., Belem, T., Samb, S. and Benzaazoua, M. Experimental characterization of the stress–strain behaviour of cemented paste backfill in compression. Springer Science Business Media (2007) 1-9.

Fall, M., Benzaazoua, M. and Ouellet S. Experimental characterization of the influence of tailings fineness and density on the quality of cemented paste backfill. Minerals Engineering 18 (2005) 41–44.

Fall, M., Benzaazoua, M. and Saa, E.G. Mix proportioning of underground cemented tailings backfill. Tunnelling and Underground Space Technology 23 (2008) 80–90.

Fall, M., Celestin, J. C., Pokharel, M., Toure, M. A contribution to understanding the effects of curing temperature on the mechanical properties of mine cemented tailings backfill. Engineering Geology 114 (2010) 397–413.

Fall, M., Nasir, O., and Celestin, J. Paste backfill responses in deep mine temperature conditions. In: 9th International Symposium of mining with backfill. Montreal, Canada: CD-Rom; 2007 paper 2522.

Fall, M., Samb, S.S. Pore structure of cemented tailings materials under natural or accidental thermal loads. Materials Characterization 5 9 (2008) 5 9 8 – 6 0 5.

Hassani, F, Razavi, S.M., and Isagon, I. A study of physical and mechanical behaviour of gelfill. Mine fill, 2007 Paper 28.

Kalinski, Michael E., Hippley, Brian T. The effect of water content and cement content on the strength of portland cement-stabilized compacted fly ash. Elsevier Ltd, Vol 84 (2005); 1812-1819.

KD2 Operator's Manual (2006) 1-24.

Khokholov, Yu. A., Kurilko, A.S. Heat exchange and filling masses in Kimberlite mining. Journal of Mining Science Vol. 40, No.1, 2004.

Manmohan, D., Mehta, P.K., (1981). Influence of pozzolanic slag, and chemical admixtures on pore size distribution and and Permeability of Hardened Cement Pastes. Journal of Cement, Concrete and Aggregates, 3, 63–67.

Neville, A. M. Properties of concrete. Forth Edition, (1995): 1-844.

Nicholson, Ronald V., Gillham, Robert W., Cherry, John A., Reardon, Eric J. Reduction of acid generation in mine tailings through the use of moisture-retaining cover layers as oxygen barriers. Canadian Geotechnical Journal, Vol. 26, (1989) 1-8.

Orejarena, L. Fall, M. Mechanical response of a mine composite material to extreme heat. Springer-Verlag (2008) 67:387–396.

Paynter, James T. Dodd, James C. The design, commissioning and operation of the golden gaint paste backfill plant. 29th annual meeting of Canadian mineral processors (division of the CIM) (1997) 382-403.

Pokharel, M. Geotechnical and environmental responses of paste tailings systems to coupled thermo-chemical loadings. University of Ottawa (2008) 1-248.

Rha, Chong Y., Kim, Chang E., Lee, Chul S., Kim, Ki I., Lee, Seung K. Preparation and characterization of absorbent polymer-cement composites. Cement and Concrete Research 29 (1999) 231-236.

Schindler, Anton K., Folliard, Kevin J. Heat of hydration models for cementitious materials. ACI Materials Journal (2005); 102-M04.

Silva, Denise A., Monteiro, Paulo J. M. The influence of polymers on the hydration of Portland cement phases analyzed by soft X-ray transmission microscopy. Cement and Concrete Research 36 (2006) 1501-1507.

Skripkiunas, G., Janavicius, E. Effect of Na2O.nSiO2 Nanodispersion on the strength and durability of Portland cement matrix. Materials Science 16 (2010).

Taylor, H.F.W., Cement Chemistry, London: Academic,1990.

Vick, 1990 S.G. Vick, Planning, BiTech Publishers Ltd, Design and Analysis of Tailings Dams (1990).

Yilmaz E., Kesimal A., Deveci H., Ercikdi B. The factors affecting the performance of paste backfill; physical, chemical and mineralogical characterization. First Engineering Sciences Congress for Young Researcher (2003).

Zhou, Q., Glasser, F. P. Thermal stability and decomposition mechanisms of ettringite at <120 º C. Cement Concrete Research 2001; 31 (9): 1333-1339.

3.6 Acknowledgement

The authors would like to acknowledge National Sciences and Engineering Research Council (NSERC), University of Ottawa and the National Research Council (NRC) of Canada.

Chapter 4

Technical Paper II

Unsaturated Hydraulic Properties of Gelfill

Abstract

From a design point of view, the durability of GF structures is considered as a key factor. Due to the fact that GF structures are cementitious porous materials, their durability depends on their ability to resist the flow of aggressive elements (water and oxygen). Thus, understanding the unsaturated hydraulic properties of GF is essential for a more cost-effective and durable design. However, there is a lack of information with regards to unsaturated hydraulic properties, the factors that affect them and their evolution with time. Hence, the unsaturated hydraulic properties of GF samples are investigated in this paper. Furthermore, functions are developed to predict the evolution of air entry values (AEVs), residual water content and fitting parameters of the van Genuchten model with degree of hydration index.

Various binder proportions (2%, 4.5%, and 6% PCI), w/c ratios (18.5, 8.2, and 6.2), and 0.4% (by weight of solids) sodium silicate type N are used. The samples are cured in room temperature for 3, 7, 28, and 90 days. Saturated hydraulic conductivity tests have been conducted; WRCs are determined by using a WP4-T dewpoint potentiameter and the saline solution method. Unsaturated hydraulic conductivity is predicted using the van Genuchten (1980) equation. The WRC is determined as the relationship between volumetric water content and suction for each mix and curing time. The van Genuchten (1980) equation is used to simulate the WRC to best-fit the experimental data. AEV, residual water content,

void ratio (*e)* and porosity (porosity*)* are also computed for each mix and curing time. Important outcomes have been achieved with regards to unsaturated hydraulic conductivity. The unsaturated hydraulic conductivity of GF decreases when the suction, binder content, and degree of hydration index increase. The effects of binder content and degree of hydration index are more obvious at low suction ranges. The results can be used to estimate the long term durability and environmental performance of GF structures.

Keywords: unsaturated hydraulic conductivity, water retention curve, air-entry value, residual water content, gelfill, cemented paste backfill

4.1 Introduction

The generation of acid mine drainage (AMD) which results from the oxidation of sulphide-bearing tailings is considered as one of the major environmental problems that is challenging the mining industry. A massive amount of sulphide-bearing tailings are generated by mine activities around the world each day. These tailings should be perfectly controlled to avoid destructive impacts on the environment. Therefore, ways to effectively and economically limit the environmental impacts caused by AMD have always been a main issue for all mining operations (Yilmaz et al., 2008). It is worth mentioning that Georgius Agricola wrote in his 16th century classic, De Re Metallica, that 'when the ores are washed, the water that has been used poisons the brooks and streams and either destroys the fish or drives them away'(Divas and Ritchie, 1986).

Several techniques have been developed in recent years to mitigate the problem associated with AMD. One of the techniques that have become increasingly popular in underground mining operations around the world is recycling the waste in the form of CPBs. CPBs are heterogeneous material produced by mixing tailings (70 - 85 wt %) with fresh or mine processed water, and hydraulic binder (3 - 7 wt %). The cost of the binder consumption is high. It can represent up to 75% of the cost of cemented backfill (Fall et al., 2008). This factor has compelled mining companies to seek alternatives that can increase the strength of the fill and reduce the binder content. Sodium silicate is the most recent chemical additive that is used to reduce the binder content in CPBs. This new product is named gelfill (GF).

GF is a new cemented tailings backfill material. It is typically made of tailings, water, binder and chemical additives (Fillset, sodium silicate gel). According to previous studies

on GF (Hassani et al., 2007 and Doucet et al., 2007), the chemical additive, sodium silicate, (like a gel, therefore the name GF) has the ability to absorb a large amount of water (cemented tailings are always prepared with excessive water to allow easy transport to underground voids), to accelerate binder hydration and promote the formation of additional C-S-H. This contributes to a substantial increase in GF strength.

Mechanical, environmental performance and durability are the most important design criteria of GF structures (Fall et al., 2009). Permeability is the key parameter that most affects the environmental performance and durability of GF. Vulnerability of GF to AMD is dependent on the reactivity of tailings contained in the GF. The reactivity in turn is reliant on the types and quantity of sulphide minerals present in the GF as well as hydraulic properties of the GF (seepage of water and diffusion of oxygen through the GF matrix). These properties can be evaluated by investigating the hydraulic conductivity of GF, in particular, the unsaturated hydraulic conductivity. In addition, the hydraulic conductivity controls the leaching and transport of pollutants through the GF to the ground water. The hydraulic conductivity can also give information about the GF pore structure, such as coarseness, connectivity, and cracking.

Mechanical properties (shear strength and UCS) are affected by the unsaturated conditions in GF structures. Increasing the suction in GF structures leads to an increase in the strength. Self-desiccation, which is mainly responsible for the development of suction at early ages of the GF, and occurs in all types of cementitious materials due to chemical shrinkage that occurs during hydration reaction, has an influence on the properties of fresh GF as well as the long-term behaviour of the GF. During self-desiccation, the largest pores empty first.

The menisci formed in these partially empty pores create capillary tension within the pore solution and reduce the internal RH of GF structures (Bentz, 2007). As a result, the compression strength of the GF structure increases, which influences the stability and durability of the GF. Decreasing the moisture content of GF structures due to higher suction (low RH) can lead to more economical GF designs. A good understanding of the unsaturated properties of GF is needed to evaluate the mechanical properties of GF in unsaturated conditions.

As GF is a new cemented material, only a few studies have discussed its mechanical properties. However, no studies have addressed the relevance of unsaturated hydraulic conductivity. There is a lack of knowledge on the unsaturated hydraulic properties of GF for different curing times and binder contents. This has inspired the author to conduct the current study.

The objectives of this study are:

- to determine the water retention curve (WRC) for the GF and its evolution with time as well as to simulate the WRC to best-fit the experimental data by using the van Genuchten (1980) equation, and
- to predict the unsaturated hydraulic conductivity of GF sample by using saturated hydraulic conductivity and WRC.

4.2 Experimental programs

4.2.1 Materials

The materials used to prepare GF include binder, tailings, sodium silicate, and water.

5.2.1.1 Binder and mixing water

PCI was used as the binder. It is the most common material used by the mining industry to produce cemented backfill. Table 4-1 shows the physical and chemical properties of the binder. Tap water was used to mix binders and tailings.

Table 4-1 Characteristics of Portland cement type I

Types of Binder	MgO	CaO	SiO_2	Al_2O_3	Fe_2O_3	SO_3	Relative Density	Specific Surface (m^2/g)
PCI	2.65	62.82	18.03	4.53	2.70	3.82	3.1	1.3

4.2.1.2 Tailings

Silica tailings (ground silica, TS) are used in this study. TS can be classified as medium tailings with 41-45 wt % fine particles (< 20 μm). The use of silica tailings allows accurate control of the mineralogical and chemical compositions of the tailings. This maintains the level of uncertainties at a minimum level (Fall et al, 2009). Natural tailings contain various reactive chemical elements, and often, sulphide minerals (which oxide and produce sulphate during contact with oxygen) that can interact with sodium silicate and/or the cement and thus affect the interpretation of the results as well as study outcomes. TS contains 99.8% SiO_2 and displays a grain size distribution close to the average of nine Canadian mine tailings (Figure 4-1). Tables 4-2 and 4-3 show the physical and chemical

properties of TS. TS are non-plastic and classified as sandy silts of low plasticity (Celestin, 2009) and the ML category in the UCCS. ML is typical for tailings from hard rock mines as also determined by Vick (1990).

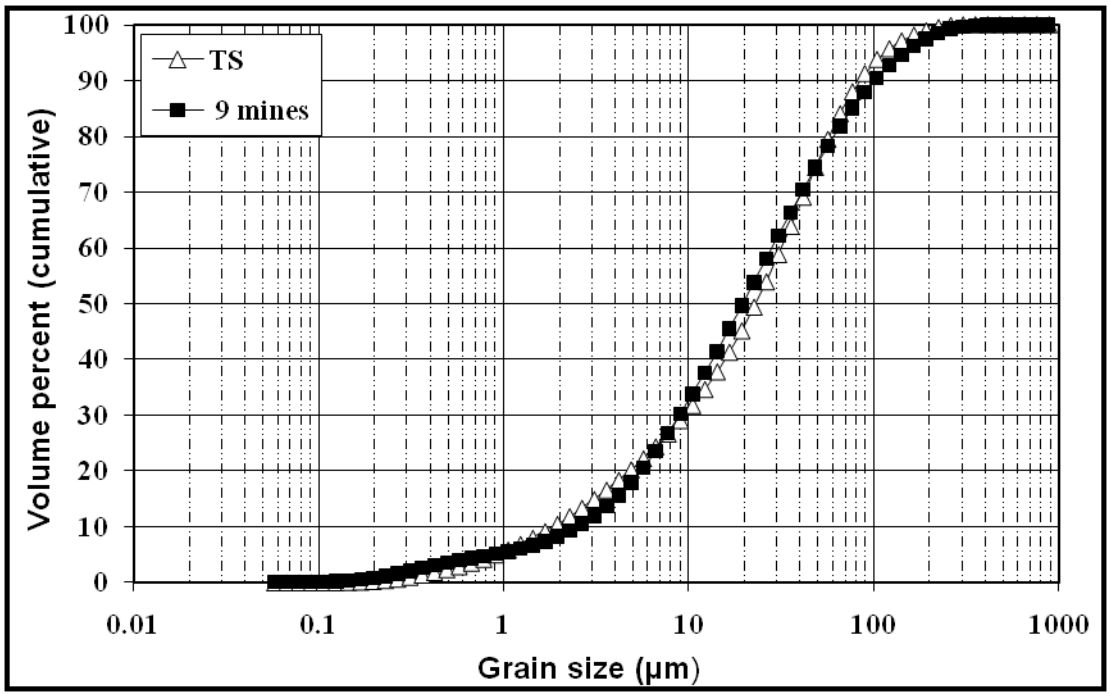

Figure 4-1 Grain size distribution of the tailings used and the average grain size distribution of tailings from nine Canadian mine

Table 4-2 Physical properties of silica tailings (TS)

Element	G_s	D_{10} (µm)	D_{30} (µm)	D_{50} (µm)	D_{60} (µm)	D_{90} (µm)	C_u	C_c
TS	2.7	1.9	9.0	22.5	31.5	88.9	16.2	1.3

Table 4-3 Main chemical elements of TS

Element	Al wt%	Ca wt%	Si wt%	Fe wt%	Na wt%	Pb wt%	S wt%	K wt%
TS	0.10	<0.01	99.80	<0.01	<0.01	0.00	0.00	0.00

4.2.1.3 Sodium silicate

A commercial solution of sodium silicate (type N) was used, in which the ratio of SiO_2 to Na_2O is 3:2. It is fabricated by mixing different ratios of sand and soda ash (sodium carbonate) at elevated temperatures. It is an inorganic chemical, a clear, colourless, and viscous liquid. Table 4-4 shows the sodium silicate properties. Sodium silicate was added to the mix in a liquid form.

Table 4-4 Sodium silicate properties (National Silicates Ltd.)

Properties	Values
Na_2O% by weight	8.90
$SiO_{2\%}$ by weight	28.66
Weight Ratio,%SiO_2 /%Na_2O	3.22
Specific Gravity @ 20°C	1.394
Solids%	37.56

4.2.2 Preparation of materials and mix proportions

Fifty GF samples were prepared to study the hydraulic properties. Tailings, binder, water, and sodium silicate were mixed using a B20F food mixer. The mixing time was 10 minutes for all mixes. Tailings, binder, and water were mixed first, followed by the addition of sodium silicate. Various binder proportions were used to prepare the mixes; 2%, 4.5%, and 6% PCI by weight with a solid mass concentration of 73% which correspond to w/c ratios of 18.5, 8.2, and 6.2, respectively. Then, 0.4% sodium silicate by weight of solids was

added to the mixes. All mixes have the same slump. The produced GF was poured into curing cylinders which are 5 cm in diameter and 10 cm in height. The prepared samples were then sealed and cured at 20°C ± 2 ° C for periods of 3, 7, 28 and 90 days.

4.2.3 Testing and analysis methods

4.2.3.1 Water retention curve (WRC)

A WP4-T dewpoint potentiameter and the saline solution method were used to measure the WRC of the GF samples. The WP4-T was used to measure the WRC of samples for periods of 3, 7, and 28 days while the saline solution method was used to determine the WRC of samples cured for 90 days. Both methods were used to measure the total suction of the samples. The reason that the WP4-T test was adopted for early age samples is to obtain all results on the same testing day because the microstructure of GF changes as hydration proceeds.

- **WRC determination by WP4-T Dewpoint PotentiaMeter**

The WP4-T is considered to be the fastest instrument for measuring water potential within five minutes. It measures water potential from 0 to 60 MPa with an accuracy of ±0.1 MPa from 0 to 10 MPa and ±1% from 10 to 60 MPa (WP4 and WP4-T manual, 2003). The method is used to only measure the total suction. Calibration was done on the WP4-T according to the procedures provided by the manufacturer. The WP4-T was placed in a temperature and humidity controlled room. It was ensured that the bottom of the PVC cup was fully covered with GF and the cup was half empty as suggested by the WP4-T manual (2003). Two samples were cut, trimmed, and levelled by using a knife and then sealed in

the PVC cups for at least 16 hours before measuring the suction. After each suction measurement, the specimen was taken out of the WP4 chamber, and then the specimen was weighed and left to air dry for about 10-15 minutes before starting on the next suction measurement. The process was repeated several times until the total suction was close to 20 MPa. When the test ended, the specimens were placed in an oven to determine the dry weight. With the dry and saturated weights of the specimens, the gravimetric water content (w) was calculated for each suction measurement.

- **Saline solution method**

After 90 days of curing, the saline solution method was employed. The hydration reactions were almost over and no further significant changes would occur in the microstructure of the GF. As well, higher suction was needed.

The saline solution method measures high suction ranges and requires 1-2 months for samples to reach equilibrium. Seven salt solutions are selected for this study (Table 4-5). Saturated solutions were prepared and poured into desiccators. The covers of the desiccators were sealed to prevent any changes in the equilibrium condition. RH and temperature were monitored using a Traceable® digital hygrometer thermometer manufactured by the Control Company. When the RH hit equilibrium, the samples were placed inside the desiccators. The samples were cut and trimmed until they were 1 cm in thickness. The volume of the desiccators was high enough compared to the volume and the number of samples. This meant that the specimen load did not disturb the ambience controlled by the saline solution and significantly increase the time needed to reach equilibrium. Two samples were used from each mix; and the curing time and average value

were taken. The weight of the samples was monitored up to the equilibrium state. At the end of the testing, the samples were placed in an oven to determine the dry weight. The water content was also calculated for each sample.

Table 4-5 Salt solution properties

Saturated Salt Solution	T (˚ C)	RH% at 25 ˚ C	Total Suction kPa	Solubility in Water (g/ml)	Supersaturated Solution (g/ml)
BaCl2 .2H2O Bariumchloride dihydrate	5-60	85.7	22603	37.5 g/100 ml (26°C)	47.5 g/100ml
K2SO4 Potassium sulphate	15-60	95.0	6987	11.1 g/100 ml (20 °C)	21.1 g/100ml
NaCl Sodiumchloride	5-60	70.8	46940	35.9 g/100 ml (25 °C)	45.9 g/100ml
Mg(NO3)2 6H2O Magnesium nitrate hexahydrate	0-50	51.0	91937	125 g/100ml at (25 °C)	135 g/100ml
MgCl2 .6H2O Magnesium chloride hexahydrate	10-50	32.7	152570	54.2 g/100 ml at (20 °C)	64.2 g/100ml
KCl potassium chloride	5-40	82.9	25545	34.0 g/100 ml(20°C)	44.0 g/100ml
LiCl Lithium chloride	20-70	11.7	291564	83 g/100 ml at 20°C)	93.0 g/100ml

4.2.3.2 Unsaturated and saturated hydraulic conductivity

Several experimental methods are available to determine the flow behaviour in unsaturated porous media. However, due to complications and significant time associated with direct measurement of unsaturated hydraulic conductivity, unsaturated flow behaviour is often predicted and not measured. It is common practice to empirically predict unsaturated

hydraulic conductivity by using the saturated hydraulic conductivity coefficient and WRC (Fredlund and Xing 1994). The van Genuchten (1980) equation was used to calculate the unsaturated hydraulic conductivity of GF. Due to the presence of cement, the microstructure of GF changes with time and variation of the binder content. In order to make this model applicable for GF at any curing time, each mix was considered as a different kind of porous media and the fitting parameters were individually calculated.

The flexible wall technique was used to determine the saturated hydraulic conductivity of the GF samples with different binder contents (2%, 4.5%, 6%) and cured for 7, 28 and 90 days. The procedure for this method is described in ASTM D5084-00 and was conducted in the constant head mode. Each sample was tested at least twice and the average value was taken as the saturated hydraulic conductivity. It should be emphasized that the results of the saturated hydraulic tests are only needed to represent the curve of unsaturated hydraulic conductivity vs. suction for the samples studied. This paper focuses on the unsaturated hydraulic properties of GF.

4.2.3.3 Determination of the binder hydration degree index

The degree of hydration index (α) was approximated from the results of UCS tests on the GF samples with different binder contents and curing times up to 120 days. Figure 4-2 presents the results of the calculations. The degree of hydration is a function of time, which ranges between 0% at the beginning of hydration, to 100% when the hydration was entirely accomplished. It is estimated using the following equation:

$$\alpha_n = \frac{UCS_n}{UCS_{final}}$$

Equation (4-1)

UCS_n : uniaxial compression strength at n curing time

UCS_{final} : uniaxial compression strength of mature GF (in this study, it is considered that the strength of GF does not increase after 120 days)

α_n: α at n curing time

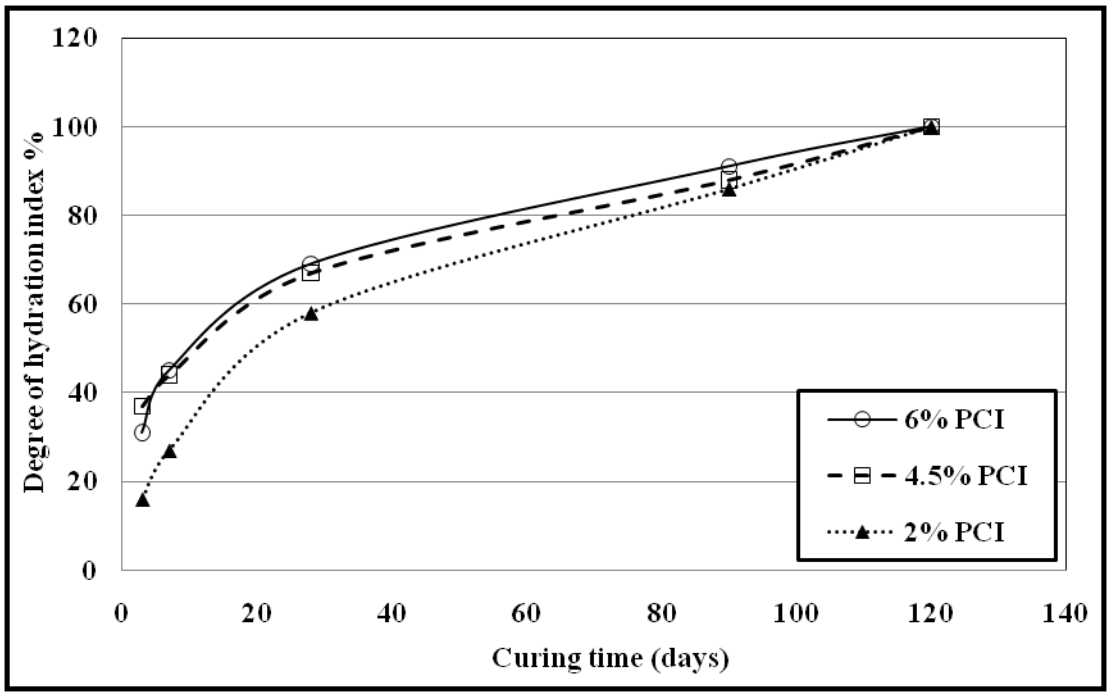

Figure 4-2 Evolution of the degree of binder hydration index with time

4.2.3.4 Microstructural analysis

The microstructure of the studied GF samples was investigated by thermal analyses ((DTG, DTA, and DSC). Tests were carried out on various prepared hcps of GF with a high w/c ratio (w/c = 2; to simulate the cement matrix of GF). The thermal analyses were undertaken using an SDT apparatus from TA Instruments which allows simultaneous registration of weight loss and heat flow along the thermal treatment of the sample. The various (dried) samples (about 30 mg each) were heated in an inert nitrogen atmosphere at the rate of 10°C per minute up to a temperature of 1000°C. Moreover, the total (overall) *n* and *e* of the GF samples were also determined.

4.3 Results and discussion

4.3.1 Water retention curves

I. **Time-dependent evolution of WRC**

The evolution of WRC with degree of hydration index for different binder contents (6%, 4.5%, 2% PCI) is illustrated in Figure 4-3. For the same binder content, it can be seen that despite the differences between the obtained curves, the overall trend of the WRCs is similar. In general, samples cured for 90 days have higher suction than samples cured for 3, 7, and 28 days. For example, for 15% volumetric water content (θ_w), the suction for the 4.5% PCI GF cured at 3 days (α_3 = 37%), 7 days (α_7 = 44%), 28 days (α_{28} = 67%), and 90 days (α_{90} = 88%) is 700, 900, 1300, and 7000 kPa, respectively (Figure 4-3b). It can be seen that the effects of curing times or degree of hydration index on WRC are obvious at both low and high suction ranges (Figure 4-3). These results indicate that GF will display

less moisture loss and deformations associated with external drying as the curing time increases. This will influence the durability of these materials.

The observed time-dependent evolution of the WRC of GF cannot be explained by the mechanisms that control the water characteristic curve of conventional soil, but rather by those that control the desorption isotherm of hardening cement paste.

There are three main states of water in hcp that need to be recalled in order to better understand the evolution of WRC with degree of hydration: (i) first, capillary water which contains free water when the capillary pores are greater than 50 nm and water held by capillary tension when the capillary pores range between 5-50 nm. The capillary pores are emptied when the ambient RH falls below about 45% (Neville, 1995); (ii) secondly, gel water which is divided into adsorbed water held by the surface force of the gel particles (removing this water causes shrinkage when the RH is less than 30%) and interlayer water held between the surfaces of C-S-H planes which can be lost only upon strong drying (11% to 0% RH) (Beaudoin, 1982) and leads to a considerable shrinkage of the C-S-H structure; and (iii) .third, chemically combined water, which is non-evaporable water, and can be only lost when hydration products decompose.

This observed increase of suction of GF as the curing time increases is explained by the fact that as hydration proceeds, the capillary pores decrease due to the increase of hydration products as demonstrated by Figure 4-4 (increasing the solids content of GF matrix leads to blockage of the capillary pores). Decreasing the porosity of the capillary pores has, as a consequence, the reduction of connectivity of these pores and thus moisture loss processes will be more controlled by the gel pores. As a result, higher suction is needed in order to remove the water from the fine pores (gel pores) due to the fact that water in these pores is

held by surface force (adsorptive force). Figures 4-4a and 4-4b illustrate the results of a thermal analysis (TGA/DTA) of cemented paste of GF cured at 7 days and 28 days, respectively. Generally, normal endothermic peaks can be noticed in the range of 50–150 °C, 450 °C, and 750 °C. These peaks at different curing times indicate the presence of CSH gel, ettringite, CH, and $CaCO_3$. A comparison of the TG/DTA diagrams of the cement pastes cured at 7 days and 28 days clearly shows that the amounts of CSH, ettringite, CH, and $CaCO_3$ that are formed in the 28 day samples are higher those formed in the 7 day sample. Indeed, it can be seen from Figure 4.4 that the mass loss which occurs in the temperature ranges of 50–150°C, 450°C, and 750°C is higher with increasing curing time.

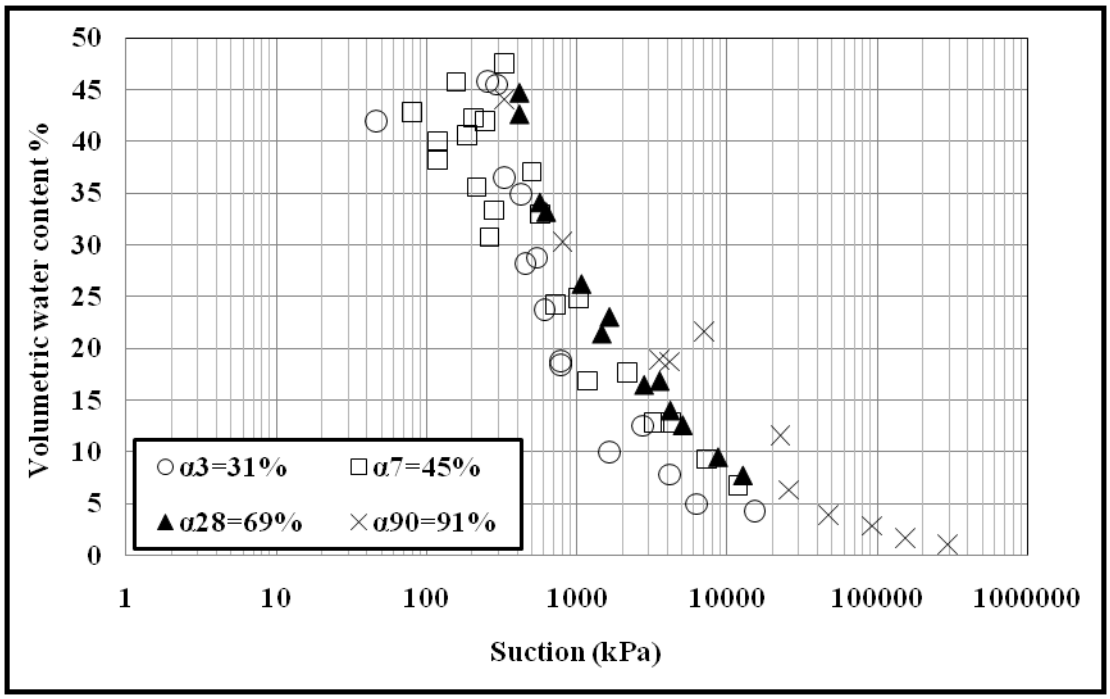

a- 6% PCI

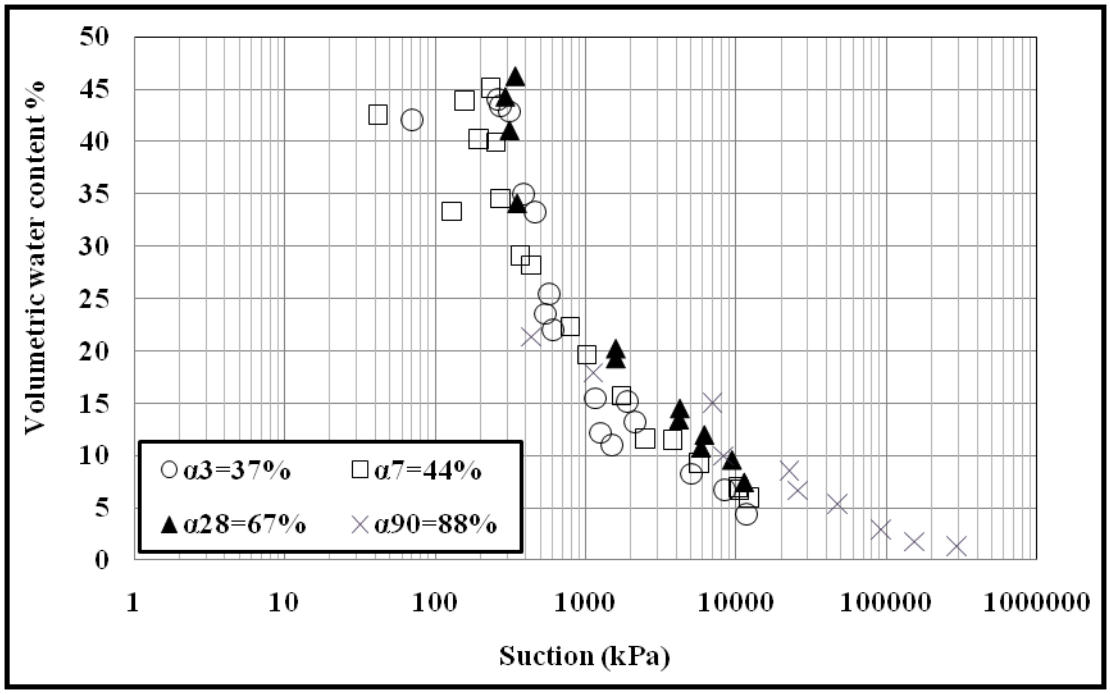

b- 4.5% PCI

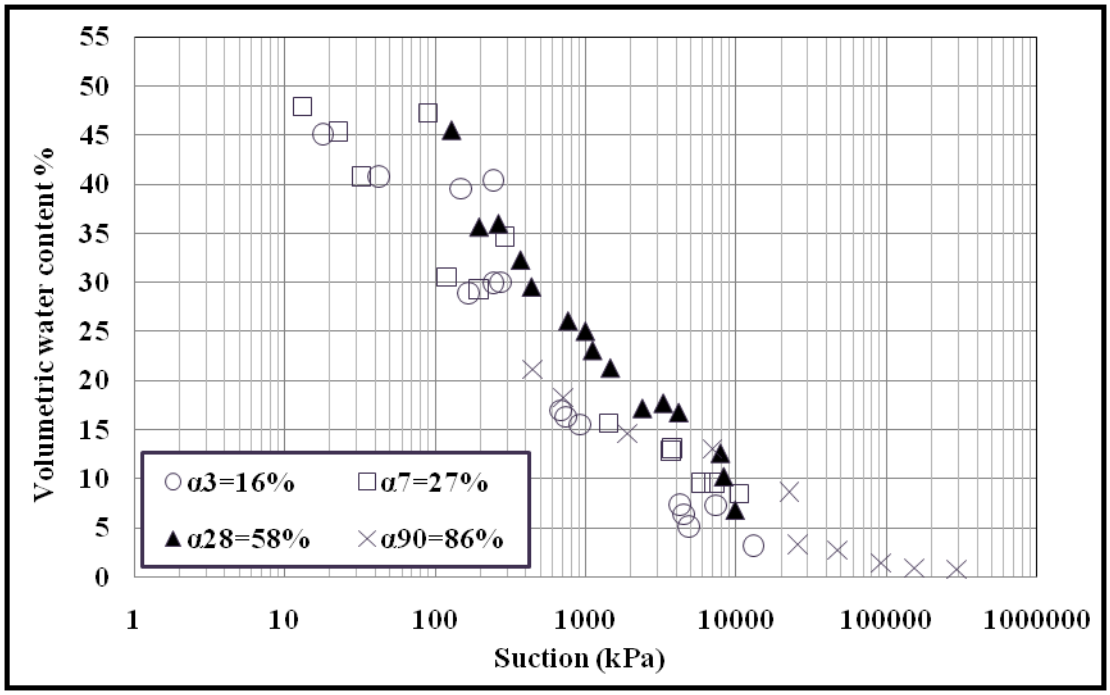

c- 2% PCI

Figure 4-3 The evolution of WRC with degree of hydration index for GF samples with (a) 6% PCI, (b) 4.5% PCI, (c) 2% PCI

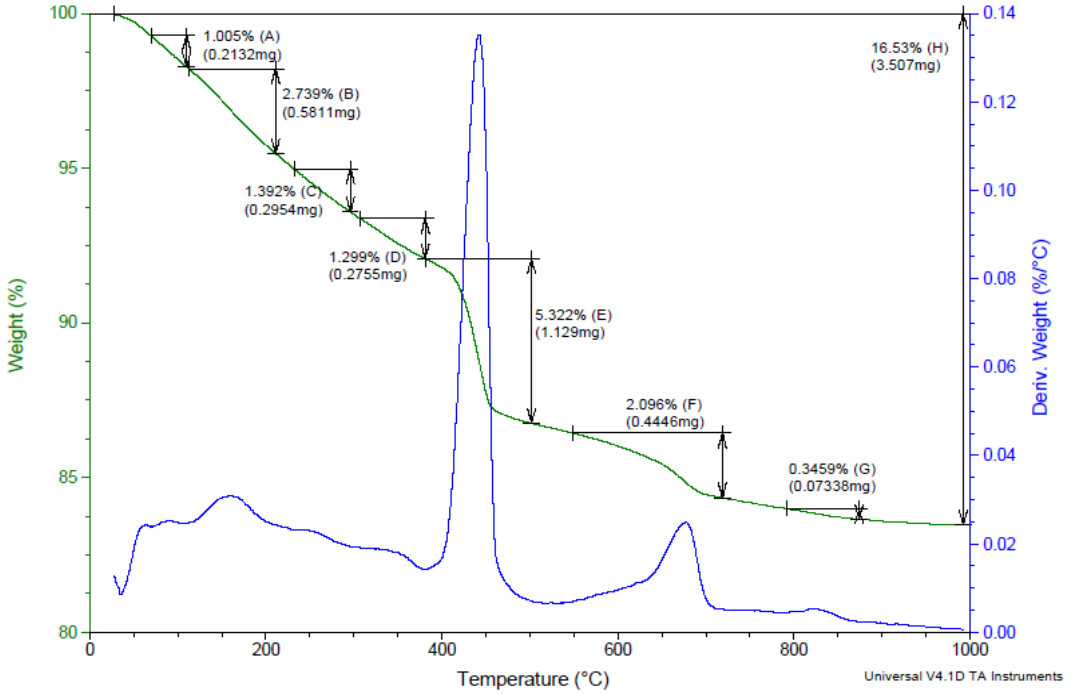

a- 7 days

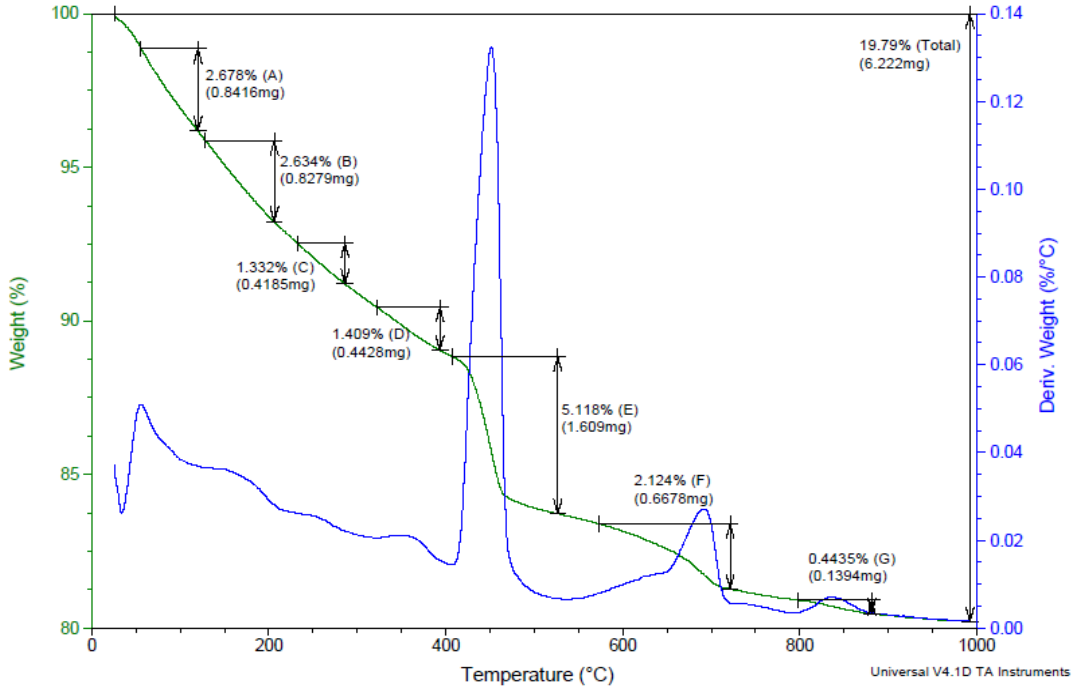

b- 28 days

Figure 4-4 Thermal behaviour (TGA/DTA) of the hardened Portland cement pastes of GF with w/c=2 cured at: a) 7 days and b) 28 days

II. **Effect of binder contents on the WRC**

Figure 4-5 shows the effect of various binder contents (6%, 4.5%, 2% PCI) on the WRC for GF samples of different ages. It can be observed that the binder proportion affects the WRC. The results show that for the same volumetric water content, a significant change in suction occurs for samples prepared with different binder contents and cured for 3, 7, 28, 90 days. However, the effect of binder on the WRCs becomes less noticeable or negligible for high suction ranges or low RH ranges. For example, when the suction is 25,000 kPa (RH = 83%, calculated by using the Kelvin equation, see Equation 4.2), the volumetric water content (θ_w) of GF samples cured for 90 days with 6%, 4.5% , and 2% PCI are 6.8%, 6.6%, 3.3%, respectively (Figure 4-4d); the θ_w is 3.9%, 5.4%, 2.7% when the suction is 46,940 kpa (RH = 70%); and when the suction value is 150,000 kPa (RH = 32%), the θ_w values are 1.6%, 1.5%, and 1.1%. This observed reduced or negligible impact of binder content on the WRC at high suction ranges (i.e. low RH) is consistent with the experimental observations made by Baroghel-Boung (2006) on hcp, who found that with a given cement below a given RH (i.e. above a given suction), the WRCs of hcp are identical or close to each other regardless of the mix (i.e. the mix parameters such as cement content, w/c has no significant influence on the WRC anymore). The results from Baroghel-Boung showed that for RH < 44%, the isotherms of all the hcp remain close, which illustrate that this range of RH (or suction) moisture equilibrium takes place in a pore structure (internal to C-S-H gel) that is not influenced by the mix parameters (Baroghel-Boung and Chaussadent, 1995; Baroghel-Boung, 1998). The author demonstrated that the mix parameters have important effects on the WRC only when RH > 76% (low range suction) while they have only a mitigated influence when $50\% \leq RH \geq 76\%$.

$$\psi = -\frac{RT}{v_{wo} w_v} \ln(RH)$$ Equation 4-2

where

ψ = total suction (kPa)

R = universal (molar) gas constant [8.31432 J/mol K]

T = absolute temperature [273.16 + t° (K)]

t° = temperature (°C)

v_{wo} = specific volume of water [$(1/\rho_w)$ (m³/kg)]

w_v = molecular mass of water vapour (18.016 kg/ml)

RH = relative humidity

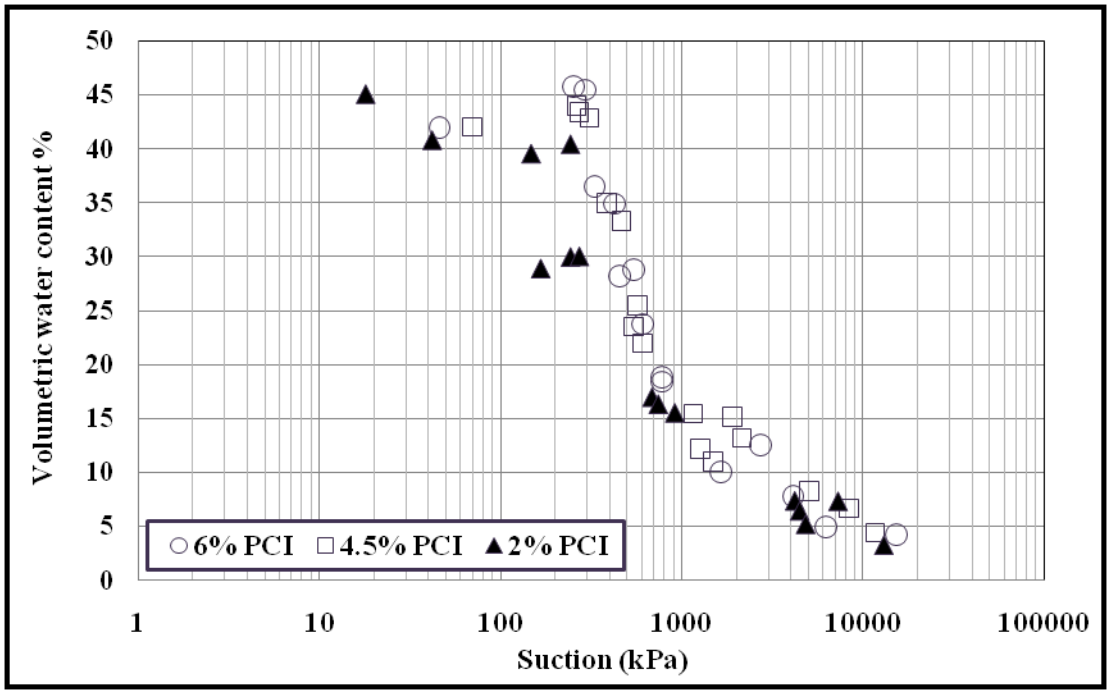

a- curing time of 3 days

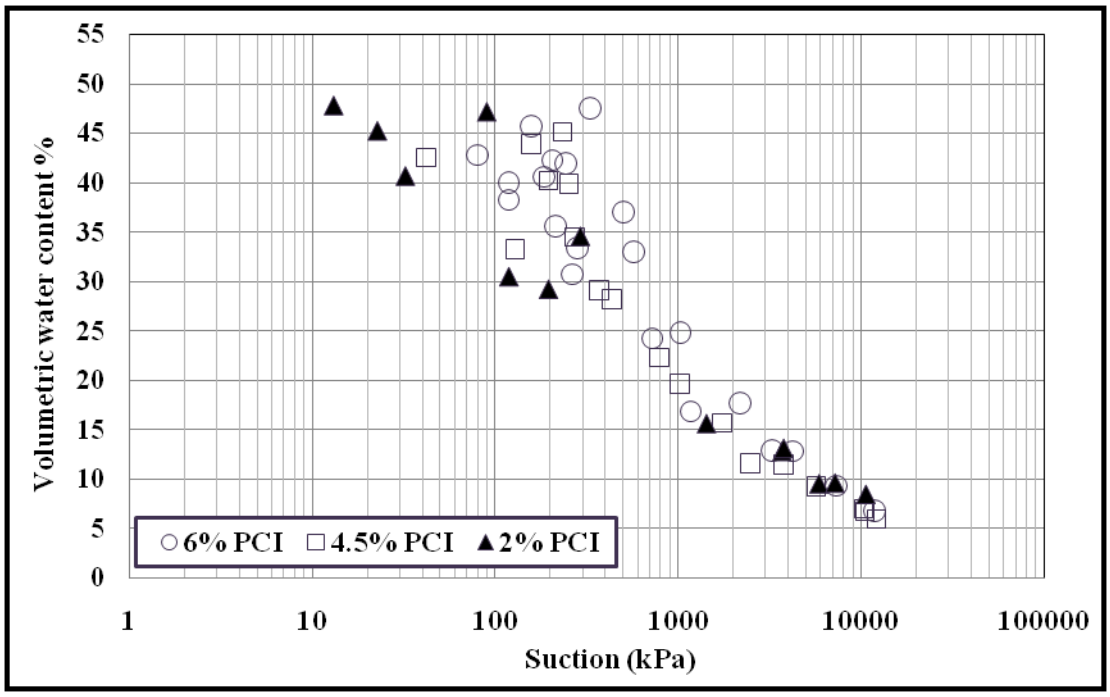

b- curing time of 7 days

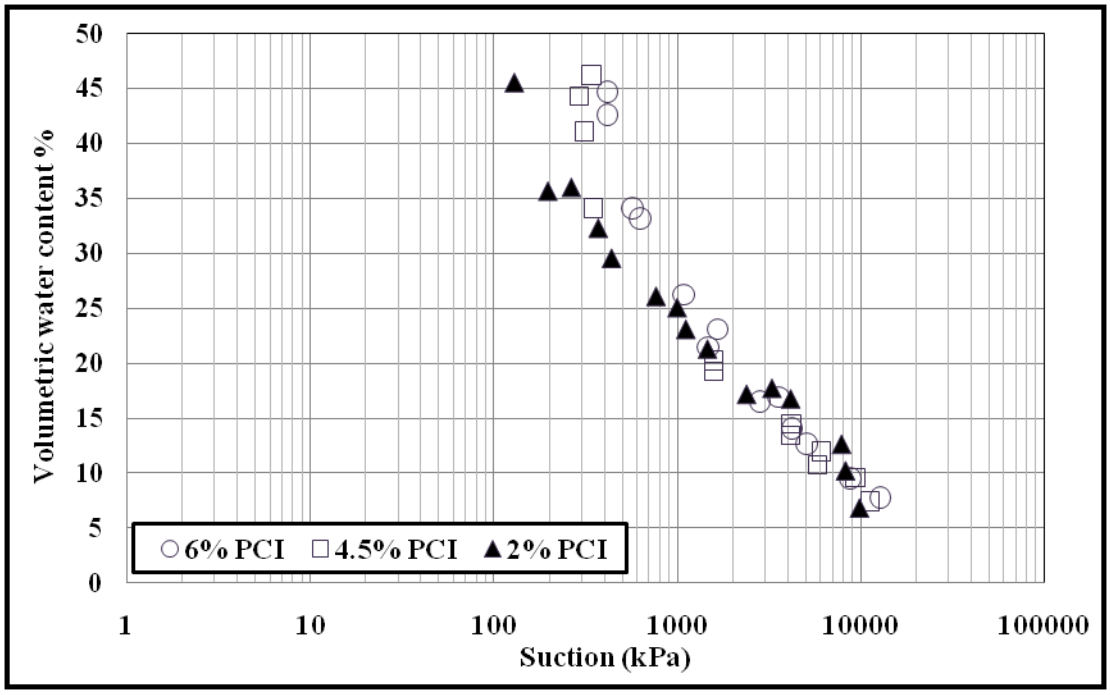

c- curing time of 28 days

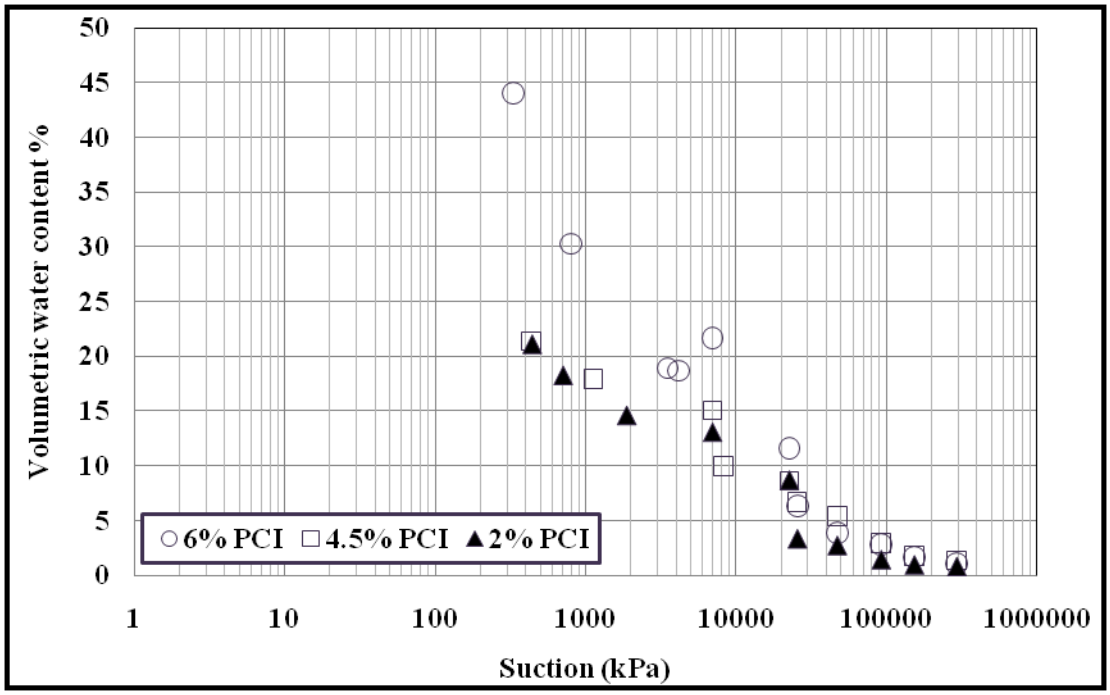

d- curing time of 90 days

Figure 4-5 Effect of various binder contents (6%, 4.5%, 2% PCI) on WRC for curing time of: (a) 3 days, (b) 7 days, (c) 28 days, (d) 90 days

The observed decrease of the volumetric water content of the GF samples at low suction ranges as the cement content decreases can be attributed to the fact that increases in the binder content will increase the rate of binder hydration (Figure 4-2) and the quantity of binder hydration products formed, such as C-S-H and CH. Formation of more hydration products is associated with the refinement of the pore structures of the GF (Figures 4-6 and 4-7). Consequently, GF samples with lower cement content will have larger and high proportions of capillary pores than the samples with higher cement content. Lower suction is needed to remove the water from the capillary pores. This refinement of the GF pore structure as the binder content increases is graphically demonstrated by Figures 4.6 and 4.7. The variations of void ratio and porosity with respect to curing time for different binder proportions of GF samples are shown in Figures 4-6a and 4-6b, respectively. It can be noted that increases in the binder content significantly decreases the void ratio and the total porosity of the GF samples (up to 28 days). Furthermore, Figure 4-7, which illustrates the effect of binder content on the MIP pore size distribution of GF, shows that increases in the binder content are associated with lower proportions of macroporosity (> 1 μm).

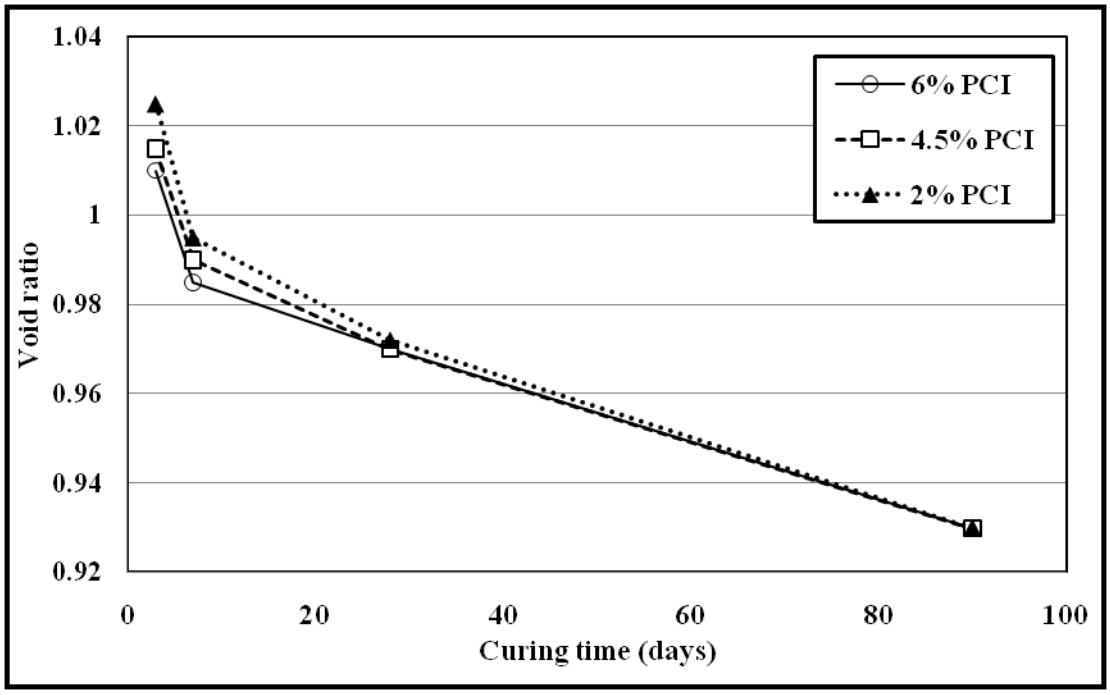

a- Void ratio

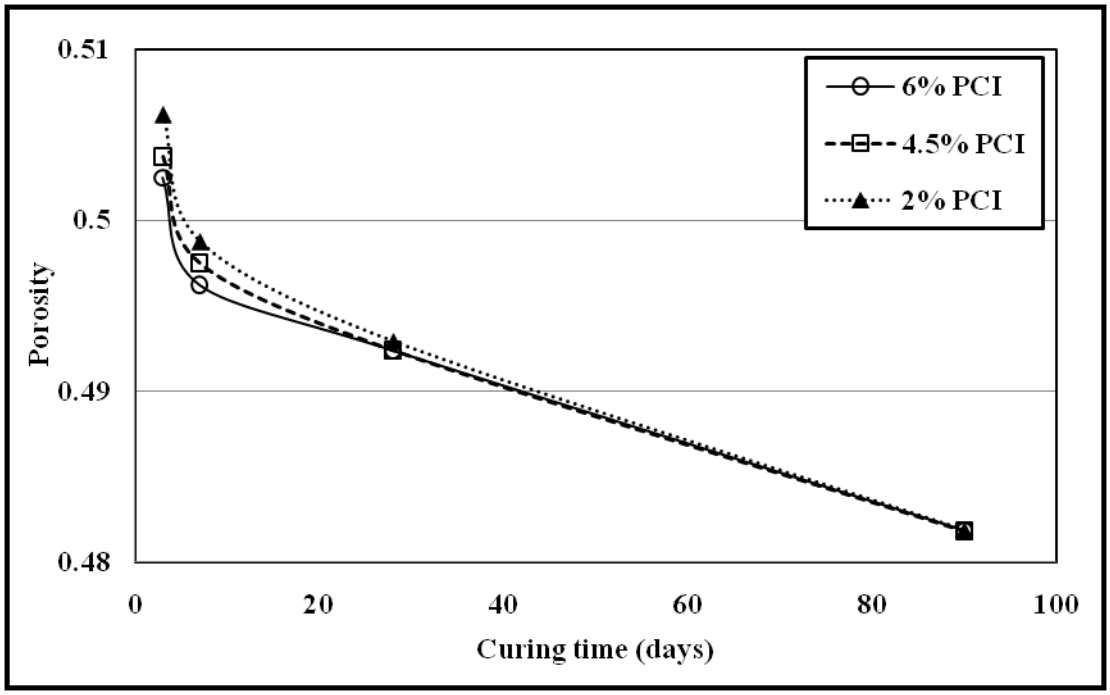

b-Total porosity

Figure 4-6 Evolution of the a) void ratio and b) porosity of GF with curing time for various binder contents

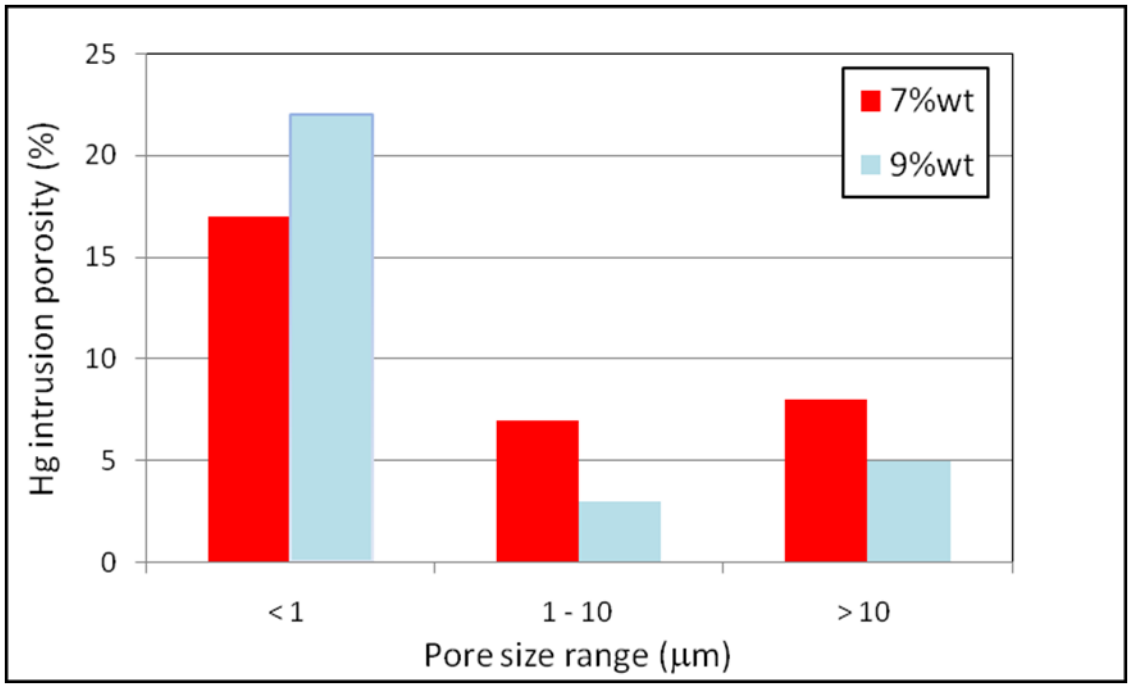

Figure 4-7 Effect of binder content on the pore size distribution of GF paste backfill cemented with PCI/slag vs. content of fines and pore size range
(data from Hassani et al., 2007)

III. Air-entry value and residual water content

The key features of WRC are the AEV and the residual water content. AEV and residual state conditions are essential parameters to geotechnical and geo-environmental engineers. The AEV represents the suction that is required to cause desaturation of the largest pores. It is important to define the AEV because it indicates the initiation of the desaturation state. It is also necessary to define the residual state condition in order to obtain the fitting parameters that are used in numerical models to predict unsaturated hydraulic conductivity. The AEV of GF is obtained by extending the maximum slope portion of WRC to intersect with the line extending from saturated volumetric content (θ_s). The corresponding value of suction is taken as the AEV. The residual water content is considered as the degree of saturation at which the liquid phase becomes discontinuous. The residual water content can

be defined as the point where a line that extends along the curve from 1,000,000 kPa intersects with the tangent to the maximum slope portion as shown in Figure 2-20.

The evolution of AEVs with curing time and degree of hydration for different binder proportions is plotted in Figure 4-8. It can be noted that the AEVs increase with curing time and degree of hydration index. This can be explained by the refinement of the pore structure during hydration process (Figures 4-6). As hydration proceeds, the solid content of the paste increases and blocks the capillary pores. Therefore, these capillaries turn into capillary pores interconnected by gel pores (Neville, 1995). The relationship between suction and pore radius are inversely proportional according to the Laplace law (Equation 4-3) (Mokarem, 2002).

$$p_v - p_c = \frac{2\sigma}{r} cos\ \theta \qquad \text{Equation 4-3}$$

where σ is the surface tension of water/water vapour interface, θ is the moistening angle, p_c is the pressure in water, p_v is the pressure in water vapour, r is the radius of pores where there is a meniscus.

In unsaturated conditions, there is an access radius. All capillaries with a radius less than the access radius are filled with water while the capillaries with a radius larger than the access radius are empty (Hau et al., 1995). Hence, as the pore size becomes smaller, higher suction is needed to be applied on the GF samples. Furthermore, it can be seen that after 90 days, the binder content does not have any significant influence on the AEVs.

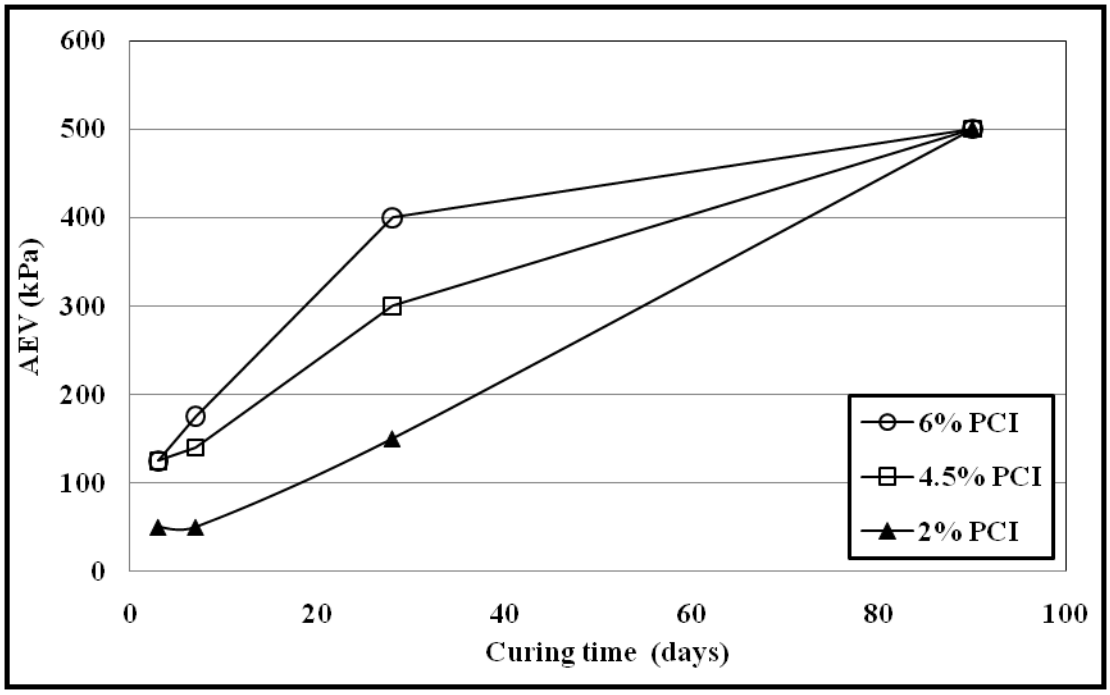

a- Curing time

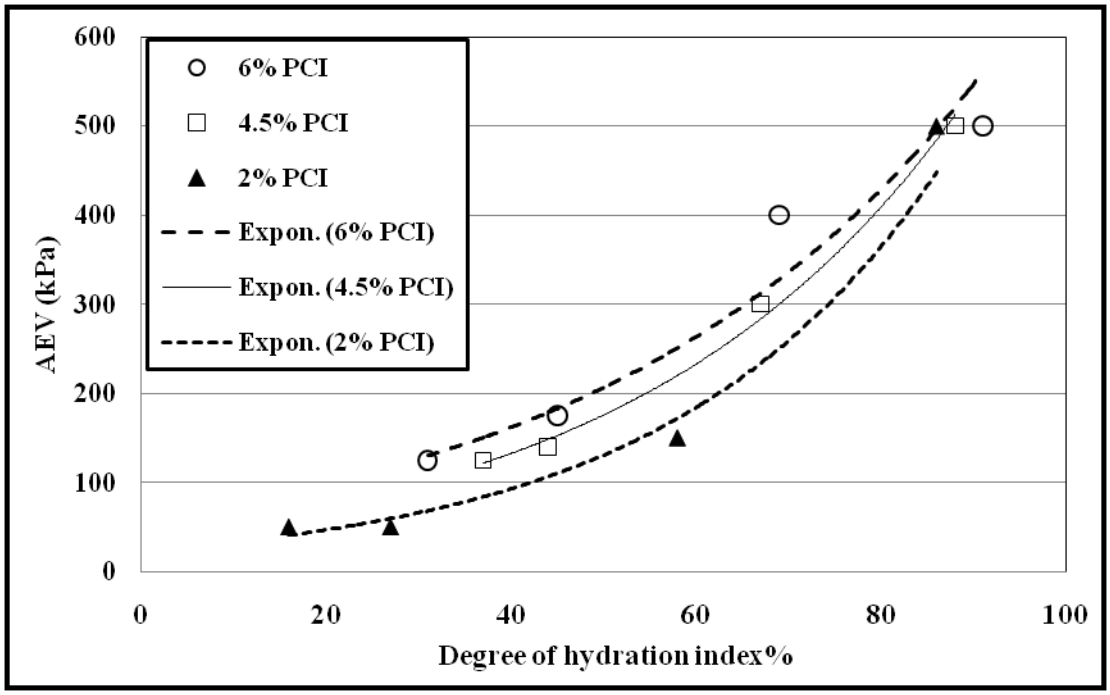

b- Degree of hydration index

Figure 4-8 Evolution of air-entry value with (a) curing time , (b) degree of hydration index for various binder proportions

The evolution of AEVs with degree of hydration index for different binder contents was formulated based on regression analysis on data sets by using Excel software (Equation 4-4):

$$AEV = ae^{b\alpha} \qquad \text{Equation 4-4}$$

where AEV is the air-entry values in kPa, α is degree of hydration index %, and a and b are the constants parameters to be determined for each GF mix. The values of a and b for this study are: 6% PCI, a = 61.05, b = 0.0244; 4.5% PCI, a = 42.89, b = 0.028; and 2% PCI, a = 23.64, b = 0.034.

To verify the applicability of the model, the predicted function was validated by using the experimental data (not used to develop the function) obtained from the GF samples in this study. In addition, for better validation of the developed model, AEV values obtained by another researcher (Godbout, 2005) on CPB samples with various mix components (binder contents and types) and cured at various times (3-28 days) were used. The outcomes of the validation are presented in Figure 4-9. It can be noticed that a good agreement is found between the predicted and experimental values. Therefore, this model can be useful for estimating the AEV of cemented backfill materials.

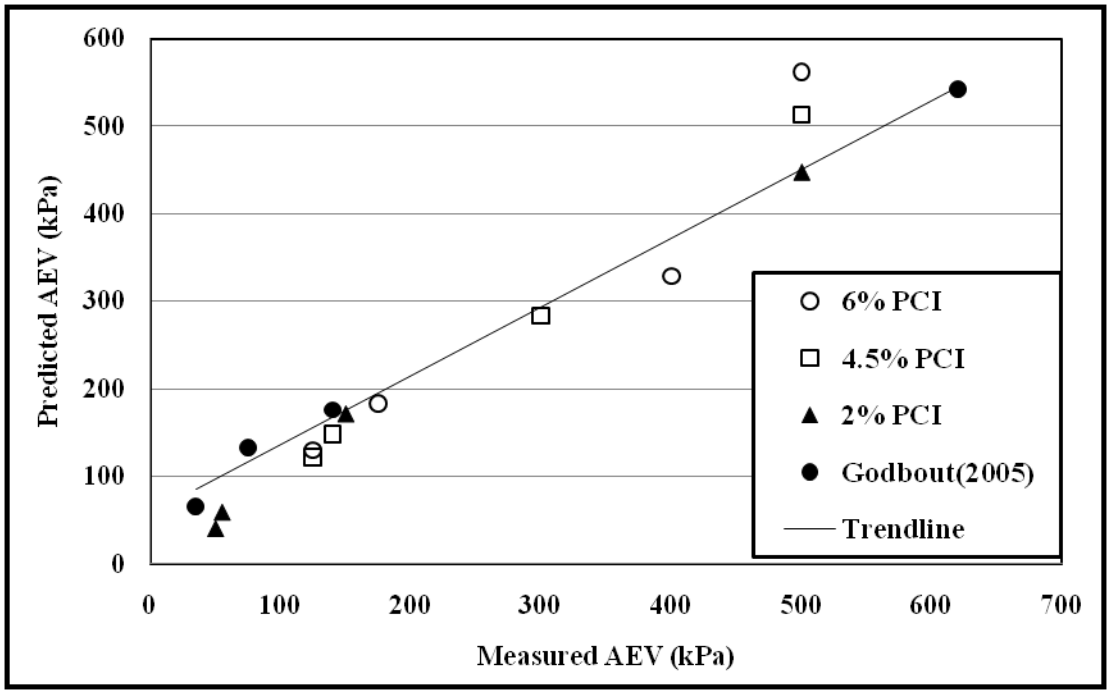

Figure 4-9 Predicted vs. measured AEV for various cemented backfill

The effect of binder proportions, curing times, and degree of hydration index on residual water content is shown in Figure 4-10. The effect of binder contents on residual water content is limited to early ages only. It seems that binder content and degree of hydration index have only slight impacts on the residual water content. The range of variations of residual water content is 8-11% (which corresponds to high suctions of 30-9 MPa) for all GF mixes. This observation is again consistent with results of Baroghel-Boung (2006) which indicate that below a given RH (44%), the mix parameters have no significant effect on the isotherm of hcp as explained above.

Using the experimental data of the present study, the evolution of residual water content with degree of hydration index for different binder contents was formulated based on a regression analysis on data sets by using Excel software (Equation 4-5).

$$RWC = ae^{-b\alpha}$$ Equation 4-5

where RWC is residual water content%, α is degree of hydration index %, and a and b are the constants parameters to be determined for each GF mix. The values of a and b for this study are: 6% PCI, a = 10.85, b = 0.003; 4.5% PCI, a = 12.16, b = 0.005; and 2% PCI, a = 11.53, b = 0.004.

To confirm the applicability of the model, the predicted function was validated by using the experimental data (not used to develop the function) obtained from the GF samples in this study. The outcomes of the validation are presented in Figure 4-11. It can be noticed that there is a good agreement between the predicted and experimental values.

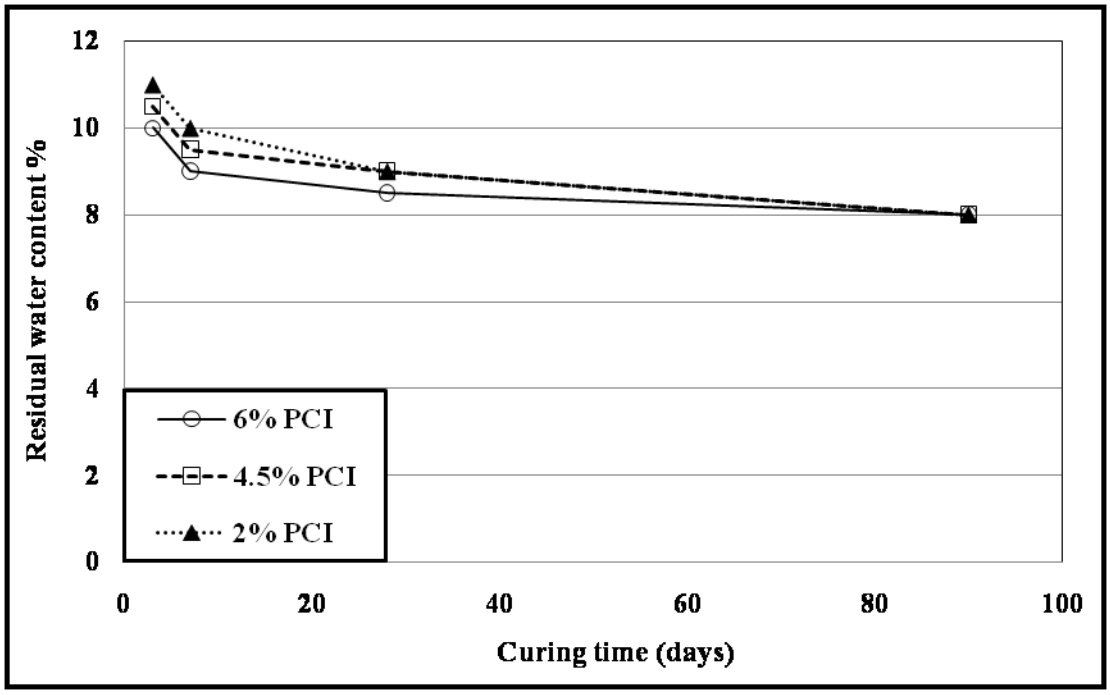

a- Curing time

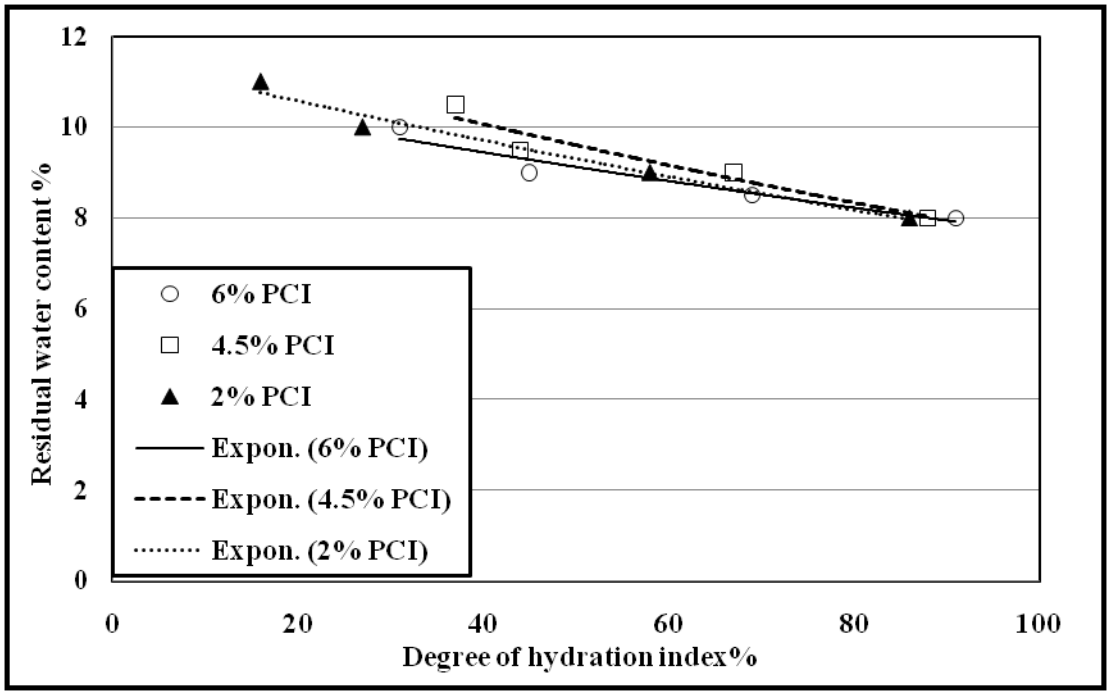

b- Degree of hydration index

Figure 4-10 Evolution of residual water content with (a) curing time, (b) degree of hydration index for various binder proportions

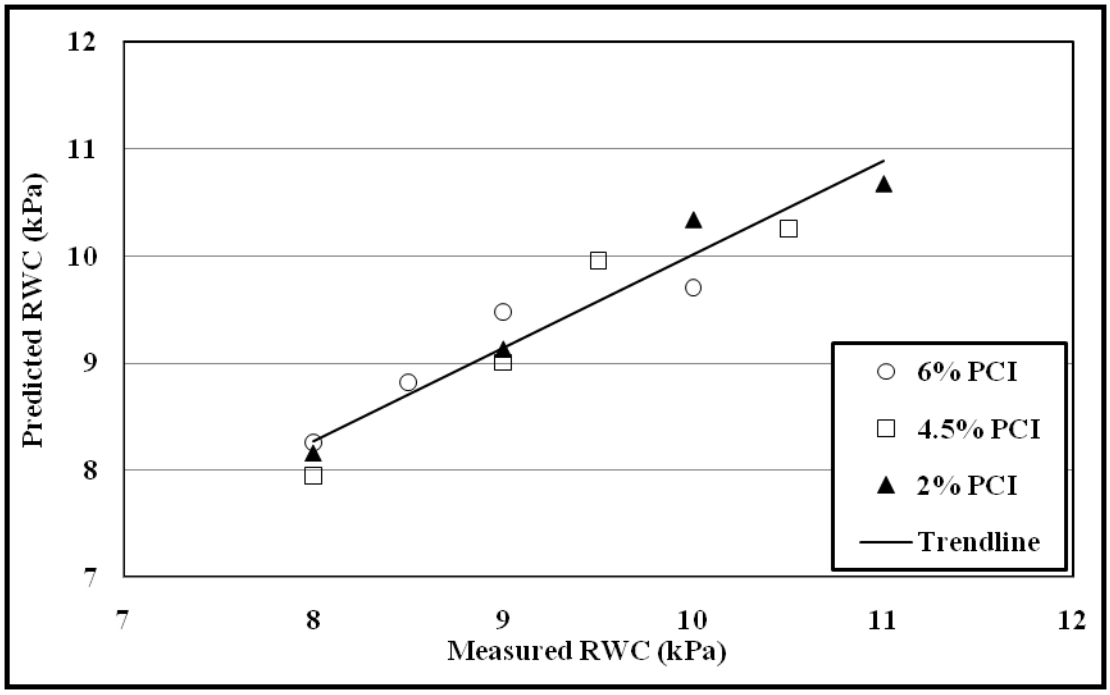

Figure 4-11 Predicted vs. measured RWC of GF with various binder contents

IV. Model fit to experimental data

Numerous empirical equations have been proposed to simulate the WRC. The van Genuchten (1980) and Fredlund and Xing (1994) models were used to fit the experimental data of this study (Equations 4-6 and 4-7, respectively). However, the van Genuchten (1980) model is the best fit curve to the experimental data as shown in Figure 4-12a. Figures 4-12, 4-13, 4-14, and 4-15 show the van Genuchten model as the best-fit curve to the experimental data for different binder contents and curing times. It can be seen that there is a good agreement between the predicted WRC and measured values.

$$\theta = \theta_r + \frac{(\theta_s - \theta_r)}{[1 + (\alpha\psi)^n]^m}$$

Equation 4-6

$$\alpha = \frac{1}{\psi_P}\left(2^{1/m} - 1\right)^{1-m}$$

$$m = \left(1 - exp(-0.8S_P)\right)\ 0 \leq S_P \leq 1$$

$$m = 1 - \frac{1}{n}$$

$$S_P = \frac{1}{\theta_s - \theta_r}\left|\frac{d\theta}{d(log\psi)}\right|$$

$$\left|\frac{d\theta}{d(log\psi)}\right| = ln(10)\psi\frac{d\theta}{d\psi}$$

where:

ψ = matrix suction (kPa)

θ = volumetric water content

θ_s = saturated water content

θ_r = residual water content

α , n, m = fitting parameters

S_P = slope which is halfway between θ_s and θ_r at point P

$$\theta_w = C(u_a - u_w)\frac{\theta_s}{\left\{\ln\left[e + \left((u_a - u_w)/a_f\right)^{n_f}\right]\right\}^{m_f}}$$ Equation 4-7

where:

θ_w = volumetric water content

θ_s = volumetric water content at saturation

e = 2.718

$(u_a - u_w)$ = soil suction

a_f = soil parameter approximating the air entry of the soil

n_f = soil parameter related to the rate of desaturation

m_f = soil parameter related to residual water content conditions

$C(u_a - u_w)$ = correction factor to ensure that the function goes through 1,000,000 kPa of suction at zero water content

The presence of binders leads to changes in the pore structures of GF with curing time. Also, different binder proportions cause variations in the pore structure. As the binder hydrates, the volume of pores decreases. Furthermore, increasing the binder content leads to the production of more hydration products which reduce the interconnectivity and size of the pores (Figures 4-6 and 4-7). Therefore, fitting parameters are individually calculated for each mix and curing time. The progress of the fitting parameters with degree of hydration index is plotted (Figures in Appendix) and formulated using Excel software (Equations 4-8, 4-9, and 4-10)

$$Alpha = ae^{-b\alpha}$$ Equation 4-8

$$m = c\alpha^{-d}$$ Equation 4-9

$$n = e\alpha^{-f}$$ Equation 4-10

where alpha, m, and n are the fitting parameters of the van Genuchten model, α is the degree of hydration index, a, b, c, d, *e*, and f are the constants parameters to be determined for each GF mix. For this study, a = 0.006, b = 0.014, c = 0.54, d = 0.084, *e* = 1.73, f = 0.008 for 6% PCI; a = 0.018, b = 0.035, c = 0.49, d = 0.046, *e* = 1.9, f = 0.02 for 4.5% PCI; and a = 0.014, b = 0.024, c = 0.7, d = 0.17, *e* = 2.5, f = 0.114 for 2% PCI.

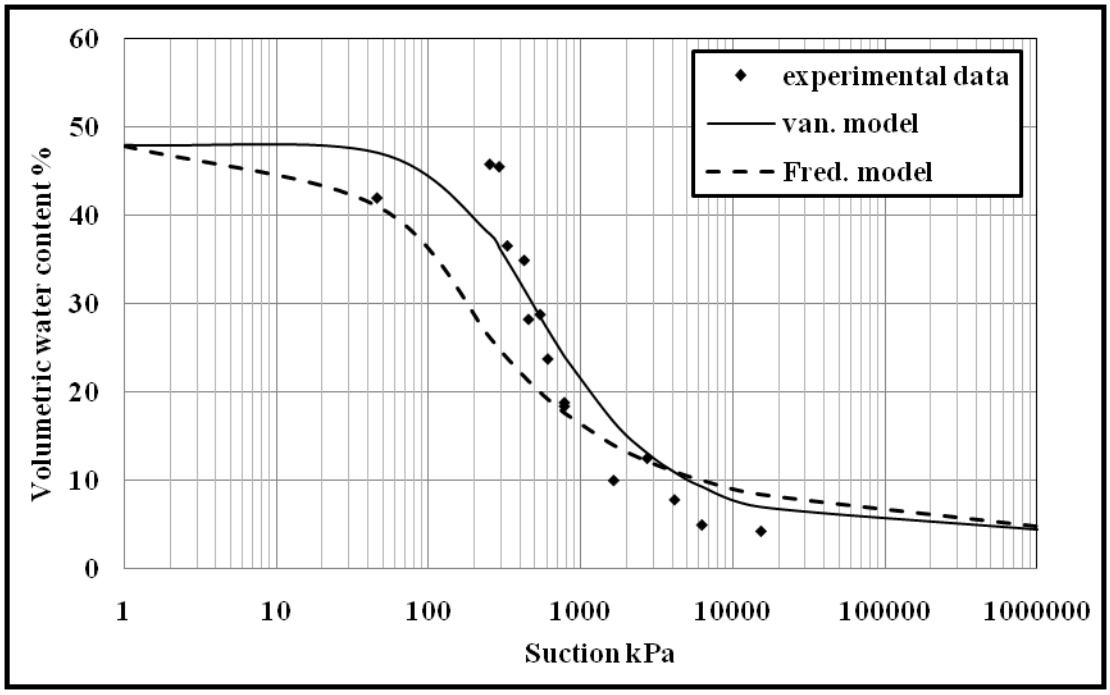

a- 6% PCI and curing time of 3 days (α=0.0037 kPa^{-1}, m=0.407, n=1.687)

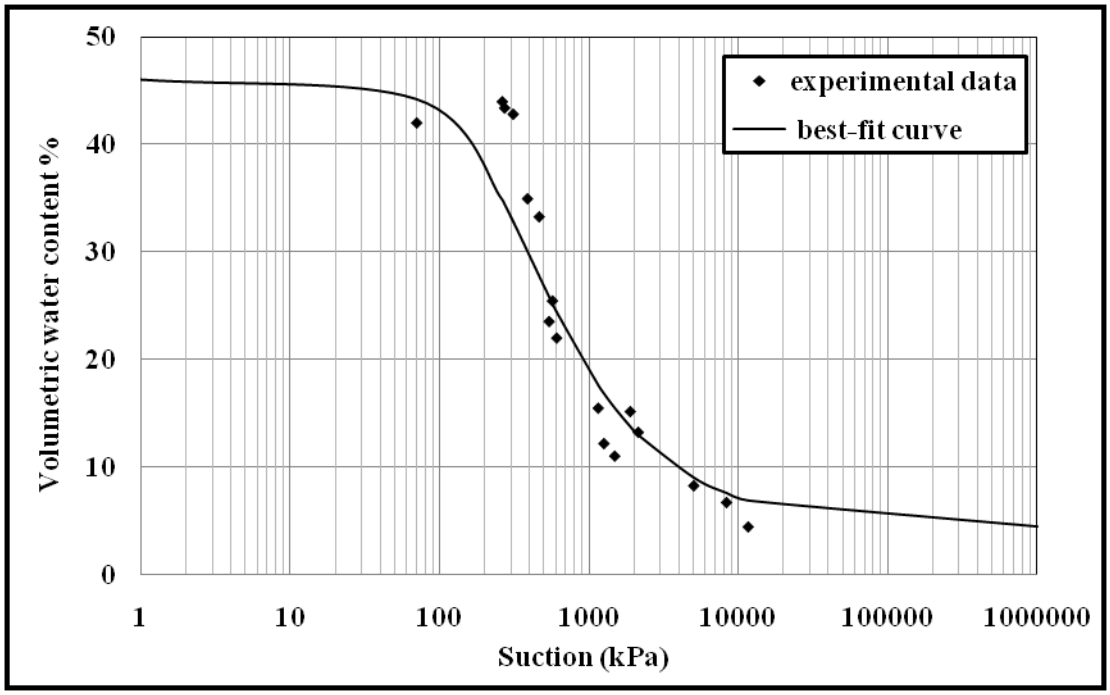

b- 4.5% PCI and curing time of 3 days (α=0.004 kPa^{-1}, m=0.422, n=1.729)

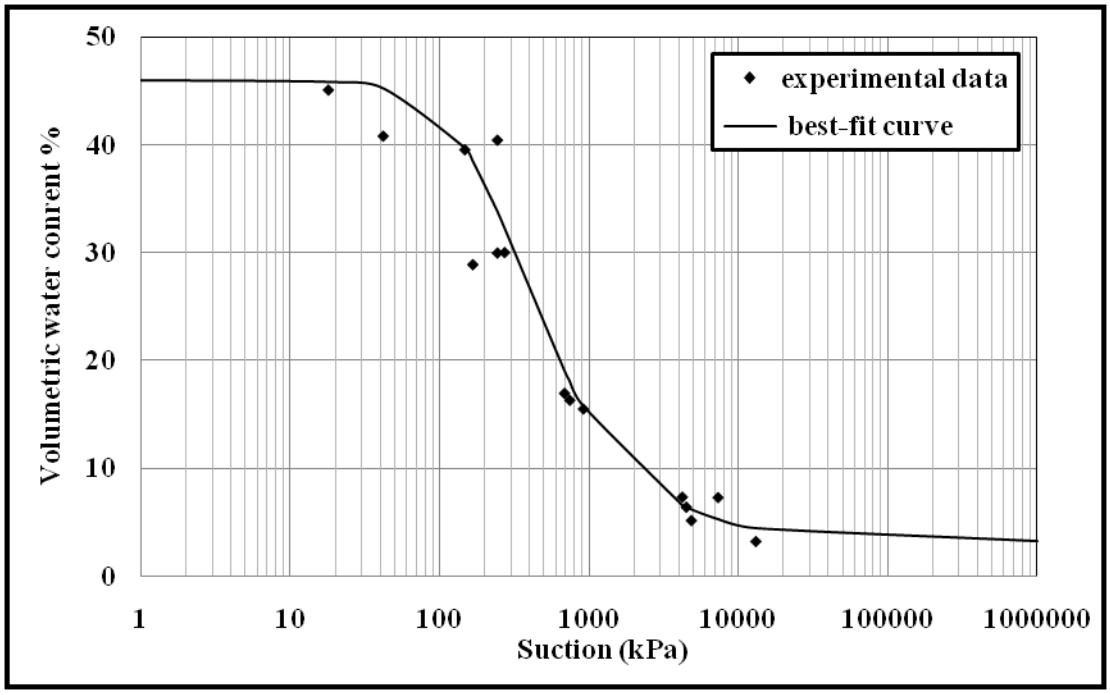

c- 2% PCI and curing time of 3 days (α=0.0042 kPa^{-1}, m=0.469, n=1.886)

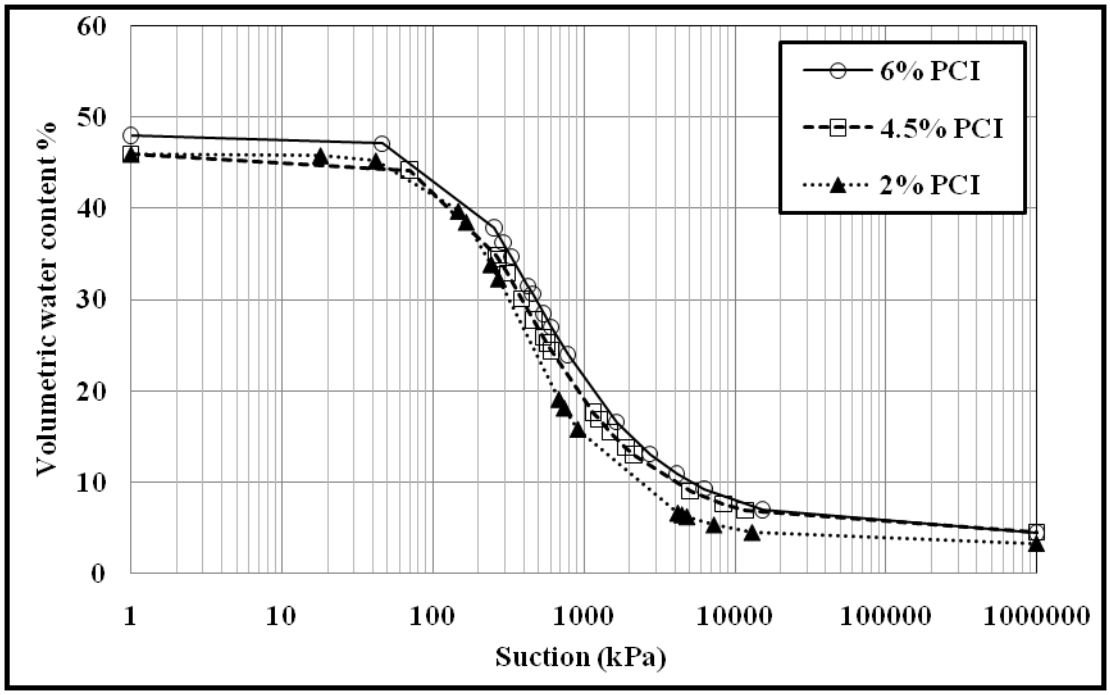

d- van Genuchten model for curing time of 3 days

Figure 4-12 Model prediction for WRC for curing time of 3 days (a) 6% PCI, (b) 4.5% PCI, (c) 2% PCI, (d) van Genuchten model for various binder contents (6%, 4.5%, 2% PCI)

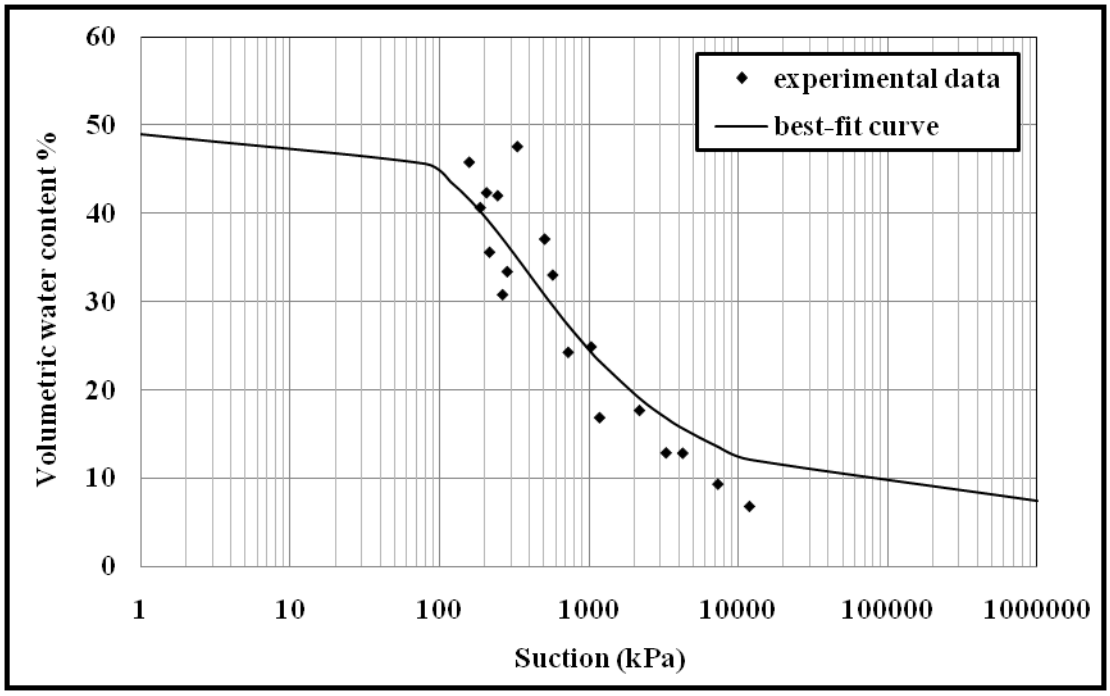

a- 6% PCI and curing time of 7 days (α=0.0054 kPa^{-1}, m=0.334, n=1.501)

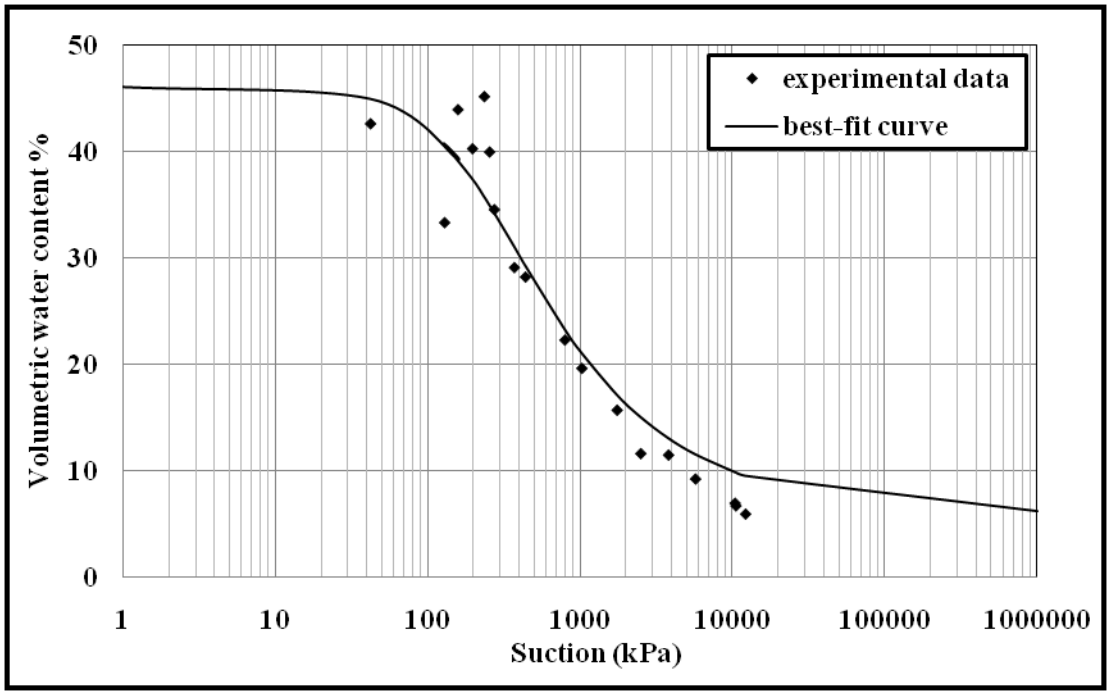

b- 4.5% PCI and curing time of 7 days (α=0.0048 kPa^{-1}, m=0.372, n=1.593)

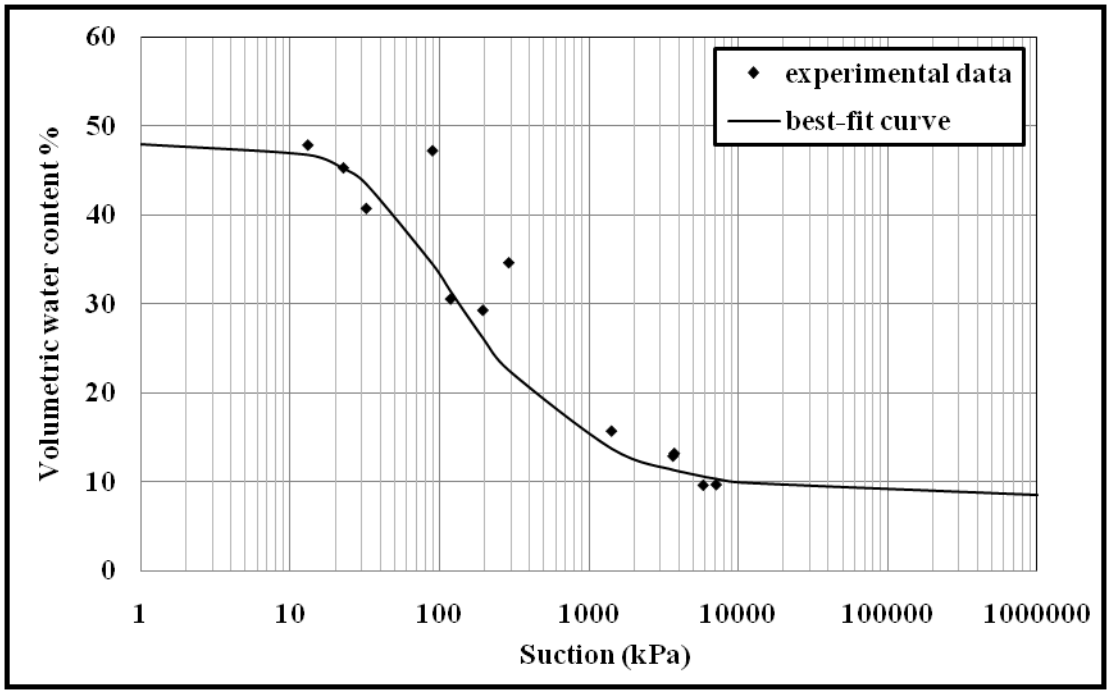

c- 2% PCI and curing time of 7 days (α=0.0166 kPa^{-1}, m=0.389, n=1.635)

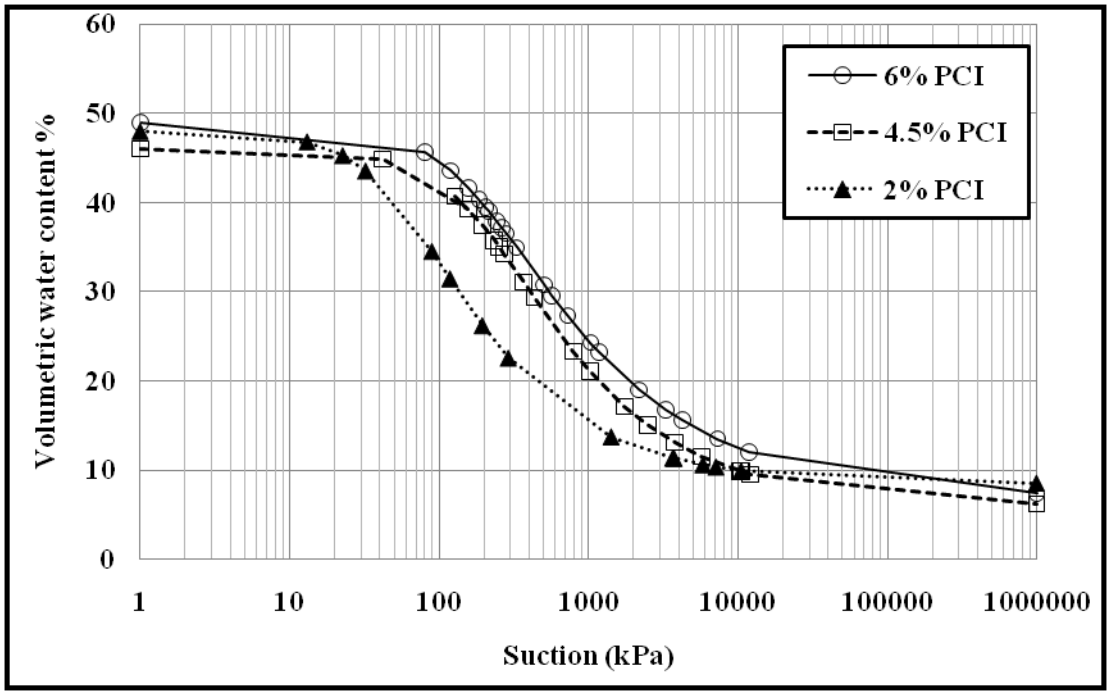

d- van Genuchten model for curing time of 7 days

Figure 4- 13 Model prediction for WRC for curing time of 7 days (a) 6% PCI, (b) 4.5% PCI, (c) 2% PCI, (d) van Genuchten model for various binder contents (6%, 4.5%, 2% PCI)

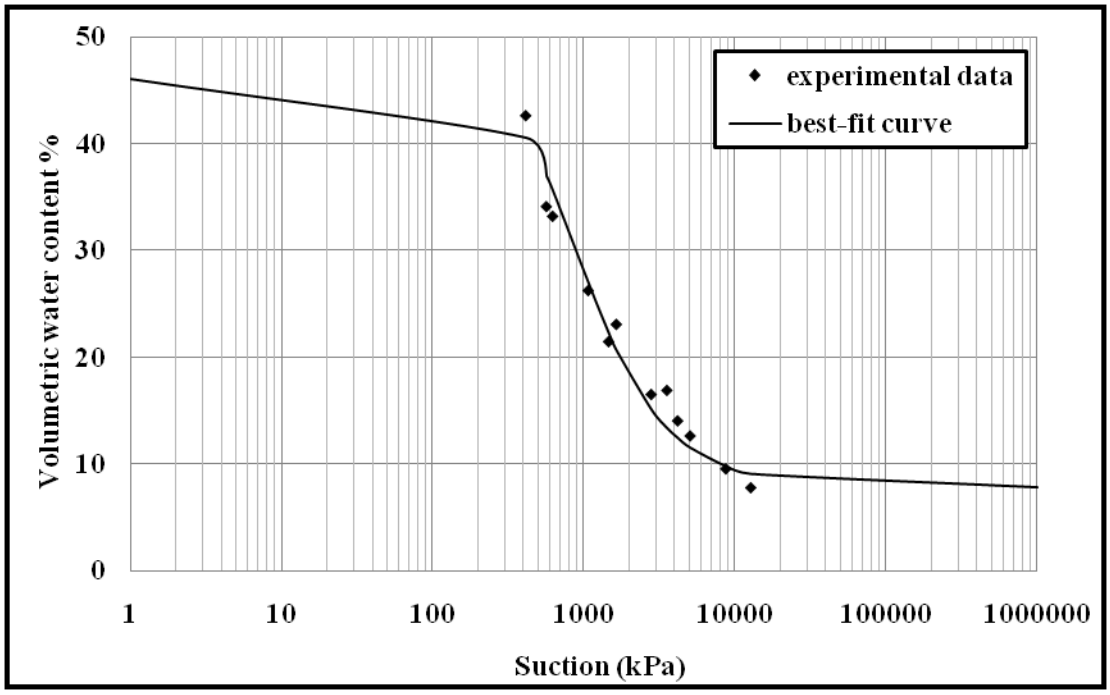

a- 6% PCI and curing time of 28 days (α=0.0014 kPa^{-1}, m=0.538, n=2.164)

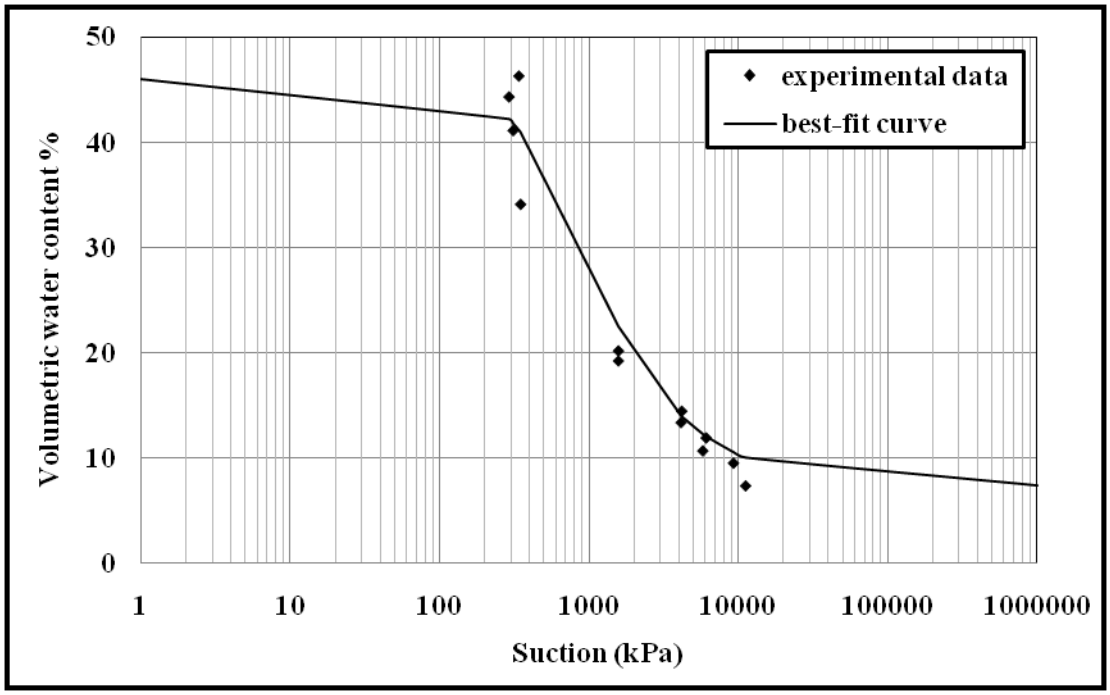

b- 4.5% PCI and curing time of 28 days (α=0.0016 kPa^{-1}, m=0.478, n=1.914)

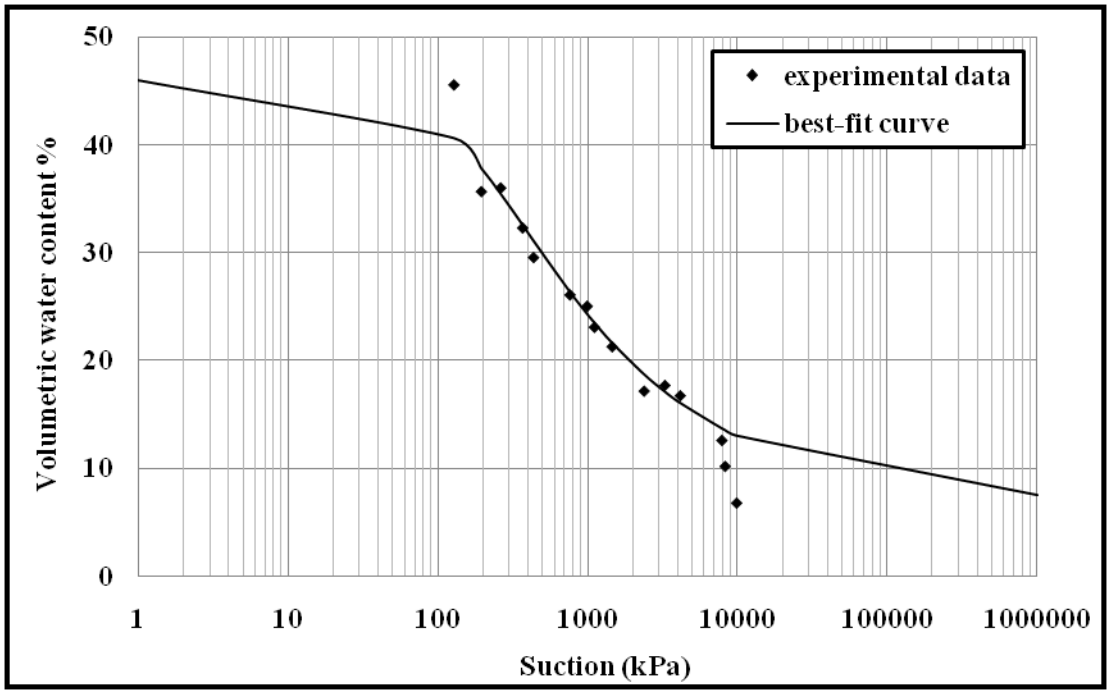

c- 2% PCI and curing time of 28 days (α=0.0054 kPa^{-1}, m=0.315, n=1.461)

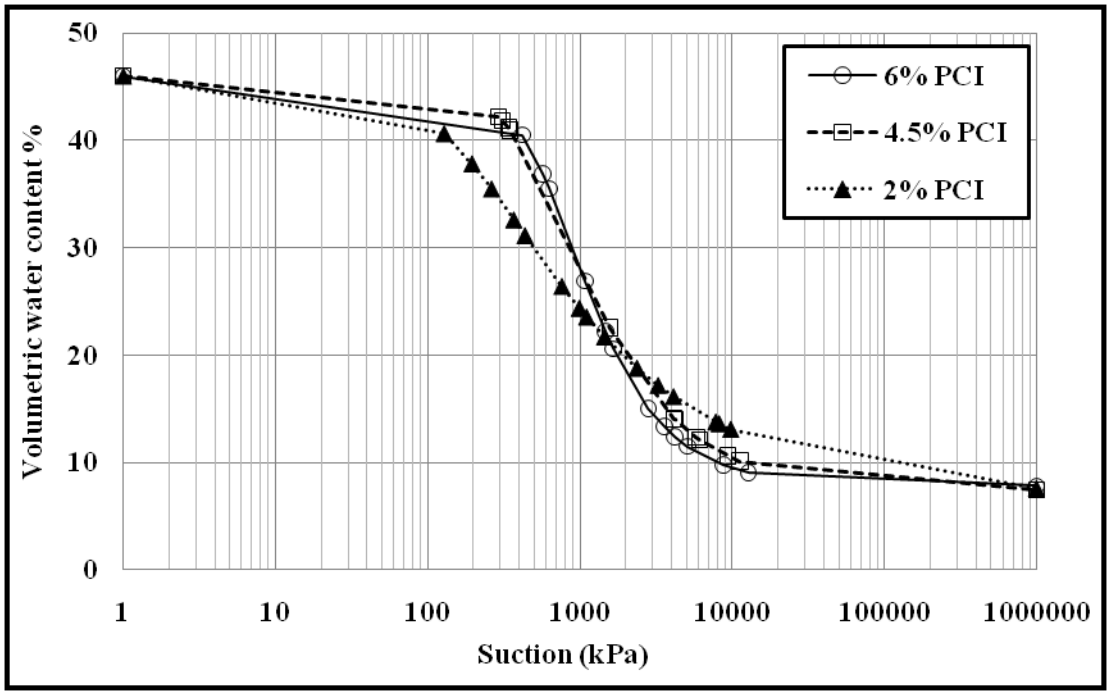

d- van Genuchten model for curing time of 28 days

Figure 4-14. Model prediction for WRC for curing time of 28 days (a) 6% PCI, (b) 4.5% PCI, (c) 2% PCI, (d) van Genuchten model for various binder contents (6%, 4.5%, 2% PCI).

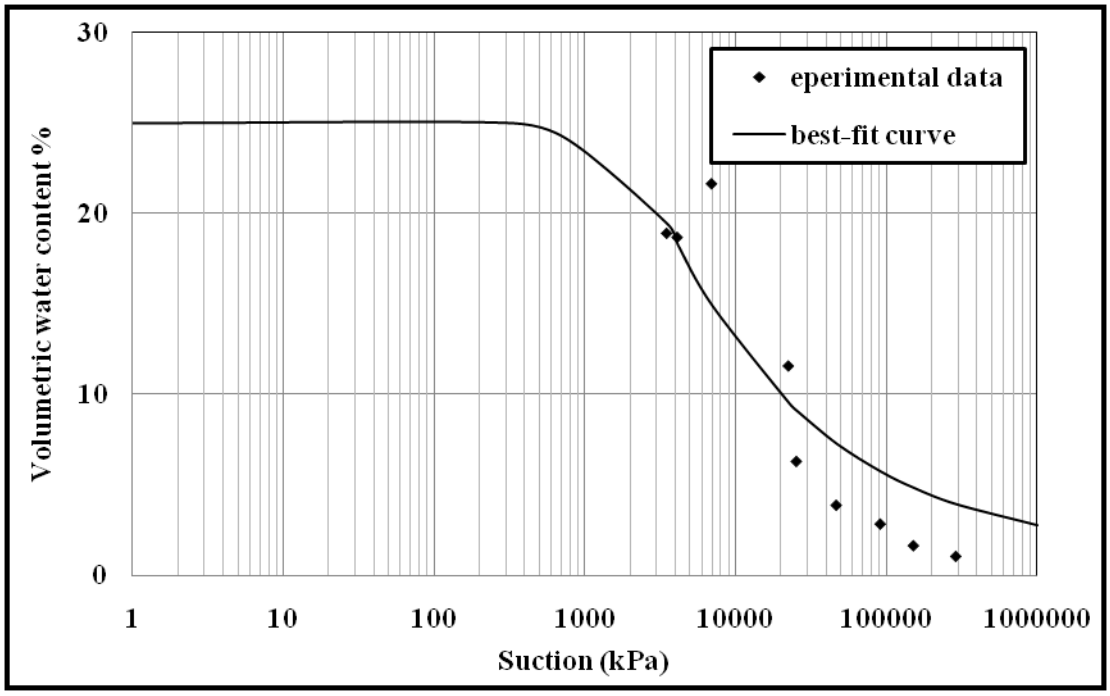

a- 6% PCI and curing time of 90 days (α=0.0024 kPa^{-1}, m=0.298, n=1.425)

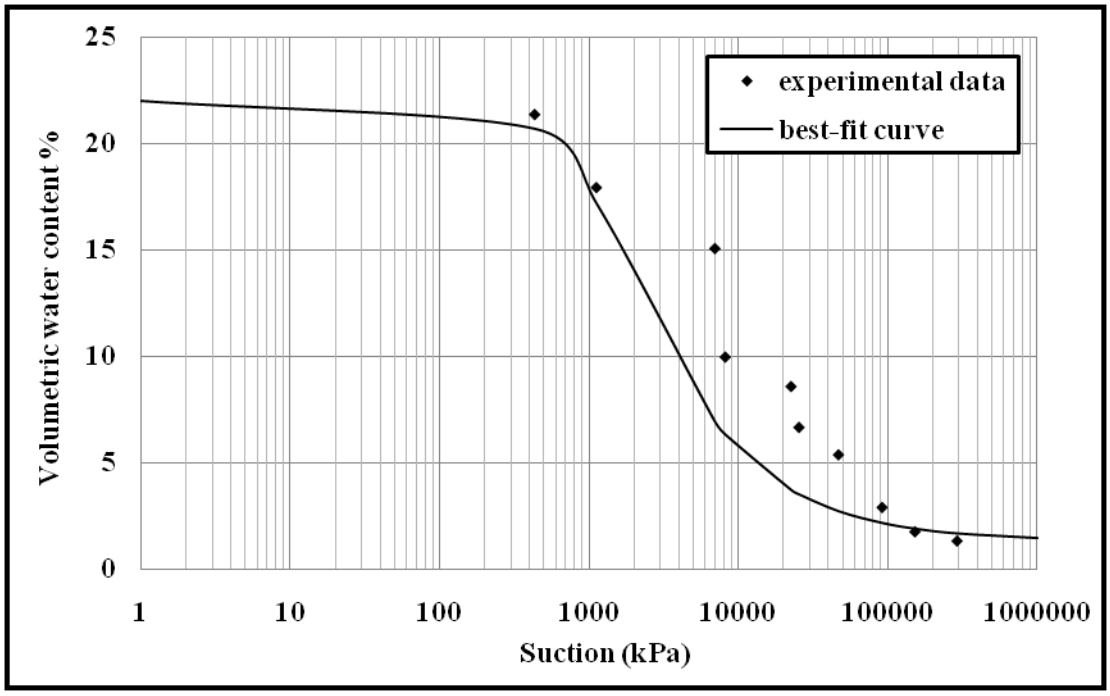

b- 4.5% PCI and curing time of 90 days (α=0.0008 kPa^{-1}, m=0.424, n=1.736)

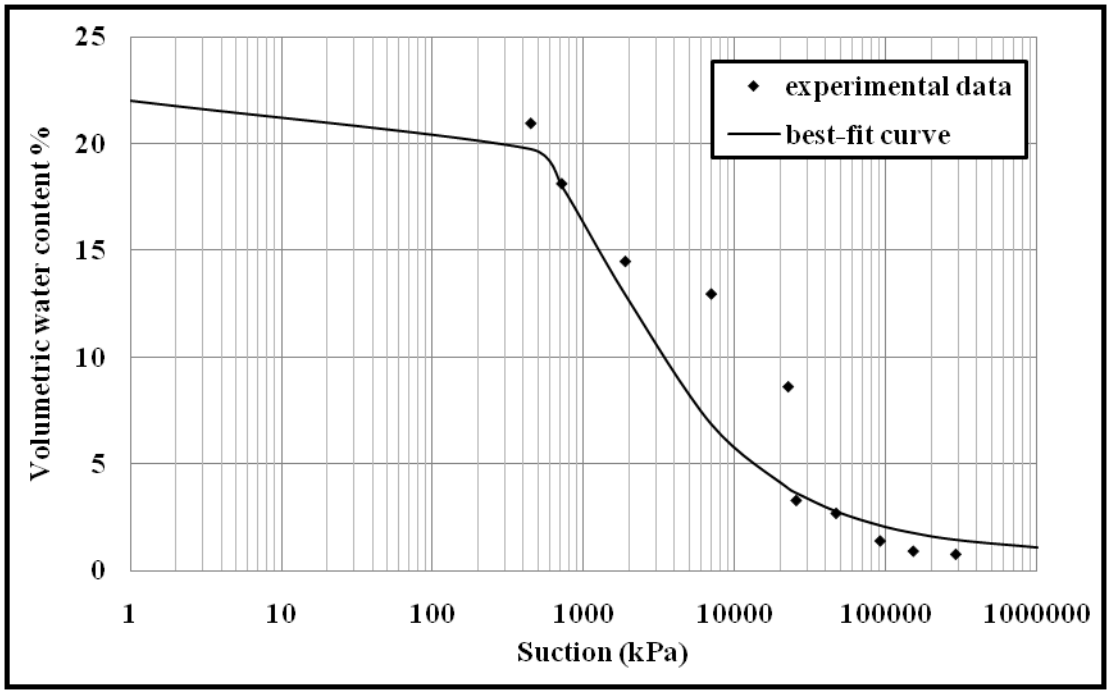

c- 2% PCI and curing time of 90 days (α=0.0012 kPa^{-1}, m=0.37, n=1.587)

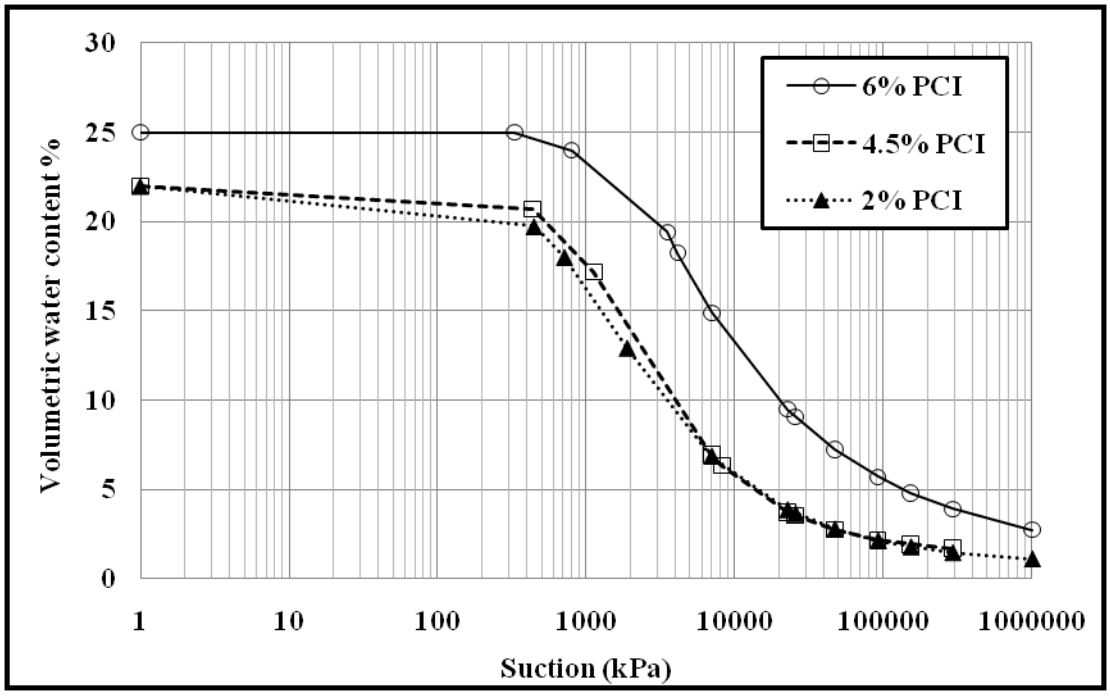

d- van Genuchten model for curing time of 90 days

Figure 4-15 Model prediction for WRC for curing time of 90 days (a) 6% PCI, (b) 4.5% PCI, (c) 2% PCI, (d) van Genuchten model for various binder contents (6%, 4.5%, 2% PCI)

4.3.2 Unsaturated hydraulic conductivity

The unsaturated hydraulic conductivity obtained by the van Genuchten (1980) model (Equation 4-11) versus suction for various binder contents and curing times is plotted in Figures 4-16 and 4-17. As expected, the unsaturated hydraulic conductivity of GF decreases as the suction increases. Furthermore, as the binder content and degree of hydration index increase, the unsaturated hydraulic conductivity of GF decreases. This is more obvious at low suction ranges. This can be explained by the fact that unsaturated hydraulic conductivity is a function of WRC and saturated hydraulic conductivity. As the hydration process proceeds, more hydration products are produced (Figure 4-4). The formation of these products in the pores with curing time leads to a reduction of porosity (Figure 4-6) and the refinement of the pore structure of GF materials which creates a barrier to water movement in the pores. As a result, saturated hydraulic conductivity decreases which in turn leads to lower unsaturated hydraulic conductivity. In brief, as the degree of hydration increases, unsaturated hydraulic conductivity is reduced (Figure 4-16). The effect of binder contents on the unsaturated hydraulic conductivity of GF is easily noticed at low suction ranges. It can be seen that increasing the binder content will reduce the unsaturated hydraulic conductivity (Figure 4-17). As mentioned earlier, when the binder proportion is increased, more cement hydration products are produced, and this refines the pore structure of the GF materials.

It is important to state that all the factors that affect the WRC and saturated hydraulic conductivity are applicable for unsaturated hydraulic conductivity.

$$kr = \frac{\{1-(\alpha\psi)^{n-1}[1+(\alpha\psi)^{n}]^{-m}\}^{2}}{[1+(\alpha\psi)^{n}]^{m/3}}$$

Equation 4-11

$$kr = \frac{k_{unsat}}{k_{sat}}$$

Equation 4-12

kr = relative coefficient of permeability

ψ = matrix suction (kPa)

α , n, m = fitting parameters

k_{unsat} = unsaturated hydraulic conductivity

k_{sat} = saturated hydraulic conductivity

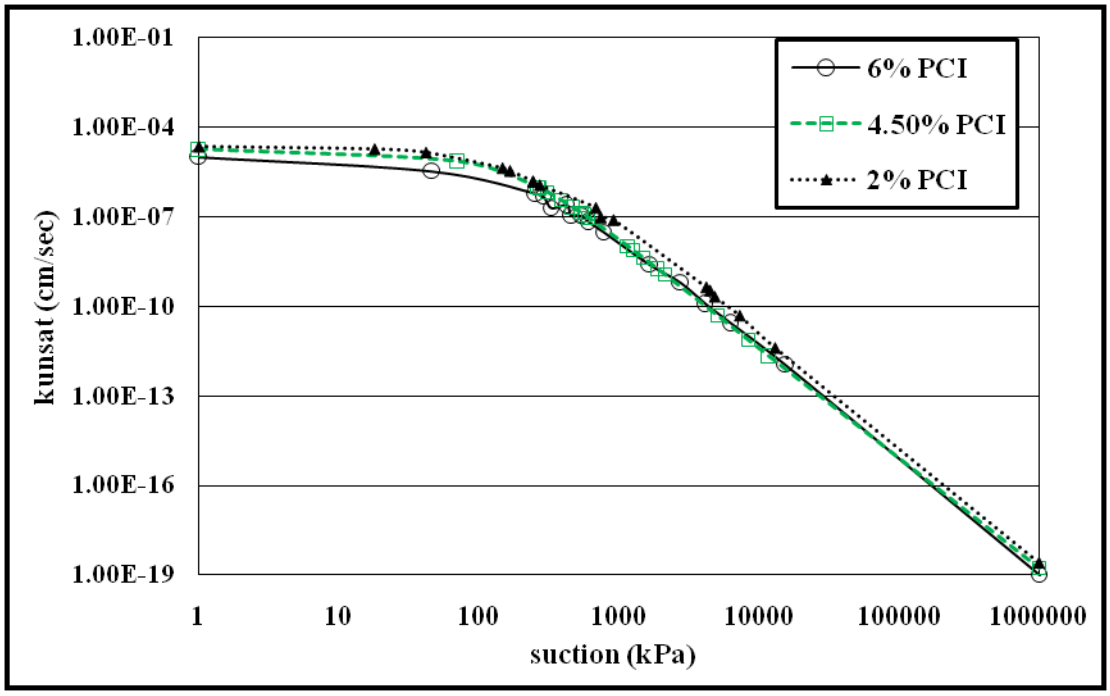

a- curing time of 3 days

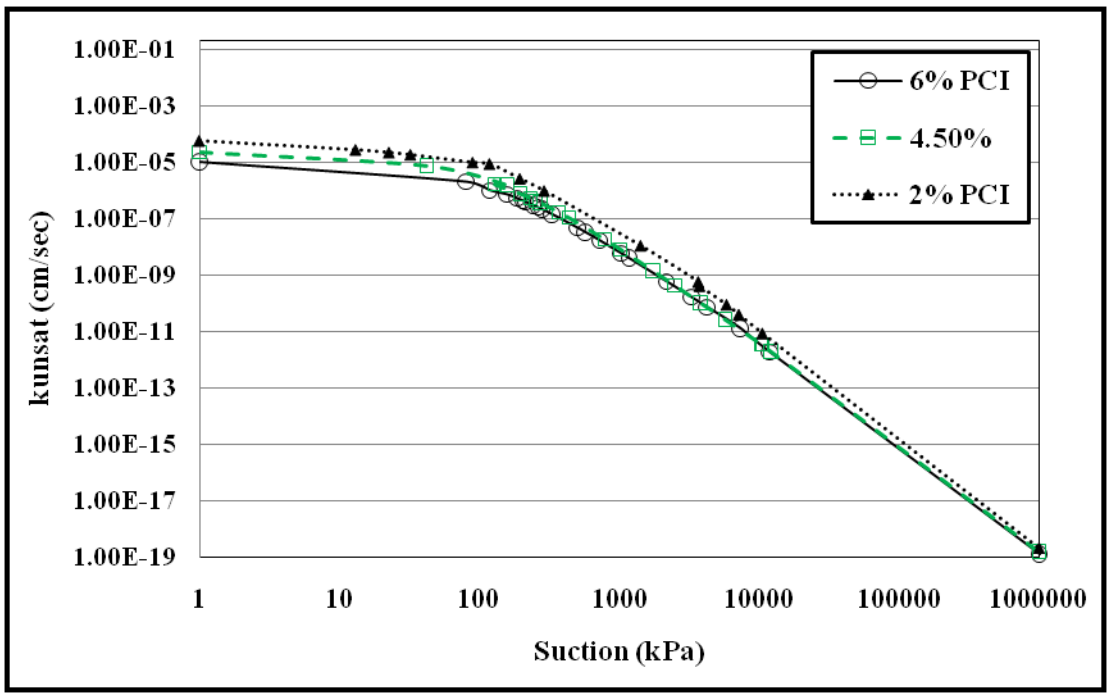

b- curing time of 7 days

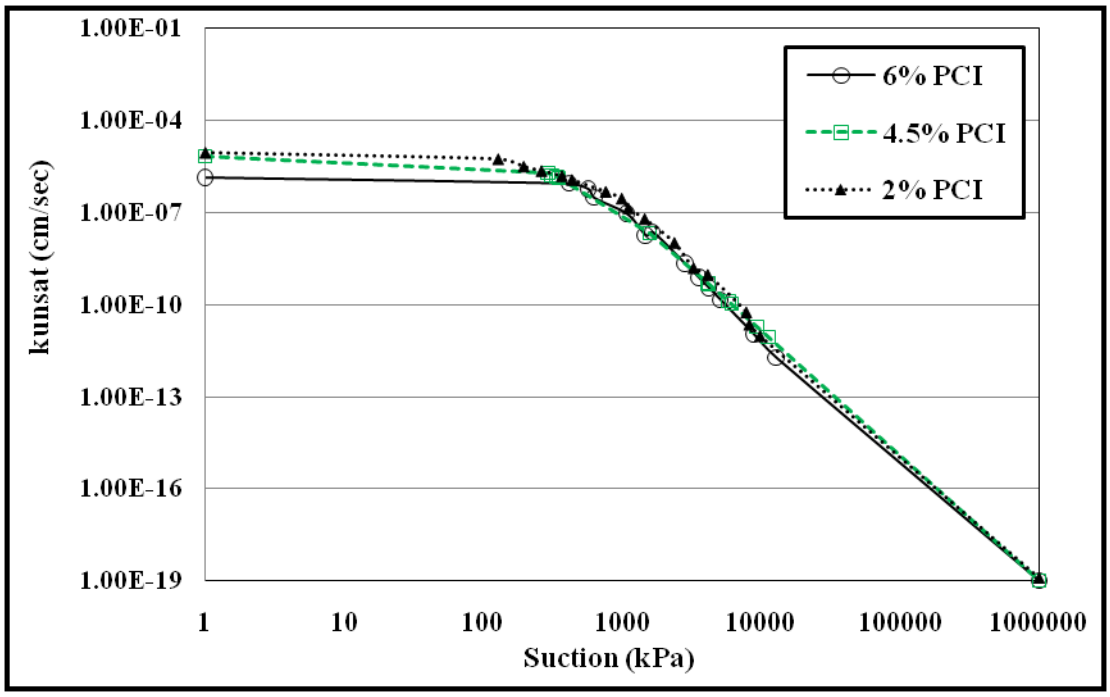

c- curing time of 28 days

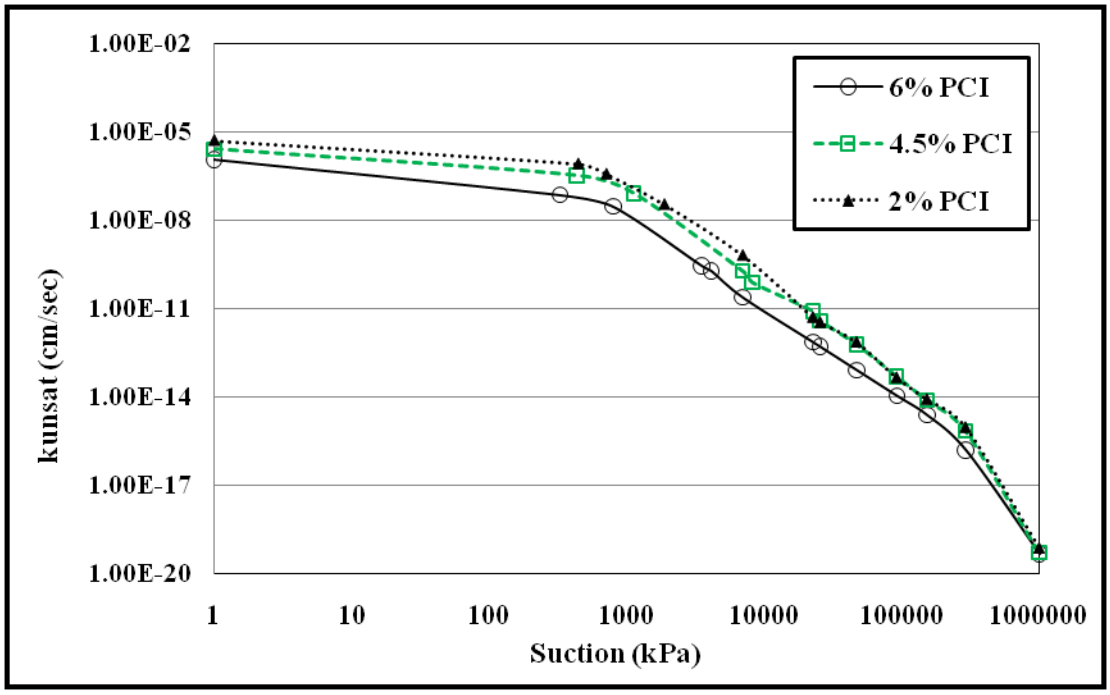

d- curing time of 90 days

Figure 4-16 Unsaturated hydraulic conductivity of GF vs. suction for various binder contents and curing time of (a) 3 days, (b) 7 days, (c) 28 days, (d) 90 days

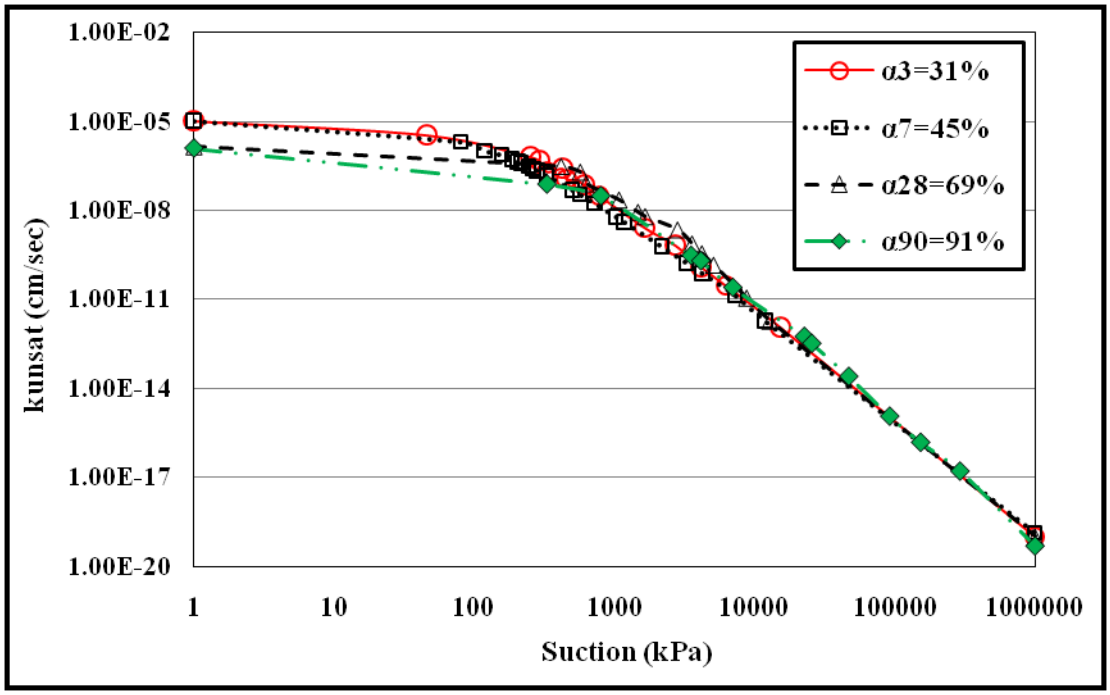

a- 6% binder content

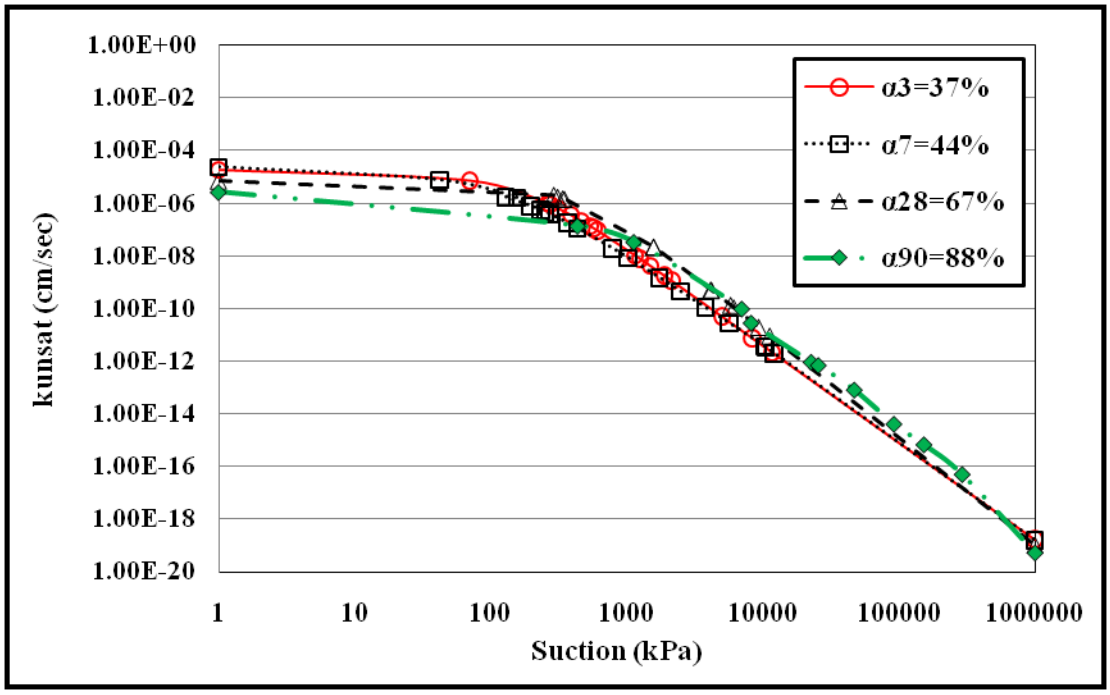

b- 4.5% binder content

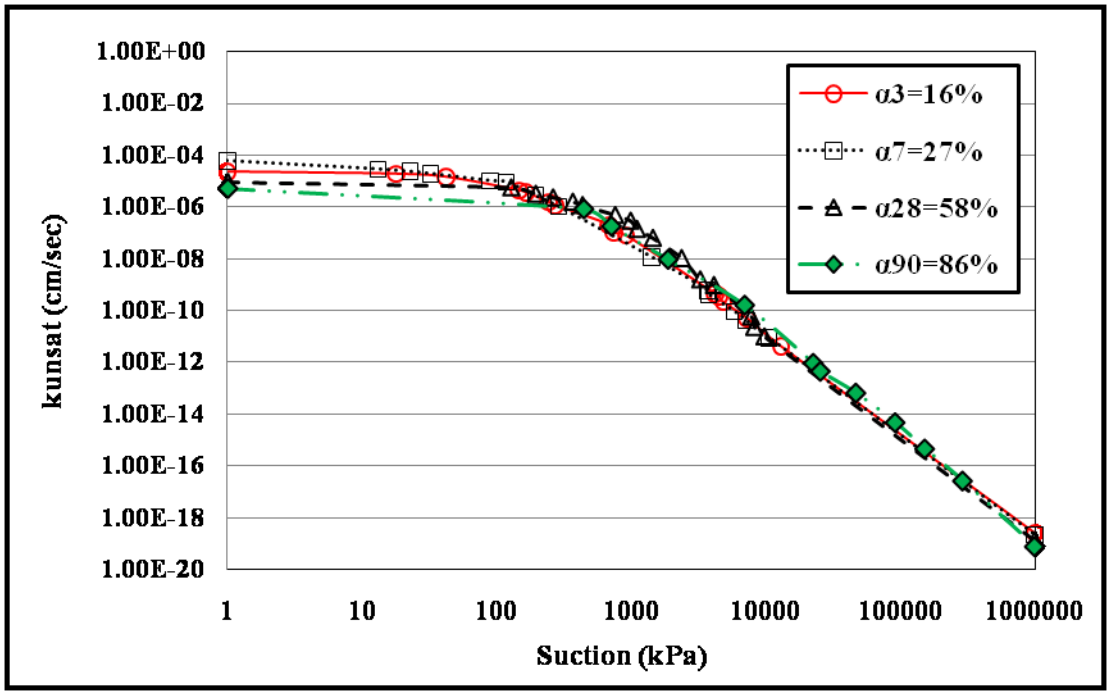

c- 2% binder content

Figure 4-17 Unsaturated hydraulic conductivity of GF vs. suction for various degrees of hydration: (a) 6% PCI, (b) 4.5% PCI, (c) 2% PCI

4.4 Summary and conclusions

The unsaturated hydraulic properties of GF have been investigated in this study. The van Genuchten (1980) model is used to estimate the unsaturated hydraulic conductivity of GF samples. In order to predict the unsaturated hydraulic conductivity, saturated hydraulic conductivity and WRC are required. The latter is measured in the laboratory by using two different techniques, which include a WP4-T dewpoint potentiameter and the saline solution method. Based on the outcomes obtained, the following conclusions can be drawn:

While the effect of curing times (or degree of hydration index) on WRC is obvious at both low and high suction ranges, the binder proportion influences the WRC at low suction ranges only.

It is noted that the AEVs increase with an increase in curing time and decrease of void ratio values, while the binder content influences the AEVs at early ages only. On the other hand, binder proportions, curing times, and degree of hydration index have slight effects on residual water content.

Functions to predict the evolution of AEVs, residual water content, and the fitting parameters from the van Genuchten model with degree of hydration index for various binder contents are proposed. These formulas can be useful for preliminary design phases of GF structures, verification of the validity of experimental results, and also estimations of the possible variations of unsaturated properties that can be expected during the service of a given GF structure.

It is observed that the unsaturated hydraulic conductivity of GF decreases when the suction increases, as well as when binder content and degree of hydration index increase. The effects of binder content and degree of hydration index are more obvious at low suction

ranges. Unsaturated hydraulic conductivity is a function of saturated hydraulic conductivity and WRC. For this reason, each factor that affects these parameters has an impact on unsaturated hydraulic conductivity.

Valuable outcomes have been obtained with regards to unsaturated hydraulic conductivity. The results can be used to assess the long term durability and environmental performance of GF structures as well as the stability and behaviour of GF structures at early ages. The findings of this study can also help to predict the potential formation of AMD in GF systems. However, it is essential to mention that only the desorption (drying) part of the WRC is investigated in this study. Therefore, the hysteresis of WRC due to adsorption-desorption isotherms needs to be addressed in further studies.

4.5 References

Barbour, S. L. Nineteenth Canadian geotechnical colloquium: The soil-water characteristic curve: a historical perspective. Canadian Geotechnical Journal 35: (1998) 873-894.

Barighel-Bouny, V., Mainguy, M., Lassabatere, T., Coussy, O. Characterization and identification of equilibrium and transfer moisture properties for ordinary and high-performance cementitious materials. Cement and Concrete Research 29 (1999) 1225-1238.

Beaudoin, J. J. Effect of humidity and porosity on fracture of hardened Portland cement. Cement and Concrete Research 12 (1982); 705-716.

Bentz, D. B. A review of early-age properties of cement-based materials. Cement and Concrete Research 38 (2008) 196-204.

Baroghel-Bouny, V., Chaussadent, T. Pore structure and moisture properties of cement-based systems from water vapour sorption isotherms. Materials Research Society (1995); 245-254.

Baroghel-Bouny, V. Texture and moisture properties of ordinary and high-performance cementitious materials. Proceedings of the International RILEM Conference Concrete: From Material to structure (1998): 144-165.

Celestin, J.C. Geotechnical properties of cemented paste backfill and tailings Liners: effect of mix components and temperature. University of Ottawa, (2008) 1-221.

Davis, G. B., Ritchie, A. I. M. A model of oxidation in pyritic mine wastes: part 1 equations and approximate solution. Applied Mathematical Modelling Vol. 10 (1986), 314-322.

Fall, M., Adrien, D., Celestin, J.C., Pokharel, M., Toure, M. Saturated hydraulic conductivity of cemented paste backfill. Minerals Engineering 22 (2009) 1307-1317

Fernández-Jiménez A., Palomo A., Revuelta D.. Alkali activation of industrial by-products to develop new earth-friendly cements. Proceeding of the 11th International Conference on Non-Conventional Materials And Technologies (NOMAT 2009) 6-9 September 2009, Bath, UK

Fisseha, B., Bryan, R. & Simms, P. Unsaturated flow and evaporation in multilayer deposits of gold paste tailings. Canadian Geotechnical Conference Edmonton: 818-823.

Fredlund, D. G. and Rahardjo, H. Soil mechanics for unsaturated soils, (1993) 1-510.

Fredlund, D. G., Xing, A., Huang S. Predicting the permeability function for unsaturated soils using the soil-water characteristic curve. Canadian Geotechnical Journal, 31(3): (1994) 521-532.

Fredlund, D.G. and Xing, A. Equations for the soil-water characteristic curve. Canadian Geotechnical Journal, 31(3): (1994) 521-532.

Fredlund, Murray D., Wilson, G.W., Fredlund, Delwyn G. Estimation of hydraulic properties of an unsaturated soil using a knowledge-based system. Department of Civil Engineering University of Saskatchewan, Saskatoon, Sask., Canada. (1997) 1-7.

Godbout, J., Bussiere, B., Aubertin, M., Belem, T. Evolution of cemented paste backfill saturated hydraulic conductivity at early curing time. Canadian Geotechnical Conference Ottawa 2007: 2230-2236.

Grabinsky, M., Bawden, W., Simon, D., Thompson, B. In situ properties of cemented paste backfill in an Alimak Stope. Canadian Geotechnical Conference Edmonton (2008) 1-7.

Hau, C., Acker, P., Ehrlacher, A., Analyses and Models of the Autogenous Shrinkage of Hardened Cement Paste, Cement and Concrete Research 25 (7): 1995.

Leong, E.C. and Rahardjo, H. Permeability functions for unsaturated soils. Journal of Geotechnical and Geo-environmental Engineering. (1997) 1118-1126.

Leong, E.-C., Tripathy, S. & Rahardjo, H. Total suction measurement of unsaturated soils with a device using the chilled-mirror dew-point technique. Ge´otechnique (2003) 53, No. 2, 173–182.

Mbonimpa, M., Cissokho, F., Bussiere, B., Maqsoud, A., Aubertin, M., A numerical study of oxygen flux through inclined covers with capillary barrier effects. Canadian Geotechnical Conference Edmonton (2008) 1-8.

Mokarem, D. W. Development of concrete shrinkage performance specifications. Virginia Polytechnic Institute and State University (2002) 1-225.

Neville, A. M. Properties of Concrete. Forth Edition, (1995) 1-844.

Persson, B. Self-desiccation and its importance in concrete technology. Building Materials Division of Lund University (1997) 1-13

Petry, Thomas M., Jiang, C. Evaluation and utilization of the WP4 Dewpoint PotentiaMeter phase I & II. University Transportation Center Program at the University of Missouri-Rolla (2003).

Pokharel, M. Geotechnical and environmental responses of paste tailings systems to coupled thermo-chemical loadings. University of Ottawa. (2008) 1-248.

Simon, D. Microscale analysis of cemented paste backfill. University of Toronto (2005) 1-282.

Sreedeep, S., and Singh, D. N. Methodology for determination of osmotic suction of soils. Geotechnical and Geological Engineering (2006) 24: 1469–1479.

Sreedeep, S., and Singh, D. N. Nonlinear curve-fitting procedures for developing soil-water characteristic curves. Geotechnical Testing Journal (2003) 29: 1-10.

Tang, A., Cui, Y. Controlling suction by the vapour equilibrium technique at different temperatures and its application in determining the water retention properties of MX80 clay, CERMES-ENPC, Institute Navier, France (2005) 1-32.

Thakur, Vikas K.S., Sreedeep, S., and Singh, Devendea N. Laboratory investigations on extremely high suction measurements for fine-grained soils. Geotechnical and Geological Engineering (2006) 24: 565–578.

Thakur, Vikas K.S., Sreedeep, S., Singh, Devendra N. Parameters affecting soil–water characteristic curves of fine-grained soils. Journal of Geotechnical and Geoenvironmental Engineering ASCE (2005)131:4(521).

van Genuchten, M. TH. A Closed-form equation for predicting the hydraulic conductivity of unsaturated soils. Soil Science Society of America Journal (1980) 44:892-898.

Vick, 1990 S.G. Vick, Planning, BiTech Publishers Ltd, Design and Analysis of Tailings Dams (1990).

WP4 and WP4-T Operator's manual. Version 2.2, (2003) 1-83.

Yilmaz, E. How efficiently the volume of wastes produced from mining operations can be reduced without causing any significant environmental impact? Environmental Synthesis Report, UQAT, Canada, (2007)1-45.

4.6 Acknowledgement

The authors would like to acknowledge National Sciences and Engineering Research Council (NSERC), University of Ottawa and the National Research Council (NRC) of Canada.

Chapter 5

Technical Paper III

Thermo-Hydro-Mechanical Behaviour of Gelfill in Column Experiments

Abstract

Two columns have been built to simulate the THM behaviour of GF under drained and undrained conditions. The columns are insulated using insulating foam sealant to maintain temperature differences. The columns are built and filled in three filling sequences of 50 cm over 3 days. To prepare the mix, a binder content of 4.5%, w/c ratio of 8.2, and 0.4% (by weight of solids) sodium silicate type N have been used to prepare the mix. The GF columns are cured at room temperature for 28 days. The suction and temperature developments during the hydration process are monitored. When the curing phase has been completed, the cylindrical samples are taken out from the columns to study the THM behaviour of GF. UCS, saturated hydraulic conductivity, and thermal conductivity tests are conducted. The outcomes of the aforesaid tests are compared with the results obtained by testing the mould samples. The results show that the mechanical, hydraulic and thermal behaviour of GF columns are coupled. The UCS values of GF are strongly coupled to heat development, saturation and suction development within the GF. In addition, the UCS outcomes, K tests for samples obtained from the GF columns show higher values than small samples and saturated hydraulic conductivity from the GF columns show lower values than small samples

Keywords: drained and undrained conditions; gelfill; cement; tailings; column.

5.1 Introduction

Cemented backfill is extensively used in mining operations for underground mine support, the maximization of ore recovery, and tailings waste management. The most important performance properties of cemented backfill include mechanical (e.g. UCS), hydraulic (e.g. hydraulic conductivity), and thermal (e.g. thermal conductivity) properties. Several studies (Fall et al., 2010; Celestin and Fall, 2009; Fall et al., 2009; Ylimaz et al., 2003) have been performed to study the factors that affect the performance properties of cemented backfill. However, most of these studies dealt with rockfill, hydraulic backfill and cemented paste backfill. Only a few studies have focused on GF (a mix of tailings, water, cement, and sodium silicate), the most recent type of cemented backfill. In addition, most of the previous studies on cemented backfill, in particular, GF, are performed on small (mould) laboratory samples. However, there is growing recognition that the actual in situ properties of cemented backfill material are significantly different from the laboratory material. It is important to understand the properties of the field material in order to optimize the cemented backfill mix design. Indeed, studies show that for a given mix and curing time, the UCS of in situ cemented backfill cored samples can be 2 to 4 times higher than those of the same mix poured into moulds (e.g, Le Roux et al., 2002; Cayouette, 2003; Revell, 2004). The differences in UCS could be related to the cemented backfill hardening conditions in the stope, such as stope size and geometry, as well as the coupled THM that occurs in cemented backfill. Increasing the size of the GF structure will increase hydration heat, which in turn, enhances the UCS of GF. However, since GF is new cemented material, there have been no studies conducted to investigate the coupled THM processes that occur in GF. There is the need to gain more knowledge on the THM behaviour of GF.

The objectives of this paper are:

- to investigate the coupled thermal, hydraulic and mechanical behavior of cemented GF by conducting column experiments, and
- to compare the outcomes of the columns experiment with the results obtained from small samples that have the same mix proportion and curing time.

5.2 Experimental Programs

5.2.1 Materials

The materials used to prepare the GF mix include binder, tailings, sodium silicate, and water.

5.2.1.1 Binder and mixing water

PCI was used as the binder. It is the most common binder material used by the mining industry to produce cemented backfill. Table 5-1 shows the physical and chemical properties of the binder. Tap water was used to mix the binder and tailings.

Table 5-1 Characteristics of Portland cement type I

Types of Binder	MgO	CaO	SiO_2	Al_2O_3	Fe_2O_3	SO_3	Relative Density	Specific Surface (m^2/g)
PCI	2.65	62.82	18.03	4.53	2.70	3.82	3.10	1.30

5.2.1.2 Tailings

Ground silica tailings (TS) were used in this study. The advantage of selecting TS as tailings material is to accurately control the mineralogical and chemical composition of the tailings. Furthermore, natural tailings contain various amounts of sulphate and other undesirable minerals which can interact with cement hydration and sodium silicate, and thus lead to uncertain results. This can significantly affect the outcomes of the study. TS contains 99.8% SiO_2 and displays a grain size distribution close to the average of nine Canadian mine tailings (Figure 5-1). It can be observed that TS has about 45 wt.% fine particles (< 20 μm) and can be classified as medium tailings. Tables 5-2 and 5-3 show the physical and chemical properties of TS.

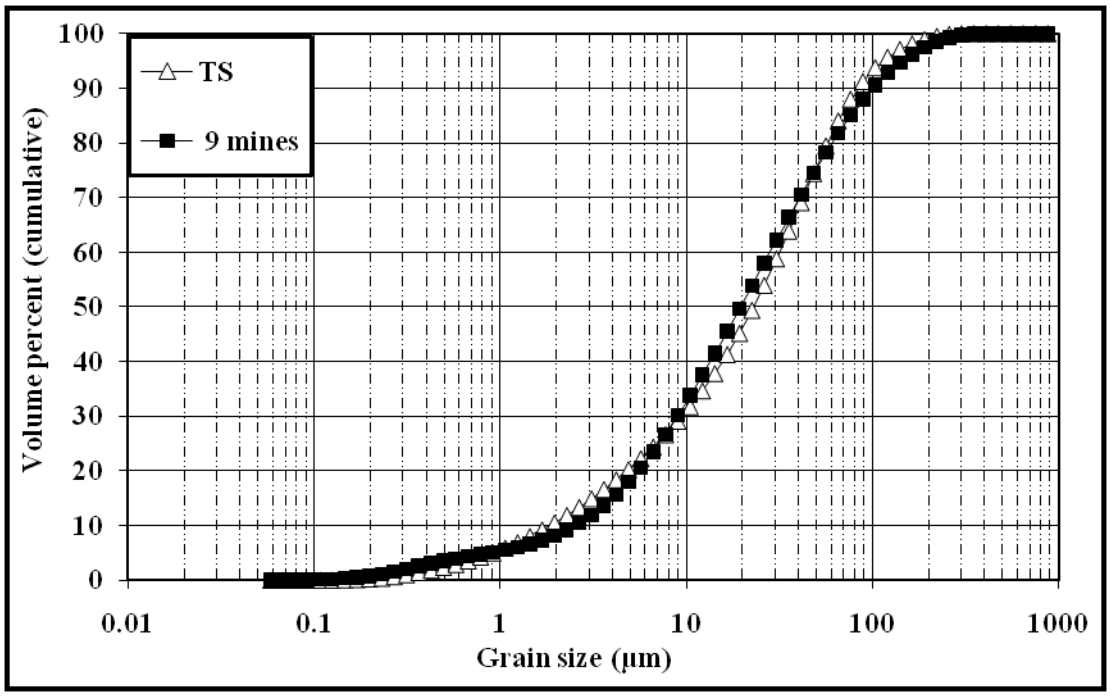

Figure 5-1 Grain size distribution of the tailings used and the average grain size distribution of tailings from nine Canadian mines

Table 5-2 Physical properties of artificial tailings (TS)

Element	G_s	D_{10} (µm)	D_{30} (µm)	D_{50} (µm)	D_{60} (µm)	D_{90} (µm)	C_u	C_c
TS	2.7	1.9	9.0	22.5	31.5	88.9	16.2	1.3

Table 5-3 Main chemical elements of TS

Element	Al wt%	Ca wt%	Si wt%	Fe wt%	Na wt%	Pb wt%	S wt%	K wt%
TS	0.1	<0.01	99.8	<0.01	<0.01	0.0	0.0	0.0

5.2.1.3 Sodium silicate

Sodium silicate type N was added to the mix in liquid form. It is an inorganic chemical, made by mixing various ratios of sand and soda ash (sodium carbonate) at high temperatures. It is described as a clear, colourless, and viscous liquid. Sodium silicate is manufactured by National Silicates Ltd. Table 5-4 gives the sodium silicate properties.

Table 5-4 Sodium silicate properties (National Silicates Ltd.)

Properties	Values
Na_2O% by weight	8.90
$SiO_{2\%}$ by weight	28.66
Weight ratio,%SiO_2 /%Na_2O	3.22
Specific Gravity @ 20°C	1.394
Solids%	37.56

5.2.1.4 Columns

KING Pltp Ltwall builder's tubes, sized 8.5" x 8', and 12" x 8' were used as the formwork to build the GF columns**.** A small tube was placed inside a large tube. The gap between the tubes was filled with foam as illustrated in the following section.

5.2.1.5 Foam

Insulating foam sealant, GREAT STUFF^{TM}, was used to fill the gap between the two tubes. The foam is used to fill, seal, and insulate gaps up to 1 inch. It expands to take the shape of the cracks and voids. Also, the insulating foam sealant forms a permanent, airtight, and water-resistant bond. Table 5-5 gives the foam properties.

Table 5-5 Properties of foam from Manufacturer

Properties	Values
k-factor (thermal resistance) per meter ASTM C518 @24°C mean temp., W/m˚C	0.033
Compressive strength, ASTM D1621, parallel to rise, kPa	82.05
Apparent density, ASTM D1622, kg/m^3	22.9

5.2.2 Developed experimental set-up of column experiments

Two columns that are 21.25 cm in diameter and 150 cm in height were developed to simulate the GF placement in underground mining with drained and undrained conditions

(Figure 5-2). Figure 5-3 shows a schematic diagram of the experimental set-up. The columns were insulated using insulating foam sealant to maintain temperature differences between the GF column and the atmosphere, which was achieved by placing a small builder tube (21.25 cm) inside a big builder tube (30 cm). The gap between the two columns was filled with the insulating foam. The top of the columns was left uncovered in order to allow desiccation. The idea was to simulate underground mining conditions. In most cases, the surface of backfill is exposed and can be used as a mucking floor while the sides and the bottom are protected by the adjacent rocks. The base of the undrained column was sealed to prevent any leakage while a funnel was placed at the base of the drained column. The funnel was filled with crushed coarse aggregate with a maximum size of 10 mm. The aggregate was topped with geotextile material. The aggregate was saturated in water for 24 hours to avoid any absorption of the drained water by the aggregate. Then, the surface of the aggregate was air dried (to achieve the environment of the saturated air dried surface for the coarse aggregate). Both columns were placed on a steel table that was designed for this purpose. A scale and a container were put under the drained column to measure the weight of the drained water. Temperature sensors model TH-T manufactured by ROCKTEST and soilmoisture model No.2100F tensiometers by Soilmoisture Equipment Corporation were placed at three levels in the center of each column prior to filling (Figure 5-3). A Temperature and humidity sensor was used to monitor the changes in room temperature and RH during the curing period.

Figure 5-2 Set-up of columns (drained (D; to the left), and undrained (UN; to the right), conditions)

5.2.3 Preparation of gelfill material, filling, and curing of the column

The GF mix contained 0.4% wt sodium silicate, 4.5% PCI with a solid mass concentration of 73% which correspond to a w/c ratio of 8.2. The mixing time was 10 minutes for all mixes. Mixing was done using a B20F food mixer. The columns were filled up to the height of 150 cm in three filling sequences of 50 cm each. Each lift was allowed to set for 24 hr, then a new layer was placed. This allows GF placement close to field conditions and evaluation of the impact of filling on GF THM properties. Temperature sensors and tensiometers were fixed at the centre of each layer ahead of filling in order to monitor temperature and suction developments with time (Figure 5-3). When the filling phase was

over, both columns were left to cure in room temperature for 28 days (room temperature and RH% were measured during curing time, Figure 5-4). Temperature and suction readings were monitored almost every hour for the first five days and twice a day for the rest of the curing period. The tensiometer readings became unreliable when they reached 70 kPa on the seventh day of curing, and for this reason, the suction readings were terminated after that period of time. Negative pore water pressure that was measured by a tensiometer was limited to approximately 90 kPa due to the possibility of cavitation of water in the tensiometer.

The drained water was collected and weighed by the container and the electronic scale placed under the funnel that was attached to the bottom of the drained column. When the curing step was completed, the samples were taken out from different depths of the columns (25 cm, 75cm, and 125 cm); this method of sampling was also adopted by Le Roux et al. (2005) and it is called block sampling. The columns were first cut into big pieces and then samples that are 5 cm in diameter and 10 cm in height were carved from the blocks.

In this study, the samples were subjected to UCS, hydraulic conductivity, and thermal conductivity tests. The results of the tests carried out on the column samples were compared with the results obtained from tests on the small samples (5 cm x 10 cm). The experimental program was carried out on the small GF samples and the results obtained are available in Technical Paper I of this thesis.

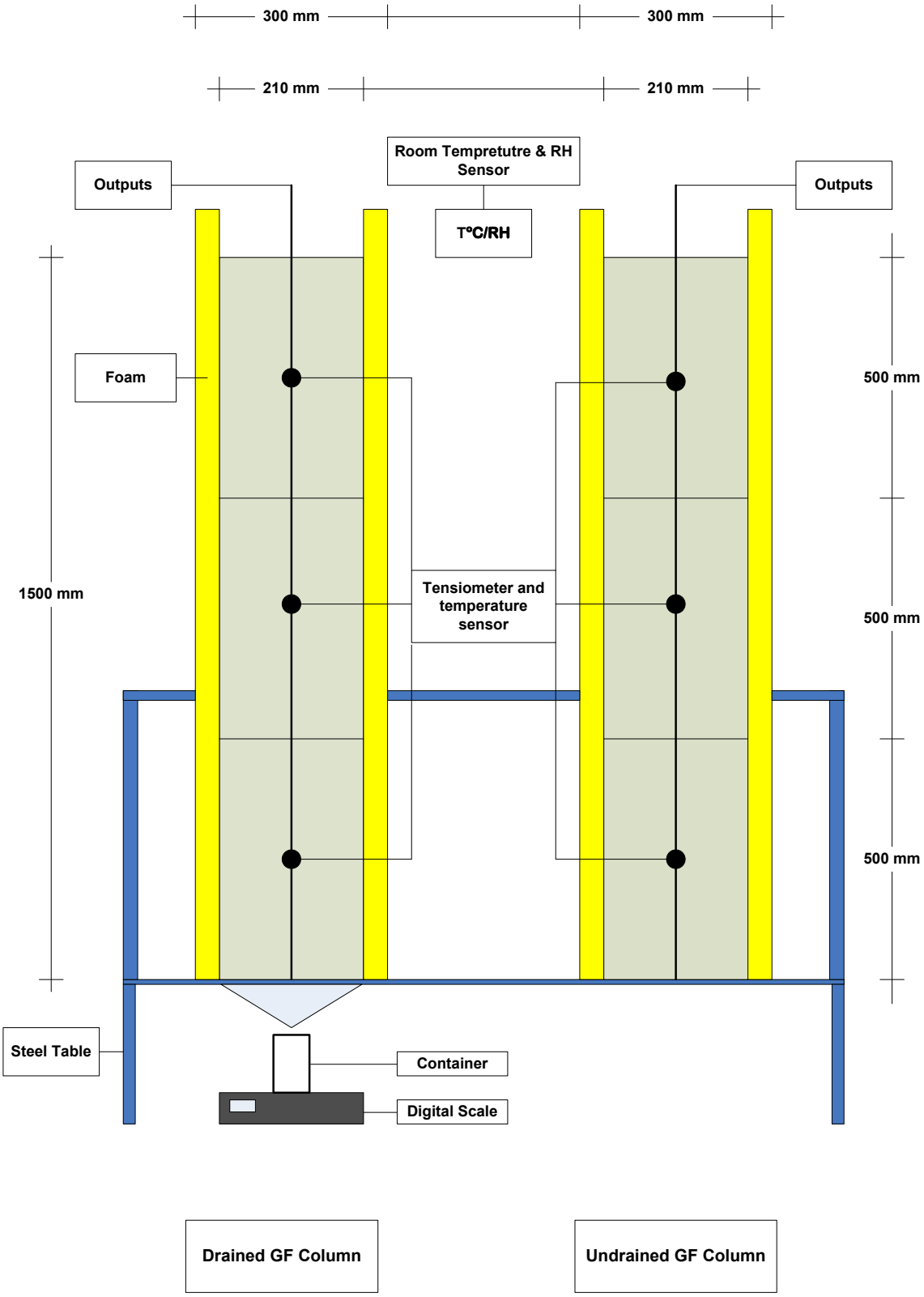

Figure 5-3 Schematic diagram of the experimental set-up

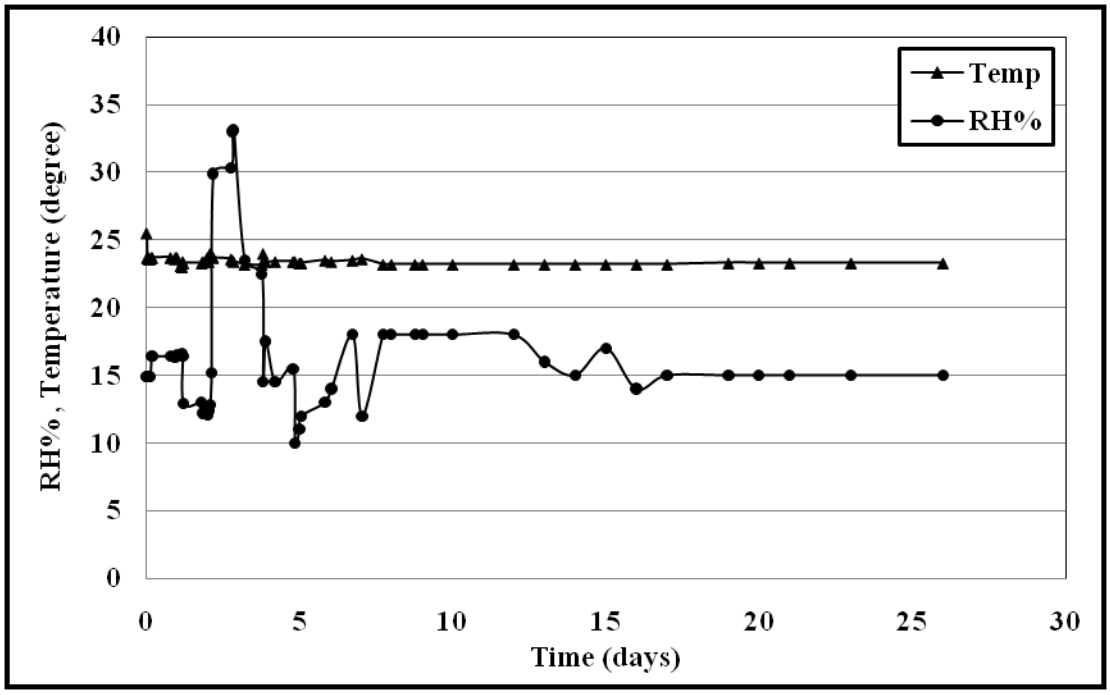

Figure 5-4 Evolution of the room temperature and air RH% during curing time

5.2.4 Preparation and curing of the gelfill mould (small) samples

Around 70 GF mould samples were prepared. The tailings, binder, water, and sodium silicate gel were mixed using a B20F food mixer for 10 minutes. The tailings, binder, and water were mixed first, followed by the addition of sodium silicate gel. The binder proportion used to prepare the mixes is 4.5% of PCI with a solid mass concentration of 73% which correspond to a w/c ratio of 8.2. The prepared GF was poured into cylindrical plastic moulds, 5 cm in diameter and 10 cm in height. The prepared samples were then sealed and cured in a laboratory environment at 20°C ± 2 °C for a period of 28 days. Mechanical, hydraulic conductivity and thermal conductivity tests were carried out on the samples after their curing. It should be mentioned that the results of the tests performed on the small GF samples are used in this thesis only for comparison purposes. A detailed

presentation and analysis of the results are available elsewhere (Technical Paper I of this thesis).

5.2.5 Testing and analysis methods and procedures

5.2.5.1 Mechanical tests

UCS tests were performed on samples taken out from the columns at depths of 25 cm, 75 cm, and 125 cm after 28 days of curing time. UCS tests were also performed on GF mould samples. The specimens were tested according to ASTM - C 39 using a computer-controlled mechanical press. The press has a normal loading capacity of 50 kN. All samples were tested at a constant deformation rate of 1 mm/min. All test data were collected using a computerized data logging system. The results were saved using LabView computer software. Two to three samples were tested for each layer and GF cylinder, and then, the average was determined to represent the compression strength of the layer or GF small sample.

5.2.5.2 Determination of the hydraulic properties

I. Saturated hydraulic conductivity tests

Saturated hydraulic conductivity tests were conducted on the GF column and GF mould samples. After 28 days of curing time, the samples were taken out from the columns at depths of 25 cm, 75 cm, and 125 cm. The specimens were tested according to ASTM D5084-00 using a TRI-FLEX II system. A flexible wall technique in constant head mode was used. The samples were saturated in water for 24 hours prior to the testing. Each

hydraulic conductivity test was repeated at least twice to ensure that the results always fall within an accurate limit.

II. Suction measurement

Small tip tensiometers with a flexible coaxial tube were used to measure the suction in GF columns. The tensiometers were installed and calibrated using the procedure provided by the manufacturer (Soilmoisture Equipment Corporation). The purpose of the calibration is to remove air bubbles from the ceramic tip and the tube. It is essential to have an air-free tensiometer tube in order to ensure correct readings. Deaired water is used to fill the tube and the tip. The ceramic tip is soaked in water prior to its use to avoid desaturation due to evaporation from the tip. The tensiometers were fixed at the side of the columns and the ceramic tips were placed at the center of each layer prior to casting.

5.2.4.3 Determination of the thermal properties and heat development

I. Thermal conductivity tests

A KD2 thermal properties analyzer manufactured by Decagon Devices was used to measure the thermal conductivity of GF columns as well as that of the GF mould samples. The KD2 sensor needle contains both a heating element and a thermistor; care was taken to prevent bending of the probe. The device computed the values of thermal conductivity and resistivity by monitoring the dissipation in heat from a line source given a known voltage (KD2, 2006). The thermal conductivity was measured with an accuracy of 5%. The test is considered as a quick test, as the measurement speed is 1.5 minutes. The tests were conducted according to the guidelines provided by the manufacturer. Three readings were

taken for each layer at depths of 50 cm, 100 cm, and 150 cm after 28 days of curing time of the column as well as the GF mould samples.

II. Temperature development within the GF columns

Model TH-T temperature sensors manufactured by ROCKTEST were used to monitor the temperature development in GF columns. The external casing is made of an extruded stainless steel shell built to withstand long term use without corrosion. It encapsulates a highly sensitive and a reliable thermistor (instruction manual). The standard themistor used in the TH-T sensor is a 3 kΩ thermistor. Equation (5-1) is used to convert the output of the sensors from ohms to degree Celsius; this equation is provided by the manufacturer. The sensors were calibrated using thermometers. The calibration results showed a good agreement with the conversion table provided by the manufacturing company.

$$T = \frac{1}{A+B\ln R_T+C\ln^3 R_T} - 273.15 \qquad \text{Equation (5-1)}$$

where:

T = Temperature in degrees

A, B, C, = constant factors depend on themistor type

R_T = readings in ohms

5.3 Results and discussion

5.3.1 Evolution of thermal properties and heat development

5.3.1.1 Thermal conductivity

The effect of drained and undrained conditions on the thermal conductivity for the GF columns is presented in Figure 5-5. It is shown that the effects of drained and undrained conditions are insignificant. In addition, the variation in thermal conductivity values along the GF columns is minor. The range of thermal conductivity is 2 - 1.8 W/mºC for the drained column while the range for the undrained column is 2.1 - 1.7 W/mºC. The thermal conductivity of the drained and the undrained columns are higher than that of the small samples (which is 1.4 W/mºC). This is because the density of the GF columns is higher than small samples (taller samples imply better compaction and higher density). The dry density of the GF columns is 1.45 g/cm^3 while the dry density of the small samples of GF is 1.38 g/cm^3. Furthermore, from Figure 5-5, it can be observed that the thermal conductivity of the top layers is slightly lower than that of the middle and bottom layers. This can be attributed to the evaporation induced desaturation of the top layers. This is in good agreement with the results of the suction measurements shown in Figures 5-10 and 5-11. From these figures, it can be observed that the top layers have higher matrix suction (lower degree of saturation) than the middle and bottom layers. The results confirm that the thermal conductivity is strongly coupled to suction or degree of saturation. This decrease of the thermal conductivity of GF with lower saturation degree (or higher suction) can be explained by the fact that as the saturation degree decreases, the water or moisture in GF is partially replaced by air. Since water has a thermal conductivity about 25 times that of air, it is obvious that when the air content increases, the thermal conductivity of the GF will

also decrease. Similar observations were made on classical concrete (Short and Kinniburg 1978, Schnider 1982, Morabito 1989, Ashworth 1991) and cemented paste backfill (Celestin and Fall, 2008).

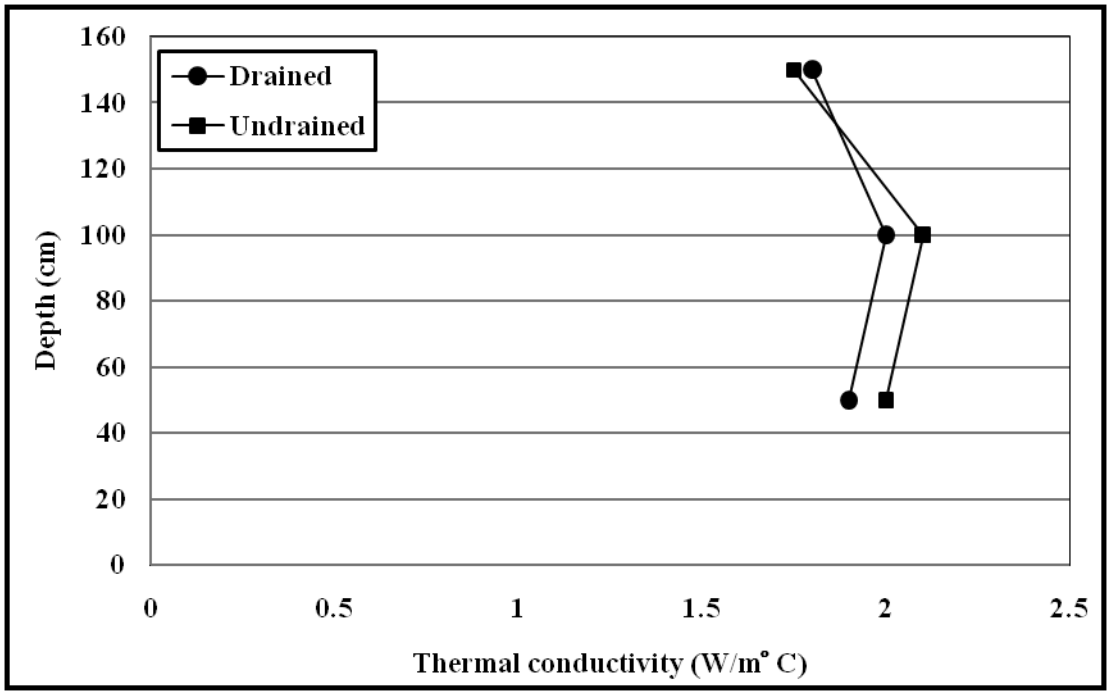

Figure 5-5 Evolution with depth of the thermal conductivity of the GF in drained and undrained conditions

5.3.1.2 Temperature development

Temperature development for the columns during the hydration process for both drained and undrained conditions is illustrated in Figures 5-6 and 5-7, respectively. It can be seen that the variations in the temperature of the bottom and the middle layers are similar, whereas for the top layers, the values are lower. A small amount of heat loss occurred because the tops of the columns were uncovered. In addition, the evolution of temperature

with time for both columns was close, which means that the drained and the undrained conditions had slight effects on temperature evolution. It can be seen that the three layers from the undrained column achieved a slight increase in temperature than the drained column at peak only. The maximum temperatures for the undrained column are 25.3ºC, 24.4ºC, and 22.7ºC for the bottom, middle, and top layers, respectively, while the maximum temperatures for the drained column are 23.6ºC, 23.6ºC, and 22.2ºC for the bottom, middle, and top layers, respectively. It seems that the rate of hydration was faster in the undrained column for the first few days. Temperature development is dependent on the rate of hydration. As the rate of hydration increases, more heat rises from the GF columns (e.g. Neville, 1995).

Also, it can be observed that a large part of the temperature released by the hydration of the GF columns occurs in the first three days. Neville (1995) stated that about one-half of the total heat is evolved between 1 and 3 days, three-quarters in 7 days, and 83% to 91% of the total heat in 6 months. This is because at early stages of hydration, different compounds of cement hydrate at different rates (e.g. C_3S and C_3A hydrate faster than C_2S); the rate of heat evolution depends on the chemical composition of the cement and the sum of heat of the individual compounds. It is well known that C_3S and C_3A liberate higher rates of heat than C_2S (Lerch and Bogue, 1934).

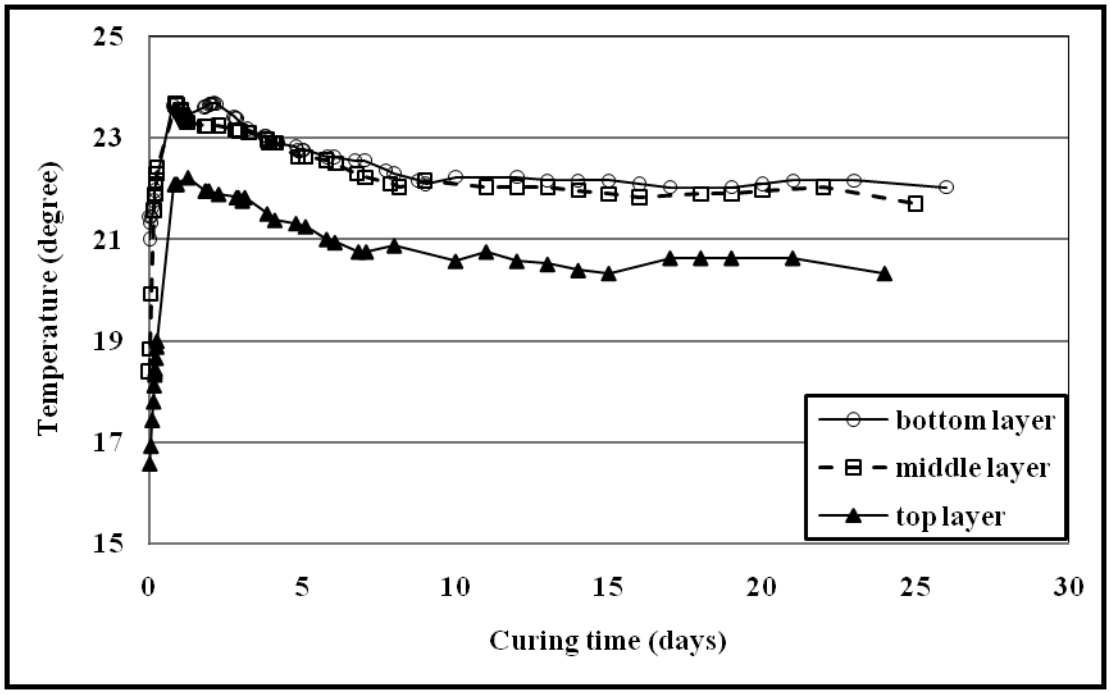

Figure 5-6 Temperature development during the hydration process for drained column

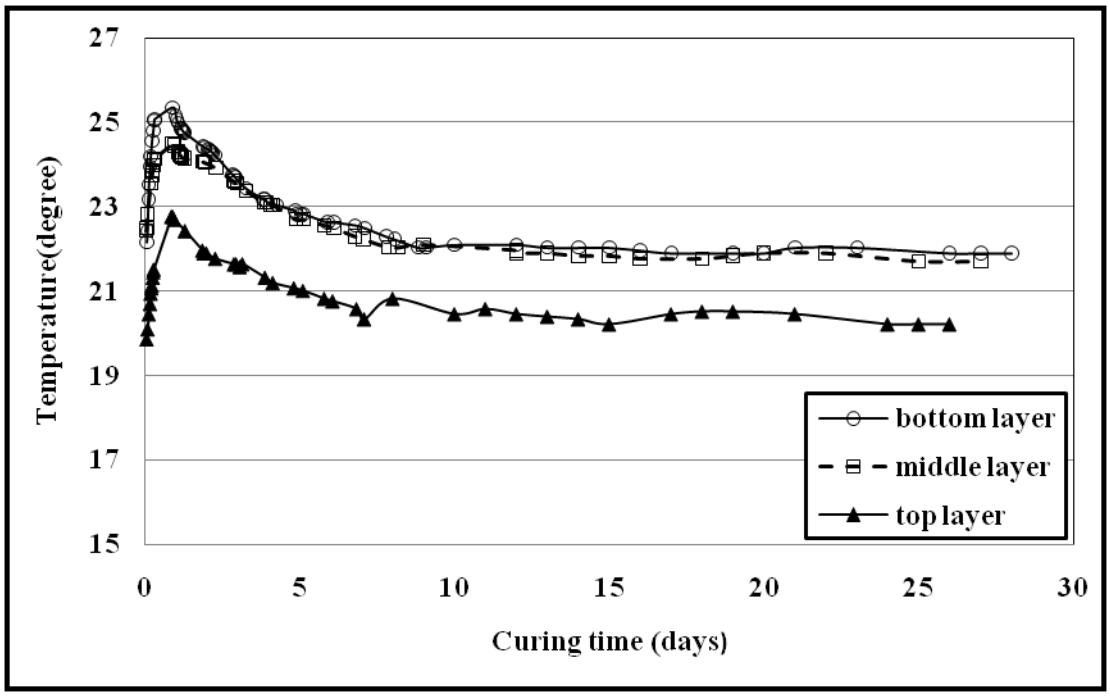

Figure 5-7 Temperature development during the hydration process for undrained column

5.3.2 Evolution of the hydraulic properties

5.3.2.1 Saturated hydraulic conductivity

The evolution of saturated hydraulic conductivity with the depth of the drained and undrained GF columns is shown in Figure 5-8. The range of the saturated hydraulic conductivity values of the drained GF column is 5.29×10^{-6} - 5.66×10^{-6} cm/s, while the range for the undrained GF column is 4.5×10^{-6} - 5.9×10^{-6} cm/s. This indicates there are no significant differences between the hydraulic conductivity values in the drained and undrained columns. Only a slight change in saturated hydraulic conductivity can be observed for the undrained column with depth, whereas the variation in saturated hydraulic conductivity of the drained column is negligible. It seems that the pore structure of the drained column is almost the same for all of the layers. Hydraulic conductivity can provide relevant information about the pore structure of cementitious materials (Fall et al., 2009). A slightly lower hydraulic conductivity observed in the bottom layer of the undrained column can be attributed to the impact of cement hydration heat on the refinement of the pore structure of cementitious material. From Figure 4-7, it can be seen that the bottom layer of the undrained GF column shows the highest peak temperature (25.3°C). This higher temperature resulted in faster binder hydration in the bottom of the undrained GF column than in the other layers of the undrained GF column and in the drained column.

Both columns showed slightly lower saturated hydraulic conductivity values than the small samples. The saturated hydraulic conductivity of the small samples is 6.8×10^{-6} cm/s (Figure 5-9). This is due to the fact that the GF columns are better packed than the small samples. They were subjected to a heavier weight when they were part of the GF columns, and this enhanced the compaction of the fresh material. Furthermore, heat development (Figures 5-6 and 5-7) in the GF (due to cement hydration) results in faster binder hydration in the GF

columns than the small samples. This means that more hydration products in GF columns lead to the refinement of their pore structures. However, in general, it should be mentioned that the saturated hydraulic conductivity of the GF columns and the small samples fall within the same range.

5.3.2.2 Suction development with time

Matrix suction (u_a-u_w, u_a is pore air pressure, u_w is pore water pressure) is one of the stress state variables in unsaturated porous media. The matrix suction component is commonly associated with the capillary phenomenon that arises from the surface tension of water. Matrix suction development with time for drained and undrained columns is illustrated in Figures 5-10 and 5-11, respectively. It is noticed that after 24 hours and prior to the addition of the middle layer, the bottom layer of the drained column achieves higher matrix suction (42 kPa) than the bottom layer of the undrained column which reaches a suction value of 26 kPa. When binder hydration process starts, the GF material undergoes self-desiccation; this decreases the internal RH or increases suction and can lead to empty pores. Self-desiccation is considered as the main mechanism responsible for the increase of suction with time in cementitious materials. Self-desiccation is the chemical shrinkage that arises during the hydration process. Furthermore, the bottom layer of the drained column loses some of its water which reduces the water content of this layer and increases the suction in comparison to the undrained layer. After placing the second GF layer, the matrix suction values decrease for both columns. This is due to the fact that the underlying layers absorb part of the water of the fresh layers. After 24 hours of placing the middle layer, it was observed that the suctions in the two layers converge to values that are quite close. In addition, the suction in the fresh layer rises at a much higher rate than the suction during

the initial drying of the bottom layer (before adding the middle layer) of the undrained column, while the situation is reversed for the drained column. This is because in addition to self-desiccation, the middle layer of the undrained column lost some of its water to the bottom layer. This reduced the water content and increased the suction of the middle layer to a higher level more than at the initial drying stage of the bottom layer of the undrained column. However, for the drained condition, it seems that the bottom layer drained more water at the initial drying stage in comparison to the middle layer.

The same observation was noticed when the third layers were placed. On the seventh day, the measurement of suctions was stopped due to cavitation in the tensiometers. The suction values for each layer for both conditions are explained below.

The top layer for both condition reaches matrix suction values that are higher than the other layers due to desiccation (top of columns were left uncovered). The middle layers achieved a matrix suction of 65 kPa while the bottom layers achieved values of 67 and 60 kPa for the drained and undrained columns, respectively.

It can be seen that in most cases, the drained column achieves higher matrix suctions than the undrained column. The reduction in the moisture content for the drained column leads to an increase in the matrix suctions.

From a design point of view, it is important to take into consideration the increase and drop in suction with time during the filling process. It is well documented that the increase in suction will increase the UCS value for GF structures. Studies found that in a fine porous media, an increase in the negative pore water pressure (i.e. suction) results in increases in the cohesion which in turn leads to increase in confinement of porous media particles (Haines' 1925, 1927). However, these suction values change with time during the filling

process and at some point, reach zero. This process could have a notable impact on the strength of GF, and thus on the mechanical stability of the GF structure.

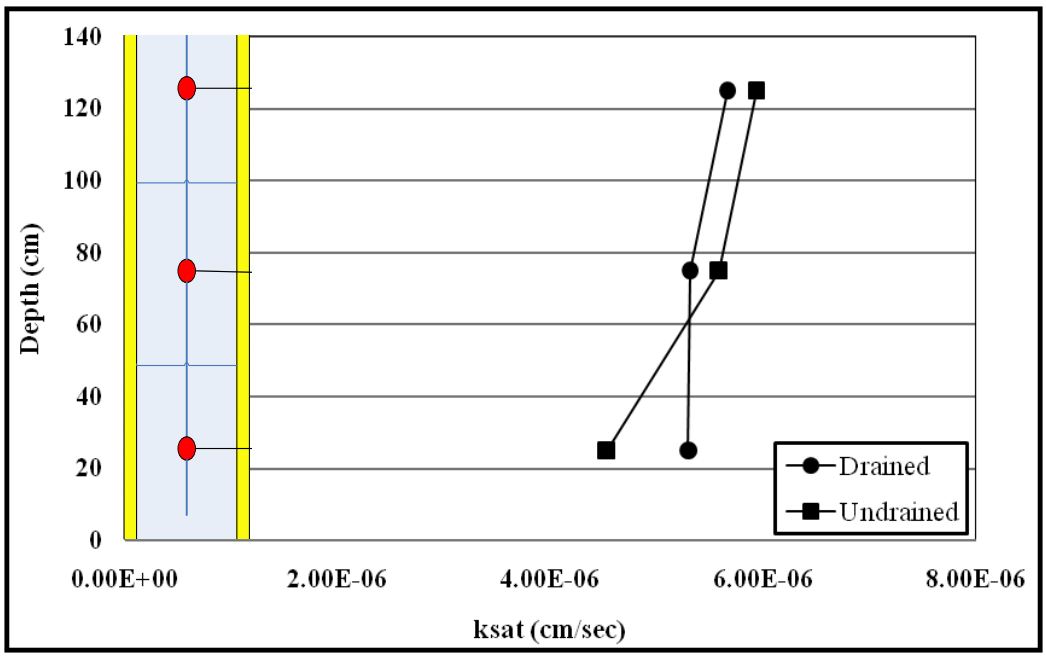

Figure 5-8 28 days saturated hydraulic conductivity of GF columns in drained and undrained conditions vs. depth

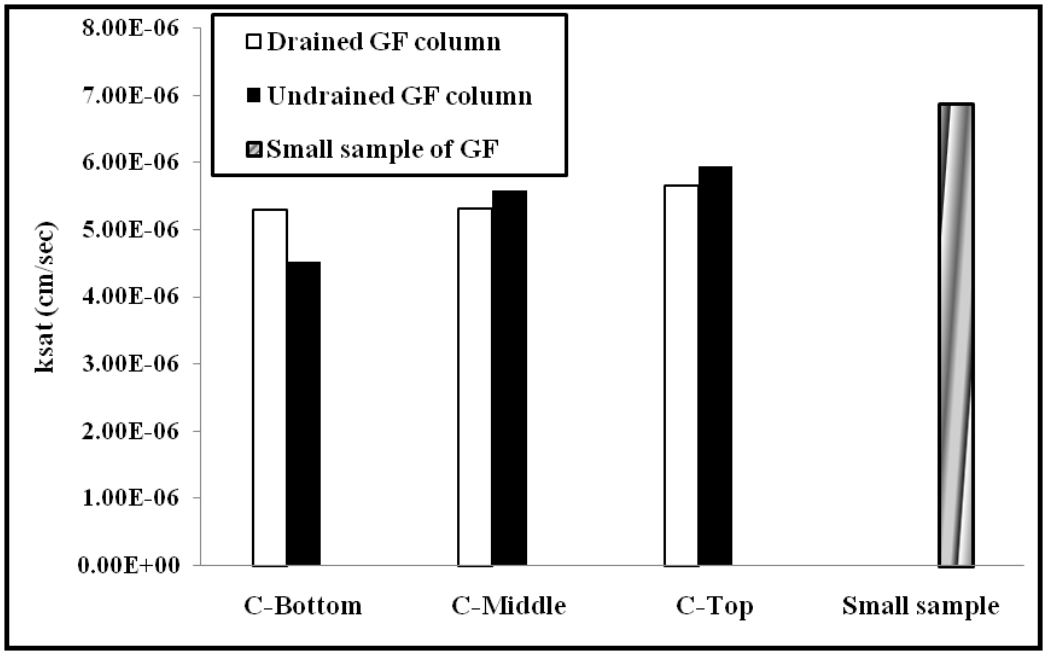

Figure 5-9 Comparison of the saturated hydraulic conductivity of GF columns and small GF samples

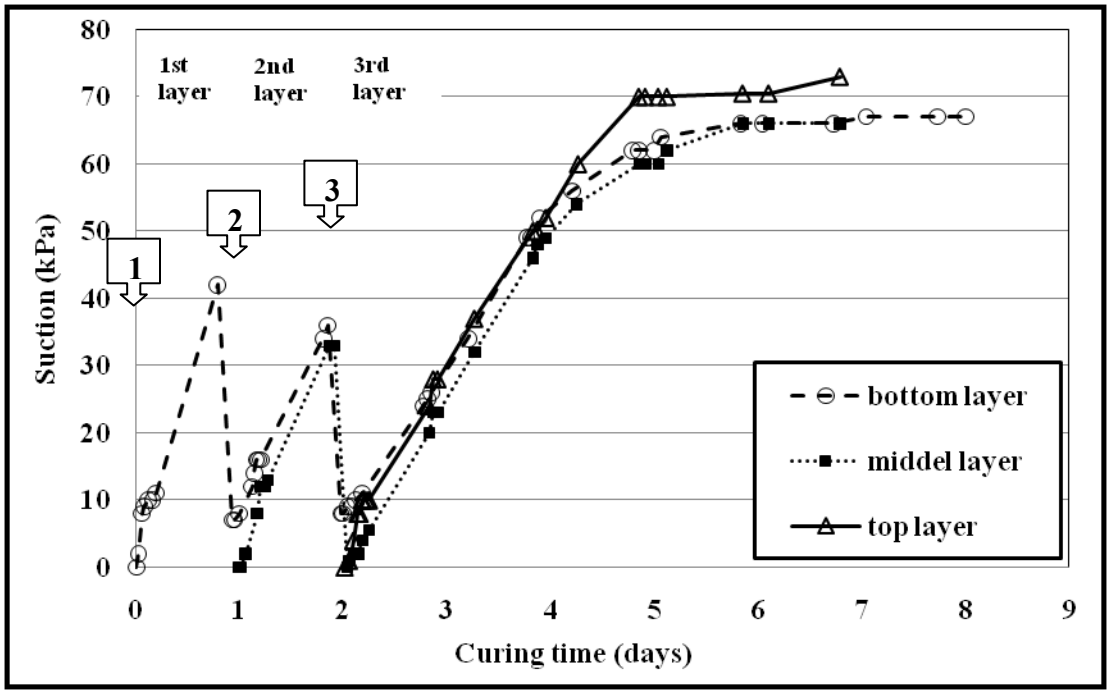

Figure 5-10 Development of matrix suction with time and depth for drained column

1= first filling, 2= second filling, 3= third filling

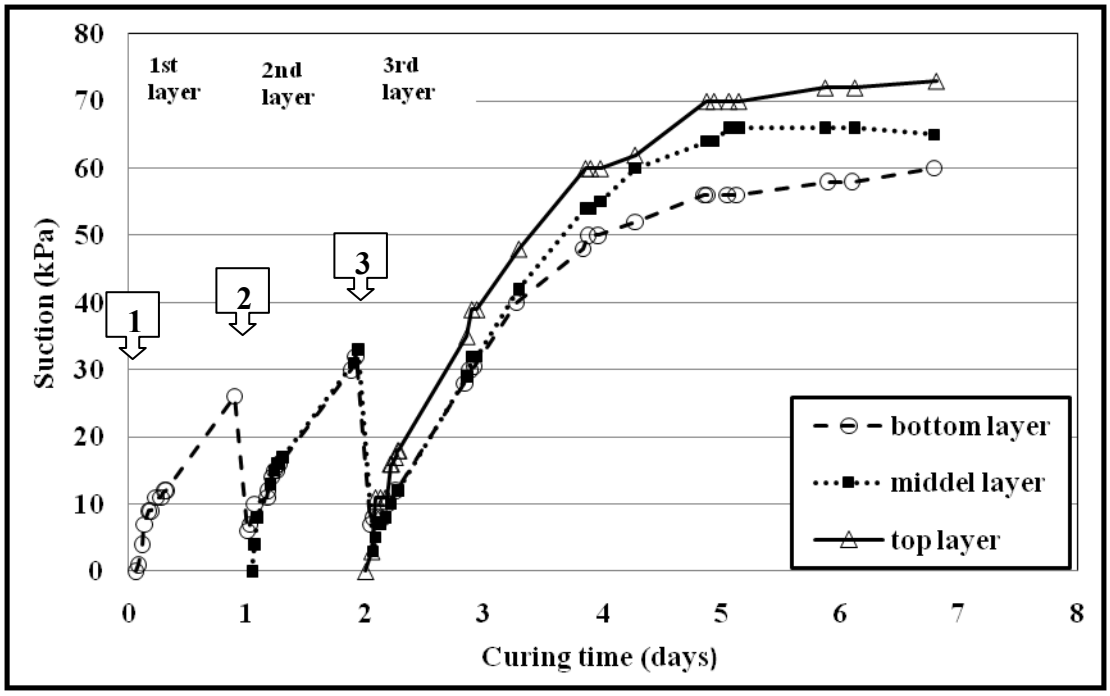

Figure 5-11 Development of matrix suction with time and depth for undrained column

1= first filling, 2= second filling, 3= third filling

5.3.2.3 Water drainage

Immediately after pouring the bottom layer, the water started to seep from the funnel attached to the column base, and this continued for four hours. The weight of the water collected from this layer is 305 g which corresponds to 2.77% of the initial quantity of the bottom layer of water. Figure 5-12 shows the evolution of the drained water with time. No increase in the weight of the drained water was recorded the next day when the middle layer was poured. The reduction in the drained water can be related to the advancement of binder hydration (refinement of pore structure) and the presence of sodium silicate in the mix used in the present investigation. Furthermore, according to Doucet et al., (2007) and Hassani et al. (2007), sodium silicate gel has the ability to capture water, which in turn, will result in a minimal reduction of the amount of drained water.

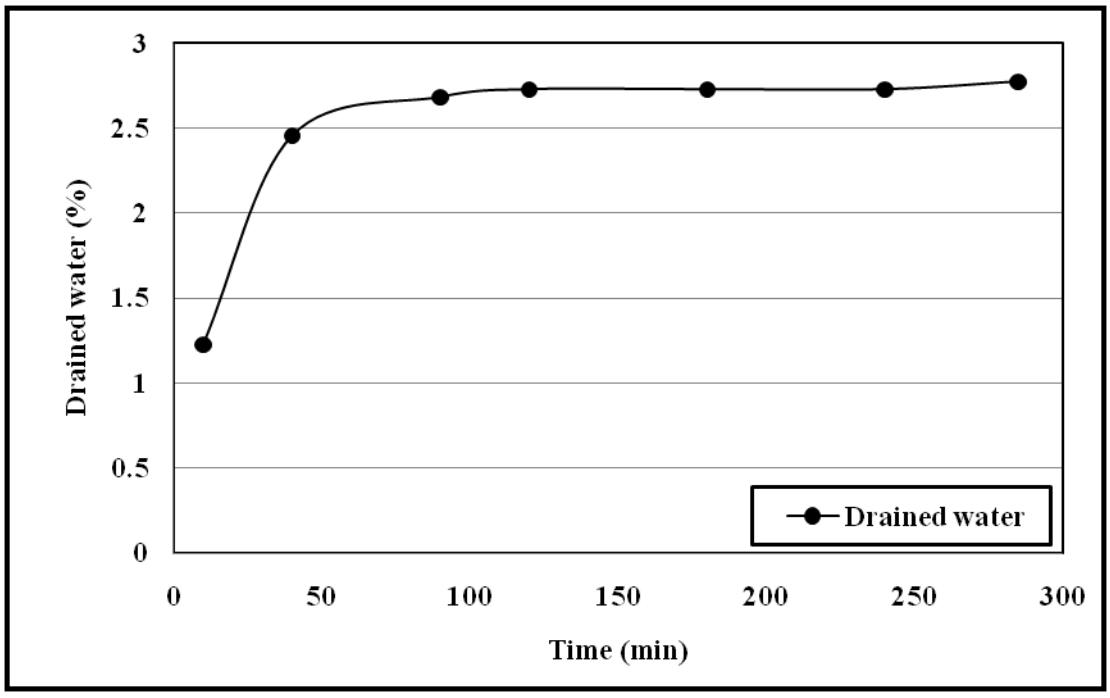

Figure 5-12 Drained water vs. time from the bottom layer of the GF drained column

5.3.3 Mechanical properties

Figure 5-13 presents the variation in UCS values of the GF columns with depth in the drained and undrained columns. The range of variation in UCS is 556 - 585 kPa for the drained column, while the range of variation for the undrained column is 537 - 614 kPa. For the bottom and the middle layers, the results showed that the undrained GF gains higher strength than the drained GF, whereas this is reversed for the top layer. This is attributed to the fact that the water was only drained from the bottom layer (as mentioned in Section 5.3.2.3). The drained water collected from the bottom layer is about 2.77% of the initial quantity of the bottom layer of water. After 24 hours, this layer solidified and it was impossible for the water in the middle layer to drain out through the bottom layer. The weight of the drained water collected at the base of the column stayed the same after casting the middle layer (Figure 5.12). However, the drained bottom layer absorbed some water from the fresh middle layer. As a result, the water content of the bottom layer was again increased. This decrease and increase in water content for the bottom layer of the drained column could have caused some destabilization to the cement hydration in this layer. This led to a slight decrease in the strength. Furthermore, the drained water could have eliminated some of the clinker from the bottom layer of the drained column. This would result in less clinker available for cement hydration for the bottom layer of the drained GF in comparison to the other layers and the undrained column. Future geochemical analyses of drained water would help to support this argument.

For the bottom layer in the undrained column, the water content is more stable than the drained case as mentioned earlier. For this reason, the strength of the GF column of the bottom and middle layers of the undrained column is slightly higher than the same samples of the drained column. Furthermore, heat development between the bottom and middle

layers in the undrained and drained columns is responsible for the difference of strength observed between the two layers. From Figures 5-6 and 5-7, it can be noticed that the peak temperatures in the middle and bottom layers of the undrained columns are higher than those in the same layers of the drained column. It is well known that higher temperature results in higher early strength in cementitious material (e.g. Celestin, 2009).

From Figure 5-13, it can be observed that the UCS value of the top layer in the undrained column is lower than that of the top layer in the drained column. The UCS value is also lower than that of the bottom and middle layers. This can be attributed to the difference of moisture gradients (thus of drying rate) between the drying surfaces of the top layers of the undrained and drained columns. It is well known that the highest tensile stresses occur in the exposed surface layer where the moisture gradients are the highest. The moisture gradients are responsible for the differential drying (and thus shrinkage) of the cementitious material (e.g. Grasley and Lange, 2002). When the induced tensile stresses exceed the tensile strength of the cementitious material, cracking will immediately occur, thereby negatively affecting its mechanical (e.g. strength) and durability (e.g. permeability) properties. In the case of the drained GF, the water loss is not only due to internal drying (self-desiccation) and external drying (e.g., desiccation), but also to water drainage. This means that the undrained GF has higher water content available for desiccation, and thus the potential to develop higher moisture gradients with the RH of the ambient air. This will mean that the undrained GF may develop higher tensile stress and suffer higher drying rates and shrinkage strains. The higher drying rate of the top layer of the undrained column is in agreement with the results of the suction increase rates of the top layers presented in Figures 5-10 and 5-11. From these figures, it can be seen that between 2 and 3 days, the

slope of the suction increase in the top layer of the undrained column is higher than that of the drained column. This can suggest a higher drying rate.

The UCS values for the GF columns (both drained and undrained) are compared with the UCS of the small samples (mould samples) that have the same binder content, w/c ratio, and curing time as illustrated in Figure 5-14. It can be seen that the UCS values for the GF columns are higher than the mould samples. This is because the GF columns are better packed than the small samples. As well, the GF columns samples were subjected to a heavier weight when they were part of the GF columns, and this enhances the compaction of the fresh material. Furthermore, heat development (Figures 5-6 and 5-7) in the GF (due to cement hydration) results in faster binder hydration in the GF columns. Faster cement hydration leads to higher UCS. Indeed, faster cement hydration results in precipitation of larger amounts of cement hydration products, such as C-S-H and CH. C-S-H is primarily responsible for the strength of cementitious material (Neville, 1995).

From the results presented, it can be concluded that the strength development of GF is strongly coupled to heat development, saturation degree or suction development within the GF.

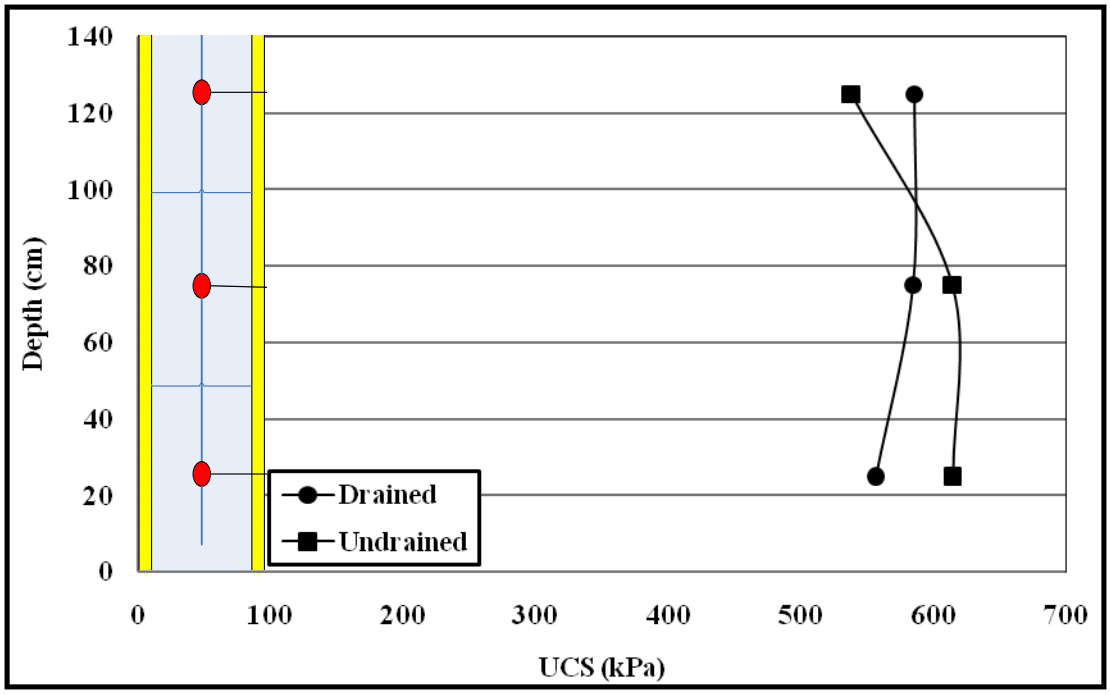

Figure 5-13 28 days UCS of GF columns in drained and undrained conditions vs. depth

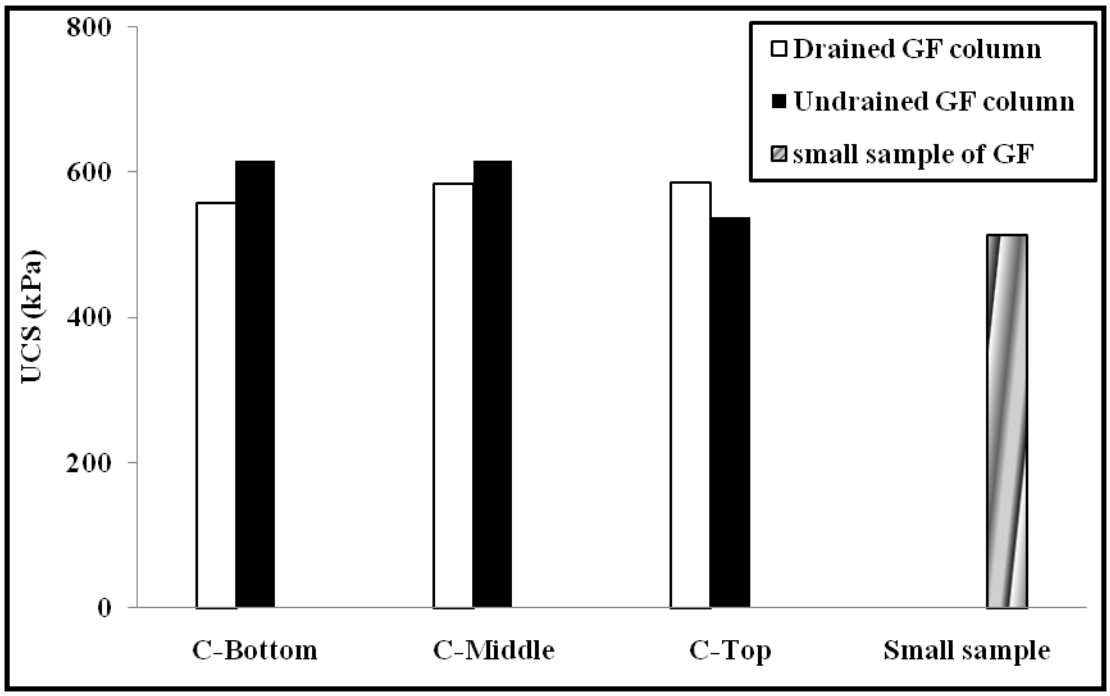

Figure 5-14 Comparison of UCS of GF columns and small samples of GF

5.4 Summary and conclusions

In this paper, the THM behavior of GF columns in drained and undrained conditions has been studied. UCS, saturated hydraulic conductivity and K tests are conducted on samples that are taken from the columns (block samples) and GF mould samples. Suction and temperature development was monitored during the hydration process. The outcomes of these tests are then compared with the results obtained from small (mould) samples that have the same mix proportion and curing time. The following conclusions can be drawn:

The bottom and the middle layers of the undrained column gains higher UCS than the drained column, while the top layer of the drained column achieves a higher UCS. The water content of the bottom and middle layers of the drained column is disturbed which negatively affects the hydration reaction of these layers. Also, the heat development in the undrained GF column is higher than the drained column, and this leads to a faster hydration reaction and then to a higher UCS. On the other hand, the UCS of the top layer of the undrained column is lower than that of the top layer of the drained column and those of the bottom and middle layers of the undrained column. This is due to the differences of moisture gradients between the drying surfaces of the top layers of the undrained and drained columns. Furthermore, the strength of the drained and the undrained samples is higher than the strength of the small samples. This is attributed to the fact that the columns are compacted under their weight, and also the heat development in the GF (due to cement hydration) results in faster binder hydration in the GF columns than the small samples. This faster cement hydration leads to a higher UCS. The outcomes of this paper show that the mechanical properties of GF are strongly coupled to heat development, saturation and suction development within the GF.

Negligible changes in the saturated hydraulic conductivity of the drained column were observed while there was a slight variation in the saturated hydraulic conductivity of the undrained column. The bottom layer of the undrained column shows a lower value than the other layers. This slightly lower hydraulic conductivity can be attributed to the impact of cement hydration temperature on the refinement of the pore structure of cementitious material; the bottom layer of the undrained GF shows the highest peak temperature (~25.5°C). In brief, the hydraulic properties of GF structures are affected by heat development. The saturated hydraulic conductivity of the GF columns falls within the same range of the small samples.

In most cases, the drained column achieves higher matrix suction than the undrained column. The drained column has the advantage of reducing the GF moisture content which leads to an increase in the matrix suction.

The effect of the drained and the undrained conditions is insignificant on the values of thermal conductivity. In addition, the variation in thermal conductivity values along the GF columns is minor. The thermal conductivity of the drained and the undrained GF columns displays higher values than the small samples. Furthermore, the evolution of temperature with time shows slight higher values for the undrained column than the drained column at early ages while the effect of the drained and the undrained conditions was insignificant on temperature evolution at advanced ages.

The test results obtained showed that the mechanical, hydraulic and thermal properties of GF columns are different from samples cured in plastic moulds. The main reason behind

the differences between the GF columns and small sample properties is the THM coupling effects.

This paper shows that the mechanical properties, hydraulic properties (suction and water content), and temperature development are coupled.

The present investigation and its obtained results add to the fact that GF material properties demonstrate enhanced behaviour when used in real structures, and strong coupled processes occur in GF structures in the field. These coupled processes need to be considered in the design of GF structures.

5.5 References

Cayouette, J. Optimization of the paste backfill plant at Louvicourt mine, CIM Bulletin, 96 (1075). (2003) 51-57.

Celestin, J.C. Geotechnical properties of cemented paste backfill and tailings liners: effect of mix components and temperature. University of Ottawa, (2008) 1-221.

Celestin, J. C. H., Fall, M. Thermal conductivity of cemented paste backfill material and factors affecting it. International Journal of Mining, Reclamation and Environment (2009) 1-17.

Doucet, C., Tarr, K., and Swan, G. Evaluation of the effect of mixing method, sequence and time on the properties of gelfill. Minefill 2007, 2488.

Fall, M., Adrien, D., Celestin, J.C., Pokharel, M., Toure, M. Saturated hydraulic conductivity of cemented paste backfill. Minerals Engineering 22 (2009) 1307-1317.

Fall, M., Celestin, J. C., Pokharel, M., Toure, M. A contribution to understanding the effects of curing temperature on the mechanical properties of mine cemented tailings backfill. Engineering Geology 114 (2010) 397–413.

Fall, M. and Samb S.S. Pore structure of cemented tailings materials under natural or accidental thermal loads. Materials Characterization. 5 9 (2008) 5 9 8 – 6 0 5.

Fall, M., Benzaazoua, M. and Saa, E.G. Mix proportioning of underground cemented tailings backfill. Tunnelling and Underground Space Technology 23 (2008) 80–90.

Fall, M., Nasir, O., and Celestin, J. Paste backfill responses in deep mine temperature conditions. 9th International Symposium of mining with backfill. Montreal, Canada: CD-Rom; 2007 paper 2522.

Fisseha, B., Bryan, R. & Simms, P. Unsaturated flow and evaporation in multilayer deposits of gold paste tailings. Canadian Geotechnical Conference Edmonton (2008): 818-823.

Fredlund, D. G. and Rahardjo, H. Soil mechanics for unsaturated soils, (1993) 1-510.

Grabinsky, M., Bawden, W., Simon, D., and Thompson, Ben. In situ properties of cemented paste backfill in an Alimak Stope. Canadian Geotechnical Conference Edmonton (2008): 790-796.

Grasley, Zachary C., Lange David A. Modeling drying shrinkage stress gradients in concrete. Journal of Testing and Evaluation, (2002) 1-13.

Han-Kook, K., Sang-Eun, K., Jin-Keun, K., Yang, S. An experimental study on thermal conductivity of concrete. Cement and Concrete Research 33 (2003) 363–371.

Hassani, F, Razavi, S.M., and Isagon, I. A study of physical and mechanical behaviour of gelfill. Minefill, 2007 Paper 28.

KD2 Operator's Manual (2006) 1-24.

Le Roux, K. A., Bawden, W. F., Grabinsky, M. W. F. Assessing the interaction between hydration rate and fill rate for cemented paste backfill, in proceedings on the 55th Canadian Geotechnical and 3rd joint IAH-CNC Groundwater specialty Conferences. (2003) 427-432.

Le Roux, K., Bawden, William F. and Grabinsky, Murray F. Field properties of cemented paste backfill at the Golden Giant mine, Mining Technology (Trans. Inst. Min. Metall. A). (2005) 1-16.

Lerch, W., Bogue, R. H. Heat of hydration of Portland cement pastes. Journal of research of the National Bureau of Standards. (1934) 1-30.

Nasir, O. Modeling of coupled processes in hydrating cemented paste backfill structures and application to the analysis of their performance. University of Ottawa. (2008) 1-144.

Pokharel, M. Geotechnical and environmental responses of paste tailings systems to coupled thermo-chemical loadings. University of Ottawa. (2008) 1-248.

Revell, M.B. Paste-How strong is it? In proceeding of the 8th International Symposium on Mining with Backfill. (2002) 286-294.

Schindler, Anton K., Folliard, Kevin J. Heat hydration models for cementitious materials. ACI Materials Journal, 2005: 24-33.

Williams, T. J., Denton, D. K., Larson, M. K., Rains, R. L., Seymour, J. B., Tesarik, D. R. Geomechanics of reinforced cemented backfilling an underhand stope at the Lucky Friday Mine, Mullan, Idaho. U.S. Department of health and human services (2001).

Ylimaz E., Kesimal A., Deveci H., Ercikdi B. The factors affecting the performance of paste backfill; physical, chemical and mineralogical characterization. First Engineering Sciences Congress for Young Researcher (2003).

5.6 Acknowledgement

The authors would like to acknowledge National Sciences and Engineering Research Council (NSERC), University of Ottawa and the National Research Council (NRC) of Canada.

Chapter 6

Summary, Conclusions and Recommendations

Over 200 cylindrical GF block and mould specimens (5 cm ×10 cm) have been tested in this investigation to determine the thermal, hydraulic, and mechanical properties of GF structures. Two columns made of GF that are 21.25 cm in diameter and 150 cm in height are developed to simulate the THM behaviour of GF under drained and undrained conditions. Various binder proportions (2%, 4.5%, and 6% PCI) are used for the mould samples while 4.5% PCI is used for the GF columns. Added to the mixes is 0.4% (by weight of solids) sodium silicate type N. The mould samples are cured for 3, 7, 28, 90, and 120 days, whereas the GF columns are cured for 28 days. UCS, saturated hydraulic conductivity and K tests are conducted on the mould and block samples taken from the GF columns. Microstructural analyses (XRD and TGA/DTA) are performed and α is approximated. WRCs were measured by using a WP4-T dewpoint potentiameter and the saline solution method, while unsaturated hydraulic conductivity is predicted for mould samples by using the van Genuchten (1980) equation. Prior to the filling of the columns, temperature sensors and tensiometers are fixed in the centre of each layer inside the columns in order to monitor temperature and suction developments with time.

6.1 Conclusions

The following conclusions can be drawn from the present study:

1. Mechanical properties are affected by binder content, binder types, and curing time. The evolution of UCS values is a function of curing time or degree of hydration index and binder content. Also, it is found that using PCI-slag as a binder in the GF mix gives higher strength than a mix that only contains PCI.

   The strength of the block samples from the drained and undrained GF columns is higher than that of the mould samples.

   The bottom and the middle layers of the undrained column gain higher UCS than those of the drained column, whereas the top layer of the drained column achieves a higher UCS.

2. The saturated hydraulic conductivity of GF is affected by binder contents, especially at early ages. The hydraulic conductivity of GF decreases as the binder content increases.

   A direct relationship is found between the UCS and the saturated hydraulic conductivity. As the UCS increases, the saturated hydraulic conductivity decreases.

   The saturated hydraulic conductivity of the GF columns falls within the same range of the mould samples.

3. The effect of curing time (or degree of hydration) on WRC is obvious at both low and high suction ranges while the binder proportion influences the WRC at low suction ranges only. It is found that the variations in void ratio and porosity are minor during the hydration process. On the other hand, the AEVs increase with an increase in curing time and decrease of void ratio values, while the binder content

only affects the AEVs at early ages. Binder proportions, curing times, and degree of hydration index have a slight effect on residual water content.

The evolution of AEVs, residual water content, and the fitting parameters from the van Genuchten model with degree of hydration index for various binder contents has been proposed in simple formulas. These formulas can be useful for the preliminary design phases of GF structures.

4. The unsaturated hydraulic conductivity of GF decreases when the suction, binder content, and degree of hydration index increase. These observations are more obvious at low suction ranges. The unsaturated hydraulic conductivity is a function of saturated hydraulic conductivity and WRC.
5. The thermal conductivity increases as binder contents and curing time increase. The thermal conductivity of GF samples is lower than the thermal conductivity of CPB samples because sodium silicate has a low thermal conductivity (0.65 W/m°C). The thermal conductivity of the drained and the undrained GF columns displays higher values than the small samples.
6. The evolution of temperature and suction with time for both columns is similar. However, in most cases, the drained column achieves a higher matrix suction than the undrained column.
7. TGA/DSC and XRD analyses show that loss of weight and intensity of CH are higher in GF than CPB, which means that sodium silicate accelerates the binder hydration process.
8. The results obtained from the GF column experiment show that the effects of the drained and undrained conditions are insignificant in most cases. On the other hand,

the outcomes of this study confirm that thermal, chemical, hydraulic, mechanical and microstructural properties are strongly time-dependent or affected by the degree of binder hydration index. Also, the present investigation has shown that the above said factors are strongly coupled.

6.2 Recommendations

The following recommendations are suggested:

1. For future studies and a more reliable simulation to the in situ condition, a model that is notably larger than the columns used in the present investigation can be built and subjected to the same environment in which real GF structures can be found. The new model can be enclosed from the sides and the bottom with small rocks to closely simulate actual conditions. In order to quicken the mixing and casting process, a larger mixer (concrete mixer) can be used instead of the food mixer used in the present study. In the author's opinion, valuable results can be obtained and a greater understanding of GF behaviour in actual structures will be achieved when the aforementioned method is adopted;
2. Build and test GF columns at various curing times (7, 28, 90 and 150 days) to study the evolution of THM behaviour;
3. Set up a dial gage or linear variable differential transformer (LVDT) at the top of the GF columns to measure the settlement. Furthermore, monitor the suction evolution with the GF columns for longer curing times;
4. Determine the degree of binder hydration;

5. Investigate the pore structure or microstructure of GF in more detail. The impact of sodium silicate on the modification of the nano-structure of the C-S-H formed within the GF should be further investigated;
6. Study the hysteresis of WRCs;
7. Use GF that contain Slag as mineral admixture since the Slag-GFs show higher UCS than the PC_GF; and
8. Develop a mathematical model to predict the thermo-chemo-hydro-mechanical (TCHM) behaviour of GF.

Appendix

Photos and Figures from the Study

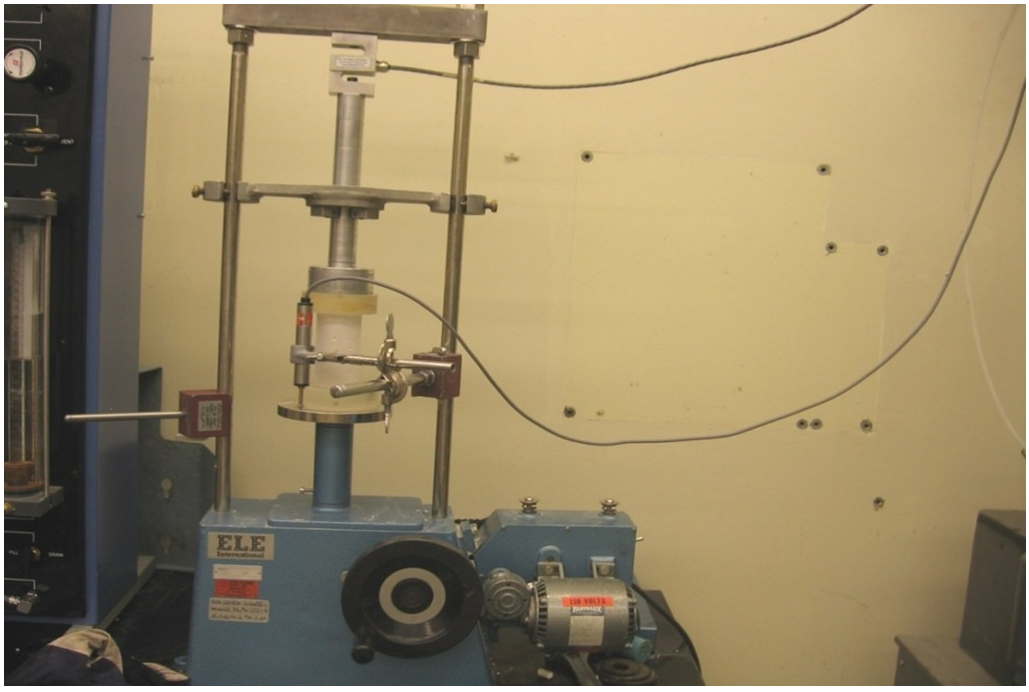

UCS test

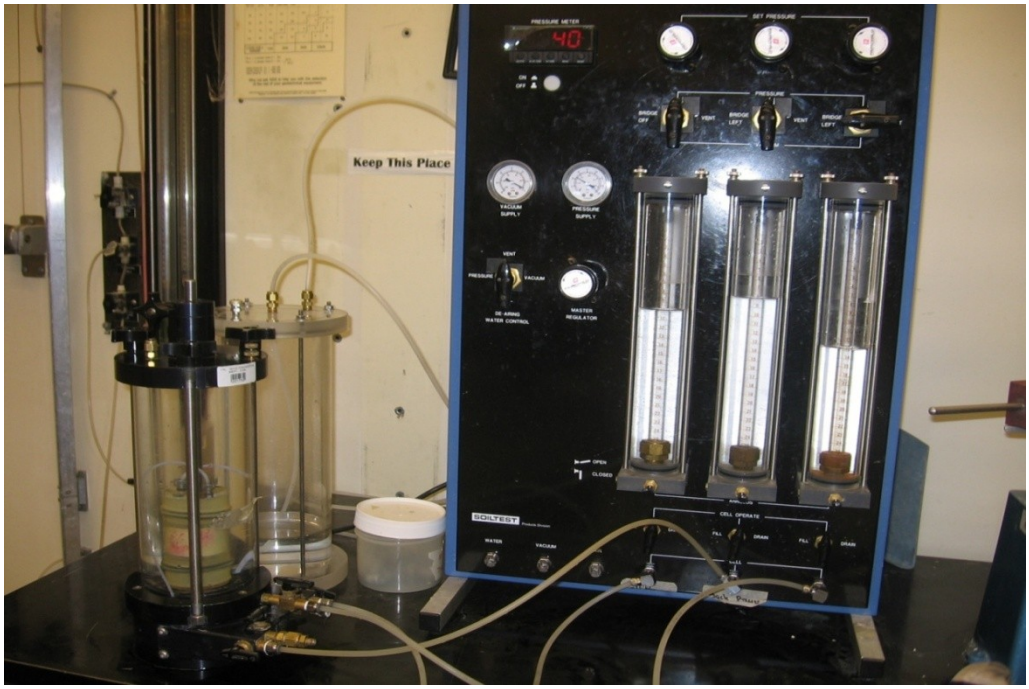

Saturated hydraulic conductivity test

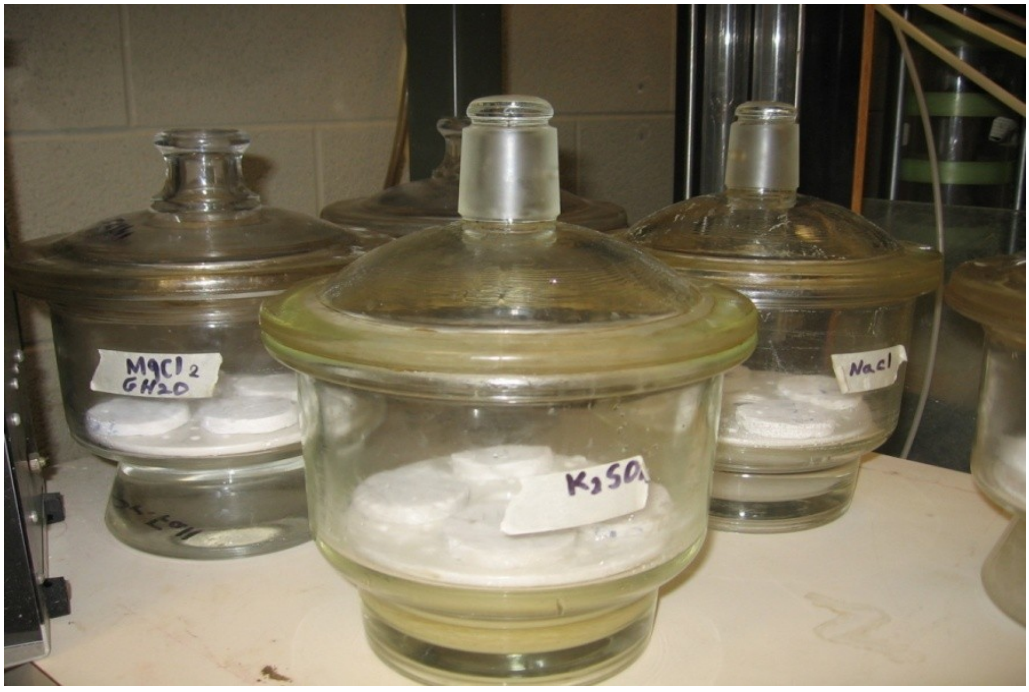

Saline solution methods

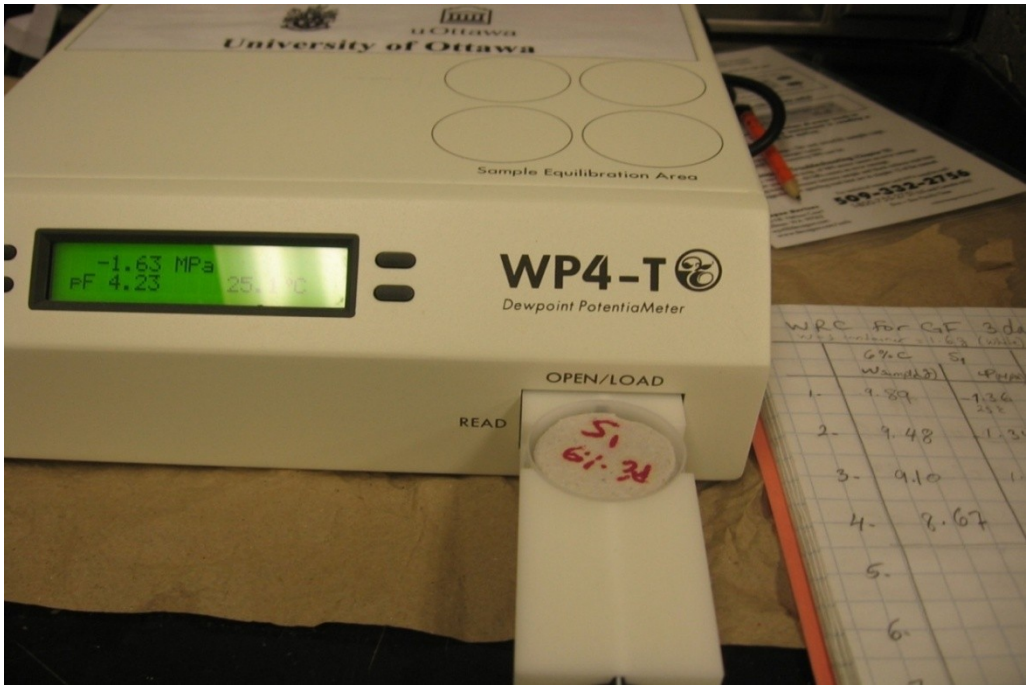

WP4-T test

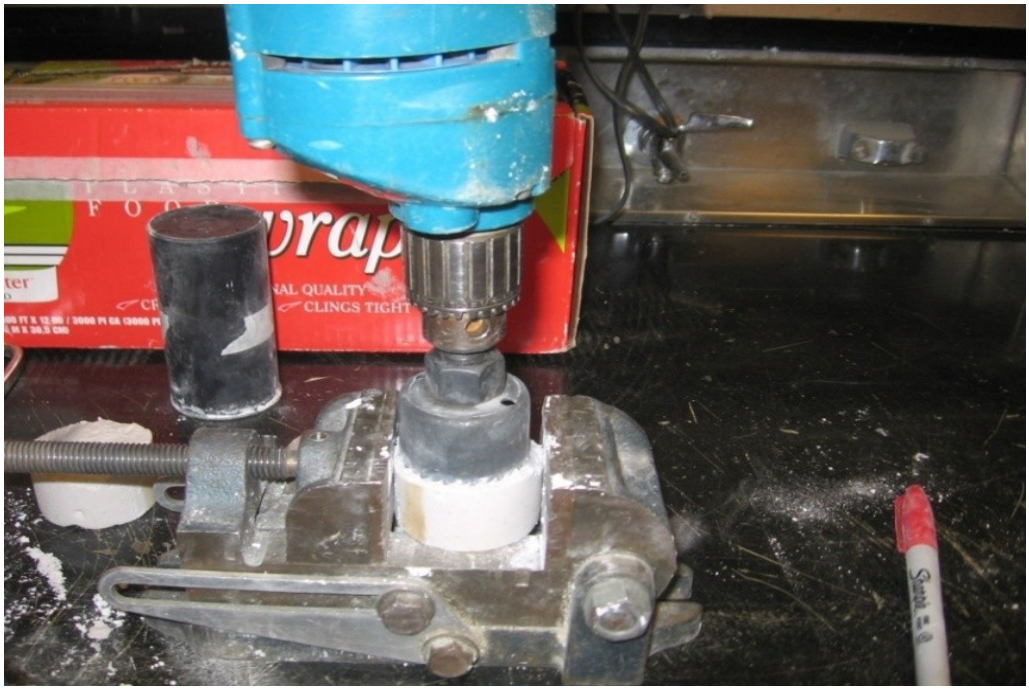

Preparation of samples for WP4-T test; step 1

Step 2

Step 3

Step 4

Thermal conductivity test

Drained column

Tensiometers fixed on the columns

Tesiometer tip and temperature sensor

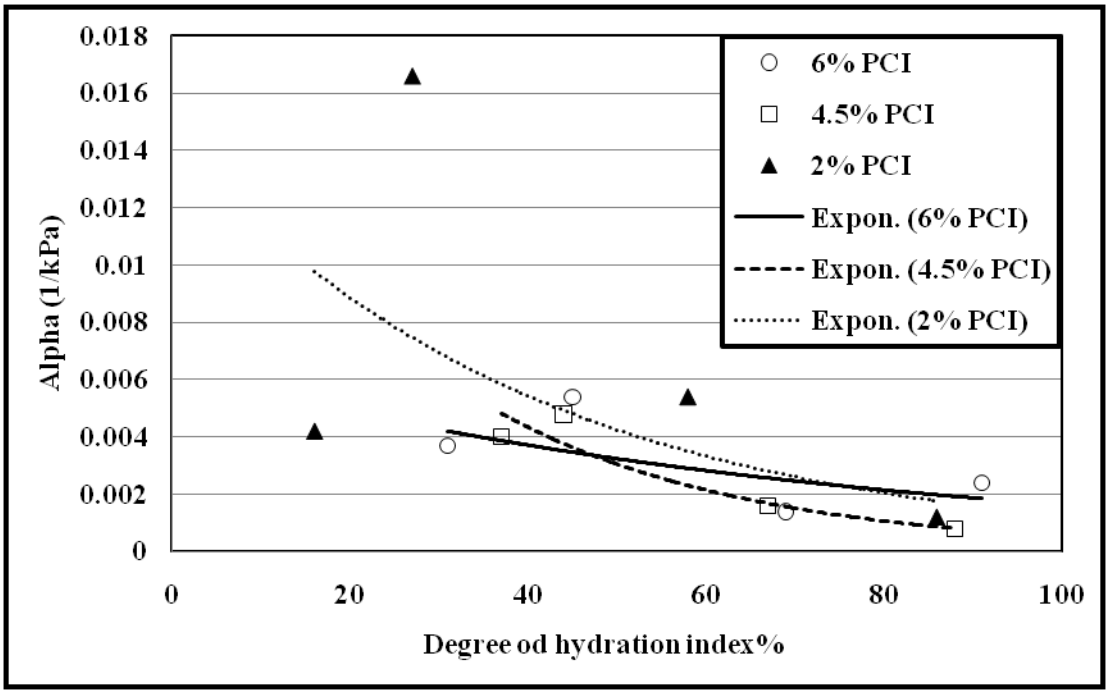

The evolution of α (fitting parameter) with degree of hydration index for various binder contents (6%, 4.5%, and 2% PCI)

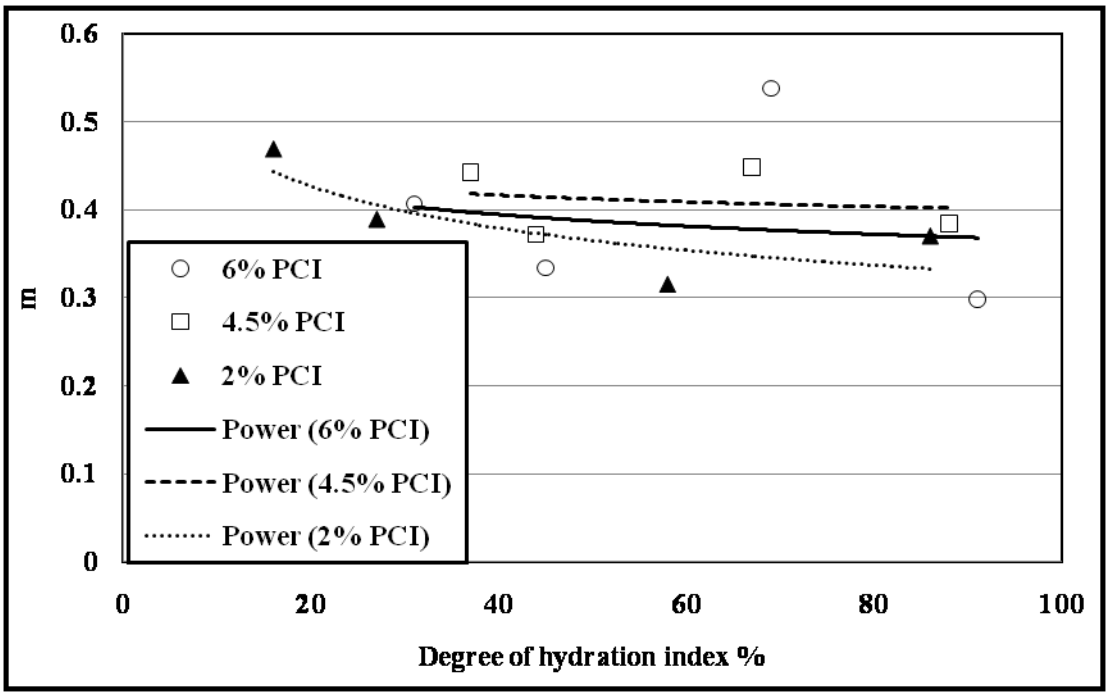

The evolution of m (fitting parameter) with degree of hydration index for various binder contents (6%, 4.5%, and 2% PCI)

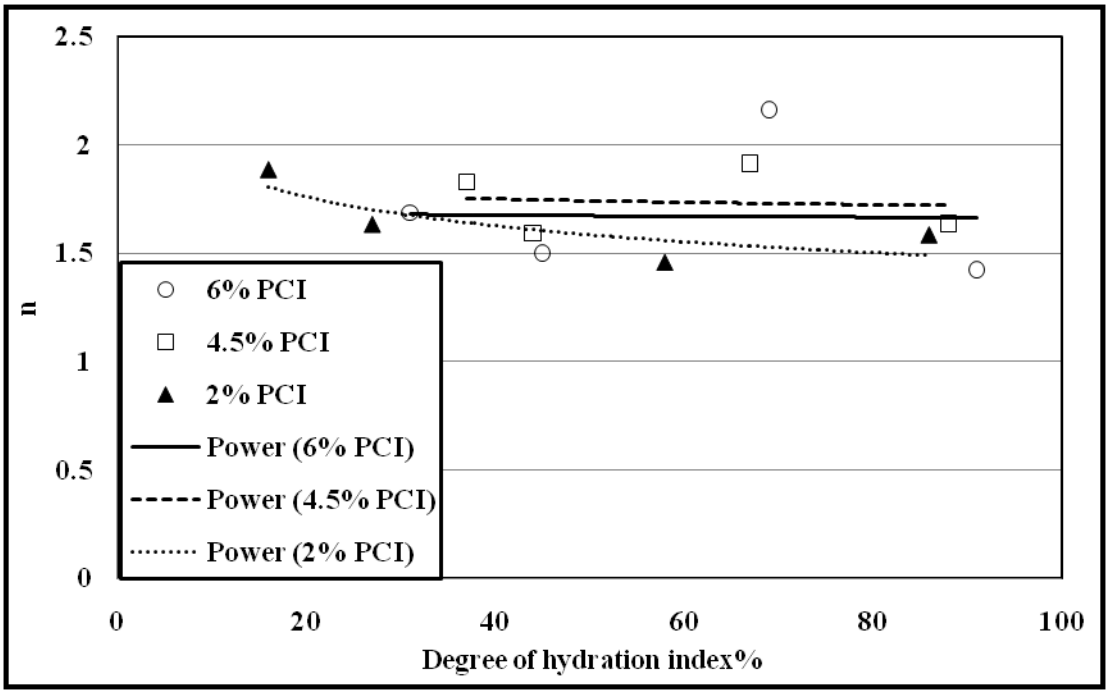

The evolution of n (fitting parameter) with degree of hydration index for various binder contents (6%, 4.5%, and 2% PCI)

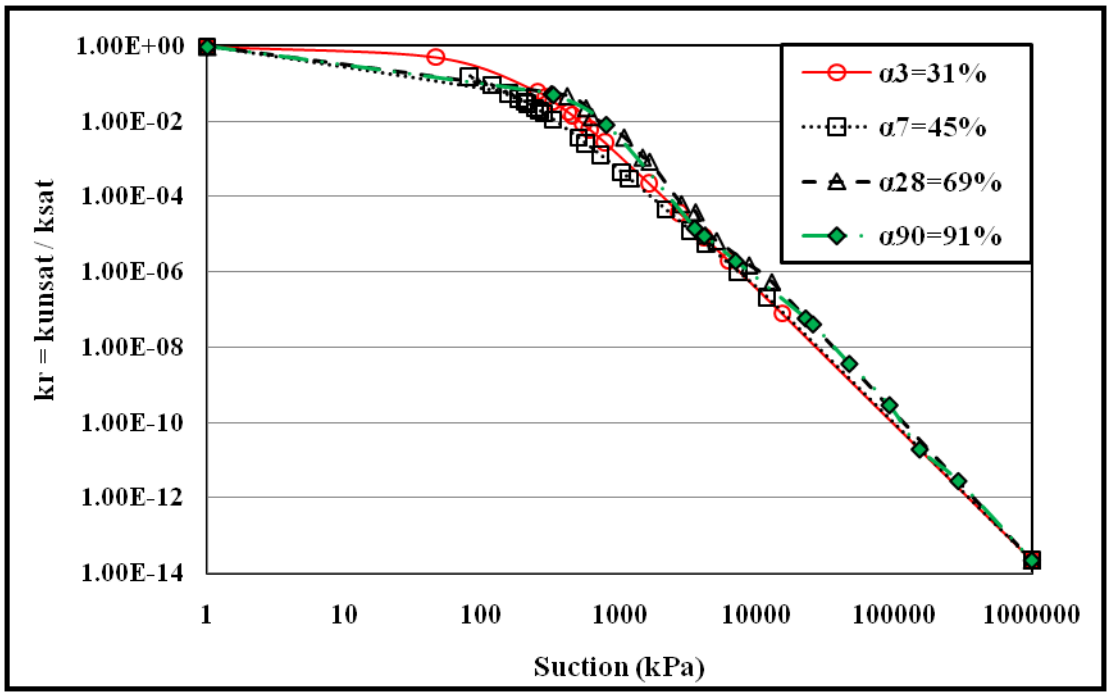

a- 6% PCI

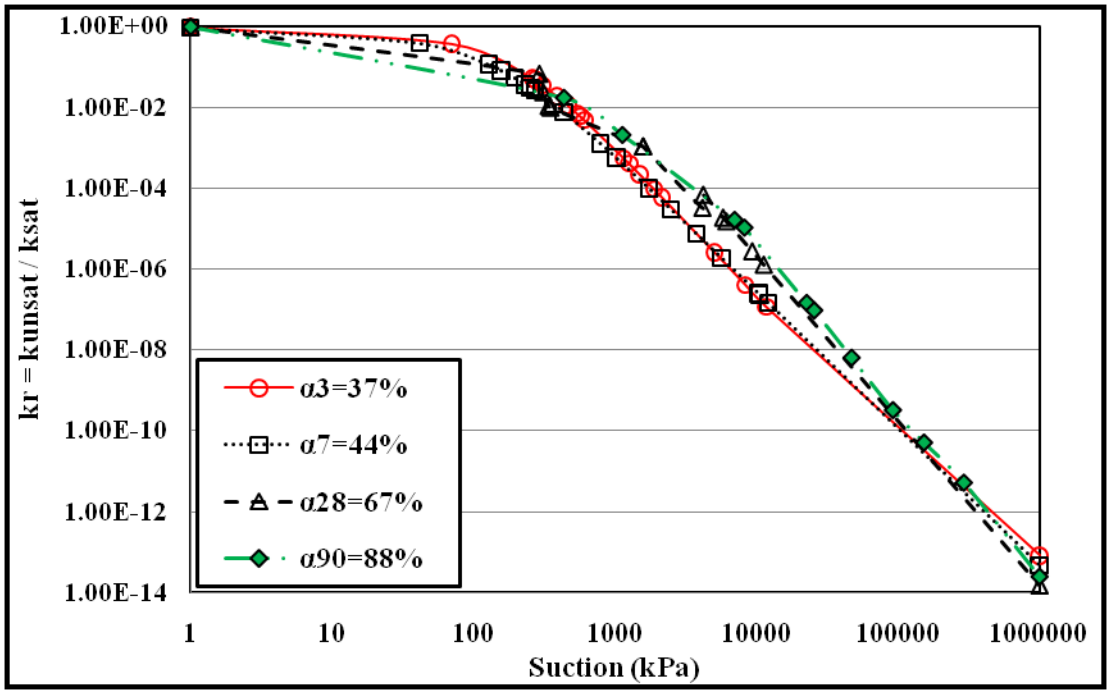

b- 4.5% PCI

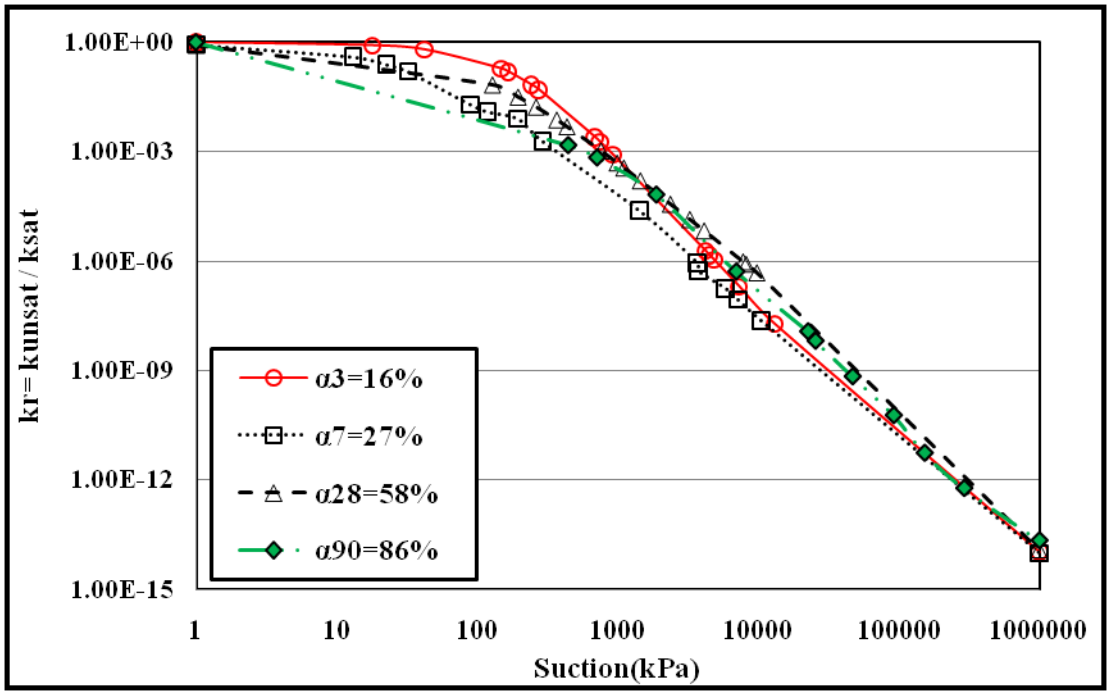

c- 2% PCI

The relative coefficient of permeability vs. suction for GF samples with various degrees of hydration and (a) 6% PCI, (b) 4.5% PCI, and (c) 2% PCI